# PRECIOUS METAL GEOCHEMISTRY AND MINERALOGY OF THE OVOID ZONE OF VOISEY'S BAY MAGMATIC SULFIDE DEPOSIT, LABRADOR, CANADA

by



A thesis submitted to the

School of Graduate Studies

in partial fulfillment of the requirements for the degree of

Master of Science

Department of Earth Sciences

Memorial University of Newfoundland

# ABSTRACT

The Voisey's Bay Ni-Cu-Co deposit, located in northern Labrador, is considered to be a PGE poor, magmatic sulfide deposit, but anomalous regions containing elevated concentrations of Pt, Pd, Au and Ag have been reported during routine assay. Only limited data is available which documents the types of precious metal occurrences that are present in these regions. In this thesis, a thorough investigation of the PGE and precious metal-minerals has been conducted for the Ovoid, Mini-Ovoid and Discovery Hill deposits. The results were compared to previously documented occurrences in a hornblende-gabbro dyke in the Southeast Extension zone. The significance of these occurrences has been evaluated in reference to potential for recovery of Pt, Pd, Au and Ag, and the genesis of the mineralization in the anomalous regions. Because the concentrations of precious metals at Voisey's Bay deposit are low, unconventional methods of analysis were used to concentrate and analyze the mineral phases present. The dominant mineral phases that are present are sperrylite and froodite. Electrum, stützite and volyksite account for minor to trace proportions of the precious metal minerals. Analysis of sulfide minerals for Pt, Pd, Au and Ag by LA-ICPMS revealed that, in regions that represent very fractionated magma, most of the precious metal mass is present as discrete mineral phases containing Bi, Te, As, Sn and Sb, and only small proportions of Pd are found in solid solution in pentlandite and galena. The presence of semi-metals in the sulfide melt is the key component necessary to crystallize domains rich in PGM. Semi-metals were likely inherited through local crustal interactions of parental magma with Tasiuyak gneisses.

The major conclusions drawn from this study are 1) that even at low-PGE grade deposits such as Voisey's Bay, PGM are able to crystallize if sufficient amounts of semi-metals are present; and 2) recovery of the Pt, Pd, Au and Ag at Voisey's Bay may be possible because the majority of the precious metal mass is associated with minerals that are already recovered in the Ni or Cu concentrates, or they are present as mineral grains large enough to be concentrated alone.

# ACKNOWLEDGEMENTS

This thesis was generously funded by Vale Ltd. I am grateful for the assistance and expert guidance that was provided by Vale Ltd. staff, Dawn Evans-Lamswood, Peter Lightfoot and Robert Wheeler. Their experience and knowledge of Voisey's Bay deposit is invaluable and has added appreciable insight to this thesis.

I would like to acknowledge the following people for their dedicated and thorough assistance which has made this thesis possible:

I would like to thank the staff at Memorial University for their excellent support with the analytical work that was conducted: Michael Shaffer and David Grant for their assistance with all MLA and SEM analysis; Nancy Leawood for her assistance with ICP-MS analysis; and, Wilfred Diegor, Mike Tubrett and Kate Souders for their help with analysis of LA-ICP-MS; Dr. Derek Wilton for his review of my thesis and helpful comments. I would also like to thank Yanin Liu from the University of Toronto for her assistance with EPMA, and Joe Petrus for his assistance with supplementary LA-ICP-MS from Laurentian University.

I am grateful to have received such superior instruction and training from Dr. Louis Cabri who has dedicated his career to the study of platinum-group minerals.

I would also like to give a special thank you to Dr. Paul Sylvester for his excellent supervision. I have gained valuable knowledge from his wisdom, and I am forever grateful for his direction, encouragement and support.

Finally, I would like thank my husband, Andrew, and my children, Ben and Thomas, for their continuous support and inspiration.

# Table of Contents

# List of Tables

# List of Figures

# List of Commonly Used Abbreviations and Mineral Formula

PGE: Platinum-Group Elements

PGM: Platinum-Group Minerals

PMM: Precious-Metal Minerals

MSS: Monosulphide Solid Solution

ISS: Intermediate Solid Solution

VB: Voisey's Bay

NPS: Nain Plutonic Suite

LA-ICPMS: Laser Ablation Inductively Couple Mass Spectrometry

EPMA: Electron Probe Microanalysis

EPD: Electric Pulse Dissagregation

MLA: Mineral Liberation Analyzer

Po: Pyrrhotite, $Fe_{(1-x)}S$

Pn: Pentlandite, $(Fe,Ni)_9S_8$

Cpy: Chalcopyrite, $CuFeS_2$

Mt: Magnetite, $Fe_3O_4$

Fr: Froodite, $PdBi_2$

Spy: Sperrylite, $PtAs_2$

Poalovite, $Pd_2Sn$

Acanthite, $Ag_2S$

Michenerite, (Pd,Pt)BiTe

Electrum, Au-Ag alloy where Au>Ag

Stutzite, $Ag_{(5-x)}Te_3$

Volynskite, $AgBiTe_2$

# CHAPTER 1: INTRODUCTION

Platinum-group elements (PGE) have two major applications: 1) their production is essential to sustain our technology-driven world, and 2) PGE occurrences in nature can reveal an understanding of Earth's evolution because of their selective behavior in geologic systems. These elements, Pt, Pd, Ir, Os, Rh and Ru, are a group of high density metals (group VIII on the periodic table) with similar properties. They are non-reactive, exhibit strong electrical conductivity and have excellent catalytic properties. For these reasons, PGE are in high demand for their many uses such as conversion of crude oil to gasoline, manufacturing nitrate fertilizers, and as catalysts to reduce emissions from vehicle exhaust (Johnson Matthey Platinum Today, 2013a; McDonald and Hunt, 1982). From a petrogenetic perspective, PGE can be an important tool for evaluating the history of a deposit because their chalcophile nature allows them to partition into Fe and S rich magmas over silica rich magmas. The concentrations and PGE present in a geological system can give insight into the types of magma that produced the system and the history of the magma upon cooling. In either case, the mode of occurrence of PGE has proven to have significant importance to both applications.

The majority of the Earth's total PGE are concentrated in the mantle (0.05 wt.%, Lorand, 1990) because of their preference for Fe rich magmas and their high densities. Very rarely, PGE are found at high enough concentrations in areas of the crust where they can be mined either as a primary product (e.g. mafic layered intrusions where PGE concentrations can reach up to 50 to 100's of ppm at some deposits) or as a by-product at large base-metal sulfide deposits. With increasing technological advancements in ore processing, extraction of PGE from low-grade deposits is possible (e.g. Raglan, Northern Quebec and Jinchuan, China). As the demand for PGE grows and the PGE reserves at high grade deposits become more limited due to exceeding capacity or political and environmental factors, the low-grade PGE deposits are becoming more important sources of PGE.

In this thesis, rare precious-metal (PM) occurrences at the Voisey's Bay magmatic sulfide deposit are examined. Voisey's Bay, which is principally mined for Ni and Cu, is located in northern Labrador and is hosted by a 1.34 Ga troctolite intrusion emplaced within Enderbitic and Nain orthogneisses. The deposit is unusually low in its average content of PGE compared to other magmatic Cu-Ni deposits, but rare, anomalous concentrations of Pt and Pd (>0.5 ppm Pt+Pd) have been detected in some areas of the deposit during routine assay by Vale Ltd. The reasons for investigating these rare occurrences are to evaluate the potential for recovery of Pt or Pd as a by-product if future exploration at Voisey's Bay reveals any zones of enriched PGE; and secondly, to outline a model for the genesis of the PGE mineralization at Voisey's Bay which may have useful references for the entire genetic history of Voisey's Bay, and also to other deposits that have similar mineralization styles. In particular, the model involves evolution of PGE mineralization from a highly differentiated semi-metal rich melt.

From both an economic and paragenetic standpoint, a detailed account of the precious-metal minerals (Pd, Pt, Au and Ag), which extends beyond a qualitative assessment is critical for interpretation. In this work, the PGM are rigorously characterized and a mass-balance of the PGE, Au and Ag occurrences within the Ovoid is calculated. The findings are compared to occurrences within Discovery Hill zone and from a hornblende-gabbro dyke in the Southeast Extension zone (Huminicki et al., 2008). Localized contamination of semi-metals from crustal gneisses is considered as one possibility for any differences in the PGM assemblages observed between the three zones.

**Types of PGE Deposits and Mineralization**

The type of deposit which hosts PGE occurrences depends of the type of magma that produced the deposit and what processes took place to concentrate the PGE. The deposits that are mined specifically for PGE are associated with reef-type deposits in ultramafic to mafic layered intrusions (Bushveld

Complex, Great Dyke, Stillwater and Lac des Iles). In these deposits, PGE are enriched near or in chromitites (UG2, 5-7 ppm), at the base and sidewalls of the intrusions (Platreef, Bushveld Complex, up to 5ppm of PGE) or in the center of the intrusion (Merensky Reef, Bushveld, 5-7 ppm and J-M reef at Stillwater, Montana, up to 20 ppm of PGE) (summarized in Maier, 2005).

Deposits where PGE are mined as a by-product are normally associated with large magmatic Cu-Ni-sulfide deposits. These deposits are usually hosted by a mafic-ultramafic dyke system or komatiite and picrite lava channels. The sulfide magma is formed within traps of conduits where they are able to precipitate high Ni and Cu tenor, disseminated to massive sulfides. Low- to moderate-scale PGE mineralization can occur at these types of deposits and are recovered as a by-product during recovery of Ni and Cu (Sudbury Igneous Complex, Norils'k, Kabanga, Ungava deposits; Naldrett, 1999; Cabri, 1992). If economically significant amounts of PGE were discovered at Voisey's Bay, they would also be recovered as a by-product.

In order to make a general comparison of the relevance of PGE occurrences at Voisey's Bay to occurrences at other deposits, a brief summary of documented PGE mineralogy from selected PGE bearing deposits has been compiled in Table 1. The deposits are listed by country in order of estimated reserve capacity (USGS Open file report, Wilburn and Bleiwas, 2002; Maier, 2005).

Even though the majority of the world's PGE are mined from reef-type deposits, PGE by-production from Ni-Cu deposits is still considered an asset. Approximately 71% of the world's PGE reserves (primarily Pt) are contained in the Bushveld Complex, South Africa; however, the actual exported supply of Pt from South Africa has decreased from 78% in 2004 to 71% in 2013, while the global demand for PGE has increased steadily from 198 tonnes in 2004 to 262 tonnes in 2013 (based on data from Johnson Matthey, 2013b). The increasing demand for PGE compounded with a slow decrease in South Africa PGE exports signifies the importance of Ni-Cu-(PGE) deposits to the future PGE mining industry. Russia is the next

major contributor (13% PGE reserves), which is mostly mined from Noril'sk as a by-product of Ni and Cu.

A common mineralogical characteristic amongst the deposits listed in the table is the presence of PGE-arsenide, bismuthides and tellurides. The PGE sulfide phases tend to be less prominent, and appear to occur in larger quantities in the mafic-layered intrusion reef-type deposits (chromitite bearing).

**Table 1-1:** Compilation of Some PGE Producing Deposits

| Location* | Reserve Base* | %Reserves | Deposit Name | Setting Type | PGE Mineralogy | PGE Geochemistry |
|---|---|---|---|---|---|---|
| South Africa | 34000000 | 71.44 | Bushveld Complex (UG2, Merensky Reef, Platreef) | mafic layered intrusion | Pt, Pd, Ru sulfides and Pt-Fe alloys (western limb), PGE-arsenide-telluride phases (eastern limb) (Cabri, 1992) | Pd, Ru, Rh in solid solution in base-metal sulphides (Cabri, 1992; Osbahr et al., 2012) |
| Russia | 6100000 | 12.82 | Norilsk | Komatiite/basaltic lava flows | Pt-Fe alloy (isoferroplatinum) and cooperite (mainly disseminated sulfides); Pt-Pd sulfides, tellurides and bismuthotellurides (massive sulfide) (Genkin and Evstigneeva, 1986) | Pd in pentlandite (Cabri et al., 2002) |
| | | | Imandru/ Burakovsky | | Bismuthotellurides and arsenides; sperrylite, laurite, erlichmanite, hollingworthite, daomanite, cooperite; other unnamed Pt minerals (Barkov and Fleet, 2004) | Ru, Os, Ir in pyrite |
| Zimbabwe | 5300000 | 11.14 | Great Dyke | mafic layered intrusion | Bismuthotellurides, arsenides (moncheite, maslovite, michenerite, kotulskite, sperrylite); PGE sulfides/sulpharsenides (cooperite, laurite, braggite, hollingworthite) ( Oberthür et al 1997; Coghill and Wilson, 1986) | Pt in Pyrite |
| Canada | 910000 | 1.91 | Deposits of the Sudbury Igneous Complex | meteorite impact/Ni-Cu-(PGE) | Pt, Pd tellurides/bimuthotelluride/aresenides (froodite, sperrylite, michnerite/moncheite, sudburyite); Pt-Fe alloys; PGE sulfides/sulpharsenides (cooperite, laurite) (Cabri and Laflamme, 1976; Dare et al., (2011) | Pt, Pd in gerdorffite and cobaltite; Pd in pentlandite (Cabri and Laflamme, 1976) |
| | | | Raglan | ultramafic-komatiite/Ni-Cu-(PGE) | Arsenides, tellurides/bimuthotellurides (sperrylite, sudburyite, merkensyite, maucherite) (Seabrook et al., 2004) | Pd in pentlandite |
| | | | Lac des Iles | reef-type/ mafic layered intrusion | Pt-Pd sulfides (vysotskite) and Pt-Pd bismuthotellurides (kotulskite) (Watkinson and Dunning, 1979) | Pd in pentlandite (Cabri and Laflamme, 1979) |
| US | 900000 | 1.89 | Duluth Complex | Ultramafic/Ni-Cu-PGE | Bimuthotellurides, tellurides, arsenides | |
| | | | Stillwater | mafic layered intrusion | PGE sulfides; arsenides (sperrylite) Pt-Fe alloys (Talkington and Lipin, 2008) | Pd, Ru and Rh in pentlandite (Cabri et al., 1989) |
| Other | 380000 | 0.80 | Nuasahi, India | Chromiferous Ultramafic-mafic | Sudburyite, michenerite, palladian-bismuthian melonite, irarsite (Mondal and Baidya, 1997) | |
| | | | Kambalda, Australia | mafic-ultramafic/Ni-Cu-(PGE) | Arsenides (sperrylite, palladoarsenide); tellurides/bismuthotellurides (moncheite, merenskyite, stibiopalladinite, michenerite) (Hudson, 2008) | Pd in melonite (Hudson, 2008) |
| | | | Jinchuan, China | ultramafic/Ni-Cu-(PGE) | Bismuthotellurides/bismuthides (froodite, michenerite), arsenides (sperrylite), selenides (padmaite), Ir-sulfidearsenide (irarsite) (Prichard et al., 2005) | |
| | | | Rum Deposit, Scotland | ultramafic/Ni-Cu-(PGE) | Bimuthotellurides and arsenides; Pd-Cu alloys; Pt-Fe alloys, native-Pt, laurite, moncheite, sperrylite, isomeriete, cooperite, braggite; other less common arsenide and bismuthotellurides (Power et al., 2005) | |

*Data from Wilburn and Bleiwas (2002) and Maier (2005)
PGE reserves is the total reserves of combined Pt, Pd, Ir, Ru, Rh and Os

**Evolution of sulfide deposits and Voisey's Bay Deposit**

Since PGE differentiation is so strongly dependent on ore genesis, general aspects of magmatic sulfide deposit evolution that are important to the formation of Voisey's Bay are briefly reviewed in the following text.

To form any magmatic sulfide deposit, a parental magma must be derived through partial melting of a mantle component. The composition of the mantle derived magma is dependent on the degree of partial melting as the minerals that make up the mantle peridotites have different melting temperatures. A larger degree of partial melting will produce ultramafic melts (more abundant in Mg), whereas a lesser degree of melting will produce mafic melts. Since an increase of pressure increases the melting temperature of a mineral, the position of the melt within the mantle will also affect the composition of the melt. A magma formed higher in the mantle will have a different composition than magma with the same degree of partial melting in the lower mantle. The type of magma produced by partial melting will determine what trace elements are present in the melt. The partition coefficient (D) predicts how trace elements are partitioned between magma and residual solid. More detailed information pertaining to partition coefficient calculations can be found in such works summarized in McIntire (1963).

Maier and Barnes (1999) suggest that the majority of PGE in the mantle are hosted by sulfides and the sulfides would be one of the first phases to melt. At low degrees of melting, an abundant amount of sulfide would be present and could develop and segregate an immiscible sulfide liquid. The PGE will partition into the immiscible sulfide depleting the remaining melt of PGE. At this point, the melt will begin to ascend leaving behind the PGE rich sulfide melt. Thus, large degrees of partial melting (at least 25%) are necessary to form magma parental to PGE rich deposits.

As a melt ascends, it may react with other bodies of magma within the vicinity or interact with and assimilate crustal components. The parental magma will also begin to crystallize during ascent and may

fractionate residual melts during the process. These steps condition magma to become sulfur saturated. Although it is possible for magma to leave the mantle already saturated in sulfur, it is believed that most deposits have assimilated sulfur by interacting with crustal rocks (evidence for this can be found in the amount of crustal S measured in rocks of the deposit, e.g. Ripley et al., 2000). If the magma has acquired enough sulfur, an immiscible sulfide melt may segregate from the existing parental magma. Many Cu-Ni-sulfide deposits show strong evidence for crustal interaction which is reflected in their S-isotope signatures.

Another mechanism which can trigger sulfide saturation might be contamination of the magma with external silica during assimilation of the crustal components because silica may lower the solubility of sulfur within the magma (Irvine, 1975; Li and Naldrett, 1993). Evidence for this can be determined through oxygen isotope studies (e.g. Ripley et al., 2000). A third possibility that has been suggested to trigger sulfur saturation is the crystallization and fractionation of Fe-bearing silicates and oxides. Because $Fe^{2+}$ is bonded to S in magma form, the crystallization of Fe-rich minerals (olivine, pyroxene, magnetite) can increase the sulfur content and segregate an immiscible sulfide melt (Haughton, 1974).

After a sulfide melt has segregated from its parental melt, it must collect the necessary metals to form economic mineral deposits, such as Ni, Cu and PGE. Campbell and Naldrett (1979) showed that the concentration of PGE within the sulfide melt is a function of the initial PGE concentration in the parental melt ($C_o$), D and the mass ratio of sulfide to silicate magma (R) and is described by:

$$C_s = C_o * D(R+1)/(R+D)$$

Lightfoot et al. (2011) attributed the low level concentrations of PGE at Voisey's Bay to the timing of sulfur saturations. In that study, initial Ni, Cu, PGE and Au concentrations of samples from rocks that

formed Voisey's Bay and other mafic intrusions of the Nain Plutonic Suite were calculated and it was inferred that their parental magmas ascended as a PGE poor residual melt, and sulfur saturation of the ascended magma occurred in the crust, during interaction with the Tasiuyak gneisses.

**Fractionation of PGE within a Sulfide Melt**

Genetic models for PGE mineralization have been proposed for a number of deposits. These models are based on textural associations of the PGM and the proportion of PGE present in solid solution in sulfide phases. In the majority of deposits, a model encompasses either exsolution of PGM at low temperatures (Dare et al., 2011), direct crystallization of PGM from an immiscible semi-metal rich melt (Cabri and Laflamme, 1976), or concentration of PGE through hydrothermal fluids. A quantitative assessment of the PGE occurrences can help to better identify which mode of PGM crystallization has occurred.

It is well known that upon cooling the sulfide melt will begin to crystallize and will often fractionate a residual melt. The first phase to crystallize is the high-temperature Fe-Ni-S monosulfide phase (MSS) (pyrrhotite and sometimes pentlandite) at temperatures >1000°C (Ebel and Naldrett, 1996). At this point, an intermediate residual Cu-rich melt fractionates (ISS). At temperatures of 500-550°C (Kullerud and Yund, 1969), chalcopyrite will crystallize and at temperatures <300°C (e.g. Buerger, 1947; Cabri, 1973), the ISS will recrystallize and pyrrhotite will exsolve pentlandite. In some cases, it has been suggested that the PGE sulfide phases will exsolve from the base-metal sulfide phases during low temperature recrystallization.

In most deposits, it is observed that PGE partition between the MSS and ISS. By synthesizing equilibrated MSS and sulfide liquid with the addition of PGE at a range of temperatures (1040°C and below), it is found that Ir, Os, Ru and Rh are highly compatible with MSS and will remain in the MSS, and Pt, Pd and Au are very incompatible with MSS and will partition into the ISS (Distler et al, 1977;

Fleet et al., 1993; Barnes et al., 1997). Fleet et al. (1999) showed that the partition coefficients of Ir, Os and Rh in the MSS will decrease with decreasing S content producing a more alloy saturated system. Since most natural sulfide systems contain $O_2$, Mungall, et al. (2005) performed a similar experiment by synthesizing MSS and sulfide liquid plus a quartz-magnetite-fayalite (QMF) buffer system to fix $O_2$ conditions. The results indicated that the calculated D values were similar to previous experiments and are minimally affected by $fO_2$ and temperature. The general consensus is that, under a wide range of conditions, Ir, Os, Ru and Rh are highly compatible with MSS and will remain in MSS during sulfide magma differentiation, while Pt, Pd and Au are highly incompatible with MSS and will be partitioned out of the MSS. More recent studies where technological advancements have enabled very low levels of PGE to be detected in sulfide phases have shown that Pd and Pt are normally not found in Cu rich phases (ISS) (Holwell and McDonald, 2010). It is suggested that Pt and Pd are not only incompatible with MSS, but are also either incompatible with the Cu-rich ISS, (Peredogova, 2007; Helmy et al., 2007 and 2008), or subsequently leave or diffuse from ISS during some cooling paths (Dare et al., 2010).

Derivation of PGM from a differentiated semi-metal melt was first proposed by Cabri and Laflamme (1976) for samples taken from the Sudbury area because the majority of the PGE in that area were carried by tellurides, arsenides and bimuthides. Helmy et al. (2008 and 2013a/b) recognizes the importance of semi-metals such as Te, Sb and As to PGM formation in magmatic environments. In these studies, they performed experiments equilibrating MSS and sulfide liquid to determine partitioning behaviour of PGE with the addition of other semi-metals, Bi, Sb, As and Te. It was noted that PGE tend to complex with semi-metals over sulfur. In undersaturated liquids, PGE and semi-metals (Pt-As) may self-organize to form nano-associations at supersolidus temperatures. One conclusion drawn from this study is that PGE distribution may not be only controlled by their chemical compatibility within a particular phase, but is also controlled by the surface properties of the nano-sized clusters.

The Pd and Pt to semi-metal ratio in magma will strongly influence the distribution of Pt and Pd within a deposit because Pt and Pd easily complex to semi-metals, Bi, Te, Sb and As. If the Pd and Pt to semi-

metal ratio is low, the majority of Pd and Pt will accumulate discrete PGM rather than being concentrated in solid solution in sulfide phases. If this ratio is high, excess Pt and Pd will enter sulfide phases.

In many PGE deposits, PGE occur as discrete semi-metal bearing minerals, and less commonly (particularly Pt and Pd) as sulfide phases. When PGE sulphide phases do occur, it appears that Ir, Ru or Pt bearing sulfide phases are more common and are more frequent in chromitite rich deposits (Table 1).

Many deposits that host high grade PGE have been affected by overprinting of subsequent magmatic and/or metamorphic activity which may have upgraded the PGE content during remobilization from hydrothermal fluids. Examples include PGE mineralization in the Sudbury and Raglan ores. In these deposits, PGM are in many cases associated (near or in contact) with altered hydrous and Cl-bearing phases, and are found along footwall contacts and in chalcopyrite-rich veins (Farrow and Watkinson 1997; Seabrook et al., 2004).

**Geological Background**

Voisey's Bay deposit is a world class Ni-Cu-Co magmatic sulfide deposit. Naldrett (1997) indicates that Voisey's Bay is a unique magmatic sulfide deposit because of its setting. He has grouped sulfide deposits into four categories based on their associated magmatism: Category I represents sulfide deposits emplaced within Archean greenstone belts (komatiites and tholeiites which can sometimes be found associated with one another) (e.g. Munni Munni, Australia and Radio Hill intrusions); Category II deposits are emplaced within rifted continental environment (e.g. Jinchuan, China); Category III sulfide deposits intrude cratonic environments (e.g. Norils'k-Talnakh, Russia and Duluth complex, USA); Category IV are associated with orogenic belts. Voisey's Bay is considered category III. Normally these types of deposits are associated with flood basalt magmatism. Voisey's Bay is the only category III type deposit to be associated with anorthositic magmatism, and because of this, Naldrett (1997) stressed the importance of three key factors necessary for the development of Voisey's Bay. The three key factors

include the following: 1) the host magma must become sulfur saturated in order to segregate an immiscible sulfide liquid; 2) the sulfide must concentrate within restricted localities (within conduit width changes or entry point of feeder dyke are examples) so that the sulfide may 3) react with adjacent silicate magma to collect chalcophile elements (Cu and Ni). In this case, Naldrett (1997) references Voisey's Bay as being a "classic example" of the relevance of the three key factors necessary for the generation of Ni-Cu-sulfide deposits.

The 1.34 Ga troctolite intrusion that hosts the sulfide mineralization at Voisey's Bay is a member of the Nain Plutonic Suite. The intrusion is situated across a contact between the Nain and Churchill Province boundaries. On the west end, the intrusion intersects graphite-garnet-sillimanite bearing Tasiuyak gneiss, and intrudes enderbitic orthogneisses on the east end. The main sulfide components of Voisey's Bay are restricted to two troctolite chambers (an upper and a lower chamber) and to areas of a subvertical feeder dyke that connects the two chambers. Ryan (2000) describes the local geology of the Voisey's Bay intrusion and of other granitic and dioritic intrusions that comprise the Nain Plutonic Suite. The Voisey's Bay intrusion has been dated by Amelin (2000) and Lambert et al. (2000 and 2001).

The ore generation at Voisey's Bay deposit likely occurred as the result of a two stage magma event (Li and Naldrett, 1997; Naldrett 1999; Li and Naldrett, 2000). The first magma pulse (upper chamber) interacted with local Tasiuyak gneisses and upgraded the sulfur content of the system. Evidence for crustal contamination can be found in Li and Naldrett (2000), Ripley et al. (2000 and 2001) and Lambert et al. (2000 and 2001). While ultramafic to basaltic magma progressed along the feeder sheet, a second magma pulse rose up and interacted with cumulates of first generation magma and upgraded the system in Ni and Cu concentrations. A decreasing trend in Ni versus forsterite content among mafic-ultramafic cumulates indicates crystallization of olivine from the troctolite magmas, and an abrupt decline in this trend in areas proximal to the upper chamber is remnant evidence of the two separate magma pulses (Li and Naldrett, 2000).

Voisey's Bay deposit is divided into six ore-bearing regions (Figure 1). From west to east, the ore zones consist of Reid Brook, Discovery Hill, the Mini-Ovoid, Ovoid, Southeast Extension and Eastern Deeps. Reid Brook and Discovery Hill are contained within in the upper chamber, the Mini-Ovoid, Ovoid and Southeast Extension occupy areas of the feeder dyke, and the Eastern Deeps resides in the lower chamber. Evans-Lamswood et al. (2000) indicate that the ore bodies crystallized within geometric inflection points of the conduit system. The changes in conduit geometry allowed the sulfide magma to become trapped and accumulate as sulfide ore.

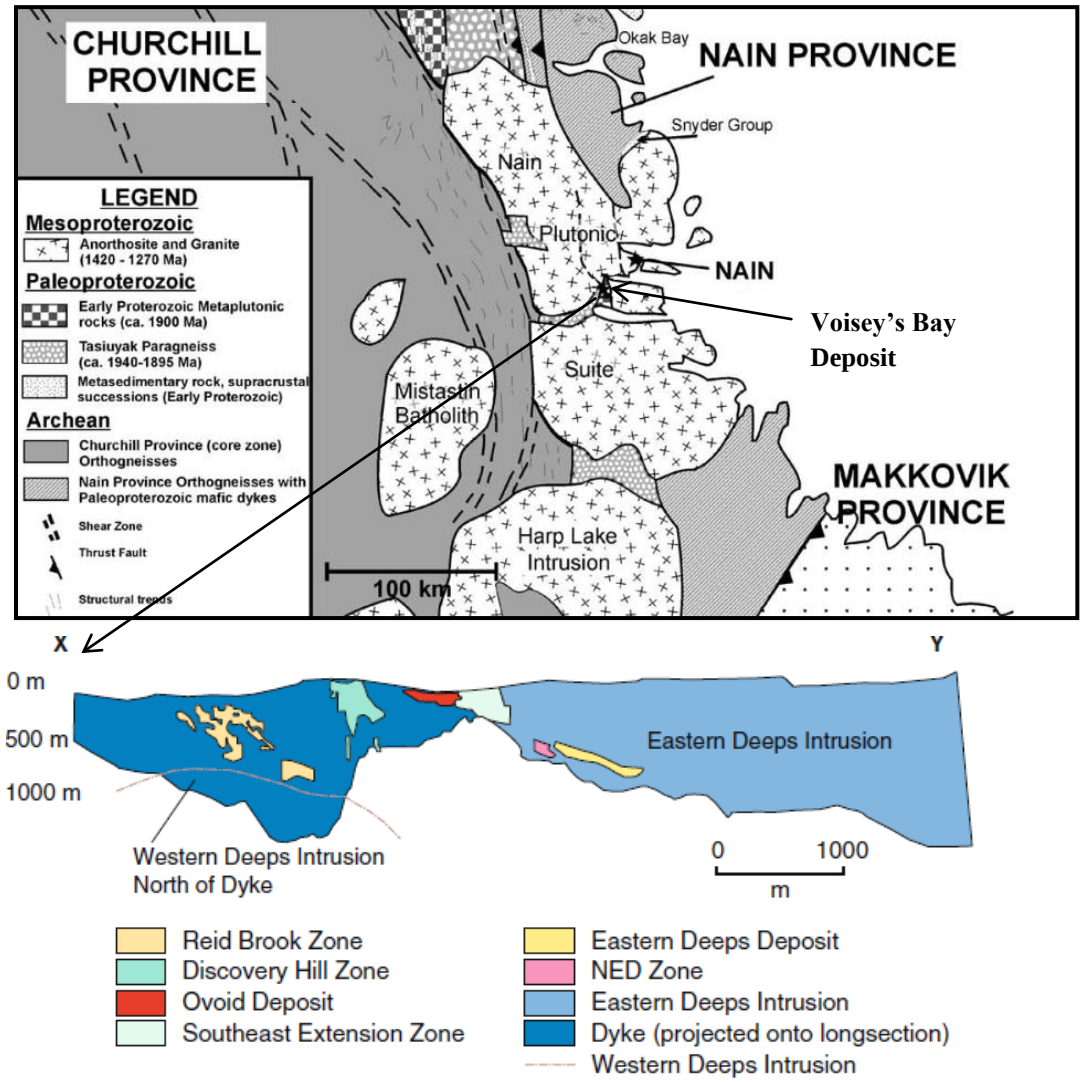


**Figure 1-1: General Geology of Voisey's Bay Area** (A.modified from Rawlings-Hinchey et al, 2003; B. modified from Lightfoot et al., 2011)

Documentation of PGE occurrences at Voisey's Bay deposit is included in Naldrett et al. (2000), Lightfoot et al. (2011) and Huminicki et al. (2008). Collectively, it is thought that Pd and Pt concentrations increase toward the centre of the Ovoid body as a result of fractional crystallization of the sulfide magma and an inward cooling. Huminicki et al. (2008) offers the only description of PGE mineralogy at Voisey's Bay for occurrences within a hornblende-gabbro dyke in the vicinity of the Southeast Extension zone. The major PGM documented include sperrylite, froodite ($PdBi_2$) and paolovite ($Pd_2Sn$). Other precious metal minerals present are native Ag, electrum, stutzite and hessite. Palladium was found in pentlandite and galena. The PGM and PMM are dominantly associated with the Cu rich mineral assemblages. Huminicki et al. (2008) provides evidence for magmatic origin for PGE that is related to a differentiated ISS and concludes that the PGE mineralization has not been affected by late magmatic-hydrothermal activity.

The interaction of the troctolite magma with the crustal gneisses may have an important connection to formation of the PGM at Voisey's Bay. It has been suggested that at other deposits such as Sudbury (Creighton mine, Dare et al., 2010 and 2011) and the deposits of the Bushveld complex (Hutchinson and McDonald, 2008), that sulfide magma inherited semi-metals through crustal contamination. Different contaminations in separate areas of a single deposit may give rise to variations in PGE mineral assemblages observed throughout the deposits. Becuase crustal interactions play such a significant role in the development of ore at Voisey's Bay, it is possible that some of the semi-metals that are associated with the PGE may have been inherited from the surrounding gneisses. Li and Naldrett (2000) also point out that variation in the degree of crustal interactions across the Voisey's Bay deposit is apparent based on the amount of partially digested gneissic fragments present at each zone. The possibility that any variation observed in PGM assemblages at Voisey's Bay is due to localized contaminations is also considered in this thesis.

**Applications to Extractive Metallurgy and Geometallurgy**

It is important to understand how PGE occur in order to determine if a possibility for PGE by-production at Voisey's Bay exists. Whether the PGE occur in solid solution or as discrete mineral phases will have an impact on how the ore is processed. Characteristics such as PGM grain-size, ease of liberation upon grinding, and association will further impact the recovery of the PGE. Where PGM have larger grain-sizes and are easily liberated during routine grinding, conventional gravitation or flotation methods can be used to directly recover the PGM. The PGM-rich concentrate can then be smelted and refined to extract the PGE metals. This is occasionally performed at deposits where PGE are principally mined and the PGM occur in high enough proportions to be recovered more easily (e.g. UG2 chromitite ore, Bushveld Complex; Xioa and Laplante, 2008; Jones, 2005).

In most deposits, however, PGE occur as very fine-grained discrete mineral inclusions that are very difficult to liberate by routine grinding, or they occur in solid solution in sulfide phases at trace levels. In these types of occurrences, understanding association is crucial for determining how the PGE will be recovered. At many base-metal sulfide deposits where PGE are recovered as a by-product, routine ore processing generates Ni and Cu concentrates which are smelted to a matte and then shipped to a refinery. The type of concentrate from which the PGE will be recovered to ultimately depends on the occurrence and association of the PGE. Once recovered to the Ni or Cu concentrates, the PGE may be extracted during the refining stage.

For the Voisey's Bay ore, three types of concentrates are produced and include a high grade Ni concentrate, a Ni middling concentrate that contains Ni and Cu, and a Cu concentrate. It is important to note that any Pb that is present in the form of galena will likely be recovered to Cu concentrate because some precious metals (such as Ag) are known to be associated with galena (Fleischer, 1955). Both galena and chalcopyrite are floatable under similar conditions (Bulatovic, 2007) and separation of the two minerals during ore processing could be difficult to achieve if galena has not been accounted for. By

combining a detailed assessment of the PGM occurrence with a quantitative mass balance of the PGE (and other precious metals) an estimated proportion of PGE that will be recovered to each concentrate can be calculated.

A detailed assessment of PGE and other precious metal occurrences within a deposit may also provide useful applications to geometallurgical exploration. Since most PMM that occur in base-metal sulfide deposits are fine-grained and are present in trace quantities (examples summarized in Howlell and McDonald, 2010 and Cabri, 1992), recovery at some deposits may be limited, particularly where the PGE and precious-metals (PM) are associated with pyrrhotite or silicate gangue. If any domains containing elevated levels of PGE at Voisey's Bay are able to be defined, the PGE entitlement of that domain could be calculated based on the proportion of PGE and other precious metals are amenable to routine recovery methods.

The thesis is divided into two manuscripts. The first manuscript presents the results of the PGE, Au and Ag characterization and mass-balance within the Ovoid deposit and describes general, first-order observations on the potential to recover Pt and Pd as a by-product from the Ovoid samples. The second manuscript builds on the results from the PM characterization and mass-balance to present a detailed genetic model for the PGE occurrences within the Ovoid, Southeast Extension and Discovery Hill zones (Figure 1).

## References


Amelin, Y., Li, C., Valeyev, O., Naldrett, A.J. (2000) Nd-Pb-Sr isotope systematics of crustal assimilation in the Voisey's Bay and Mushuau intrusions, Labrador, Canada. Economic Geology, v. 95, p. 815–830.

Amelin, Y., Li, C., Naldrett, A.J. (1999) Geochronology of the Voisey's Bay intrusion, Labrador, Canada by precise U-Pb dating of coexisting baddeleyite, zircon and apatite. Lithos v 47, p 33-51

Barkov, A.Y., Fleet, M.E., Nixon, G.T., Levson, V.M., (2004) Platinum-group minerals from five placer deposits in British Columbia, Canada. The Canadian Mineralogist 43:1687-1710

Barnes, S-J., Naldrett, A.J., Gorton, M.P. (1985) The origin of platinum-group elements in terrestrial magmas. Chemical Geology v 53, p 303-323

Bulatovic, S.M. (2007) Handbook of Flotation Reagents – Chemistry, Theory and Practice, Volume 2 – Flotation of Sulfide Ores: Elsevier

Cabri, L. (1973) New data on phase relations in the Cu-Fe-S system. Economic Geology. v 68 p. 443-454

Coghill, B.M., Wilson, A.H. (1993) Platinum-group minerals in the Selukwe Subchamber, Great Dyke, Zimbabwe: implications for PGE collection mechanisms and post-formational redistribution. Mineralogical Magazine 57:613-633

Cabri, L.J., Laflamme, J.H.G. (1976) The mineralogy of the platinum-group elements from some copper-nickel deposits of the Sudbury area, Ontario. Economic Geology v 71, p 1159-1195

Dare, A.S., Barnes, S-J., Prichard, H.M., Fisher, P.C. (2010) The timing and formation of platinum-group minerals from the Creighton Ni-Cu-Platinum-group element sulfide deposit, Sudbury, Canada: early crystallization of PGE-rich sulfarsenides. Economic Geology v 105, p 1071-1096

Dare, A.S., Barnes, S-J., Prichard, H.M., Fisher, P.C. (2014) Mineralogy and geochemistry of Cu-rich ores from the McCreedy East Ni-Cu-PGE deposit (Sudbury, Canada); implications for the behavior of platinum group and chalcophile elements at the end of crystallization of a sulfide liquid. Economic Geology v 109, p 343-366

Ebel, D.S., and Naldrett, A. J. (1996) Fractional Crystallization of Sulfide Ore Liquids at High Temperature. Economic Geology v 91 p. 607-621

Evans-Lamswood, D.M., Butt, D.P., Jackson, R.S., Lee, D.V., Muggridge, M.,G., Wheeler, R.I. and Wilton, D.H.C. (2000) Physical controls associated with the distribution of sulfides in the Voisey's Bay Ni-Cu-Co deposit, Labrador. Economic Geology v 95, p. 749-769

Farrow, C.E.G., Watkinson, D.H. (1999), An evaluation of the role of fluids in Ni-Cu-PGE-bearing, mafic ultramafic systems: Geological Association of Canada Short Course, v 13, p 31-98

Fleet, M.E., Stone, W.E. (1991) Partitioning of platinum-group elements in the Fe-Ni-S system and their fractionation in nature. Geochimica and Cosmochimica v 55, p 245-253

Fleischer, M. (1955) Minor elements in some sulfide minerals. Economic Geology 50$^{th}$ anniversary. V971-1024

Genkin, A.D., Evstigneeva, T.L. (2008) Association of platinum-group minerals of the Noril'sk copper-nickel sulfide ores. Economic Geology. 81:1208-1212

Hanley, J. (2005), The aqueous geochemistry of the platinum-group elements (PGE) in surficial, low T hydrothermal and high-T magmatic hydrothermal environments: Mineralogical Association of Canada Short Course v 35, p 35-56

Helmy, H.M., Ballhaus, C., Fronseca, R.O.C., Wirth, R., Nagel, T., Tredoux, M. (2013a) Noble metal and nanoclusters and nanoparticles precede mineral formation in magmatic sulfide melts. Nature Communications 4:2505

Helmy, H.M., Ballhaus, C., Fronseca, R.O.C. (2013b) Fractionation of platinum, palladium, nickel, and copper in sulfide-arsenide systems at magmatic temperature. Contrib Mineral Petrol v 166, p 1725-1737

Helmy, H.M., Ballhaus, C., Wohlgemuth-Ueberwasser, C., Fonseca, R.O.C., Laurenz, V. (2010) Partitioning of Se, As, Sb, Te and Bi between monosulfide solid solution and sulfide melt - application to magmatic sulfide deposits. Geochimica and Cosmochimica v 74, p 6174-6179

Helmy, H.M., Ballhaus, C., Berndt, J., Bockrath, C., Wohlgemuth-Ueberwasser, C. (2007) Formation of Pt, Pd and Ni tellurides: experiments in sulfide-telluride systems. Contributions to Mineralogy and Petrology v 153, p 577-591

Holwell, D.A., McDonald, I. (2010) A review of the behavior of platinum-group elements within natural magmatic sulfide ore systems. Platinum Metals Rev v 54, p 26-36

Huminicki, M.A.E., Sylvester, P.J., Lastra, R., Cabri, L.J., Evans-Lamswood, D., Wilton, D.H.C. (2008) First report of platinum-group minerals from a hornblende-gabbro dyke in the vicinity of the Southeast Extension Zone of the Voisey's Bay Ni-Cu-Co deposit, Labrador. Mineralogy and Petrology v 92, p 129-164

Huminicki, M.A.E., Sylvester P J, Shaffer M, Wilton D H C, Evans-Lamswood D, Wheeler R I (2012) Systematic and Integrative Ore Characterization of Massive Sulfide Deposits: An Example from Voisey's Bay Ni-Cu-Co Ovoid Orebody. Exploration and Mining Geology v 20, p 53-86

Huminicki, M.A.E., Sylvester, P.J., Cabri, L.J., Lesher, C.M., and Tubrett, M. (2005) Quantitative mass balance of platinum-group elements in the Kelly Lake Ni-Cu-PGE deposit, Copper Cliff offset, Sudbury. Economic Geology, v. 100, p. 1631–1646.

Huminicki, M.A.E (2007) A comprehensive geological, petrological, and geochemical evaluation of the Voisey's Bay Ni-Cu-Co sulfide deposit: an integration of empirical data and process mechanics, PhD Thesis, Memorial University of Newfoundland

Hutchinson, D., McDonald, I. (2008) Laser ablation ICP-MS study of platinum-group elements in sulfides from the Platreef at Turfspruit, northern limb of the Bushveld Complex, South Africa: Mineralium Deposita v 43, p. 695–711.

Johnson Matthey Precious Metals Managment (2013a). Platinum Today - History of PGM. www.platinum.matthey.com

Johnson Matthey Precious Metals Managment (2013b). Platinum Today - PGM Market Reports and and Market Data Tables. www.platinum.matthey.com

Kullerud, G., Yund, R.A. and Moh, G.H. (1969) Phase relations in the Cu-Fe-S *in Wilson, H.D.B., ed., Magmatic ore deposits, a symposium: Economic Geology*. v 4 p. 323-343

Lambert, D.D., Frick, L.R., Foster, J.G., Li, C., Naldrett, A.J. (2000) Re-Os isotope systematics of the Voisey's Bay Ni-Cu-Co magmatic sulfide system, Labrador, Canada: II. Implications for parental magma chemistry, ore genesis, and metal redistribution. Economic Geology v 95, p 867-888

Lambert, D.D., Foster, J.G., Frick, L.R., Li, C., Naldrett, A.J. (1999) Re-Os isotopic systematics of the Voisey's Bay Ni-Cu-Co magmatic ore system, Labrador, Canada. Lithos v 47, p 69-88

Li, C., Naldrett, A. J. (2000) Melting Reactions of Gneissic Inclusions with Enclosing Magma at Voisey's Bay, Labrador, Canada: Implications with Respect to Ore Genesis. Economic Geology v 95, p. 801-814

Li, C., Lightfoot, P.C., Amelin, Y., Naldrett, A.J. (2000) Contrasting petrological and geochemical relationships in the Voisey's Bay and Mushuau Intrusions, Labrador, Canada: Implications for ore genesis. Economic Geology v 95, p 771-799

Lightfoot, P.C., Keays, R.R., Evans-Lamswood, D., Wheeler, R. (2011) S Saturation History or Nain Plutonic Suite mafic intrusions: origin of the Voisey's Bay Ni-Cu-Co sulfide deposit, Labrador, Canada. Miner Deposita v 47 p23-50

Lorand, J.P., 1989. Abundance and distribution of Cu-Fe-Ni sulfides, sulphur, copper and platinum-group elements in orogenic-type spinel lherzolite massifs of Ariege (northeastern Pyrenees, France). Earth Planet. Sci. Lett. 93:50-64

Maier, W.D. (2005) Platinum-groupe element deposits and occurrences: Mineralization styles, genetic concepts and exploration criteria. Journal of African Earth Sciences. V 41-3 p 165-191

Maier., W.D., Barnes, S-J., 1999. Platinum-Group Elements in Silicate Rocks of the Lower, Critical and Main Zones at Union Section, Western Bushveld Complex. Journal of Petrology 11:1647-1671

Mc Donald, D. and Hunt, L. A history of platinum and its allied metals. Johnson Matthey. Eurpoa Publications Ltd. London, England (1982)

McIntire, W.L. (1963) Trace element partition coefficients- a review of theory and applications to geology. Geochimica et Cosmochimica Acta V 27 p 1209-1264

Mondal, S.K., Baiyda, T.K., Rao, G.K., Glascock, M.D. (2001) PGE and Ag mineralization in a breccia zone of the Precambrian Nuasahi Ultramafic-Mafic Complex, Orissa, India. The Canadian Mineralogist, 39: 979-996

Naldrett, A.J. (2010) From the mantle to the bank: the life of a Ni-Cu-(PGE) sulfide deposit. South African Journal of Geology v 113, p 1-32

Naldrett, A.J., Singh, J., Kristic, S., Li, C. (2000a) The mineralogy of the Voisey's Bay Ni-Cu-Co deposit, Northern Labrador, Canada: Influence of oxidation state on textures and mineral compositions. Economic Geology v 95, p 889-900

Naldrett, A.J., Asif, M., Krstic, S., Li, C. (2000b) The composition of mineralization at the Voisey's Bay Ni-Cu sulfide deposit, with special reference to platinum-group elements: Economic Geology v 95, p 845-865

Naldrett, A.J. (1999) World-class Ni-Cu-PGE deposits: key factors in their genesis. Mineralium Deposita. 34: 227-240

Osbahr, I., Klemd, R., Oberthür, T., Brätz, H., Schouwstra, R. (2012) Platinum-group element distribution in base-metal sulfides of the Merensky Reef from the eastern and western Bushveld Complex, South Africa. Mineralium Deposita. v 48 p 211-238

Peregoedova, A.V. (1998) The experimental study of Pt-Pd-partitioning between monosulfide solid solution and Cu-Ni sulfide melt at 900-840ºC. In 8th International Platinum Symposium abstracts. Geol Soc South Africa and South African Inst Min Metal, Symposium Series, S18, p 325-373

Rawlings-Hinchey, A.M., Sylvester, P.J., Myers, J.S., Dunning, G.R. and Kosler, J. (2003). Paleoproterozoic crustal genesis: calc-alkaline magmatism of the Torngat orogen, Voisey's Bay area, Labrador. Precambrian Research v 125, p 55-85.

Ripley, E.M., Park, Y-R. (2000) Oxygen isotope studies of the Voisey's Bay Ni-Cu-Co deposit, Labrador, Canada. Economic Geology v 95 p 831-844

Ripley, E.M., Park, Y-R., Li, C., Naldrett, A.J. (1999) Sulfur and oxygen isotopic evidence of country rock contamination in the Voisey's Bay Ni-Cu-Co deposit, Labrador, Canada. Lithos v 47, p 53-68

Ryan, B. (2000) The Nain-Churchill boundary and the Nain Plutonic Suite: A regional perspective on the geological setting of the Voisey's Bay Ni-Cu-Co deposit. Economic Geology v 95, p 703-724

Seabrook, C.L., Prichard, H.M., Fisher, P.C. (2004) Platinum-group minerals in the Raglan Ni-Cu-(PGE) Sulfide Deposit, Cape Smith, Quebec, Canada. The Canadian Mineralogist 42:485-497

Talkington, R.W., Lipin, B.R. (1986) Platinum-group minerals in chromite seams of the Stillwater Complex, Montana. Economic Geology. 81:1179-1186

Tredoux, M., Lindsay, M. N., Davies, G., McDonald, I. (1995) The fractionation of platinum-group elements in magmatic systems, with the suggestion of a novel causal mechanism. S. Afr. J. Geol. v 98, p 157-167

Watkins, D.H., Dunning., G. (1979) Geology and Platinum-group mineralization, Lac-Des-Ils Complex, Northwestern Ontario. The Canadian Mineralogist 17:453-462

Wilburn, D.R., Blewais, D.I., 2005. Platinum-Group Metals – World Supply and Demand. United States Geological Survey (USGS), Open File Report http://pubs.usgs.gov/of/2004/1224/2004-1224.pdf

Wilson S. A., Ridley W. I., Koenig A. E. (2002) Development of sulfide calibration standards for the laser ablation inductively-coupled plasma mass spectrometry technique. Journal of Analytical Atomic Spectrometry, 17, 406-409.

# CHAPTER 2: MINERALOGY OF RARE OCCURRENCES OF PRECIOUS METAL ENRICHED MASSIVE SULFIDE IN THE VOISEY'S BAY Ni-Cu-Co OVOID DEPOSIT, LABRADOR

Chapter 2 of this thesis has been published in a special issue of the Canadian Mineralogist on Platinum-Group Element Mineralogy (*Kelvin, M.A., Sylvester, P.J., Cabri, L.J. (2011) Mineralogy of rare occurrences of precious-metal-enriched massive sufide in the Voisey's Bay Ni–Cu–Co Ovoid deposit, Labrador, Canada. Canadian Mineralogist v 49, p 1505-1522*.)

**Abstract**

The Voisey's Bay Ovoid Ni-Cu-Co magmatic sulfide deposit, Labrador, is generally poor in precious metals (Pt, Pd, Ag, Au) but unusual occurrences with elevated levels (Pt+Pd >0.5 ppm) are present. We present a detailed and quantitative description of the precious metal mineralogy of four such occurrences within massive sulfides. The four samples, all from near the center of the Ovoid, were examined by SEM-based Mineral Liberation Analysis for characterization of precious metal minerals. Distributions of precious metals among the major sulfide minerals were estimated using mass-balance calculations based on bulk assays of the samples and the proportions and compositions of the minerals. A quantitative model for the distribution of precious metals will have useful applications for ore processing should domains with economic abundances of precious metals be identified in the Ovoid or the other underground deposits at Voisey's Bay in the future.

The results indicate that the majority of precious metals are present as discrete mineral phases including sperrylite, froodite, michenerite, Au-Ag alloy, völynskite, stützite and acanthite, whereas minor to moderate amounts of Pt, Pd, Ag and Au are found in solid solution in the

sulfide phases, pyrrhotite, pentlandite, chalcopyrite and galena. The precious metal minerals are normally associated with pentlandite, galena, chalcopyrite, pyrrhotite and magnetite, and rarely with breithauptite (NiSb), altaite (PbTe), other precious-metal minerals and native bismuth. With the exception of sperrylite, which is coarse grained and liberated easily by electric pulse disaggregation, the precious metal minerals are most commonly found as fine inclusions in pentlandite and galena, and less so as larger attachments. The associations are consistent with previously reported precious-metal mineral data from a hornblende-gabbro dyke of the Southeast Extension Zone at Voisey's Bay, demonstrating similar modes of crystallization, which are likely related to crystallization of a highly differentiated sulfide magma in both areas.

Processing of Pt from sperrylite and perhaps Pd from froodite could be achieved in ores with a mineralogy similar to the samples described here by grinding, and gravity or flotation methods but the Au-Ag alloy, völynskite and stützite would likely be too fine to recover as discrete grains for Ag and Au concentration. Instead, the Ag and Au could be recovered as a by-product of Ni-Cu-Co processing of the pentlandite and chalcopyrite, which are the major hosts of the Ag and Au minerals.

## Introduction

The Voisey's Bay Ovoid magmatic sulfide deposit, located in northern Labrador, Canada, is currently being mined in an open pit by Vale. The Ovoid is one of several deposits at Voisey's Bay; the original deposit before mining commenced contained 31,910,000 tonnes of proven ore with grades of 2.79 wt% Ni, 1.65 wt% Cu and 0.140 wt% Co (Bacon & Cochrane 2003). The Voisey's Bay ore contains lower concentrations of platinum-group elements (PGE) compared to other major Ni-Cu sulfide deposits; on average, concentrations of Pt + Pd in massive sulfides at Voisey's Bay are <0.5 ppm (Naldrett et al. 2000a). However, elevated concentrations of Pt+Pd (> 0.5 ppm) occur rarely within areas of the deposit. Preliminary assays show that anomalously elevated concentrations of Pb (~500-1500 ppm) are associated with some of the Pt+Pd enrichments.

### *Background Information*

Much of the reported scientific research on Voisey's Bay mineralization has been concerned with the physical and chemical processes that concentrated Ni, Cu and Co in the sulfides, and the unusual relationship of the ores with troctolitic host-rocks (Li & Naldrett 1999, Evans-Lamswood et al. 2000). With the exception of the study of Huminicki et al. (2008), there is little information on the precious metal mineralogy (platinum-group minerals (PGM), Au and Ag mineralogy) at Voisey's Bay. Thus the origin of occurrences of precious metal enrichments in these ores is not clear, and strategies for the recovery of these metals as a by-product of Ni-Cu-Co recovery at Voisey's Bay would be difficult to establish if further exploration leads to recognition of domains containing economic levels of precious metals in the Ovoid or other known underground deposits that are not yet mined.

Our goal in this study to present a quantitative mineralogical description of four massive sulfide samples from the core of the Ovoid body, selected on the basis of having unusually elevated levels of precious metals. Scanning electron microscope (SEM)-based mineral liberation analysis (MLA) is used to determine the mineralogy of the ores, and the modal abundances, grain sizes, associations and liberation characteristics of the minerals. The major and minor element concentrations of the sulfide and precious-metal minerals are determined by electron-microprobe analysis. Trace-element concentrations of precious metals present in solid solution in the sulfide phases are determined by laser ablation-inductively coupled plasma-mass spectrometry (LA-ICP-MS) (Sylvester 2001, Cabri et al. 2003). These data are used to determine how the precious-metals are apportioned among the mineral phases present in the ores based on quantitative mass-balance calculations. The results are compared to those reported by Huminicki et al. (2008) for a precious metal occurrence in a hornblende gabbro dyke in the Southeast Extension Zone of the Voisey's Bay deposit. Finally, we relate the characteristics of the precious metal occurrences to recovery techniques that might have useful implications to processing ore with mineralization styles similar to the occurrences described here.

Recent advances in mineral processing have increased a need for accurate documentation of the distribution and occurrence of base and precious metals among ore and gangue minerals in order to determine the most suitable method of recovery. In particular, the recovery method chosen will depend on whether the precious metals occur in solid solution with base-metal sulfides or as discrete precious-metal minerals (PMM) including PGM. It is also important to document how intimately the PMM are intergrown with the major minerals, i.e., whether they are liberated, included or attached onto particles of processed ore (Cabri 2010).

*Geological Context*

At Voisey's Bay, mineralization is magmatic in origin (Li & Naldrett 1999, Evans-Lamswood et al. 2000). The deposit evolved as part of the Nain Plutonic Suite, which is composed of a number of granitic, dioritic, anorthositic and troctolitic bodies that intruded Archean and Paleoproterozoic gneisses and paragneisses (Ryan 2000) (Fig. 1). The main Ni-Cu-Co mineralization is hosted by ca. 1.33 Ga troctolite-gabbro feeder dykes that may have connected two troctolite magma chambers, the Reid Brook chamber at depth and the Eastern Deeps chamber at a higher level in the crust. The chambers and conduit dyke system are known collectively as the Voisey's Bay Intrusion. The eastern half of the feeder troctolite intruded Enderbitic orthogneiss, whereas the western portion entered the Tasiuyak paragneiss (Rawlings-Hinchey et al. 2003). A detailed description of the geology and mineralogy of Voisey's Bay area and the mineralized regions can be found in Li & Naldrett (1999), Evans-Lamswood et al. (2000), Ryan (2000) and Naldrett (2004).

The deposit is divided into five distinct ore-bearing zones: from west to east, the Reid Brook Zone, Discovery Hill Zone, Mini-Ovoid and Ovoid, Southeast Extension Zone and Eastern Deeps Zone. The Ovoid, the zone of particular interest in this study, is a bowl-shaped body containing massive sulfide mineralization up to 110 m that is situated above brecciated, fragment-poor conduit troctolite-gabbro containing 10-50% sulfide (Evans-Lamswood et al. 2000, Naldrett & Li 2000). To the west, the Ovoid body extends to form a smaller massive sulfide bulge (Mini-Ovoid), which also overlies fragment-poor conduit troctolite-gabbro.

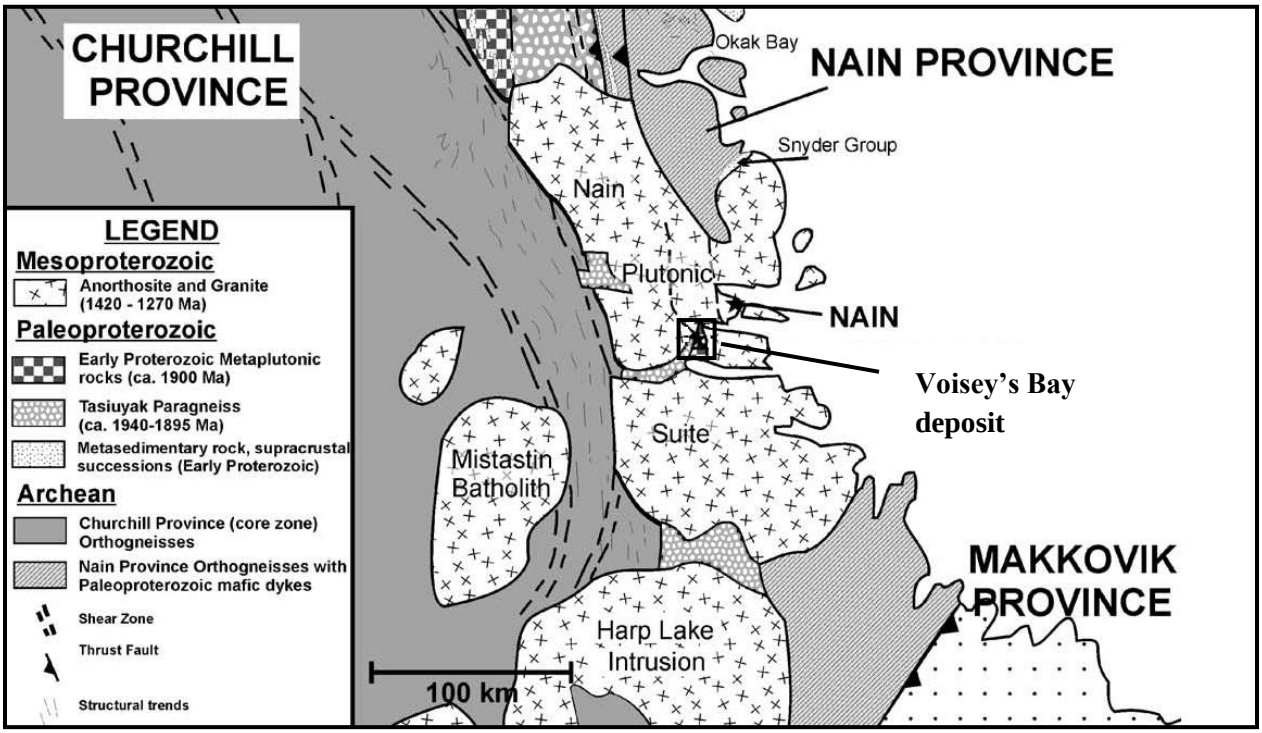


**Figure 2-1: General geology of Voisey's Bay area** showing the location of Voisey's Bay deposit within the Nain Plutonic Suite (modified from Rawlings-Hinchey *et al.* 2003)

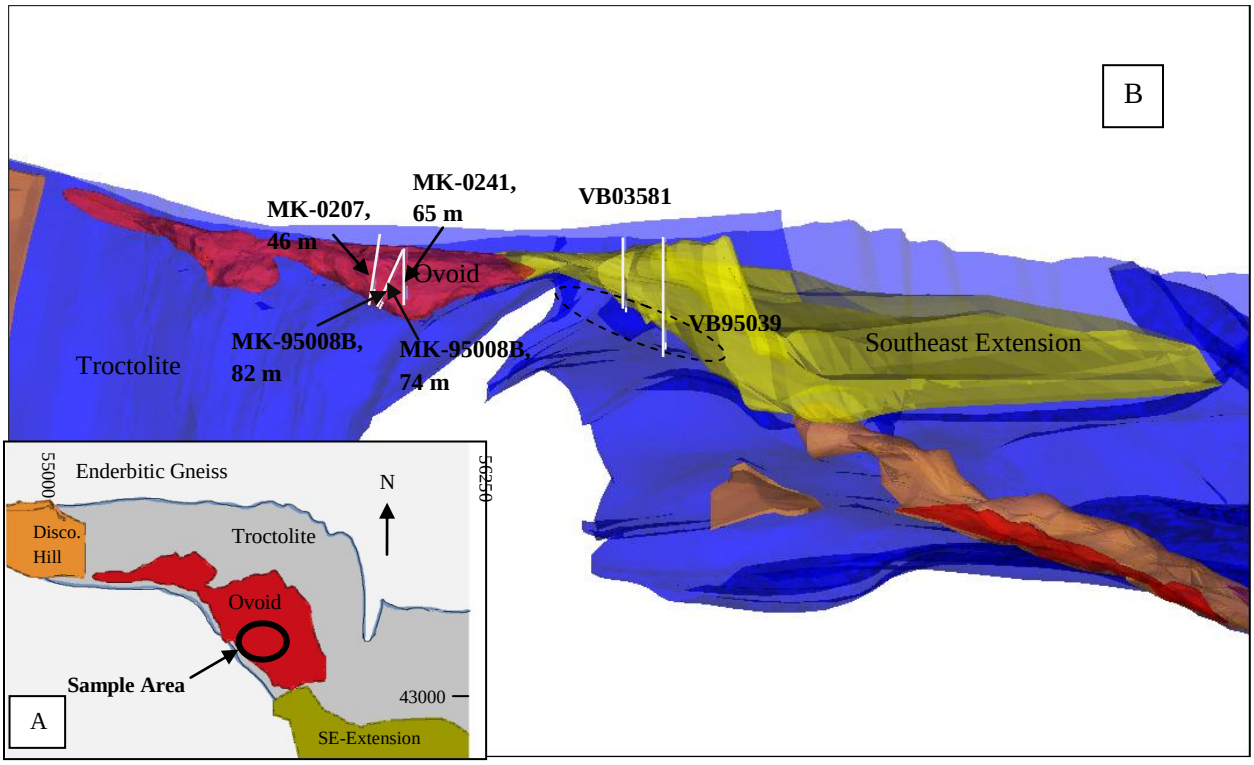


**Figure 2-2A-B**: A. Plan view map of Ovoid area. B. Projected view facing northeast showing relative location of samples and respective drill holes. The VB03581 and VB95039 drill holes intersect a hornblende-gabbro dyke of the SE Extension Zone. This location is the site of a previous PGM study conducted by Huminicki et al. (2008). The dashed circle represents the general vicinity of the hornblende-gabbro dyke.

*Mineralogy*

The portions of the Voisey's Bay magmatic system that are of ore grade consist of three main textural types: massive sulfide (>85% sulfide by volume), semi-massive sulfide (25-85% sulfide by volume) and disseminated sulfide (<25% sulfide by volume). In general, the sulfide minerals are composed of varying amounts of pyrrhotite ($Fe_{1-x}S$), chalcopyrite ($CuFeS_2$) and pentlandite [$(Fe,Ni)_9S_8$] with trace amounts of other phases. In the massive sulfide of the Ovoid, coarse hexagonal pyrrhotite exhibiting troilite lamellae forms the groundmass for interstitial chalcopyrite and large grains (1-2 cm) of pentlandite. Variable amounts of exsolved cubanite ($CuFe_2S_3$) are present in chalcopyrite. Magnetite is present as crystal aggregates at 1-5% by volume in the massive sulfide (Naldrett & Li 2000b). Huminicki (2007) defined a

variety of petrographic textures in the massive sulfide ores, distinguished by intergrowths of pentlandite-chalcopyrite in “loops”; variations in grain size and degree of alignment of magnetite; development of pseudohexagonal fracture in pyrrhotite; and the nature of exsolution in chalcopyrite and pyrrhotite. Normally, the massive sulfide of the Ovoid region does not contain galena; however, in some areas, including those studied here, anomalous occurrences of galena are present at the trace level (up to 0.25% by volume). The distribution and occurrences of anomalous galena and precious metals within the Ovoid are not well understood, but the unpublished data by Vale indicate a possible positive correlation between elevated Pt+Pd and elevated Pb. Massive sulfide samples containing these anomalous occurrences are the focus of this study.

Currently, the only documented occurrence of discrete PGM from the Voisey’s Bay area is that reported by Huminicki et al. (2008). The region studied by Huminicki et al. (2008) is situated directly east and down dip of the Ovoid (Fig. 2). The PGE-mineralized sulfide occurs in a hornblende gabbro dyke that intrudes troctolite and enderbite of the Southeast Extension Zone, just below an interval of massive sulfide. The dyke contains minor amounts of disseminated sulfide (<5%). The dominant PGM are sperrylite ($PtAs_2$), paolovite ($Pd_2Sn$), Sn-bearing stibiopalladinite [$Pd_{5-x}(Sb,Sn)_{2-x}$], michenerite (PdBiTe), froodite ($PdBi_2$) and maslovite (PtBiTe), with lesser amounts of PGE-Sn-Sb alloys. Following conventional crushing and sieving to particle sizes < 300 µm, the majority of these minerals were either completely liberated (28%) or associated with chalcopyrite ($CuFeS_2$), galena (PbS), bornite ($Cu_5FeS_4$) (56%) and other Ag-bearing phases (13%). The remainder were associated with silicate minerals (3%).

## Methodology

*Sample descriptions*

Four samples of massive sulfide from the core of the Ovoid were selected for this study on the basis of whole rock assays with elevated levels of Pt+Pd (and Pb) compared to typical massive sulfide assemblages or the presence of galena in dissected core. The samples were taken from the three drill holes located in Figure 2. All four samples contain galena, as well as mineral assemblage of pyrrhotite (± troilite), pentlandite, chalcopyrite (± cubanite), and magnetite typical of the Ovoid.

All four samples have textures similar to those shown in Figure 3. Pentlandite and chalcopyrite form a patch-like texture (1-5 cm) as opposed to strings or loops, which are a common texture (Evans-Lamswood *et al*. 2000, Huminicki 2007) seen in typical massive sulfides in the Ovoid. Some of the grains exhibit exsolved cubanite in chalcopyrite and exsolved troilite in pyrrhotite. The magnetite in the samples studied here is normally present as large, unaligned chains of crystals. This differs from the magnetite textures commonly seen elsewhere in the Ovoid, which have more of a finer-grained, speckled appearance, or form chains with a preferred alignment (Huminicki 2007). Galena, occasionally seen optically, is present in amounts of $\leq 0.25\%$ by volume where magnetite is most abundant. The galena occurs between crystals of the aggregated magnetite, or peripheral to chalcopyrite.

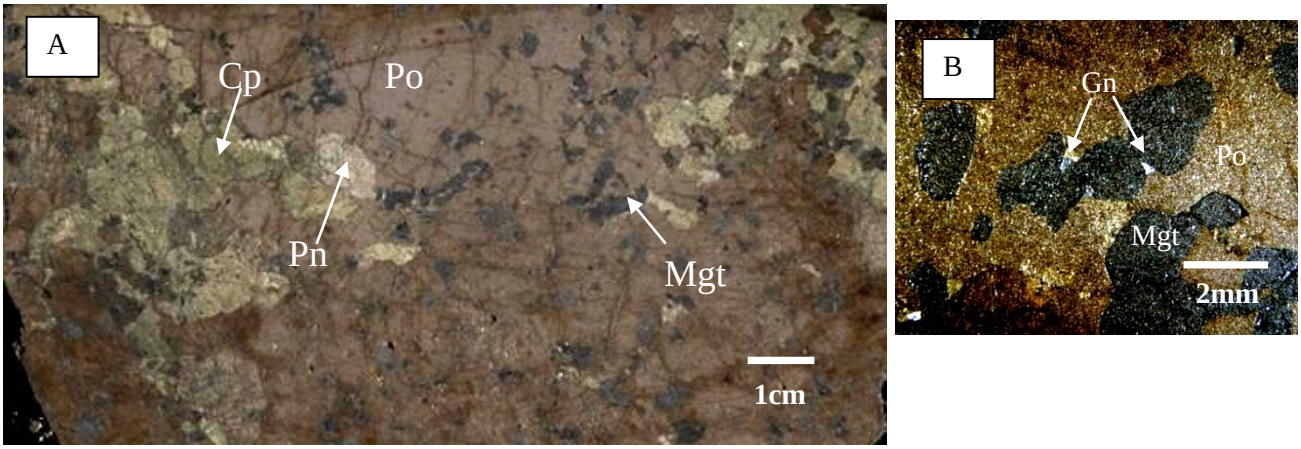


**Figure 2-3A-B: Photomicrographs of Ovoid Samples** A) Optical photograph of split massive sulfide core sample showing the textures of the sulfides. B) Magnified by 20x (Pn= pentlandite, Gn= galena, Mgt= magnetite, Po= pyrrhotite, Cp=chalcopyrite)

*Sample preparation*

Each of the four samples represents a 1 m interval of transversely split drill core, broken into <10 cm size pieces. In order to obtain an accurate representation of PMM associations and modes of occurrence, electric pulse disaggregation (EPD) was performed to liberate minerals instead of using conventional crushing. EPD uses explosive forces to liberate grains along preferential zones of weakness (see Rudashevsky *et al.* 1995 for the earliest relevant paper and Lastra *et al.* 2003 for the earliest potential application to mineral processing). EPD preserves the original sizes and shapes of trace mineral grains compared to crushing, which may potentially damage and break apart a single grain into several pieces, producing biases with respect to the original representation of grain sizes (Cabri *et al.* 2008). The EPD processing was performed at Overburden Drilling Management (ODM) Ltd, Ottawa, Ontario, using CNT Mineral Consulting Inc.'s Spark-2 EPD (see http://www.cnt-mc.com/).

*Analytical methods*

The EPD residues were sieved to grain size fractions of -175+125, -125+75 and -75 µm. Hydroseparation (HS) using the CNT HS-11 was performed on the sieved products to isolate the heavier minerals from the lighter material. Representative subsamples (0.1-1 g) of the HS concentrates were collected using a micro-riffler and were mounted as mono-layers in epoxy, polished, and examined by SEM-based Mineral Liberation Analysis at the Inco Innovation Centre (IIC) of Memorial University. The Mineral Liberation Analysis searches for, and quantifies the areal distribution of the minerals of interest exposed in the mount using back-scattered electron (BSE) imaging. The BSE grayscale of a mineral reflects the mean atomic number, and provides mineral identification when combined with energy-dispersive X-ray (EDX) analysis for elemental detection in the phase. This method is particularly useful for our study because of the high-resolution capabilities of the SEM, allowing automated searches for the PMM, which typically have fine grain-sizes but bright grayscales (Fandrich *et al.* 2006). This routine was performed on the four samples for each size fraction to search for the rare PMM. Once detected, the PMM occurrences were documented, and their area was mapped and calculated using the MLA software. The major sulfide-magnetite mineralogy of each sample was characterized by the MLA in the mounted EPD residues that were not processed by the HS.

Electron probe-microanalysis (EPMA) was performed on the PMM detected to confirm their mineral identities on the basis of major element concentrations. EPMA analysis was carried out at the University of Toronto, Department of Geology using a Cameca SX-50. Analysis by LA-ICP-MS to determine concentrations of trace PGE dissolved as solid solution in pyrrhotite, pentlandite, chalcopyrite and galena was performed at the IIC of Memorial University. The instrument used was a Finnigan ELEMENT XR mass spectrometer equipped with GEOLAS 193 nm excimer laser-ablation system. The measurement procedure employed follows that outlined by Sylvester (2001). Three synthetic pyrrhotite calibration standards (Po41, Po689, Po727; Sylvester *et al.* 2005) were ablated before and after each spot test for all

four mineral phases. Since the Ovoid samples contain significantly high amounts of Cu and Ni and minor amounts of Zn, it was necessary to apply the interference corrections described in Sylvester (2001). The possible isotopic interferences that were corrected for in these samples include $^{40}Ar^{65}Cu$ on $^{105}Pd$, $^{40}Ar^{66}Zn$ on $^{106}Pd$ and $^{40}Ar^{68}Zn$ on $^{108}Pd$; $^{40}ArNi^{61}$ on $^{101}Ru$, and $^{40}Ar^{62}Ni$ on $^{102}Ru$ and $^{102}Pd$. Measurements requiring corrections greater than 50% were not included in the data-set. The concentrations of Rh in galena and chalcopyrite could not be determined because of the large interferences (>95%) of $^{206}Pb^{2+}$ and $^{40}Ar^{63}Cu$, respectively, on $^{103}Rh$ (100% isotopic abundance).

Whole-rock abundances of Fe, Cu, Ni, Co, Pb and Zn were determined by digesting a portion (0.5 g) of each sample into solution using nitric and bromic acids followed by analyses by inductively coupled plasma-optical emission spectrometry (ICP-OES). Acid solution preparations and ICP-OES analysis were performed at the IIC of Memorial University. Whole-rock PGE and Au concentrations were determined by Ni fire assay with an ICP-MS finish at Activation Laboratories Ltd, Ancaster, Ontario. Concentrations of Ag in the samples were established by a total digestion ICP-MS method using hydrochloric, nitric and perchloric acids at Activation Laboratories Ltd.

*Mass-balance calculations*

Mass balance calculations are required to establish the distribution of PGE and other precious metals within ore samples. For this study, we used an approach similar to that taken by Huminicki *et al.* (2005). The concentration of the precious metals, Pt, Pd, Ag and Au, in each sample that is contributed by discrete PMM must be determined by subtracting the total measured Pt, Pd, Ag and Au in solid solution from the concentrations of the same precious metals measured in the whole rocks (equation 1). This method provides the most reliable representation of the distribution of Pt, Pd, Ag and Au concentrations because obtaining accurate absolute abundances of rare PMM phases within a sample is difficult to achieve (Cabri *et al.* 2003). Equation 2 demonstrates the calculation performed to give the total amount of

Pt, Pd, Ag and Au in solid solution. The mass fraction of mineral abundances of the major sulfide phases are measured by Mineral Liberation Analysis.

$$C_{PMM(total)} = C_{WR} - C_{SS} \quad (1)$$

$$C_{SS} = C_{Cpy}*f_{Cpy} + C_{Po}*f_{Po} + C_{Pn}*f_{Pn} + C_{Gn}*f_{Gn} = \Sigma (C_{min}*f_{min}) \quad (2)$$

where

$C_{PMM(total)}$ = Concentration of each of Pt, Pd, Ag and Au contributed by *total* discrete PMM

$C_{WR}$ = Total whole rock concentration of each of Pt, Pd, Ag and Au

$C_{SS}$ = Total concentration of each of Pt, Pd, Ag and Au in solid solution in major mineral phases

$C_{min}$ = Measured concentration of each of Pt, Pd, Ag and Au in major mineral phases (Cpy=chalcopyrite, Po=pyrrhotite, Pn=pentlandite, Gn=galena)

$f_{min}$ = Mass fraction of major mineral phases determined by MLA (mass fraction)

For the mass balance of the Ovoid samples, we take this calculation a step further by combining information from the detailed PMM data (detected by MLA) and the concentrations of Pt, Pd, Ag and Au in the PMM (determined by EPMA and LA-ICPMS) to determine the relative contribution of each precious metal from each PMM phase. Thus, the total precious metal mass fraction contribution is equal to the total concentration of precious metal in a mineral phase divided by the whole rock concentration of the respective precious metal.

$$F_{Precious\ metal\ (total)} = C_{PMM}/C_{WR} \quad (3)$$

where

$F_{Precious\ metal\ (total)}$ = the total fraction of PMM contributed to the sample by a precious metal mineral

$C_{PMM}$ = Concentration of each of Pt, Pd, Ag and Au contributed by a *specific* discrete PMM

## Results

*Whole-rock analysis*

Whole-rock chemical compositions for the four galena-bearing Ovoid samples are given in Table 1. They have moderately elevated Pt (average 819 ppb), Pd (average 967 ppb), and Au (average 160 ppb) concentrations compared to typical massive sulfides from the Ovoid reported by Naldrett *et al.* (2000a), which on average contain Pt=123 ppb, Pd=252 ppb and Au=93 ppb (n=52) (Table 1). In contrast, the four samples of this study have very low abundances of Rh (4 ppb), Ru (<1 ppb) and Ir (<1 ppb), even compared to the typical massive sulfides from the Ovoid (Naldrett *et al.* 2000a). A significant amount of Ag is present in our four samples, with an average abundance of *ca.* 25 ppm. Ni and Cu contents of the galena-bearing samples are similar to those of the typical Ovoid massive sulfides. Pb contents of the four samples are elevated (mean of *ca.* 1100 ppm), reflecting the presence of the constituent galena.

Because all four samples represent massive sulfides with similar textures, their concentrations were averaged and used as the bulk values for the whole-rock abundances in the final mass-balance calculations. This was done to achieve the most representative abundances for Ovoid samples that contain galena and elevated concentrations of Pt+Pd. Because Ir, Ru, and Rh are present in such minute quantities (<5 ppb) in the bulk samples, these metals were not considered in the mass-balance calculations.

**Table 2-1. BULK CHEMICAL COMPOSITIONS OF OVOID MASSIVE SULFIDE SAMPLES**

| | Fe (wt.%) | Ni (wt.%) | Cu (wt.%) | Co (wt.%) | Pb (ppm) | Zn (ppm) | Ir (ppb) | Ru (ppb) | Rh (ppb) | Pt (ppb) | Pd (ppb) | Au (ppb) | Ag (ppm) |
|---|---|---|---|---|---|---|---|---|---|---|---|---|---|
| Detection Limit | | | | | | | 1 | 1 | 1 | 1 | 1 | 1 | 0.05 |
| Galena-bearing Ore | | | | | | | | | | | | | |
| MK-95008A | 52.6 | 5.1 | 4.2 | 0.16 | 712 | 629 | <1 | <1 | 4 | 325 | 412 | 51 | 30.5 |
| MK-95008B | 49 | 4.3 | 1 | 0.06 | 819 | 609 | 1 | <1 | 4 | 2180 | 2490 | 209 | 28 |
| MK-0241 | 46.7 | 3.2 | 2.4 | 0.13 | 1686 | 179 | 1 | <1 | 5 | 158 | 463 | 84 | 15 |
| MK-0207 | 47.9 | 4.5 | 2.5 | 0.18 | 1201 | 187 | <1 | <1 | 3 | 614 | 503 | 297 | 26 |
| Mean (n=4) | 49 | 4.3 | 2.5 | 0.13 | 1104 | 401 | <1 | <1 | 4 | 819 | 967 | 160 | 24.9 |
| SD | 2.5 | 0.8 | 1.3 | 0.01 | 440 | 252 | | | 1 | 927 | 1016 | 114 | 6.8 |
| Typical Massive Ore | | | | | | | | | | | | | |
| Mean (n=52)‡ | | 4.6 | 2.8 | | | | 2 | 17 | 8 | 123 | 252 | 93 | |
| SD | | 1.1 | 1.4 | | | | 1.1 | 10 | 3 | 111 | 115 | 130 | |

Analyses by acid dissolution with either an ICP-OES (Fe, Ni, Cu, Co, Pb, Zn) and ICP-MS (Ag) finish, and Ni-sulfide fire assay with an ICP-MS finish (PGE and Au)

‡ Massive sulfide (Naldrett *et al.* 2000a)

*Mineral -liberation analysis (MLA)*

The mineral mass fractions measured by MLA for the four Ovoid massive sulfide samples are presented in Table 2. An average abundance determined from the four samples is used as a representative abundance of the major minerals for the mass-balance calculations.

**TABLE 2-2. MASS FRACTION OF MAJOR MINERALS (wt.%)**

| Mineral | MK-0207 | MK-0241 | MK-95008A | MK-95008B | Average Abundance** |
|---|---|---|---|---|---|
| Chalcopyrite ($CuFeS_2$) | 10.4 | 6.85 | 7.8 | 2.8 | 6.96 |
| Galena (PbS) | 0.14 | 0.13 | 0.12 | 0.25 | 0.15 |
| Magnetite ($Fe_3O_4$) | 8.1 | 13.1 | 7.46 | 14 | 10.7 |
| Pentlandite $(Fe,Ni)_9S_8$ | 11 | 12 | 15.8 | 13.7 | 13.1 |
| Pyrrhotite ($Fe_{1-x}S$) | 69.2 | 66.6 | 65 | 68.1 | 67 |
| Other minerals* | 2.1 | 1.32 | 3.82 | 1.17 | 2.1 |

*Other minerals may include a combination of cubanite, sphalerite, silicate gangue and other rare phases. **Average abundances were used for mass-balance calculations.

A detailed summary of PMM identified by SEM-MLA is listed in Table 3. The results of the detected PMM from all four samples were combined. This was done to gain a more accurate representation of PMM within the sampled region of the Ovoid. The PGM that were found are sperrylite, froodite and michenerite and the Ag-PMM found are electrum Au-Ag alloy, völynskite ($AgBiTe_2$), stützite ($Ag_{5-x}Te$) and acanthite ($Ag_2S$). The sperrylite is normally present as well-developed crystals with grain sizes of >76 µm. Although only three grains of sperrylite were detected, they contribute a major portion of Pt in the samples because of their relatively large grain size. Of the three grains of sperrylite, only one grain is found attached, whereas the other two were found completely liberated. A large number of froodite grains were detected; they are normally present as either small inclusions (average <5 µm) in, or as large attachments (2 to 43 µm) to galena, pentlandite, magnetite and in some cases, pyrrhotite and chalcopyrite. Ten included grains of michenerite were detected; however, they contribute little Pd (mass apportionment =0.002) to the whole sample because of their small size and low abundance. SEM-BSE-generated X-ray spectra suggest that some grains may be Sb-bearing. No Ir, Ru, Rh or Os PGM were detected. A total of 51 Ag and Au mineral grains were detected and, they are present mostly present as <10 µm inclusions.

**Table 2-3: Summary of PMM Characteristics**

| Mineral | # of Grains | Association | | | ECD (µm) | | | | Precious metal | Precious metal mass (g) | Precious Metal Mass Apportionment |
|---|---|---|---|---|---|---|---|---|---|---|---|
| | | Liberated | Attached | Locked | Average | Min | Max | SD | | | |
| Froodite ($PdBi_2$) | 264 | 5 | 31 | 228 | 3.68 | 1.11 | 43.02 | 5.14 | Pd | 2.73E-07 | 0.998 |
| Michenerite PdBiTe or Sb-bearing Michenerite* | 10 | --- | --- | 10 | 2.55 | 1.11 | 4 | 2.05 | Pd | 3.58E-10 | 0.002 |
| Sperrylite, $PtAs_2$ | 3 | 2 | 1 | --- | 76.43 | 20.88 | 124.6 | 52.25 | Pt | 7.93E-06 | 1 |
| AgAu alloy | 10 | 1 | --- | 9 | 2.38 | 1.11 | 4.28 | 1.08 | Au<br>Ag | 4.66E-10<br>5.64E-09 | 1<br>0.4195 |
| Völynskite ($AgBiTe_2$)** | 27 | --- | 3 | 24 | 2.43 | 1.11 | 15.28 | 2.83 | Ag | 3.00E-09 | 0.2232 |
| Stützite ($Ag_{5-x}Te$)* | 12 | 1 | 3 | 8 | 4.25 | 1.11 | 9.83 | 2.96 | Ag | 4.64E-09 | 0.3452 |
| Acanthite ($Ag_2S$)** | 2 | --- | --- | 2 | 2.71 | 1.92 | 3.5 | 1.12 | Ag | 1.63E-10 | 0.0121 |

*Mineral stoichiometry has not been determined by EPMA. The masses of precious metals contributed by these minerals were estimated from the EPMA results determined by Huminicki *et al.* (2008). **EPMA not determined here or in Huminicki *et al*. (2008); stoichiometry based on theoretical value.

The minerals that are directly associated with the PMM are important to document because they can have a considerable effect on how, and if, the PMM may be recovered. As well, the mineralogical associations

provide important information regarding the genesis of the deposit. The MLA quantifies the associations of the PMM with other minerals by determining the length of shared boundaries of PMM with other grains. The results are tabulated in Figure 4. Photomicrographs depicting examples of the associations and liberation for sperrylite, froodite and völynskite are displayed in Figures 5 A through F. Nearly the entire area (92%) of the sperrylite is not associated with any other minerals (free surface). Sperrylite was found to host small inclusions of galena, froodite and breithauptite (NiSb). The froodite is associated largely with pentlandite, galena and less often with pyrrhotite, magnetite, chalcopyrite, and other PMM. Two of the froodite grains detected are attached to breithauptite and included in pentlandite (Fig. 5C), and one grain was found attached to altaite (PbTe) and included in galena. One larger froodite grain attached to galena was also attached to native bismuth and AgAu alloy. The michenerite is most often associated with pyrrhotite, galena and pentlandite but in some cases were also found attached to froodite and electrum. The Ag- and Au-PMM were commonly present as small inclusions (<5 µm) in galena, pyrrhotite, chalcopyrite, pentlandite, and with magnetite. Only six of the Ag- and Au-PMM grains were found as attachments to other phases, and two grains were fully liberated. The photomicrographs show the range in grain size of the PMM, from less than 5 µm to greater than 70 µm.

Grain size is a characteristic that is highly relevant to mineral processing. It is important to determine whether PGM are fine inclusions, which may not be easily liberated, or if they exist as larger attached grains that can be liberated upon grinding and will not be too small to become entrained during the separation process (*e.g.*, Cabri *et al.* 2009). Nearly all of the michenerite and AgAu alloy grains are present as fine inclusions (<5 µm). Liberation of these minerals would be difficult to achieve by grinding. As mentioned above, the sperrylite is usually found as coarse grains, >76 µm in size, making it easily liberated. Eleven of the 51 detected Au and Ag grains were found as large (~5-15 µm ECD) liberated particles or as attachments with other minerals. Because there are over 200 grains of froodite, a grain-size distribution was plotted (Fig. 6) in order to estimate the size fractions of froodite grains that carry the majority of the Pd. Although this distribution shows that over 90% of the grains are under 10

µm in size and probably exist as fine inclusions, the majority of the total mass of froodite present in the samples is actually present in grains >10 µm in size, and thus could be liberated by grinding.

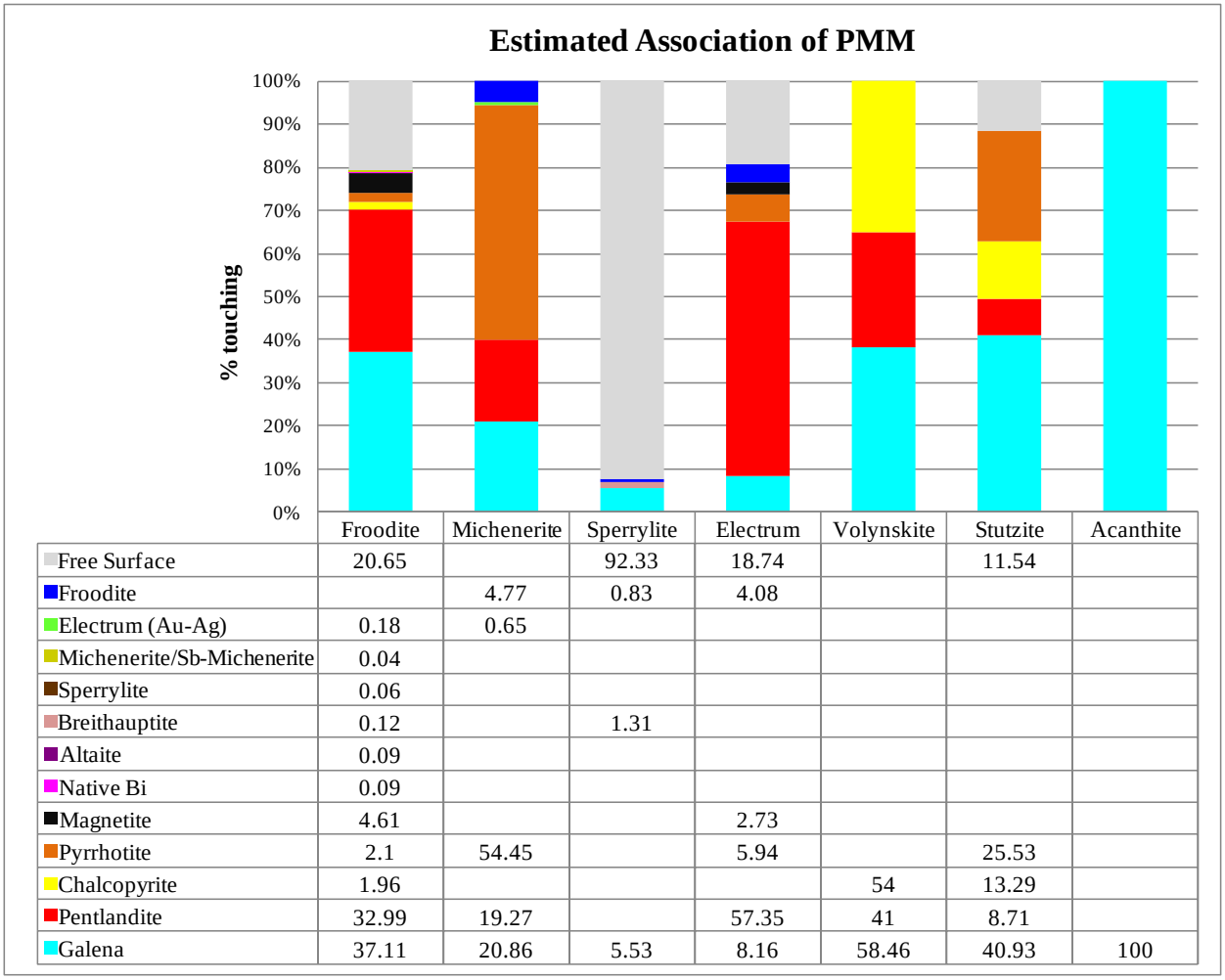


| | Froodite | Michenerite | Sperrylite | Electrum | Volynskite | Stutzite | Acanthite |
|---|---|---|---|---|---|---|---|
| Free Surface | 20.65 | | 92.33 | 18.74 | | 11.54 | |
| Froodite | | 4.77 | 0.83 | 4.08 | | | |
| Electrum (Au-Ag) | 0.18 | 0.65 | | | | | |
| Michenerite/Sb-Michenerite | 0.04 | | | | | | |
| Sperrylite | 0.06 | | | | | | |
| Breithauptite | 0.12 | | 1.31 | | | | |
| Altaite | 0.09 | | | | | | |
| Native Bi | 0.09 | | | | | | |
| Magnetite | 4.61 | | | 2.73 | | | |
| Pyrrhotite | 2.1 | 54.45 | | 5.94 | | 25.53 | |
| Chalcopyrite | 1.96 | | | | 54 | 13.29 | |
| Pentlandite | 32.99 | 19.27 | | 57.35 | 41 | 8.71 | |
| Galena | 37.11 | 20.86 | 5.53 | 8.16 | 58.46 | 40.93 | 100 |

**Figure 2-4: Estimated mineral associations of the PMM (area %)**.

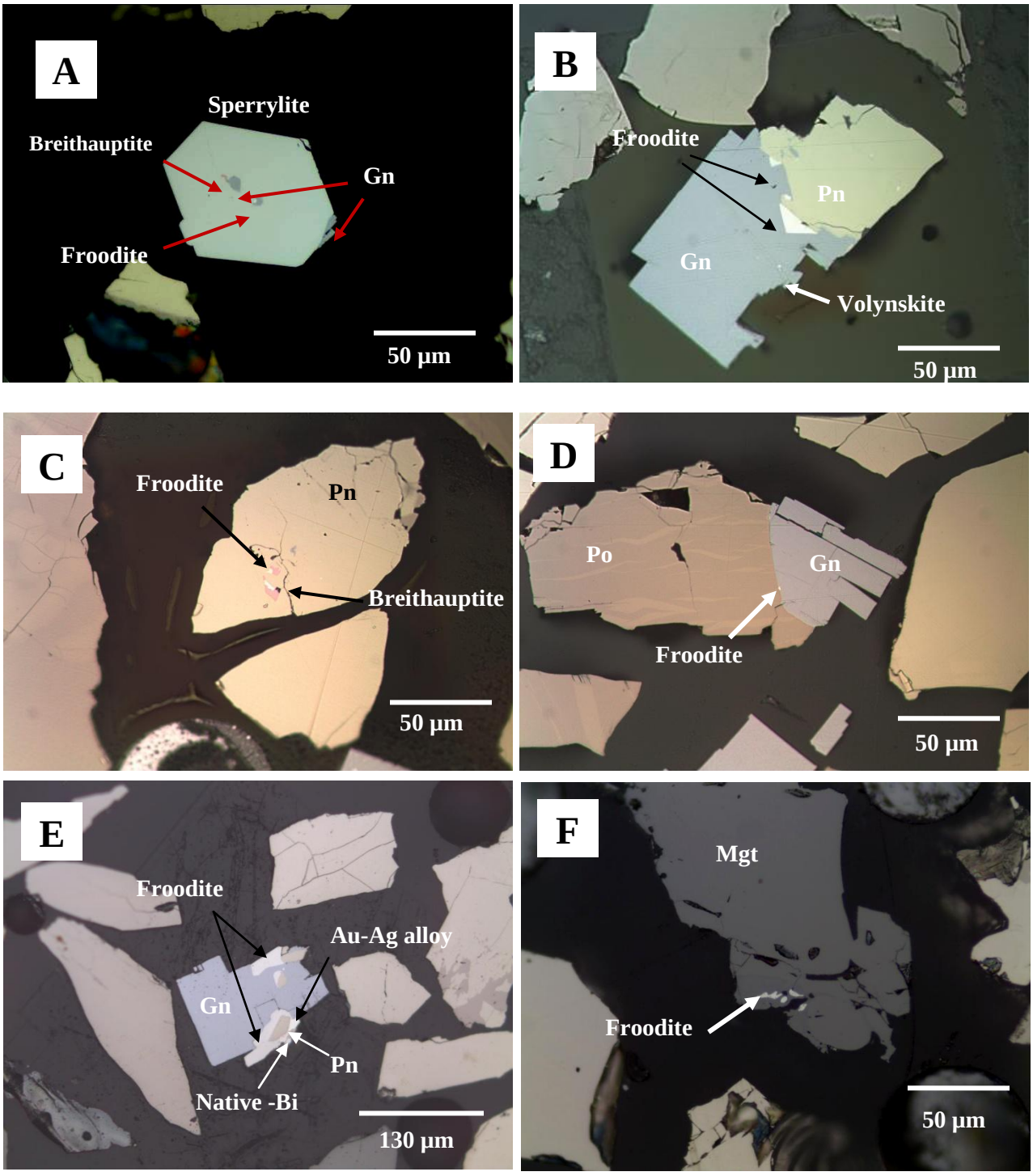


**Figure 2-5 A-F: Photomicrographs (reflected light) of PMM and PGM** A) a large, liberated sperrylite grain containing smaller inclusions of galena (Gn), breithauptite and froodite; B) greater than average size froodite grain along with a tiny grain of volynskite included in galena (Gn) and pentlandite (Pn); C) average size froodite grain included in pentlandite (Pn); D) less than average size froodite grain included in galena (Gn) and pyrrhotite (Po); E) large froodite attachment to galena (Gn) with electrum; F) small froodite grain in magnetite (Mgt).

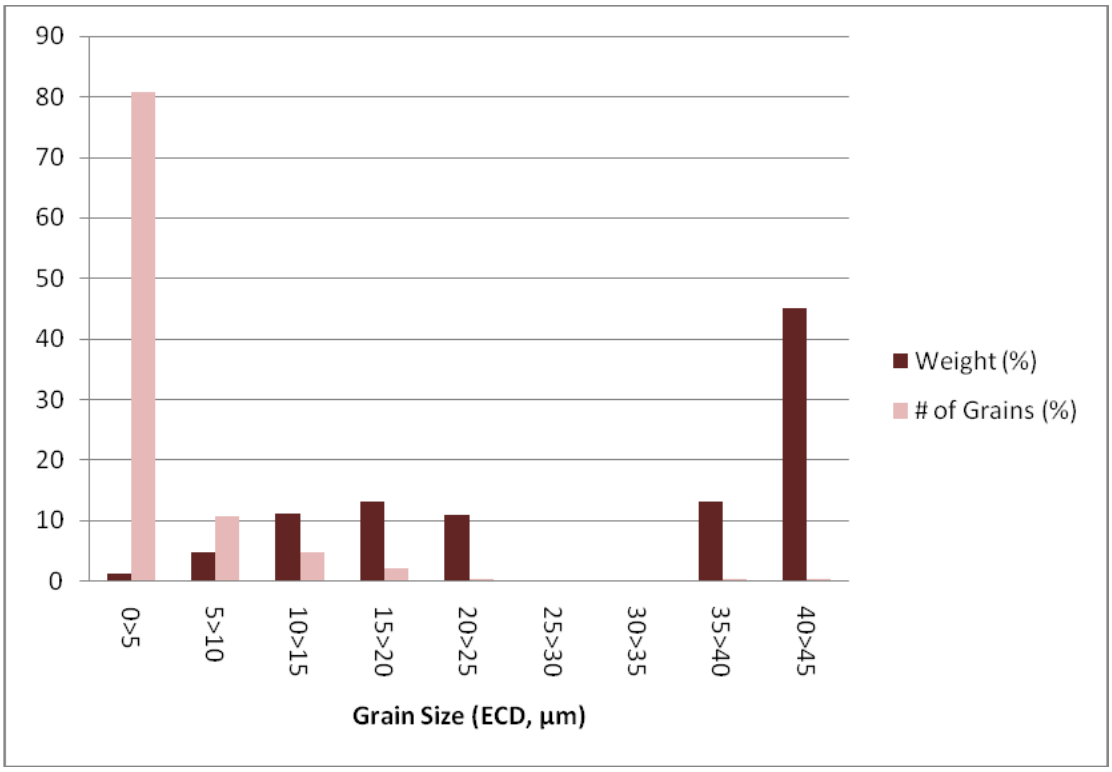


**Figure 2-6: Grain size distribution of froodite** in the 4 massive sulfide samples. The majority of the total mass of froodite is found in size fractions >10 µm.

*Electron Probe Micro-analysis (EPMA)*

The results for electron probe micro-analysis of major sulfides and trace PMM in the four samples are summarized in Table 5. The measured concentrations of Pt and Pd for sperrylite and froodite were used for the mass-balance calculations. Because of their small size, michenerite, völynskite, stützite, and acanthite were not analyzed by EPMA; for the mass-balance calculations, the compositions for these minerals are based on the EPMA data of Huminicki *et al.* (2008) or theoretical stoichiometric abundances. The trace mineral phases, breithauptite (NiSb) and altaite (PbTe) were analyzed by EPMA to confirm their identities. Cu, Ag and Bi were detected in galena; lead and selenium in sperrylite; arsenic and gold in froodite; and bismuth and arsenic in altaite. Pt and Pd are both detected in low (1-2 wt.%) abundances in breithauptite. A trace amount of Pd was measured in sperrylite.

**Table 2-5: Summary of EPMA Results (in elemental wt.%)**

| Mineral | Fe | Ni | Cu | Co | S | Pb | Pt | Pd | Ir | Re | Te | Sb | Sn | Ag | Bi | As | Au | Se | Total |
|---|---|---|---|---|---|---|---|---|---|---|---|---|---|---|---|---|---|---|---|
| **Major Sulfide** | | | | | | | | | | | | | | | | | | | |
| Pyrrhotite (n=21) | 63.07 | 0.21 | 0.02 | 0 | 36.51 | | | | | | | | | | | | | 0 | 99.81 |
| Pentlandite (n=27) | 34.29 | 31.17 | 0.02 | 1.06 | 32.97 | | | | | | | | | | | | | 0 | 99.51 |
| Chalcopyrite (n=13) | 31.03 | 0.55 | 33.39 | 0.01 | 34.53 | | | | | | | | | | | | | 0.02 | 99.50 |
| Galena (n=21) | | | 0.02 | | 13.43 | 86.83 | | | | | | 0.001 | | 0.02 | 0.14 | | | | 100.44 |
| **Trace PGM and PMM** | | | | | | | | | | | | | | | | | | | |
| Sperrylite (n=3) | 0.09 | 0.03 | | | 0 | 0.22 | 56.96 | 0.03 | | | 0.01 | 0.07 | 0 | 0.01 | 0 | 42.80 | 0 | 0.47 | 100.70 |
| Froodite (n=3) | 0.94 | 0.46 | | | 0.10 | 0 | 0 | 22.15 | | | 0.05 | 0 | | 0.07 | 76.64 | 0.15 | 0.59 | 0 | 101.16 |
| Au-Ag alloy (n=1) | 0.21 | 0.26 | 0.03 | | 0.07 | | 0.06 | | 0.03 | 0.009 | | | | 42.7 | 0.54 | 0.01 | 57.14 | | 101.06 |
| Native Bismuth (n=1) | 0.33 | 0.32 | | | | | | 1.36 | | | | 0.01 | | | 100.2 | 0.26 | 0.15 | 0.07 | 102.7 |
| Breithauptite (n=1) | 1.06 | 30.54 | | | 0.00 | 0 | 2.56 | 1.36 | | | 0 | 65.70 | | 0.08 | 0.10 | 0.26 | 0 | 0 | 101.65 |
| Altaite (n=2) | | | | | 0.84 | 59.65 | | | | | 35.41 | | | | 3.93 | 0.42 | 0.03 | 0.10 | 101.68 |

Blank spaces indicate no analysis was done for that element

*LA-ICP-MS*

The LA-ICP-MS results (Table 6) indicate that the only sulfides with a significant amount of PGE in solid solution are pentlandite and galena, each of which contain ~1.2 ppm of Pd. Figure 7 shows representative time-resolved spectra of the Pd measured in galena by LA-ICP-MS. Gold was also found in galena with an average concentration of 0.27 ppm. Silver is the most abundant precious metal detected in all sulfide phases, ranging from 0.43 ppm in pyrrhotite to 199 ppm in galena. Concentrations below detection limit were considered to be zero in the mass-balance calculations.

**Table 2-6: Concentration of Pt, Pd, Ag and Au in solid solution in sulfides (ppm)**

| | Ag | | | | Pd | | | | Pt | | | | Au | | | |
|---|---|---|---|---|---|---|---|---|---|---|---|---|---|---|---|---|
| | Mean | Min | Max | S.D. | Mean | Min | Max | S.D. | Mean | Min | Max | S.D. | Mean | Min | Max | S.D. |
| **Pyrrhotite, n=22** | 0.429 | 0 | 1.57 | 0.43 | 0.089 | 0 | 0.338 | 0.087 | 0.009 | 0 | 0.032 | 0.008 | 0.021 | 0 | 0.103 | 0.027 |
| **Pentlandite, n=24** | 3.15 | 0.5 | 13.9 | 4.15 | 1.15 | 0 | 3.61 | 0.832 | 0.013 | 0 | 0.058 | 0.016 | 0.031 | 0 | 0.209 | 0.046 |
| **Galena, n=22** | 199 | 51 | 556 | 165 | 1.27 | 0.1 | 4.56 | 1.118 | 0.03 | 0 | 0.233 | 0.065 | 0.269 | 0 | 1.1 | 0.291 |
| **Chalcopyrite, n=15** | 4.15 | 0.9 | 13.5 | 3.66 | 0.12 | 0.1 | 1.07 | 0.285 | 0.007 | 0 | 0.019 | 0.006 | 0.05 | 0 | 0.165 | 0.044 |

A detailed table outlining the LA-ICPMS is included in Appendix 4.

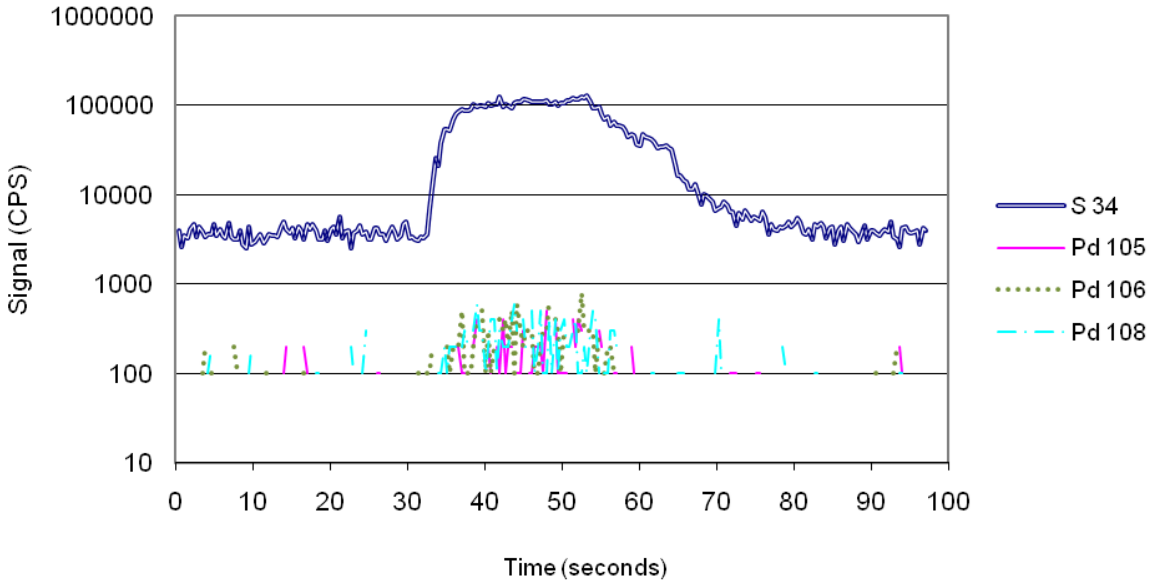


**Figure 2-7: LA-ICPMS spectra of Pd in galena**. CPS=counts per second. The laser was fired starting at about the 33 second mark and stopped at about the 55 second mark.

*Results of mass balance*

The results of the mass-balance distribution (calculated using equations 1-3) are summarized in Table 7 and Fig.8. Mass balances were calculated only for Pt, Pd, Ag and Au, because they are present in elevated abundances. A deportment calculation for Ir, Ru and Rh, which contain whole-rock abundances <5 ppb, cannot be determined accurately.

The majority of the Pd in the samples is contributed by froodite (77%), whereas michenerite was found to only contribute 0.2% Pd. The remainder of the Pd is in solid solution in pentlandite (15%), pyrrhotite (6.2%), and chalcopyrite (1.6%). Even though a fair amount of Pd was detected in solid solution with galena, this source of Pd only contributes a total of 0.20% because galena has such a low modal abundance compared to pentlandite.

Nearly all Pt in the samples is contributed by sperrylite (99%). The remaining 1% is contributed by that dissolved in solid solution within the sulfides. Most of the Au (86%) in the samples is carried by Au-Ag alloy.

The mass balance shows that the majority of the Ag (95%) in the samples is contributed by discrete PMM. The majority of Ag in the PMM is held by Au-Ag alloy (40%) and stützite (33%) and volynskite (21%) with much lesser amounts contributed by acanthite (1.2%). The remaining Ag (5.1%) is dissolved in solid solution within the sulfides, in rather similar amounts for each of pentlandite, galena, pyrrhotite and chalcopyrite.

**Table 2-7: Summary of Mass-Balance Distribution of Selected Precious Metals in Ovoid Mineralogy**

| PGE | Whole Rock Abundance (ppm) | Type of Occurrence | Mineral | Precious Metal Concentration (ppm) | Precious Metal Contribution (%) |
|---|---|---|---|---|---|
| **Pd** | 0.967 | PGM | Froodite ($PdBi_2$) | 0.748 | 77.3 |
| | | | Michenerite (PdBiTe) | 0.001 | 0.20 |
| | | | Total | 0.749 | 77.5 |
| | | Trace element solid solution | Pentlandite | 0.148 | 15.3 |
| | | | Galena | 0.002 | 0.20 |
| | | | Pyrrhotite | 0.060 | 6.20 |
| | | | Chalcopyrite | 0.008 | 0.83 |
| | | | Total | 0.218 | 22.5 |
| **Pt** | 0.819 | PGM | Sperrylite ($PtAs_2$) | 0.811 | 99.0 |
| | | Trace element solid solution | Pentlandite | 0.0017 | 0.20 |
| | | | Galena | 0.00005 | 0.0055 |
| | | | Pyrrhotite | 0.0061 | 0.74 |
| | | | Chalcopyrite | 0.0005 | 0.059 |
| | | | Total | 0.0082 | 1.0045 |
| **Au** | 0.160 | PMM | Au-Ag alloy | 0.138 | 86.3 |
| | | Trace element solid solution | Pentlandite | 0.0039 | 2.46 |
| | | | Galena | 0.0004 | 0.25 |
| | | | Pyrrhotite | 0.0142 | 8.85 |
| | | | Chalcopyrite | 0.0035 | 2.17 |
| | | | Total | 0.0218 | 13.7 |
| **Ag** | 24.9 | PMM | Au-Ag | 9.91 | 39.80 |
| | | | Völynskite ($AgBiTe_2$) | 5.27 | 21.2 |
| | | | Stutzite ($Ag_{5-x}Te$) | 8.15 | 32.7 |
| | | | Acanthite ($Ag_2S$) | 0.290 | 1.2 |
| | | | Total | 23.6 | 94.9 |
| | | Trace element solid solution | Pentlandite | 0.400 | 1.61 |
| | | | Galena | 0.298 | 1.20 |
| | | | Pyrrhotite | 0.289 | 1.16 |
| | | | Chalcopyrite | 0.289 | 1.16 |
| | | | Total | 1.28 | 5.1 |

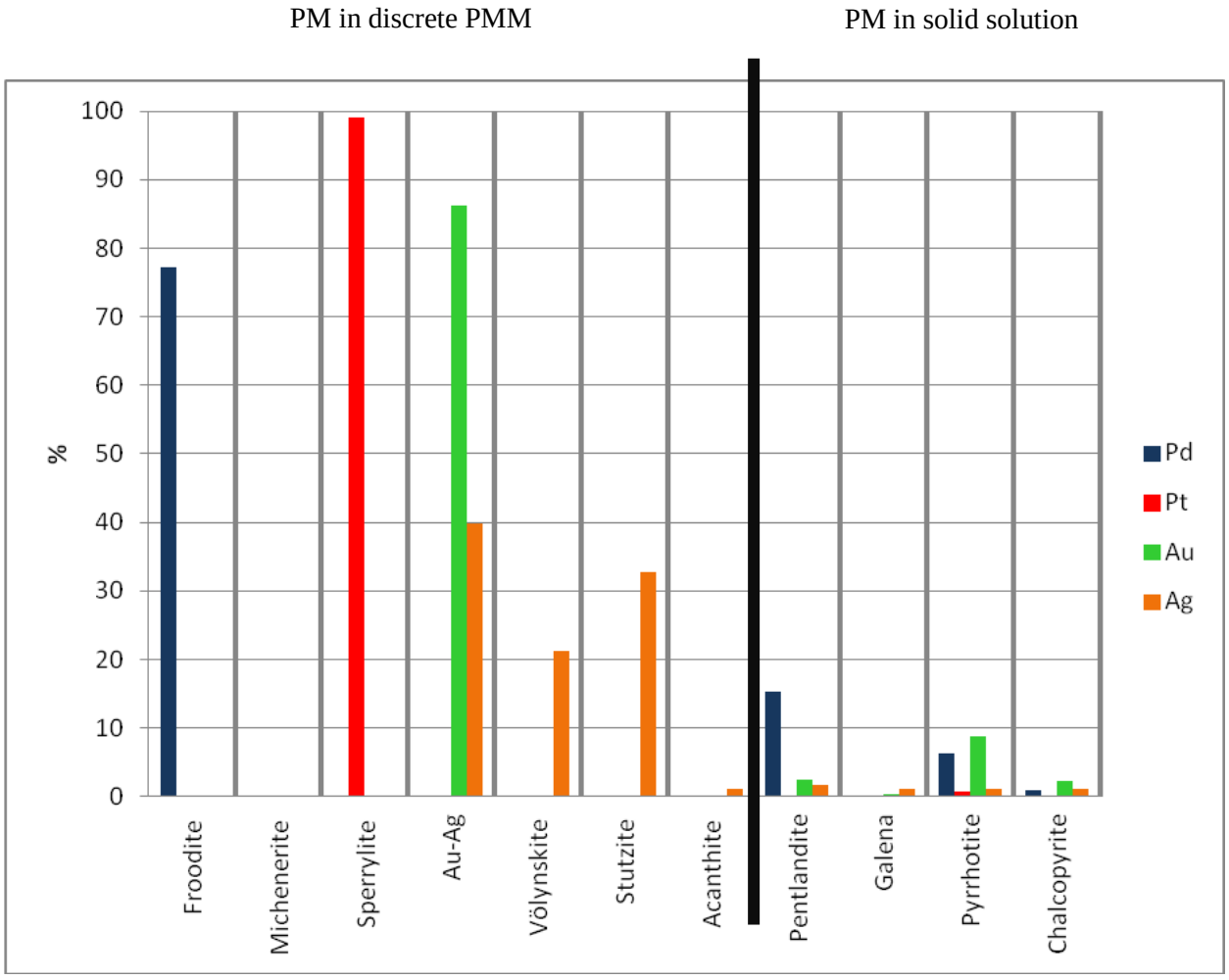


**Figure 2-8: Comparison of contribution of precious metals** from discrete precious metal minerals and in solid solution in the major and minor sulfide minerals in the Ovoid

## Discussion

*Comparison to precious metal mineralization in the SE Extension*

Comparison of the precious metal occurrences from different regions of the Voisey's Bay deposit is important for establishing genetic relationships and exploration strategies between the mineralized domains. As shown in Figures 2A and B, the four samples selected for this study are all from a region of the main Ovoid deposit located in the southeastern area of the body in plan view, and toward the middle of the body, between depths of 46 and 82 m, in cross sectional view. Comparing the results presented here

to samples from other regions of the Ovoid and other sulfide zones at Voisey's Bay will help to reveal how and why precious metal occurrences vary throughout the entire deposit. This is important for evaluating techniques for possible recovery of the precious metals from discrete domains during processing and also for developing genetic models for the orebodies of Voisey's Bay (e.g. Huminicki *et al*. 2008).

Besides the results presented here, the only other documented PMM occurrence at Voisey's Bay is that reported by Huminicki *et al.* (2008), which occurs as disseminated mineralization in the center of a hornblende gabbro dyke of the Southeast Extension Zone (Fig. 2A). Our results for the Ovoid show both mineralogical similarities and differences compared to the precious metal occurrences in the SE Extension. In general, the PMM in both locations are nearly always found associated with pentlandite, galena and chalcopyrite and less often with pyrrhotite, as well as magnetite (in the Ovoid) and silicate minerals (in the SE Extension Zone). Huminicki *et al.* (2008) suggested that the mineral associations are the result of the PGM crystallizing directly from the same sulfide melt that carried the main Cu-Ni-Co mineralization. Because little to no PGM were found to be associated with hydrous phase silicates or minerals containing Cl, PGM crystallization by late-stage hydrothermal fluids was considered unlikely by Huminicki *et al.* (2008). A cooling sulfide magma undergoing fractional crystallization first forms crystals of an Fe-S rich monosulfide solid solution (MSS) and then, later, an intermediate solid solution (ISS), from an even more differentiated sulfide magma. Since Pt and Pd are considered incompatible in MSS, they will partition into the ISS (e.g., Fleet *et al.* 1993). Most PGM are thus associated with minerals such as pentlandite (of intermediate composition), chalcopyrite and galena, which exsolve from the ISS under subsolidus conditions. The similar mineralogical relationships reported here indicate crystallization of PGM from a highly differentiated sulfide magma may have occurred in the core of the Ovoid as well.

The LA-ICP-MS results are consistent with those presented in Huminicki *et al.* (2008). Sulfides from the hornblende gabbro dyke were reported to contain average Pd contents of 2 ppm in pentlandite, 1.8 ppm in galena and 0.10 ppm in chalcopyrite, with the remaining PGE measureable in low quantities just above detection limit. This is similar to the sulfides in the Ovoid PGE occurrences, which have average Pd contents of 1.2 ppm in pentlandite (n = 24), 1.3 ppm in galena (n = 22) and 0.12 ppm in chalcopyrite (n = 15). This consistency is evidence that the ore mineralization and PGE enrichment processes in both the Southeast Extension dyke and main Ovoid deposit are related. As pointed out in Huminicki *et al*. (2008), the Pd in solid solution in galena is a significant result because it may be the first documented occurrence of PGE in galena to be reported. Palladium concentrations should be measured in galena from other magmatic deposits to determine if there are similar occurrences elsewhere. Further analysis of Ag and Au in solid solution in sulfides from the Southeast Extension Zone should also be considered for comparison to the results presented here.

A difference between the distribution of precious metals in the Ovoid and Southeast Extension zones is seen in the whole rock concentrations of PGE. Huminicki et al. (2008) reported Pt and Pd concentrations of 2-3 ppm in the samples from the Southeast Extension, which are significantly higher than the Pt and Pd levels in three (0.2-0.6 ppm) of our four samples from the Ovoid. Other differences are seen in the presence of discrete precious metal mineral phases, and in some cases with the minor mineral associations. Most significantly, in the Southeast Extension Zone, 188 grains of native Ag were detected, contributing to 24% volume of the total PMM, whereas no native silver was detected in the Ovoid. Another difference in the precious metal mineralogy between the two areas is the lack of Sn-bearing PMM in the Ovoid, whereas a variety of PMM containing Sn were detected in the Southeast Extension Zone dyke. Paolovite ($Pd_2Sn$) and antimonian stibiopalladinite [$Pd_{5-x}(Sb,Sn)_{2-x}$] contribute to a large portion of total Pd-PGM in the dyke of the Southeast Extension, whereas in the Ovoid, the main Pd carrier is froodite ($PdBi_2$). Sperrylite ($PtAs_2$) is the most abundant PGM by volume in both the Ovoid and Southeast Extension Zone dyke. Also in both the Ovoid and dyke, PMM containing As, Bi, Te and a

small amount of Sb are present. Other trace phases containing Bi, Te, Ni, As and Sb, which form minor associations with PMM, were detected in both areas. The PMM assemblages and their minor associations indicate that the differentiated melts of the Ovoid and Southeast Extension dyke were enriched in Pd, Pt, Bi, As, Sb, Te and Sn, but in different proportions. In particular, the high abundances of Sn in the dyke and the absence of Sn enrichment in the precious metal occurrences in the Ovoid may suggest differences in details of ore genesis in the two regions that require further investigation.

Finally, a large proportion of PGM (mainly sperrylite and paolovite) in the Southeast Extension dyke is associated with Cu-rich mineral assemblages, chalcopyrite and bornite, whereas only a small portion of PGM from the Ovoid were found associated with chalcopyrite. This may be due to the different techniques of sample preparation employed here *vs.* in the study of Huminicki *et al.* (2008). As we used EPD instead of conventional crushing, we were able to completely liberate sperrylite without breaking apart the original grains, and without leaving remnant sperrylite grains attached to the major mineral phases. On the basis of characteristics of sperrylite from the Southeast Extension dyke, it is possible that sperrylite in the Ovoid samples may have been strongly associated with chalcopyrite before EPD processing. On the other hand, the large sizes of sperrylite grains and their experimentally derived melting temperatures would suggest that sperrylite crystallized early from a sulfide parent melt, at high temperatures (>1400 $^{o}$C, Hansen & Anderko 1958, Bennett & Heyding 1966), prior to ISS crystallization. Detailed investigations of the sulfide and PGM crystallization processes that relate the mineralization of the dyke of the Southeast Extension Zone to the Ovoid is the subject of our ongoing studies.

*Considerations of deportment and recovery of precious metals*

Open-pit mining of the Ovoid began in August 2005 and processing began in September 2005. Two types of concentrate are produced by conventional crushing, wet grinding and differential flotation: a high-grade concentrate containing mainly Ni and Co as pentlandite, and a middlings concentrate containing

more Cu as chalcopyrite; there are also pyrrhotite tailings produced (Bacon & Cochrane 2003). Currently, Ni, Cu and Co are recovered from the concentrates by traditional smelting processes at facilities elsewhere in Canada, but starting in 2013, these metals will be extracted from the concentrates by a hydrometallurgical process at a new facility being constructed at Long Harbour, Newfoundland (Davis Engineering and Associates Ltd. & Strategic Concepts Inc. 2004). Because there are generally low levels of precious metals in Ovoid ores (Pt+Pd < 0. 5 ppm), precious metals are not currently being recovered from the concentrates treated by smelting.

Even though our samples may represent only a small portion of the total metal resource contained within the Ovoid deposit, and mining of the Ovoid is already well underway, it is useful to make some general observations about the potential to recover precious metals from samples containing elevated PGE (and Pb) based on the new data for their distribution among the minerals present in the unusual, galena-bearing, massive sulfide ores that we have characterized here. The potential exists for ongoing exploration to reveal similar precious metal occurrences in other deposits at Voisey's Bay that are not currently being mined (Discovery Hill, Reid Brook, Southeast Extension and Eastern Deeps). In addition, we recognize that nickel sulfide prospects elsewhere demonstrate styles of mineralization similar to those at Voisey's Bay such as in the Pants Lake Intrusion, Labrador (Kerr 2003), the Hulbert-Salo Property, Ontario (MacDonald Mines Exploration 2010), and Nor'East Property, Minnesota (Peterson & Ablers 2007). Further exploration of these prospects may discover occurrences of precious metals similar to those described in the Ovoid in this study.

The most common problems encountered during metal recovery are almost always related to the behavior of the mineral host of the metal during processing. To gain effective recovery of any metal, it is important to fully understand the deportment of the metals among the minerals. This is especially important for PGE and other precious metals because they are normally present in such low quantities. The above results indicate that most of the Pt, Pd, Ag and Au in the anomalous Ovoid samples of this study are present as discrete minerals, with the rest being contained in solid solution in sulfides. Sperrylite is the only mineral

that is most commonly found as nearly fully liberated, large grains. Because the mass-balance distribution indicates that 99% of Pt is carried by the sperrylite, which is coarse-grained and well-liberated, the majority of Pt should be easily concentrated by gravity methods (summarized in Xiao & Laplante 2004).

Over half (77%) of the Pd is present in froodite grains. The froodite is most often included (average grain size of ~4 µm) within galena and pentlandite or present as larger grains (reaching >40 µm) attached to galena and pentlandite. Based on the grain-size analysis shown in Figure 6, a considerable amount of the Pd from froodite is distributed in the larger, attached grains. Further grinding than what was done in this study could potentially increase the liberation of froodite, leaving grains (similar to those shown in Figs. 5B and E) amenable to gravity and flotation methods.

Silver is the most abundant precious metal in these samples. It is present in an average quantity of *ca.* 25 ppm. Although a significant amount of Ag was found to be in solid solution in pentlandite and galena, the majority of the Ag (95%) was calculated to be present as discrete PMM; however, a total of only 51 fine Ag-PMM grains were detected altogether. Similarly most of the Au (86%) in the samples is carried by Au-Ag alloy. The sizes of the Ag-PMM and Au-Ag alloy were normally less than 10 µm with an average ECD of 1-5 µm. The extreme fine-grained nature of the Ag-PMM and Au-Ag alloy makes their detection and concentration difficult. Because Ag is present at ppm levels in the samples, it is possible that more Ag-PMM may be present in size fractions finer or coarser grained than those studied here, i.e. below 75 µm or above 175 µm. Further analysis of more fine- and coarse-size fractions, and analyses to determine the concentration of Ag in solid solution in sphalerite, may help to better characterize the Ag-PMM grains and confirm the overall Ag apportionment.

The smaller inclusions of Ag-PMM, Au-Ag alloy and froodite (grains similar to those shown in Fig. 5C) in the pentlandite and chalcopyrite would be difficult to liberate by grinding, but could be collected during flotation of pentlandite and chalcopyrite. Silver, Au and Pd present as inclusions in floated pentlandite would be concentrated in a Ni-Cu-Co matte during smelting; perhaps the Ag, Au and Pd could

then be recovered as a by-product during the refinement stage of the Ni, Cu and Co. Similarly, all of the Ag, Au and Pd dissolved in solid solution in pentlandite and chalcopyrite may be recovered as a by-product of refining Ni, Cu and Co smelted concentrates. Recovery of Ag and Pd as a processing by-product of pentlandite may be particularly beneficial to consider since such a large portion of Ag and Pd in the samples occurs in pentlandite, either as micrometer-sized inclusions or "dissolved" in solid solution, and thus may be readily collected by flotation of the pentlandite.

Finally, we consider recovery of precious metals associated with galena. Although galena is present at abundances of only ≤0.25% in our samples, yielding an overall low contribution to the total Ag, Pd and Au inventory compared to the other major sulfides, a significant amount of Ag, Pd and Au was found in solid solution in each galena grain that was measured (199 ppm Ag, 1.3 ppm Pd and 0.27 ppm Au). Furthermore, 37% of froodite, 41% of stützite and 58% of völynskite are associated with galena as fine inclusions. If both the PMM inclusions and dissolved concentrations of precious metals in galena are considered together, then Ag, Pd and Au associated with galena makes up approximately 33%, 29% and 7%, respectively, of the massive sulfide samples.

Galena exhibits large grain-sizes, 50-200 µm, and is normally found completely liberated or as attached grains. These characteristics should make galena easily separated by flotation or gravity methods if recovery of Ag, Pd and Au were to be attempted. However, chalcopyrite and galena will float under similar conditions and may be more difficult to separate the two minerals. Both minerals respond well to flotation using xanthate collectors under a range of pH and Eh. In order to separate galena from chalcopyrite, a modifier or suppressant reagent must be incorporated into the milling circuit. If the Voisey's Bay ore is currently not being treated to target the flotation of galena, the galena and the precious metals that are associated with it (33% of the Ag, 29% of the Pd and 7% of the Au) would most likely be recovered to the middling concentrate which contains chalcopyrite.

**Summary**

Mineralogical characterization and mass-balance calculations suggest that elevated concentrations of Pt, Pd, Ag and Au present in four unusual, galena-bearing samples of massive sulfide from the central part of the Ovoid at Voisey's Bay are carried mainly by discrete precious mineral phases including sperrylite, froodite, stützite, völynskite and Au-Ag alloy. Moderate amounts of Pd are also contained in solid solution with pentlandite. The precious metal minerals are spatially associated with galena, pentlandite, chalcopyrite, pyrrhotite, magnetite, and very rarely with breithauptite, altaite and other PMM. Similar mineralogical associations of PMM reported previously for disseminated sulfides in a hornblende-gabbro dyke in the Southeast Extension Zone adjacent to the Ovoid suggest that the PMM in both regions of Voisey's Bay may have crystallized from a differentiated Cu-rich sulfide parent melt, as proposed by Huminicki *et al.* (2008) for the mineralization in the dyke.

Sizes and textures of the PMM in the samples have been classified as liberated from, included within, or attached to, other phases. Platinum is almost completely carried by coarse sperrylite that would be readily liberated by modest grinding, rendering it amenable to gravity or flotation methods. In contrast, froodite, which carries more than half of the Pd, is somewhat finer grained than the sperrylite and would need to be liberated with more vigorous grinding prior to gravity and flotation recovery. The bulk of the Ag-PMM and Au-Ag alloy present in the massive sulfides is even finer grained and could likely only be recovered as a by-product of Ni-Cu-Co smelting of pentlandite and chalcopyrite, which host these PMM. Such a smelting process could also potentially be used to recover the considerable amounts of Pd (15%) in the massive sulfide samples dissolved as solid solution in the pentlandite, and the lesser amounts of Au and Ag dissolved in pentlandite and chalcopyrite. The data suggest that significant amounts of the Pd (~29%), Ag (~33%) and Au (~7%) in the massive sulfides are associated with galena, either as PMM inclusions or dissolved in solid solution.

**Acknowledgments**

This project was funded by Vale. We are grateful for the excellent assistance and cooperation of the company staff, particularly Dawn Evans-Lamswood, Robert Wheeler, Peter Lightfoot and Scott Mooney, which allowed us to complete the work. Comments on the manuscript by Peter Lightfoot, Michelle Huminicki, Edward Ripley and Graham Nixon were very helpful.

## References


Bacon, W.G.. & Cochrane, L.B. (2003): Voisey's Bay project located in the province of Newfoundland & Labrador, Canada, Technical Report Pursuant to National Instrument 43-101 of the Canadian Securities Administrators, 99pp.

Bennett, S.L. & Heyding, R.D. (1966): Arsenides of the transition metals. VII: Some binary and ternary Group VIII diarsenides and their magnetic and electric properties. Can. J. Chem. **44**, p. 3017-3030.

Cabri, L.J. (2002): The platinum group minerals, *In* The Geology, Geochemistry, Mineralogy, and Mineral Beneficiation of the Platinum-Group Elements. (L.J. Cabri, ed.) Canadian Institute of Mining, Metallurgy and Petroleum, *Spec. Vol.* **54**, 12-129.

Cabir, L.J. (2010): Process mineralogy in the Pt industry and future trends *in* Abstracts, 11th International Platinum Symposium, 21-24 June 2010, Sudbury, Ontario, Canada, Jugo, P.J., Lesher, C.M. and Mungall, J.E. (eds.), Ontario. Geological Survey, Miscellaneous Release–Data, p. 269.

_____ & LAFLAMME, JHG, (1976): The mineralogy of the platinum group elements from some copper-nickel deposits of the Sudbury area. Econ. Geol. **71**, 1159-1195

_____, SYLVESTER, P., M.N., TUBRETT, PEROGOEDOVA A. & LAFLAMME, J.H.G. (2003): Comparison of micro-PIXE and LAM-ICP-MS analyses for Pd and Rh. Can. Mineral., **41**, 321-329.

_____, RUDASHEVSKY, N.S., RUDEASHEVSKY, V.N. & OVERTHÜR, T. (2008): Electric-Pulse Disaggregation (EPD), Hydroseparation (HS) and their use in combination for mineral processing and advanced characterization of ores. *Canadian Mineral Processors 40th Annual Meeting, Proceedings*, Paper **14**, 211-235.

_____, MARTIN, C.J. & NELSON, M. (2009): Deportment methodology for low-grade Ni-Cu-PGE ores. *Proceedings of 48th Conference of Metallurgists*, (C. Hamilton, B. Hart & P.J. Whittaker, eds.), 3-15.

Davis Engineering and Associates Ltd. & Strategic Concepts Inc., (2004): Voisey's Bay Nickel Project Hydromet Demonstration Facility Business Opportunities Study, Prepared for Government of Newfoundland and Labrador Department of Natural Resources under the Canada/Newfoundland Comprehensive Economic Development Agreement, 68 pp. (http://www.nr.gov.nl.ca/voiseys/)

Evans-Lamswood, D.M., Bett, D.P., Jackson, R.S., Lee, D.V., Muggridge, M.G., Wheeler, R.I. & Wilton, D.H.C. (2000): Physical controls associated with the distribution of sulfides in the Voisey's Bay Ni-Cu-Co Deposit, Labrador. Econ. Geol. **95**, 749-769.

Fandrich, R., GU, Y., Burrows, D. & Moeller, K. (2006): Modern SEM-based mineral liberation analysis; International Journal of Mineral Processing **84**, 310-320

Fleet, M.E., Chryssoulis, S.L., Stone, W.E. & Weisner, C.G. (1993): Partitioning of platinum-group elements and Au in the Fe-Ni-Cu-S system: experiments on the fractional crystallization of sulfide melt. Contrib. Mineral Petrol. **44**, 115:36

Hansen, M. & Ardenko, K. (1958): Constitution of binary alloys, 2nd edn. Metallurgy and metallurgical engineering series. McGraw-Hill Book Co, New York, 1305

Huminicki, M.A.E. (2007): A comprehensive geological, mineralogical, and geochemical evaluation of the Voisey's Bay Ni-Cu-Co Sulfide Deposit: an integration of empirical data and process mechanics: Unpublished PhD thesis, Memorial University of Newfoundland, St. John's, Canada, 354 p.

_____, Sylvester, P.J., Lastra, R., Cabri, L.J., Evans-Lamswood, D. & Wilton, D.H.C. (2008): First report of platinum-group minerals from a hornblende gabbro dyke in the vicinity of the Southeast Extension Zone of the Voisey's Bay Ni-Cu-Co deposit, Labrador: Mineral. Petrol. **92**, 129-164.

_____, Sylvester, P.J., Cabri, L.J., Lesher, C.M. & Tubrett, M. (2005): Quantitative Mass Balance of Platinum Group Elements in the Kelly Lake Ni-Cu-PGE Deposit, Copper Cliff Offset, Sudbury. Econ. Geol. **100**, 1631-1646.

Kerr, A., 2003, Nickeliferous gabbroic intrusions of the Pants Lake area, Labrador, Canada: Implications for the development of magmatic sulfides in mafic systems. Am. Jour. Sci., **303**, 221-258

Lastra, R., Cabri, L.J. & Weiblein, P.W. (2003): Comparative liberation study by image analysis of Merensky Reef samples comminuted by electric-pulse disaggregation and by conventional crusher. Proceedings, *XII International Mineral Processing Conference*, Cape Town (L. Lorenzen, D.J. Bradshaw *et al.*, eds.) 251-260.

Li, C. & Naldrett A.J. (1999): The geology and petrology of the Voisey's Bay intrusion: reaction of olivine with trapped sulfide and silicate liquids. Lithos **47**, 1-31

Naldrett, A.J. (2004): Magmatic Sulfide Deposits: Geology, Geochemistry and Exploration, Springer Verlaag, Heidelberg, Berlin, 728 pp.

_____, ASIF, M., KRISTIC, S. & LI, C. (2000a): The composition of mineralization at the Voisey's Bay Ni-Cu Sulfide Deposit, with special reference to platinum-group elements. Econ. Geol. **95**, 845-865.

_____, SINGH, J., KRISTIC, S. & LI, C. (2000b): The mineralogy of the Voisey's Bay Ni-Cu-Co Deposit, Northern Labrador, Canada: influence of oxidation state on textures and mineral compositions. Econ. Geol. **95**, 889-900.

MacDonald Mines Exploration, 2010, MacDonald Mines Exploration in the Ring of Fire, James Bay Lowlands, Northern Ontario, online presentation, www.macdonaldmines.com

Peterson, D.M. & Albers, P.B., 2007, Geology of the Nickel Lake Macrodike and its association with Cu-Ni-PGE mineralization in the northern South Kawishiwi Intrusion, Duluth Complex, northeastern Minnesota; *Institute on Lake Superior Geology Proceedings, 53rd Annual Meeting, Lutsen, MN*, **53** part 2, Field Trip

Rawlings-Hinchy, A.M., Sylvester, P.J., Myers, J. S., Dunning, G.R. & Kosler, J. (2003): Paleoproterozoic crustal genesis: calc-alkaline magmatism of the Torngat Orogen, Voisey's Bay area, Labrador. Precambrian Research **125**, 55-85.

Rudashevsky, N.S., Bukarov, B.E., Lupal, S.D., Thanlhammer, O.A.R. & Saini-Eiducat, B. (1995): Liberation of accessory minerals from various rock types by electric pulse disintegration – method and application. Trans. Inst. Min. Metall., **104**, C25-C29.

Ryan, B. (2000): The Nain-Churchill Boundary and the Nain Plutonic Suite: A Regional Perspective on the Geological Setting of the Voisey's Bay Ni-Cu-Co Deposit. Econ. Geol. **95**, 705-724.

Sylvester P.J. (2001): A practical guide to the platinum-group element analysis of sulfides by Laser-ablation ICPMS in Sylvester, P., ed., Laser-ablation ICPMS in the earth sciences. Principles and applications, Mineralogical Association of Canada Short Course Series Vol. **29**, 203-211.

_____, CABRI, L.J., TUBRETT, M.N., PEREGOEDOVA, A., MCMAHON, G. & LAFLAMME, J.H.G. (2005): Synthesis and evaluation of a fused pyrrhotite standard reference material for platinum group element and gold analysis by laser ablation-ICPMS. 10th International Pt Symposium Oulu, Extended abstract volume, 16-20.

Xiao, Z. & Laplante, A.R. (2004): Characterizing and recovering the platinum group minerals-a review. Minerals Engineering **17**, 961-979.

# CHAPTER 3: GEOCHEMICAL AND MINERALOGICAL EVIDENCE FOR SEMI-METAL CONTROL OVER PGE, AU AND AG DISTRIBUTION IN THE VOISEY'S BAY MAGMATIC SULFIDE DEPOSIT


**Abstract**

Low-grade PGE, Au and Ag mineralization in massive sulfide from the Discovery Hill and Mini-Ovoid zones of the Voisey's Bay (Labrador) Ni-Cu-Co magmatic sulfide deposit is compared to previously documented precious metal mineral (PMM; PGE, Au and Ag) occurrences from massive sulfide in the Ovoid and dissementated sulfide in the Southeast Extension zones. The purpose of the investigation was to: 1) determine the variability of PMM in the different ore zones; and 2) understand the extent and source of semi-metal (As, Se, Sb, Sn, Te, Bi) control over the PMM crystallization, in a PGE-poor magmatic sulfide deposit. PMM concentrates were prepared from mineralized samples using electric pulse disaggregation and hydroseparation, and characterized using mineral liberation analysis (MLA) and electron probe microanalysis (EPMA). Stützite is the most abundant PMM in the Mini-Ovoid, contributing to 89% of the total mass of PMM with subordinate amounts of froodite. Stützite also forms the largest number of grains at Discovery Hill although, as in the Ovoid, sperrylite represents the largest mass fraction of total PMM because of its large grain-size (86 µm). Unlike in the Mini-Ovoid and Ovoid, froodite was not found at Discovery Hill. Substantial quantities of native-Ag, electrum and paolovite are present in the Southeast Extension, but these PMM are rare (electrum) to absent in the other ore zones. Concentrations of precious and semi metals in pyrrhotite, chalcopyrite, pentlandite and galena were determined by laser ablation – inductively coupled plasma mass spectrometry (LA-ICPMS). Palladium is the only PGE present in significant amounts in these sulfides; it has consistently elevated concentrations in pentlandite (1200–2000 ppb) in all areas

except for the Mini-Ovoid. Silver is present in solid solution in nearly all sulfide phases but most enriched in chalcopyrite (ca. 45 ppm) except at Discovery Hill. Distributions of As, Se, Sn, Sb, Bi and Pd in each zone were calculated based on a combination of MLA and LA-ICPMS results. With the exception of Bi in the Ovoid, all semi-metals are strongly concentrated in discrete PMM (>70% element mass). In all analyzed ore zones, the majority of Pd is carried by discrete minerals phases containing Bi, Sn or Te. Galena was found only in the Ovoid and Southeast Extension, where it contains the largest amount of Te, Sb, Ag, Bi and Au in solid solution compared to other sulfide minerals. Bulk rock assays of mineralized and unmineralized Voisey's Bay samples and country rock gneisses were determined by ICP – optical emission spectrometry (OES) and ICPMS. Average PGE to semi-metal ratios vary from 74 in Ovoid massive sulfide; to 111 in Southeast Extension disseminated sulfide; and to 210 in Mini-Ovoid massive sulfide. Country rock Tasiuyak gneisses and Enderbitic gneisses are enriched in Se, Sn and Sb (but not Bi and Te) compared to the unmineralized Voisey's Bay troctolite (but not gabbro) units. The results indicate that PMM crystallized from a highly differentiated semi-metal melt at Voisey's Bay. Localized contamination of semi-metals from gneissic country rocks to the silicate magmas hosting the sulfide mineralization provided critical control over the variable composition and abundance of PMM in the various sulfide ore zones. The potential for small-scale domains enriched in Pd, Pt, Au and Ag may exist for unexplored or undeveloped areas of Voisey's Bay. A major conclusion drawn from this study is that, even at deposits that contain low-grade PGE, PGM may crystallize if sufficient concentrations of semi-metals are available.

## Introduction

Platinum-group elements (PGE: Pt, Pd, Rh, Ir, Ru, Os) are concentrated in magmatic sulfide deposits, at least in part, as a result of their geochemical behavior during sulfide-silicate fractionation of a magma body. It is thought that the PGE are partitioned among sulfide phases based on their compatibility within early-crystallizing, monosulfide solid solution (MSS) and the residual, intermediate solid solution (ISS)-Cu-rich sulfide melt (e.g., Naldrett, 2004). During the higher temperature stages of sulfide crystallization, Pt, Pd and Rh are incompatible within the MSS structure and are expelled into the residual sulfide melt, which crystallizes ISS, while Ir, Ru and Os partition into the MSS (Fleet et al., 1993).

Although this standard model has become a widely accepted explanation for PGE distribution in magmatic sulfide deposits, it does not explain the entire process of PGE partitioning during magmatic sulfide fractionation. In most cases, when base-metal sulfides are analyzed for PGE in solid solution, substantial quantities of Pt and Pd are rarely detected in chalcopyrite or other Cu-rich minerals exsolved from the ISS, in contradiction to expectations of PGE partitioning in the standard model (Barnes et al., 1985; Nadrett, 2010). Most often, where Pd is found in solid solution, it is in pentlandite that exsolved from MSS (Holwell and MacDonald, 2010 and references therein). One possible explanation for Pt and Pd deviating from the standard model is that they are incompatible in both MSS and ISS, and Pd is concentrated within pentlandite where there was low-temperature recrystallization of the ISS (Peregoedova, 1998).

More recently, the relationship between PGE and some semi-metals (Bi, As, Te, Sb, Sn and Se) is being recognized as an important factor governing the mineralogical distribution of PGE (Helmy et al., 2007). In both natural systems and in experimental studies of synthetic magmatic liquids, PGE's demonstrate a strong affinity to complex with semi-metal ligands (Helmy et al., 2009). PGE-semi-metal complexes comprise the dominant platinum-group minerals (PGM) at large-scale PGE producing mines such as the PGE reef deposits of the Bushveld (South Africa) and the Stillwater (Montana) complexes (e.g. Hutchinson and Kinaird, 2005; Volborth and Housely, 1984), and the base-metal sulfide deposits of the

Sudbury Basin (Ontario) (Cabri and Laflamme, 1978; Huminicki et al., 2005) and Noril'sk (Russia) (Cabri and Traill, 1966).

PGE-semi-metal associations persist even in magmatic sulfide deposits that contain economically low-grade PGE, which emphasizes the general importance of semi-metal controls on the PGE distribution in magmatic systems. An example of this relationship is observed in the PGE mineralogy at the Voisey's Bay Ni-Cu-Co magmatic sulfide deposit in northern Labrador, where the PGE are present in low levels (approximately <0.1 ppm combined average throughout the deposit). A mass balance determined by Kelvin et al (2011) indicates that the majority of Pt, Pd, and other precious metals (PM), Au and Ag, in the Ovoid deposit at Voisey's Bay are present as bismutho-telluride phases whereas only small amounts of Pd and Ag are present in solid solution in the sulfide minerals.

What remains to be confirmed is a succinct model that explains how low levels of PGE are distributed amongst the PGM and sulfide minerals of magmatic system, and at what stage(s) during the sulfide fractionation process the PGM are crystallized. Previous research on high-grade PGE deposits suggests that three models may be possible based on observed PGE and precious-metal mineralogy amongst PGE enriched deposits. The first model involves crystallization of PGM directly from a semi-metal rich melt that formed as either a highly immiscible liquid with, or an extreme differentiation product of, an ISS-, Cu-rich sulfide melt during magmatic differentiation (Cabri and Laflamme et al., 1976; Holwell and McDonald, 2007; Huminicki et al., 2008; Helmy et al., 2007, 2010; Dare et al., 2014). Recent studies propose that the PGE form complexes with semi-metals as nano-sized clusters or particles at super solidus temperatures (Tredoux et al., 1995), with the clusters/particles acting as building blocks for the differentiated/immiscible semi-metal melt (Helmy et al., 2013). The second model suggests that PGE sulfarsenides form by subsolidus exsolution from the base-metal sulfides (pyrrhotite, pentlandite and chalcopyrite) during cooling (Hutchinson and McDonald, 2008; Dare et al., 2011; Piña et al., 2011). The third model proposes crystallization of PGM from late to post magmatic hydrothermal fluids (Farrow and Watkinson, 1999; Hanley, 2005).

In this study, the PGE, Au, Ag mineralogy and geochemistry of samples selected from the Mini-Ovoid, Southeast Extension Zone and Discovery Hill zone of Voisey's Bay deposit are evaluated. The results are compared to the precious metal mineralogy (PMM) of the Ovoid (Kelvin et al., 2011) and a hornblende-gabbro dyke located in the vicinity of the Southeast Extension zone (Huminicki et al., 2008), supplemented by new geochemical analyses made here. The data are used for the purpose of developing a model for the evolution of the low-grade PGE mineralogy at Voisey's Bay. In particular, our model focuses on PGE mineralization that has derived from a differentiated/immiscible semi-metal melt that may have consisted of high temperature PGE-semi-metal clusters. Furthermore, we investigate whether a similar model can be applied to the various sulfide zones of Voisey's Bay, and to some extent, other magmatic sulfide deposits that contain similar low abundance PGE and precious metal mineralogy. Localized semi-metal contamination from surrounding country rock is considered as a possible cause for the variability of PGM throughout Voisey's Bay.

## Background

*Geology: Voisey's Bay Cu-Ni-Co Deposit, Labrador, Canada*

The Voisey's Bay Ovoid deposit is currently being mined for Ni (2.83%), Cu (1.68%) and Co (0.12%) in surface open pit by Vale Ltd. Mining of underground sulfide deposits (up to 900 m depth) is planned to begin in 2019. The geographic location and basic geology of the Voisey's Bay Intrusion is shown in Figure 1 (Rawlings-Hinchey et al., 2003; Lightfoot et al., 2011). Details of the geology, age, mineralogy and geochemistry have been described by many workers including Lightfoot et al. (1998, 2011); Amelin et al. (1999, 2000); Li and Naldrett (1999); Naldrett et al. (2000); Ryan (2000); Lambert et al. (2000); Evans-Lamswood et al. (2000); Huminicki et al. (2012).

The ore bodies formed as a product of magmatic emplacement of the Voisey's Bay Intrusion, which is one of a number of intrusions of the Nain Plutonic Suite (NPS). The NPS is composed of intrusive bodies

of granite, anorthosite, gabbro and ferro-gabbro troctolite. The Voisey's Bay Intrusion is composed of two ca. 1.34 Ga gabbro-troctolite bodies (Western Deeps Intrusion and Eastern Deeps Intrusion), which are geographically located across a suture between the Archean Nain Province to the east and the Paleoproterozoic Churchill Province to the west. The intrusion was emplaced into the Paleoproterozoic Tasiuyak gneiss (garnet-sillimanite, sulfide/graphite-bearing quartzo-feldspathic gneiss) in the west and the Paleoproterozoic Enderbitic gneiss (quartzo-feldspathic gneiss) in the east, where it was later intruded itself by the Voisey's Bay Granite-Syenite (1305Ma; Amelin et al., 2000). West-East trending rift structures were a possible control on the distribution sites of sulfide injection configuring the ore deposits within the magmatic system (Evans-Lamswood et al., 2000; Cruden et al., 2008; Lightfoot et al., 2011).

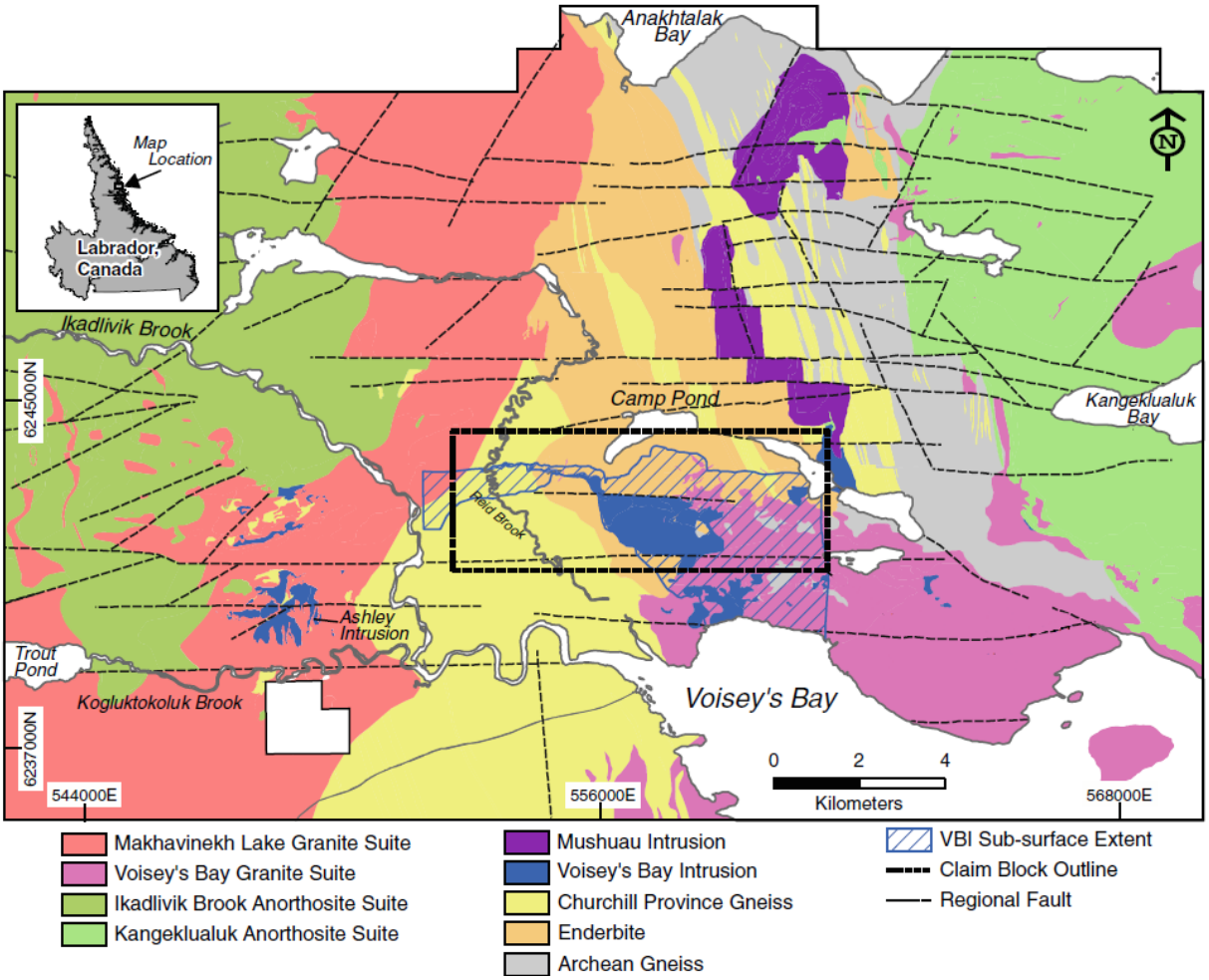


**Figure 3-1: Plan view of geology of the Voisey's Bay area** (from Rawlings-Hinchey et al., 2003; Lightfoot et al., 2011). Massive sulfide deposits are associated with the Voisey's Bay Intrusion. X-Y cross-section projection of subsurface geology shown in Fig. 2 extends from left to right across the claim block outline (dotted black rectangle).

The Western and Eastern Deeps troctolite chambers are thought to be connected by a subvertical feeder dyke (Ovoid feeder dyke). The ore bodies are divided into six geographically distinct zones, which are (from west to east): Reid Brook, Discovery Hill, Mini-Ovoid, Ovoid, Southeast Extension and Eastern Deeps (Ryan, 2000). The Ovoid, Discovery Hill and Southeast Extension zones are the focus of this study. A cross section of the zones in the subsurface is shown in Figure 2. The Eastern Deeps and the Southeast Extension zones are contained within the Eastern Deeps Intrusion, which is composed of olivine-gabbro/ferrogabbro, ferrogabbro, troctolite and olivine norite. In the Eastern Deeps, the sulfide

ore is mainly disseminated to semi-massive, although minor amounts of massive sulfide exist as small (50-100m) at the base of Eastern Deeps (Li and Naldrett, 1999).

Further east and down-plunge, the Eastern Deeps zone contains mostly disseminated to semi-massive sulfide. The Ovoid, a massive sulfide, bowl-shaped body, sits within a dilated portion of the feeder dyke (olivine-gabbro) near the contact between the Western and Eastern Deeps intrusions. To the west of the Ovoid, the massive sulfide mineralization narrows outward as a flank extending east. This smaller extension of the Ovoid is known as the Mini-Ovoid. The feeder dyke containing the Ovoid and Mini-Ovoid are in contact with the Enderbitic gneiss. A variable sized layer of "leopard troctolite" forms rims on areas of the massive sulfide of the Ovoid and Mini-Ovoid. Thin layers of brecciated fragments (consisting of large inclusions of the enderbitic gneiss incorporated into the troctolite) sit against portions of the Ovoid and Mini-Ovoid and the gneiss. The Reid Brook and Discovery Hill zones are contained within the Western Deeps Intrusion. This portion of the intrusion is composed of norite, gabbro, olivine gabbro, leucotroctolite and troctolite. In this area, the intrusion may be in chilled contact with the gneiss, or contains brecciated, fragmented inclusions (Li and Naldrett, 1999).

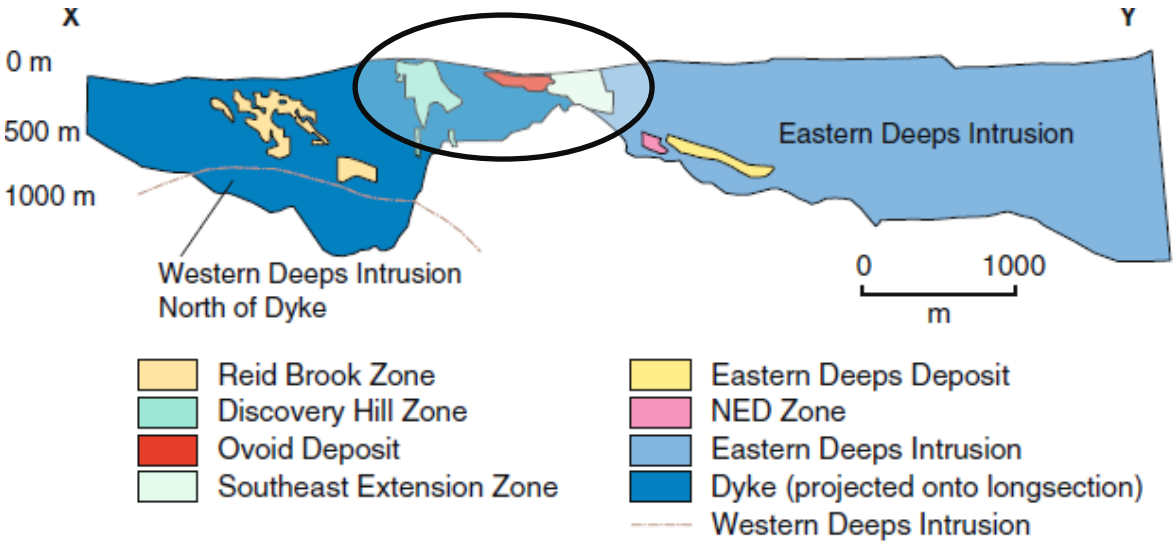


**Figure 3-2: Cross-section of Voisey's Bay deposit highlighting the main zones of mineralization** (modified from Lightfoot et al., 2011). Deposits shown within the black oval are the subjects of this study.

An important aspect of the generation of Voisey's Bay ore is the significant amount of contamination of the magmatic system by the crustal country rocks. Petrographic, mineralogical and geochemical evidence indicates that ore generation was achieved through two separate pulses of magma entering and interacting with the crustal gneisses (Li and Naldrett, 1999). Support for country rock contamination is evident from inclusions of Tasiuyak paragneiss in conduit breccia rocks, which contain reaction rims (Li and Naldrett, 2000); S and O isotope (Ripley et al., 1999, 2000) and Sr and Nd isotope (Amelin et al., 2000) studies of the Voisey's Bay intrusion and surrounding country rocks; and in Re-Os isotope data from sulfide samples from the various ore environments (Lambert et al., 1999, 2000).

*Platinum-Group Element Mineralogy at Voisey's Bay*

For the massive sulfide samples in the Ovoid, a mass balance of PGE, Au and Ag mineralization indicates that these metals are present mainly as discrete PMM of arsenide, bismuthide and telluride phases (Kelvin et al., 2011). The major phases are sperrylite ($PtAs_2$), 92.4% volume, and froodite ($PdBi_2$), 7.5% volume. The sperrylite occurs as large (76 µm on average) crystals commonly found associated with galena, PMM and breithauptite (NiSb); it is liberated easily during sample disaggregation. The froodite normally occurs as fine-grained (typically below 5 µm) inclusions or larger attachments (10-50 µm) to pentlandite and galena. Most often, the PMM were found to be associated with pentlandite and galena, less often with chalcopyrite and rarely with pyrrhotite and magnetite. Additionally, a number of the PMM were found as attachments to trace phases also containing Bi, Te, Pb and Sb (breithauptite NiSb, altaite PbTe, native Bi and tsumoite BiTe).

In the hornblende-gabbro dyke from the Southeast Extension studied by Huminicki et al. (2008), the sulfide mineralization is disseminated in leucocratic to melanocratic hornblende gabbro/gabbronorite. The sulfide mineralization consists of pyrrhotite, pentlandite, chalcopyrite, minor bornite and trace galena. Most PMM are found associated with Cu-rich sulfide assemblages (chalcopyrite and bornite) and, to a lesser extent, galena and pentlandite. The majority of these PMM are sperrylite ($PtAs_2$, 55.9% vol.),

native-Ag (24.1% vol.), stutzite ($Ag_{5-x}Te$, 7.55% vol.), electrum (Au-Ag, 2.68% vol.), paolovite ($Pd_2Sn$, 2.4% vol.), froodite ($PdBi_2$, 2.24% vol.) and Sn-stibiopalladinite [Pd(Sn,Sb), 2% vol.]. Also, Pd is present in pentlandite (2 ppm) and galena (1.8 ppm).

**Methods**

Because the abundances of PGE and precious metal minerals are so low at Voisey's Bay, conventional methods of sample preparation including disaggregation and concentration are more difficult. For this reason, we chose advanced methods of sample preparation and analysis strategies (explained below) that would increase the chances of locating the rare minerals within the bulk sample.

Eight sulfide-bearing samples containing anomalous, elevated PM concentrations in whole rock specimens were selected for this study. This included: four samples of massive sulfide from the Ovoid zone which were used in Kelvin et al. (2011) (one each from drill cores BS0241, BS0207; and two, DF6063, DF6055 from VB95008); one semi-massive sulfide sample from the Mini-Ovoid zone (BS0265); two disseminated to semi-massive sulfide samples (VX49277, VX49289) from the Discovery Hill zone (drill core VB04614); and, a PGE poor sample (Diss Ovoid) from the outer Ovoid (drill hole BS0218) that was analyzed to compare the amount of PGE, Au and Ag in solid solution in the sulfide phases to the PGE enriched samples.

The locations of the drill holes are shown in Figure 3. The mineralogy of the samples discussed in this paper may not be representative of the mineralogy in areas of Voisey's Bay deposit that contain even lower grades of PGE, Au and Ag, but do represent domains within the deposit that contain the most statistically significant numbers of PMM.

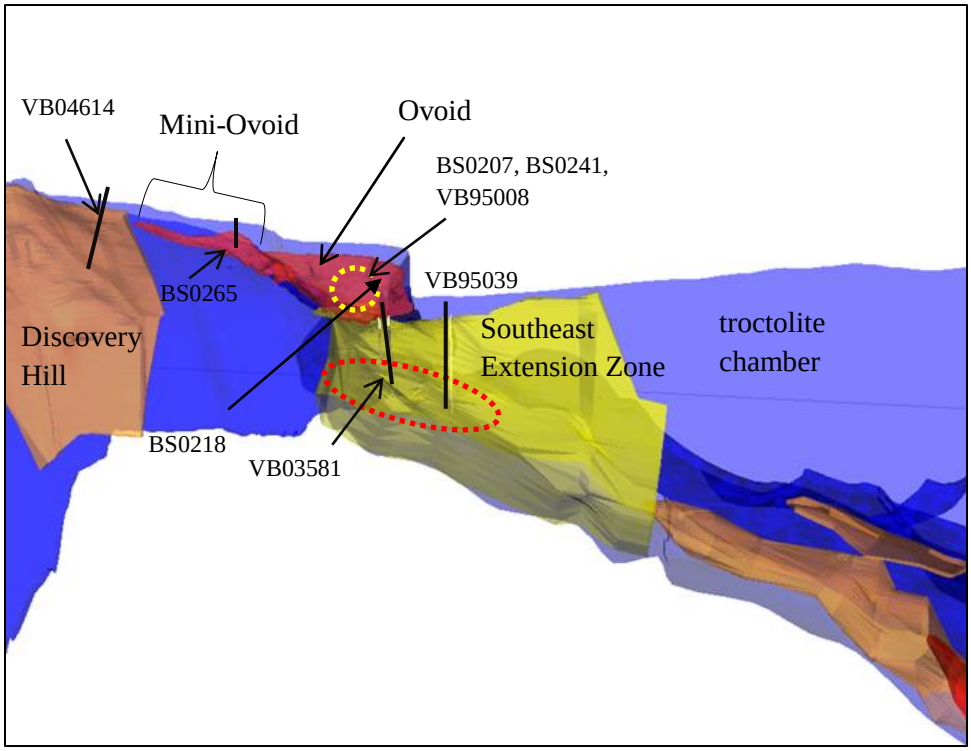


**Figure 3-3: North-west facing projection of the mid-region of Voisey's Bay deposit**. The relative locations of the samples and drill holes used in this study are shown, including those from the Ovoid (outlined by yellow dotted circle) from Kelvin et al. (2012) and Southeast Extension Zone (outlined by red dotted circle) from Huminicki et al. (2008).

Between 0.5 and 1 kg of each of the seven samples was taken from a 1m section of drill core provided by Vale Ltd. Half of each sample was analyzed for whole rock concentrations of Cu, Fe, Ni and Pb by ICP-OES and ICP-MS (at Memorial University of Newfoundland) and for PGE by Ni-fire assay and Sb, Sn, Bi, Te, Re, Ag and Au by ICP-MS (Activation Labs, Ancaster, Ontario). The same analyses for Sb, Sn, Bi, Te, Ag and Au were determined for four, PMM-enriched sulfide samples from the Southeast Extension Zone from Huminicki et al. (2008).

The remaining portions of the eight samples were broken with a hammer into centimetre-sized pieces and processed using a CNT-MC Spark-2 electric pulse disaggregator (EPD) (Cabri et al., 2008) to liberate the precious minerals. This method was used in place of conventional crushing because it separates minerals along grain boundaries using explosive forces, preserving original grain shapes. EPD was advantageous because we were able to keep the original PGM grains intact.

The EPD residues were screened into 4 size-fractions (-180/+125µm, -125/+75µm, -75/+45µm and -45µm) and were further processed with a CNT-MC H11 hydro separator (Cabri et al., 2008) to concentrate and isolate the precious metal minerals. Two monolayer polished grain mounts were prepared from the hydro separated concentrates of each size-fraction for mineralogical test work. The preparation was done by carefully distributing a single layer of the concentrate material onto double sided tape and then mounted in epoxy resin in order to avoid excessive contact of particles. Two sections of each concentrate were prepared to increase the number of particles measured by MLA.

Laser ablation inductively coupled plasma mass spectrometry (LA-ICPMS) analyses were made on the major sulfide minerals (pyrrhotite, chalcopyrite, pentlandite) and galena, to determine the concentrations of PGE, Au, Ag, Bi, Te, Sb, As and Sn present in these phases. LA-ICPMS analysis for Bi, Te, Sb, As and Sn in the sulfides were made for the Ovoid, Mini-Ovoid and Discovery Hill samples. But LA-ICPMS analysis for PGE, Au and Ag in the sulfides was determined for only the Mini-Ovoid and the Discovery Hill samples, because Kelvin et al. (2011) previously reported data for these metals in the Ovoid samples. The Ovoid and Southeast Extension zone are the only areas of the deposits that contained galena with grain sizes that were large enough to obtain accurate results with the laser beam diameter size of 30 µm. Huminicki et al. (2008) previously reported concentrations of PGEs and semi-metals in sulfides from the Southeast Extension zone.

The LA-ICPMS analysis was carried out at Memorial University of Newfoundland using an ELEMENT XR high-resolution mass-spectrometer coupled with a GEOLAS 193 nm excimer laser system for in-situ measurement; or, the measurements were completed at Laurentian University using a Thermo Fisher X Series II quadrupole LA-ICPMS. Standard reference materials, Po41, Po689, Po727 and Mass-1 (Sylvester et al., 2005; Wilson et al., 2002) were ablated before and after the set of runs for calibration. Before and after each spot test, 30 seconds of background was collected to monitor for background interferences. The LA-ICPMS procedure used for these measurements is outlined in Sylvester (2001).

Calculations to correct for isobaric mass interferences of Ni- and Cu-argides on the light PGE (Pd, Ru, and Rh) were up to 50%.

Mineralogical characterization was completed using an FEI Quanta 400 or a Quanta 650F Mineral Liberation Analyzer (MLA) (Fandrich et al., 2007) at Memorial University of Newfoundland. The characterization was completed for samples from the Mini-Ovoid and the PGE poor sample from the Ovoid. This data was compared the PGE and PM studies from Kelvin et al. (2012) and Huminicki et al. (2008).

The MLA is equipped with specialized software that quantifies mineralogical image analysis data generated by a scanning electron microscopy/energy dispersive X-ray spectroscopy (SEM-EDX) system. The software uses a combination of back-scattered electron (BSE) imaging and rapidly acquired X-rays to identify mineral species and produce colour coded particle maps. This software package includes a rare phase mineral search, which is capable of detecting micron-sized PMM within a polished section based on backscattered-electron intensity differences and identifying them using a full spectrum EDX match to a reference library of PMM. This method was ideal for our analysis since the PMMs at Voisey's Bay are low in abundance and small in size, making them difficult to locate. Electron-Probe Microanalysis (EPMA) for quantitative chemical composition was made of PMM with grain-sizes larger than 10 µm at the University of Toronto using a Cameca SX-50 instrument. Analytical details describing the run conditions are provided in Appendix 3.

The LA-ICPMS results were combined with the MLA results to produce a deportment of the Pd, Ag, Au and semi-metals (As, Se, Sn, Sb, Te and Bi). The calculations used for the deportment are summarized in Kelvin et al. (2011). The modal abundances of the sulfide phases used for these calculations are estimated based on whole-rock Cu, Ni, Fe and S concentrations, following the procedure outlined by Huminicki et al. (2005).

Finally, Ni, Cu, Fe, S and semi-metal assays were carried-out for 23 samples that represent typical magmatic and country rock types in and around the Voisey's Bay deposit. The rock-types include Tasiuyak (7 samples) and Enderbitic (5 samples) gneisses, tonalite (Enderbitic 1 sample), quartz-diorite (Enderbitic, 1 sample) which are suggested sources of sulphur and silica contamination to Voisey's Bay system (e.g., Ripley et al., 2000; Amelin et al., 2000); Voisey's Bay granite-syenite (3 samples); unmineralized gabbro (5 samples) and troctolite (3 samples) rocks of the Voisey's Bay intrusion. These samples were also used in Rawlings-Hinchey et al. (2003) and were selected based on rock type and location. The purpose of this analysis was to determine if any country rocks contain significant concentrations of semi-metals compared to unmineralized troctolites and gabbros which host the precious-metal minerals. Any semi-metal enrichments in the country rocks may suggest localized contamination of the magmatic sulfide system. No further mineralogical analysis was performed on these samples.

**Sample Descriptions**

*Massive Sulfide - Ovoid*

The mineralogy of the massive sulfide samples used for the PGE study are described in Kelvin et al. (2011) but are also summarized again here. The four massive sulfide samples from the Ovoid zone contain similar mineralogy and textures. All four samples consist of massive pyrrhotite containing exsolved lamellae of troilite and minor exsolved pentlandite. Coarse-grained, centimetre-sized, euhedral pentlandite and fine to coarse-grained mm to cm-sized chalcopyrite are present within the pyrrhotite groundmass. Normally, the pentlandite and chalcopyrite occur together forming a patch-like texture instead of chalcopyrite bands rimmed by pentlandite, which is seen in some areas of the Ovoid. Depending on grain-size, the abundances of chalcopyrite and pentlandite can vary throughout the core interval, where coarser grained areas contained more chalcopyrite and pentlandite. Care was taken to

select the sample from an area that is most representative of the core. Cumulate grains of magnetite occur interstitial to pyrrhotite and chalcopyrite. Galena is present in our samples at trace amounts and is visible within the dissected core. The galena is found mostly (>90%) between chains of cumulate magnetite grains, but also peripheral to chalcopyrite and pentlandite. Examples of the massive Ovoid sulfide mineralization are shown in Figure 4 a-d.

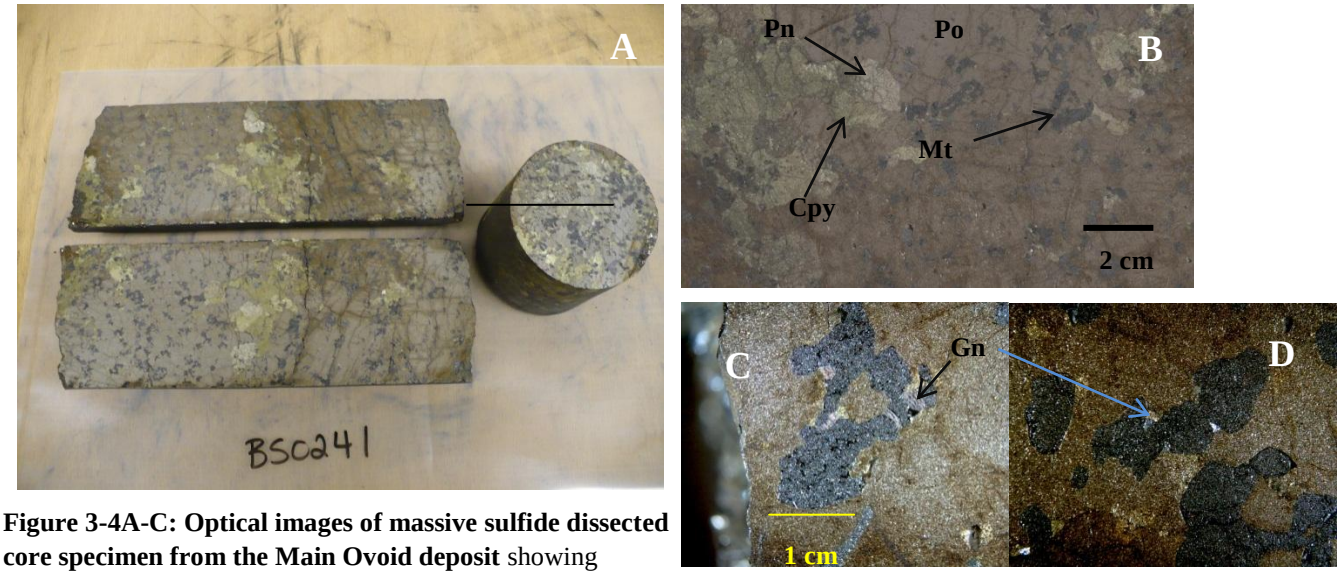


**Figure 3-4A-C: Optical images of massive sulfide dissected core specimen from the Main Ovoid deposit** showing average texture and grain-size of the four samples; Pn=pentlandite, Mt=magnetite, Cpy=chalcopyrite, Po=pyrrhotite, Gn=galena. The width of the core is 11 cm.

*Semi-massive sulfide – Mini-Ovoid*

The semi-massive sulfide sample was selected from the north side of mini-Ovoid flank near a contact between the feeder olivine-gabbro and enderbitic gneiss (depth = 83.7-85.2 m). The semi-massive sulfide bearing gneiss contains almost equal parts pyroxene and olivine (30-40%), moderate plagioclase and minor biotite. The silicate minerals are fine-grained and appear to form striated textures near the sulfide minerals. The 1 m core interval hosts large quartz inclusions and veins, 20-30 cm in width, in the upper portion of the interval.

Sulfide mineralization occurs as bands of pyrrhotite, chalcopyrite and pentlandite, and is present in amounts of 30-60% in the core interval. Pyrrhotite occurs as large bands (2-10 cm wide) rimmed by chalcopyrite-rich stringers. Chalcopyrite is more abundant than pentlandite in this sample. Some exsolution lamellae of troilite is present within in pyrrhotite, but does not occur as commonly as in the Ovoid massive-sulfide samples. Pentlandite occurs as coarse grains within pyrrhotite and sometimes with chalcopyrite. Minor amounts of fine-grained, speckled magnetite are found associated with sulfides, mostly within pyrrhotite masses. No galena is present in this sample. The section of core used for this study is shown in Figure 5.

Naldrett et al. (2000) suggested that the chalcopyrite-rich stringers from this area may have formed by the remobilization of an unfractionated (eutectic), Cu-rich liquid by subsequent magmatic influxes; or that the stringers may have crystallized from a differentiated liquid formed during initial fractional crystallization of the sulfide melt.

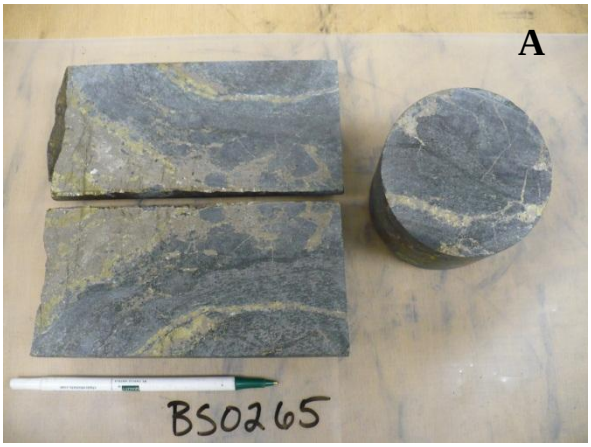


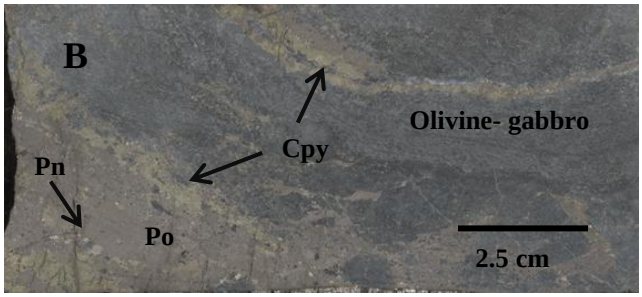


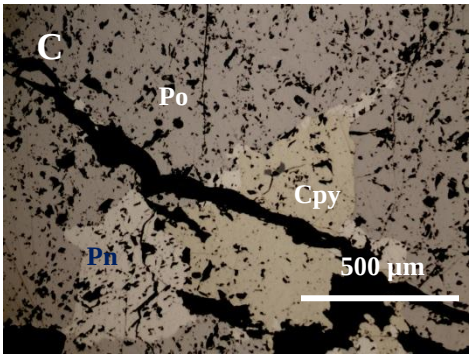


**Figure 3-5A-C: Optical images of semi-massive sulfide specimen from the Mini-Ovoid** showing texture of sulfides. C is reflected light microscopy. Pn=pentlandite, Cpy=chalcopyrite, Po=pyrrhotite. The diameter of the drill core is 11 cm.

*Disseminated – Discovery Hill*

Both of the samples from Discovery Hill are taken from the same drill core and are within the same interval. The samples contain similar mineralogy, but the sulfides differ in their proportions and textures. The sulfide minerals are hosted by olivine-gabbro. In the semi-massive sulfide sample, sulfide is present in amounts between 30-50% along the core interval and occurs as finer disseminations that are chalcopyrite rich. The chalcopyrite forms patch-like textures with fine-grained pyrrhotite and pentlandite ranging from 1-3 cm in size (Figure 6).

Pyrrhotite is the dominant sulfide mineral in the semi-massive sulfide sample. Exsolution lamellae of troilite occur much less commonly in the Discovery Hill samples than in the Ovoid samples. The pentlandite and chalcopyrite have smaller grain-sizes (<1 cm) than in the Ovoid, and tend to occur as loop structures around pyrrhotite.

Galena is present in trace amounts, has very fine grain-sizes (<10 μm) and is found as inclusions within other sulfides. Minor amounts of magnetite are present and occur as fine-grained crystals associated with both sulfides and silicate phases. The sulfide mineralogy is present in amounts of 40-70% along the core interval. Pentlandite is more abundant than chalcopyrite.

The silicate mineralogy associated with both the disseminated and semi-massive sulfide consists largely of olivine, pyroxene and plagioclase, with trace hornblende and biotite. Mostly, the silicate minerals are fine-grained (<1 cm) and occur as interstitial groundmass. No large inclusions of country rock or brecciated textures are apparent in this core sample.

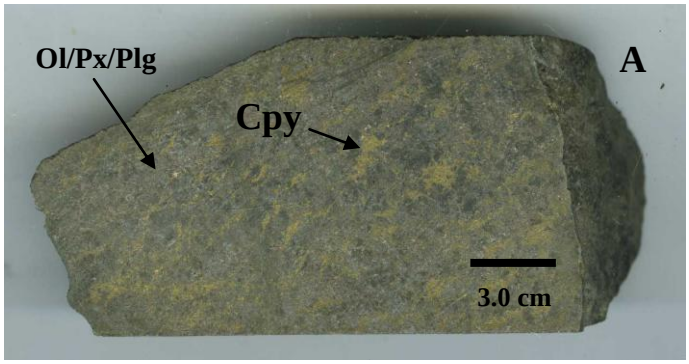


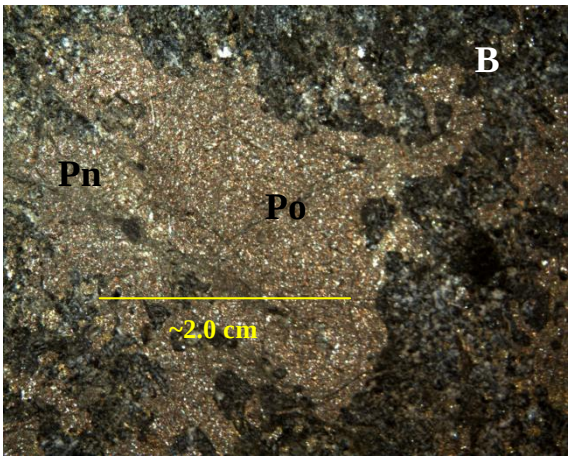


**Figure 3-6A-B: Optical images of specimen of disseminated and semi-massive sulfide core from Discovery Hill**. Pn=pentlandite, Cpy=chalcopyrite, Po=pyrrhotite. Diameter of core is approximately 8.5 cm

The PGE poor sample was included in the study in order to determine if any PGE was present in solid solution in pentlandite, pyrrhotite or chalcopyrite where PGE concentrations in the Ovoid are minimal. This sample was taken from a drill hole located at the outer portion of the Ovoid where the massive sulfide mineralization meets troctolite feeder on the southeast side. The PGE poor sample has a disseminate sulfide texture. Pyrrhotite is the dominant sulfide mineral, but is less abundant than in the massive sulfide samples. However, pentlandite and chalcopyrite are present in amounts similar to the pentlandite and chalcopyrite in the massive sulfide samples. Cubanite occurs infrequently in chalcopyrite. The sulfides produce patch-like textures (~1 cm) with one another that are interstitial to silicates. The sizes of the patch-like sulfide structures are consistent throughout the core.

The silicate minerals identified in the core are dominated by olivine and plagioclase. Minor pyroxene, biotite and hornblende are present, and may form rims around sulfide blebs. Magnetite is present in amounts of <10% and is associated with both silicate and sulfide minerals. Images are provided in Figure 3-7 to show examples of the textures.

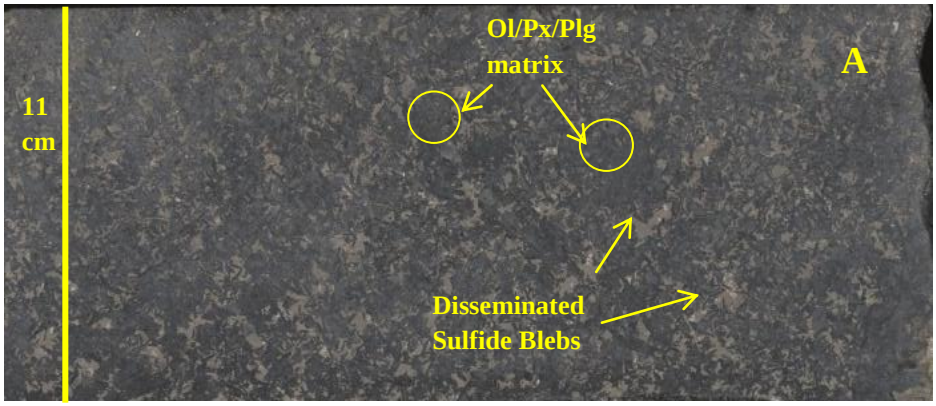


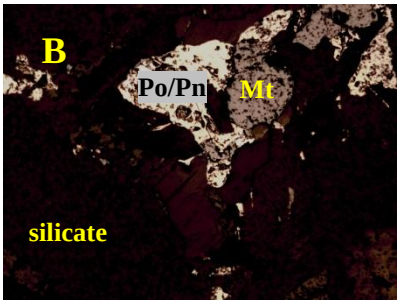


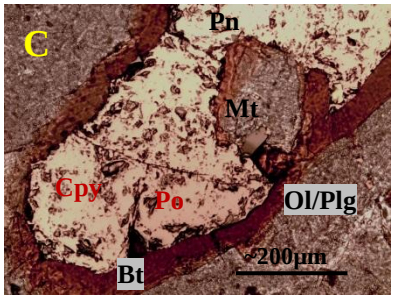


**Figure 3-7A-C: Optical images of specimen of disseminated to semi-massive sulfide "PGE" poor sample from the Outer Ovoid**. Pn=pentlandite, Cpy=chalcopyrite, Po=pyrrhotite, Ol=olivine, Plg=plagioclase. Diameter of core is approximately 8.5 cm

## Results

*MLA Results: Precious Metal Mineralogy*

A summary of the PMM and other trace phases containing, Bi, Te, As and Sb detected by the MLA from Discovery Hill and the Mini-Ovoid are presented below in Table 1. The results from Kelvin et al. (2012) and Huminicki et al. (2008) are also shown for comparison. Minerals with grain-sizes < 2µm are not detected by MLA with the run set-up. The smallest estimated average grain-size reported is 2µm.

**Table 3-1: Precious and Semi Metal Mineral Phases Detected by MLA**

| Area and Mineralization | Mineral | # of Grains | G.S | Mass (%) | Association (number of grains) | Major Assocation |
|---|---|---|---|---|---|---|
| Ovoid MASU | Froodite ($PdBi_2$) | 264 | 4 | 8.63 | Pn (136), Gn (43), Mt (22), Cpy (7), PbTe (2), NiSb (2), Sper (1), Mich (2), Elec (1), Bi (1) | Pn/Gn |
| | Michenerite PdBiTe or Sb-Michenerite* | 28 | 3 | 0.01 | Pn (16), Gn (4), Cpy (4), Po (3), Ele (1), Fr (2), BiTe (1) | Pn/Gn |
| | Sperrylite, $PtAs_2$ | 3 | 76 | 90.07 | Gn (2), Liberated (1), Breith (1), Fr (1) | Liberated/Gn |
| | Electrum, AuAg | 10 | 6 | <0.01 | Pn (4), Cpy (3), Po (3), Gn (1), Fr (1), Mich (1) | Pn/Cpy |
| | Völynskite ($AgBiTe_2$) | 27 | 2 | <0.01 | Gn (21), Pn (6), Cpy (2) | Gn/Pn |
| | Stützite ($Ag_{5-x}Te$) | 12 | 5 | 0.03 | Gn (5), Cpy (5), Po (4), Pn (4) | Sulphides |
| | Acanthite ($Ag_2S$ | 2 | 3 | 0.00 | Pn (2) | Pn |
| | Altaite (PbTe) | 14 | 10 | 0.74 | Gn (9), Cpy (3), Pn (1), Po (4), Fr (2) Bi-Te (1) | Gn/Cpy |
| | Native-Bi | 14 | 6 | 0.49 | Gn (12), Pn (3), Cpy (1), Fr (1), Other (1) | Gn/Pn |
| | Bi-Te | 32 | 2 | 0.01 | Gn (31), Pn (2) | Gn |
| | Pb-Ag-Te | 3 | 4 | <0.01 | Gn (3) | Gn |
| | Breithauptite (NiSb) | 3 | 4 | <0.01 | Pn (2), Spy (1), Gn (1), Fr (1) | Pn/PGM/Gn |
| Mini-Ovoid Semi-MASU | Froodite ($PdBi_2$) | 8 | 2 | 8.8 | Pn (8) | Pn |
| | Ir As? | 6 | 2 | 0.8 | Pn (5), Po (1) | Pn/Po |
| | ReCu/ReCuS | 5 | 2 | 0.9 | Pn (3), Cpy (2) | Pn/Cpy |
| | Völynskite ($AgBiTe_2$) | 1 | 3 | 0.4 | Pn (1) | Pn |
| | Stützite ($Ag_{5-x}Te$) | 12 | 4 | 89.1 | Po (19), Cpy (3), Pn (3), Chl (1) | Po/Cpy |
| Discovery Hill Semi-MASU to DISS | Sperrylite, PtAs2 | 1 | 86 | 99.05 | Liberated | Liberated |
| | Stutzite | 44 | 3 | 0.87 | Po (19), Pn (16), Mt (4) Cpy (4) | Po/Pn |
| | Michenerite PdBiTe or Sb- | 3 | 5 | 0.07 | Pn (2), Po (1) | Pn/Po |
| | Electrum | 1 | 10 | 0.006 | Pn (1) | Pn |
| | volynskite | 1 | 3 | 0.004 | Pn (1) | Pn |
| Southeast Extension Zone | Sperrylite, PtAs2 | 88 | NA | 55.9 | Cpy (25), Lib (20), Bn (17), Sz (14), Gn (6), Pn (6), ele (4), Prk 93), Ag (3), Px (3), PGM (1) | Cu-sulphides/lib/P |
| | Paolovite ($Pd_2Sn$) | 29 | NA | 2.4 | PGM (9), Cpy (5), Bn (5), lib (4), Pn (2), Pl (2) | PGM/Cu-S |
| | Froodite (PdBi2) | 15 | NA | 2.24 | Gn (7), Lib (4), PGM (2), Cpy (1), Px (1) | Gn/Lib |
| | Sn-Stibiopalladinite | 5 | NA | 2 | PGM (2), Lib (1), Cpy (1), Sz (1), Ag (1), Px | PGM/PMM |
| | Pd-Bi-Sb-Te (michenerite) | 17 | NA | 0.97 | PGM (9), Gn (5), Sz (3), Lib (2), Cpy (1), Ag (1) | PGM/Gn |
| | Maslovite | 5 | NA | 0.59 | Lib (5) | Liberated |
| | Platarsite | 3 | NA | 0.28 | Lib (1), Cpy (1), Gn (1) | Gn/Cpy |
| | Other Rare PGM | 22 | NA | <0.01 | | |
| | Native-Ag | 188 | NA | 24.1 | Lib (72), Bn (43), Gn (33), Cpy (29), Pn (17), Other (5) | Liberated/ Cu-S/Gn |
| | Stutzite | 61 | NA | 7.55 | Gn (32), Cpy (15), PGM (12), Lib (10), Bn (4), Other (3) | Gn/Cpy/PGM |
| | Electrum | 35 | NA | 2.68 | Lib (30), Cpy (3), Bn (1), Hn (1) | Liberated |
| | Matildite | 4 | NA | 0.12 | Gn (4) | Gn |
| | Other Rare PMM | 7 | NA | 0.08 | | |

G.S. = Estimated average grain size in μm (calculated equivalent circle diameter),Data from the Southeast Extension zone are from Huminicki et al. (2008); Pn = Pentlandite; Gn = Galena; Po = Pyrrhotite; Cpy = Chalcopyrite; Bn = Bornite; Mt = Magnetite; Spy = Sperrylite; Ele = Electrum; Fr = Froodite; Mich = Michenerite; Breith = Breithiauptite; Px = Pyroxene; Hn = Hornblende; Cl = Chlorite; Lib = Liberated

The Mini-Ovoid sample contains very few Pd-PGM and no Pt-PGM. Only 8 grains of froodite were detected. However, 6 grains of an Ir-As phase and 5 grains of Re-Cu phase were found. Both of these phases are very fine grained (<3 μm) and were present in chalcopyrite, pyrrhotite or pentlandite. Stutzite is the most abundant PMM and contributes to 89% of the total PMM mass.

In the Discovery Hill sample, sperrylite is the major PGM contributing to a large proportion of the total PMM mass because of its large grain-size. A large number of stutzite grains were identified and were mostly present in pyrrhotite and pentlandite. One grain of electrum was detected; it is situated at the boundary of a pentlandite grain. No froodite was detected in these samples, but michenerite is present. Only 3 grains of altaite, 2 grains of a Ni-As phase and one grain of breithauptite were detected in the Discovery Hill samples.

Although the PMM from the Ovoid and the Southeast Extension zone were not analyzed in this study, the results from Kelvin et al. (2011) and Huminicki et al. (2008) are summarized for comparison. In the Ovoid, a number of bismutho-telluride phases were detected along with the PMM. The bismutho-telluride phases present include altaite (PbTe), a Bi-Te phase, native-Bi, and rare grains of a Pb-Ag-Te phase and breithauptite (NiSb). The mineral identities of the Pb-Ag-Te and Bi-Te phases were not determined because they were too small to be analyzed by EPMA.

The majority of the altaite and some of the other bismutho-telluride phases have round, bleb-like textures and are very fine (<5-10 μm) inclusions in galena. In one sample (sample located at the greatest depth in Ovoid), the altaite blebs occur more frequently and are larger and easily detected optically with a microscope. These phases are also occasionally associated with pentlandite, chalcopyrite and PMM, and rarely with pyrrhotite. In a few cases, very fine stutzite grains that were associated with pyrrhotite were found within troilite lamellae (Figure 8F).

The samples from the hornblende-gabbro dyke in the Southeast Extension zone contain the most abundant PMM. In particular, native-Ag and electrum are much more abundant by mass than in the Ovoid, Mini-

Ovoid or Discovery Hill samples. No Sn-bearing PMM are detected although 34 Sn-bearing PGM were identified in the Southeast Extension zone samples. Huminicki et al (2008) also indicates that several grains of Bi-Te were also found.

BSE images acquired with the SEM are provided below to show examples of the associations, textures and grain-sizes of the PMM from the Ovoid, Mini-Ovoid and Discovery Hill. Figures 3-8A through 3-8F are images of a mounted block of massive sulfide ore taken from drill hole VB95008 and from the same 1 m interval which MK95008A and B were selected. The sample used in this polished block has not been processed by EPD to separate mineral grains in order to capture images of the in-situ associations and textures of the PMM. The in-situ textures highlight the considerable association of galena and magnetite, and between PMM and galena.

The remaining figures are BSE images of PMM grains that were detected in the samples processed by EPD. Figures 3-9A through 3-9F are images of PMM from the Ovoid. Figures 3-10A through 3-10F are photomicrographs of PMM from the Mini-Ovoid, and Figures 3-11A through 3-11F are images of Discovery Hill. The SEM images demonstrate the large grain-sizes of sperrylite and the very fine grain-sizes of the other PMM.

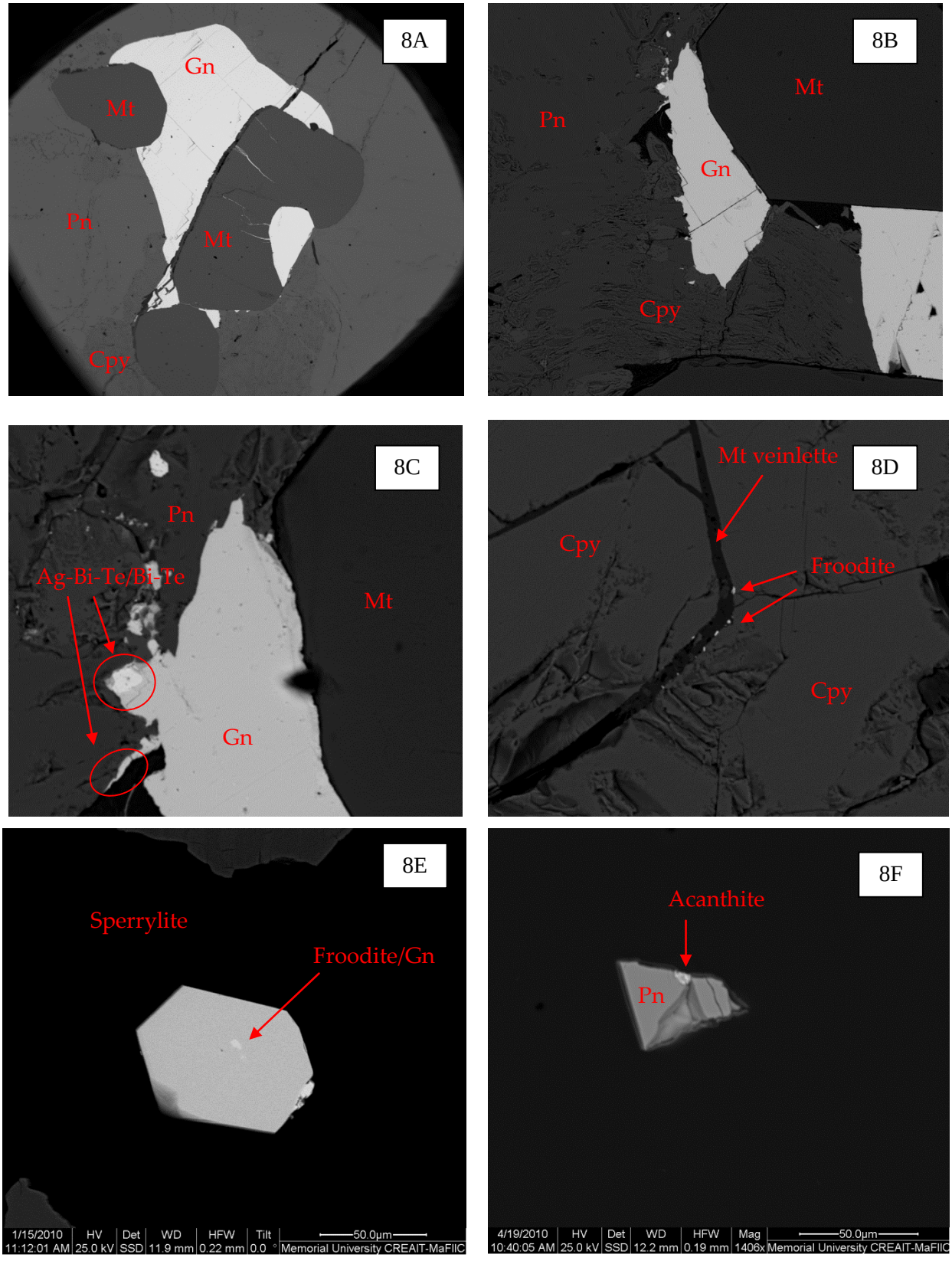


**Figures 3-8 A – F. SEM images of unprocessed massive sulfide rock from the Ovoid** mounted in a polished section showing in-situ textures of PMM and other trace phases with magnetite (Mt) and galena (Gn).

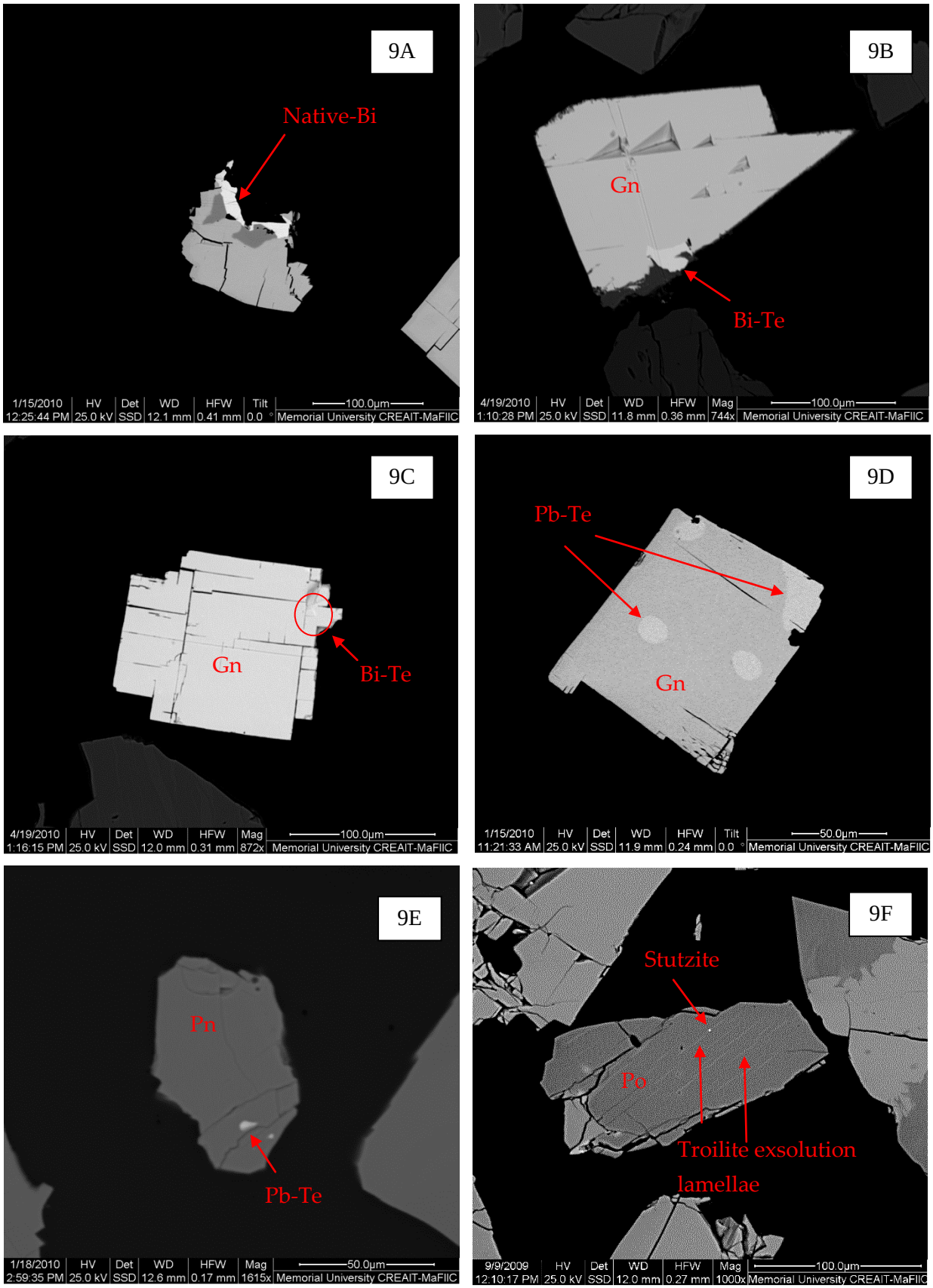


**Figures 3-9 A – F. SEM images of PMM from EPD processed massive sulfide ore from the Ovoid region**. Pn=pentlandite, Cpy=chalcopyrite, Po=pyrrhotite, Gn=galena

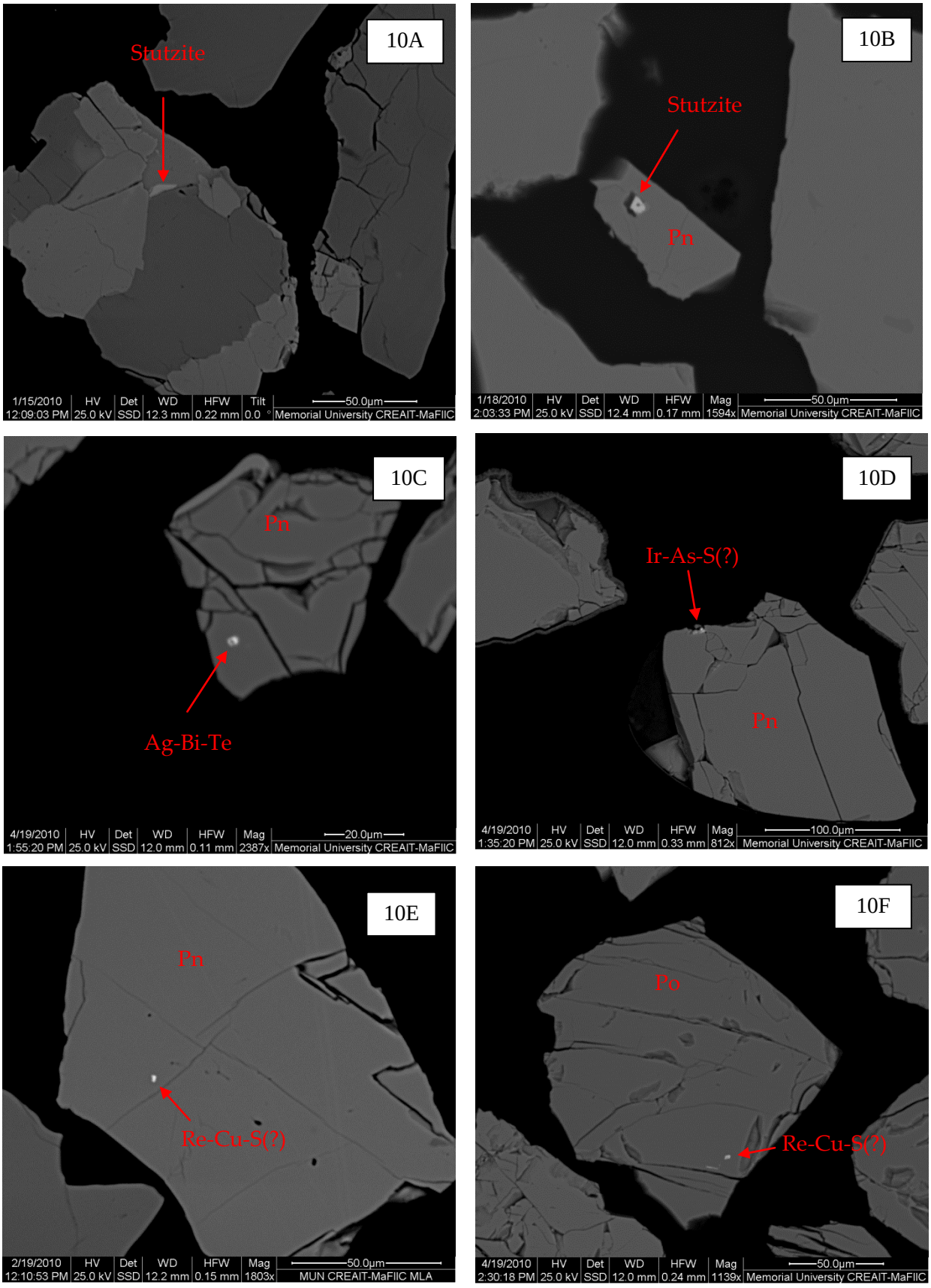


**Figures 3-10 A – F. SEM images of PMM from EPD processed semi-massive sulfide ore from the Mini-Ovoid** region. Pn=pentlandite, Cpy=chalcopyrite, Po=pyrrhotite

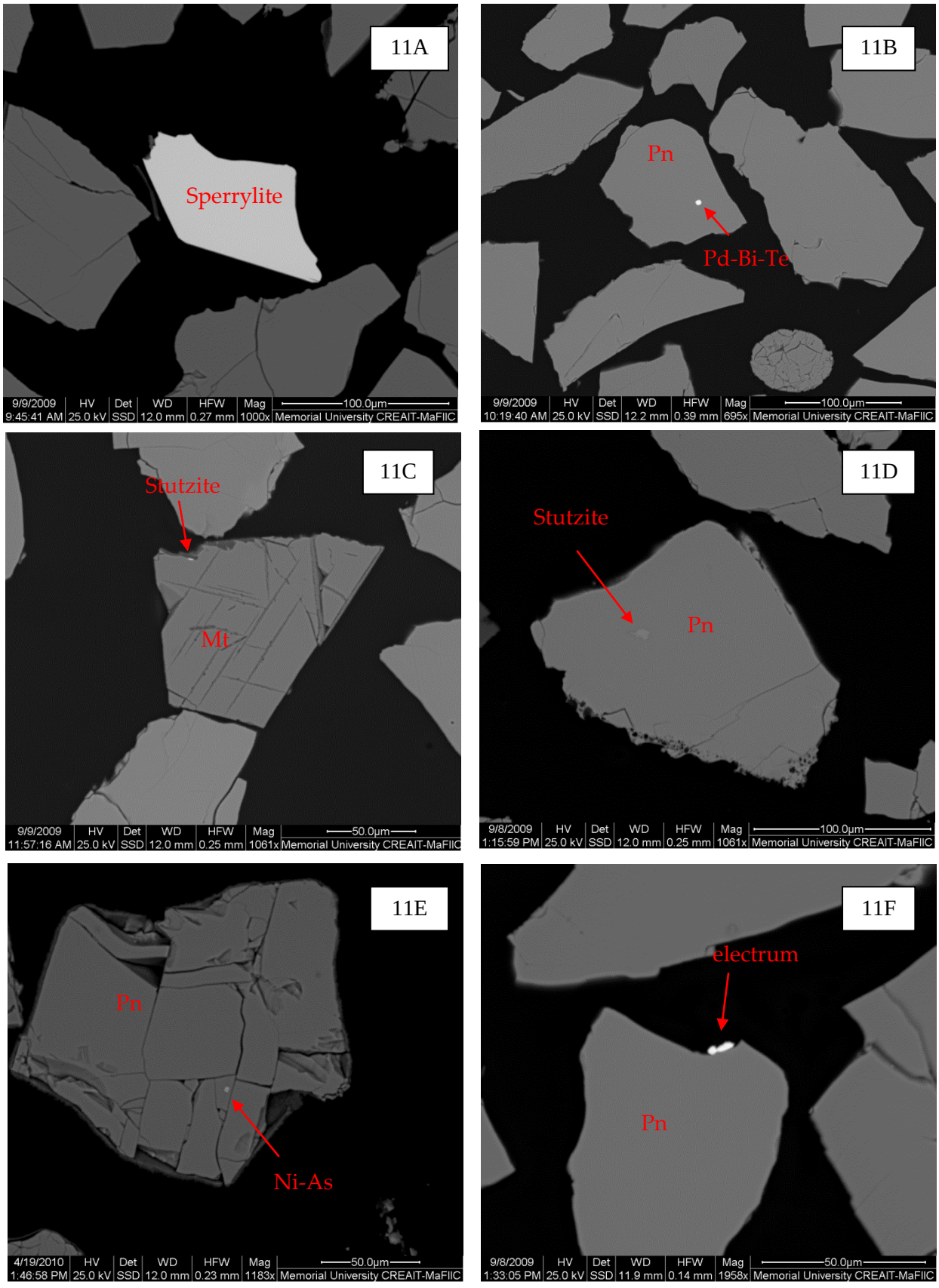


**Figures 3-11 A – F. SEM images of PMM from EPD processed semi-massive/disseminated sulfide ore from the Discovery Hill** region. Pn=pentlandite, Cpy=chalcopyrite, Po=pyrrhotite, Mt=magnetite

*EPMA of Sulfides and PMM*

The average compositions determined by EPMA for the sulfide minerals and the PMM that had grain-sizes greater than 5-10 µm are given in Table 3-2. The compositions of mineral grains that are <10 µm could not be quantified accurately by EPMA. The EPMA results from the Ovoid (Kelvin et al., 2011) are provided for comparison.

**Table 3-2: Electron Probe Micro-Analysis (EPMA) (average wt.%)**

| Mineral | Fe | Ni | Cu | Co | S | Pb | Pt | Pd | Ir | Re | Te | Sb | Sn | Ag | Bi | As | Au | Se |
|---|---|---|---|---|---|---|---|---|---|---|---|---|---|---|---|---|---|---|
| **Sulphides** | | | | | | | | | | | | | | | | | | |
| **Ovoid*** | | | | | | | | | | | | | | | | | | |
| Pyrrhotite (n=21) | 63.1 | 0.21 | 0.02 | <det | 36.5 | | | | | | | | | | | | | <det |
| Pentlandite (n=27) | 34.3 | 31.2 | 0.02 | 1.06 | 33.0 | | | | | | | | | | | | | <det |
| Chalcopyrite (n=13) | 31.0 | 0.55 | 33.4 | 0.01 | 34.5 | | | | | | | | | | | | | 0.02 |
| Galena (n=21) | | | 0.02 | | 13.4 | 86.8 | | | | | | <det | | 0.02 | 0.14 | | | |
| **Mini-Ovoid** | | | | | | | | | | | | | | | | | | |
| Pyrrhotite (n=7) | 61.7 | 0.46 | 0.01 | <det | 37.3 | | | | | | | | | | | | | |
| Pentlandite (n=7) | 30.9 | 34.2 | 0.02 | 1.19 | 33.0 | | | | | | | | | | | | | |
| Chalcopyrite (n=9) | 31.0 | 0.32 | 33.6 | <det | 34.5 | | | | | | | | | | | | | |
| **Discovery Hill** | | | | | | | | | | | | | | | | | | |
| Pyrrhotite (n=5) | 62.0 | 0.40 | 0.006 | <det | 36.9 | | | | | | | | | | | | | |
| Pentlandite (n=5) | 32.4 | 32.5 | 0.005 | 1.36 | 33.1 | | | | | | | | | | | | | |
| Chalcopyrite (n=5) | 31.4 | 0.31 | 34.0 | <det | 34.2 | | | | | | | | | | | | | |
| **TRACE PMM** | | | | | | | | | | | | | | | | | | |
| **Ovoid*** | | | | | | | | | | | | | | | | | | |
| Sperrylite (n=3) | 0.09 | 0.03 | | | <det | 0.22 | 57 | 0.03 | | | 0.01 | 0.07 | <det | 0.01 | <det | 42.8 | <det | 0.47 |
| Froodite (n=3) | 0.94 | 0.46 | | | 0.1 | <det | <det | 22.2 | | | 0.05 | <det | | 0.07 | 76.6 | 0.15 | 0.59 | <det |
| Electrum (n=1) | 0.21 | 0.26 | | | 0.07 | | 0.06 | | <det | <det | <det | | | 42.7 | 0.54 | <det | 57.1 | |
| Native Bismuth (n=1) | 0.33 | 0.32 | | | | | | 1.36 | | | <det | 0.01 | | <det | 100 | 0.26 | 0.15 | 0.07 |
| Breithauptite (n=1) | 1.06 | 30.5 | | | | <det | 2.56 | 1.36 | | | <det | 65.7 | | 0.08 | 0.10 | 0.26 | <det | <det |
| PbTe1 | <det | 0.01 | | | 0.78 | 55.6 | <det | 0.01 | <det | | 35.4 | 0.20 | | | 7.87 | 0.59 | <det | 0.1 |
| PbTe2 | 0.31 | <det | | | 0.89 | 63.7 | <det | <det | <det | | 35.4 | 0.21 | | | <det | 0.3 | 0.06 | 0.12 |
| **Discovery Hill** | | | | | | | | | | | | | | | | | | |
| Sperrylite (n=1) | 0.12 | 0.02 | | | <det | 0.27 | 57.6 | <det | <det | | <det | 3.23 | | <det | <det | 38.57 | <det | <det |

*Results from Kelvin et al. (2012)

The EPMA results indicate that the Ni content in pentlandite and the Ni in solid solution in pyrrhotite are the lowest in the Ovoid (0.21 in pyrrhotite and 31.2 in pentlandite) and the highest in the Mini-Ovoid samples (0.46 in pyrrhotite and 34.2 in pentlandite). The Cu content in chalcopyrite is similar (33-34%) in all three deposits. Cobalt is present in amounts of 1-1.4% in pentlandite, where it is the highest in

Discovery Hill and the lowest in the Ovoid. Iron in pyrrhotite is similar in each deposit, but it is slightly higher in the Ovoid region and may reflect the higher proportion of troilite in that area. Selenium was not detected in pyrrhotite, pentlandite or chalcopyrite.

Sperrylite was the only PMM that was >10µm and could be analyzed by EPMA from Discovery Hill and the Mini-Ovoid. Trace amounts of Fe, Pb, Ni and Sb were detected in this phase. The compositions of stutzite, volynskite, michenerite, Ir-As-S(?), Re-Cu-(S), Ni-As and Bi-Te that were detected in the Mini-Ovoid and Discovery Hill samples could not be could accurately quantified by EPMA because they had grain-sizes <10 µm.

*LA-ICPMS Analyses of Sulfides*

The LA-ICP-MS results for elements that were detected in solid solution are summarized in Tables 3 and 4. A completed data-set is included in Appendix 4. Figures 3-12 A - H plot the concentrations of elements measured in pentlandite, chalcopyrite, pyrrhotite and in galena where it was present. Figures 3-13 A-D show sample images of LA-ICPMS time resolved spectra of selected elements in solid solution in pentlandite, chalcopyrite and pyrrhotite.The concentration of the metals in sulfides from the hornblende-gabbro dyke determined by Huminicki (2008) are included for comparison.

Iridium, ruthenium, rhodium and platinum were either below or near detection limit, or required interference corrections that were too large (>50%) to be included reliably in this study.

The LA-ICPMS results for these elements are not presented below. Values that were below the detection limit were reported as zero.

**Table 3-3: Average Concentration of Pd, Ag and semi-metals in sulfide phases determined by LA-ICPMS (ppm)**

| | *Average L.O.D* | As *0.07* | Te *0.2* | Sb *0.03* | Sn *0.07* | Ag *0.1* | Pd *0.01* | Au *0.01* | Bi *0.01* |
|---|---|---|---|---|---|---|---|---|---|
| Ovoid* | Pn | 1.14 | 2.49 | 0.13 | 0.31 | 3.09 | 1.16 | 0.08 | 0.59 |
| | Cpy | 0.26 | 5.61 | 0.03 | 10.31 | 4.96 | 0.12 | 0.05 | 0.96 |
| | Po | 0.50 | 0.69 | 0.11 | 0.29 | 0.74 | 0.08 | <det | 0.23 |
| | Gn | 4.37 | 5672.5 | 1.06 | 10.00 | 250.10 | 1.49 | 0.50 | 3872.5 |
| Mini-Ovoid | Pn | 0.36 | 4.78 | <det | 0.18 | 1.65 | 0.43 | <det | 0.07 |
| | Cpy | 0.15 | 6.45 | 0.04 | 11.13 | 19.77 | 0.16 | <det | 0.24 |
| | Po | 0.34 | 7.15 | <det | 0.23 | 1.02 | 0.05 | <det | 0.02 |
| | Gn | | | | | | | | |
| Disc Hill | Pn | 0.21 | 2.72 | <det | 0.31 | 0.29 | 1.32 | 0.01 | 0.96 |
| | Cpy | 11.59 | 6.94 | <det | 10.31 | 0.30 | 0.30 | 0.02 | 0.84 |
| | Po | 0.14 | 0.79 | <det | 0.29 | 0.89 | <det | <det | 0.30 |
| | Gn | | | | | | | | |
| HG Dyke** | Pn | 41.79 | 4.14 | 0.17 | 0.76 | 5.32 | 2.00 | 0.08 | 0.82 |
| | Cpy | 0.93 | 6.66 | 0.10 | 63.26 | 47.00 | 0.10 | 0.08 | 0.59 |
| | Po | 1.05 | 1.36 | 0.09 | 0.36 | 1.02 | 0.03 | 0.08 | 0.37 |
| | Gn | 17.38 | 484.64 | 0.96 | 10.95 | 310.90 | 1.8 | 0.34 | 47.85 |
| PGE Poor | Pn | 0.32 | NA | 0.02 | NA | 3.41 | 1.47 | 0.02 | NA |
| | Cpy | 0.11 | NA | 0.02 | NA | 4.96 | 0.12 | 0.02 | NA |
| | Po | 0.36 | NA | 0.02 | NA | 0.53 | 0.20 | 0.03 | NA |
| | Gn | | | | | | | | |

<det indicates measurement was below detection limit; Blank spaces indicate mineral was not present; Values highlighted in brown were not analyzed. * Pt, Pd, Au and Ag data from Kelvin et al. (2011); **Data from Huminicki (2007); A more complete data-set is included in Appendix 4.

**Table 3-4A: Number of LA-ICPMS analyses above detection limit / Total Number of Analyses**

| | | As | Te | Sb | Sn | Ag | Pd | Au | Bi |
|---|---|---|---|---|---|---|---|---|---|
| | | ppm | ppm | ppm | ppm | ppm | ppm | ppm | ppm |
| | *Average LOD* | *0.07* | *0.2* | *0.03* | *0.07* | *0.1* | *0.01* | *0.01* | *0.01* |
| Ovoid | Pn | 33/50 | 26/28 | 30/50 | 26/28 | 50/50 | 48/50 | 6/24 | 26/28 |
| | Cpy | 13/20 | 5/11 | 12/20 | 5/9 | 20/20 | 19/20 | 19/20 | 5/9 |
| | Po | 27/32 | 8/8 | 1732 | 8/8 | 17/32 | 11/32 | 3/27 | 8/8 |
| | Gn | 0/26 | 8/8 | 14/26 | NA | 15/26 | 21/26 | 15/26 | 4/8 |
| Mini-Ovoid | Pn | 14/16 | 10/10 | 11/16 | 3/10 | 6/6 | 14/16 | 0/6 | 10/16 |
| | Cpy | 11/16 | 6/6 | 8/16 | 6/6 | 15/16 | 15/16 | 0/16 | 6/6 |
| | Po | 4/5 | 8/8 | 0/5 | 5/5 | 13/13 | 10/13 | 1/5 | 5/8 |
| | Gn | | | | | | | | |
| SE Extension | Pn | 6/12 | NA | 0/12 | NA | 5/12 | 8/12 | 3/12 | NA |
| | Cpy | 4/12 | NA | 0/12 | NA | 6/12 | 3/12 | 5/12 | NA |
| | Po | 5/12 | NA | 0/12 | NA | 5/12 | 0/12 | 1/12 | NA |
| | Gn | | | | | | | | |
| PGE Poor | Pn | 6/6 | NA | 0/6 | NA | 6/6 | 6/6 | 3/6 | NA |
| | Cpy | 3/6 | NA | 0/6 | NA | 6/6 | 6/6 | 3/6 | NA |
| | Po | 6/6 | NA | 3/6 | NA | 6/6 | 6/6 | 5/6 | NA |
| | Gn | | | | | | | | |

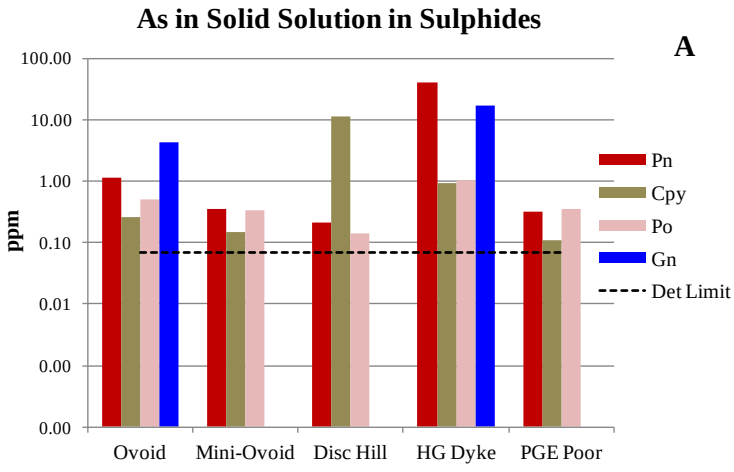


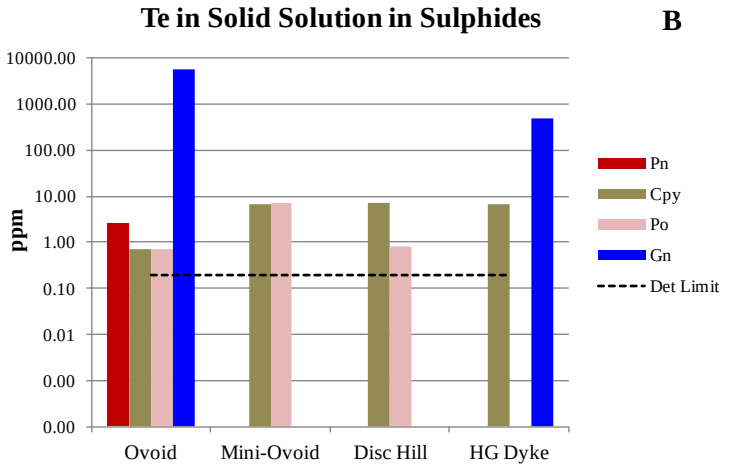


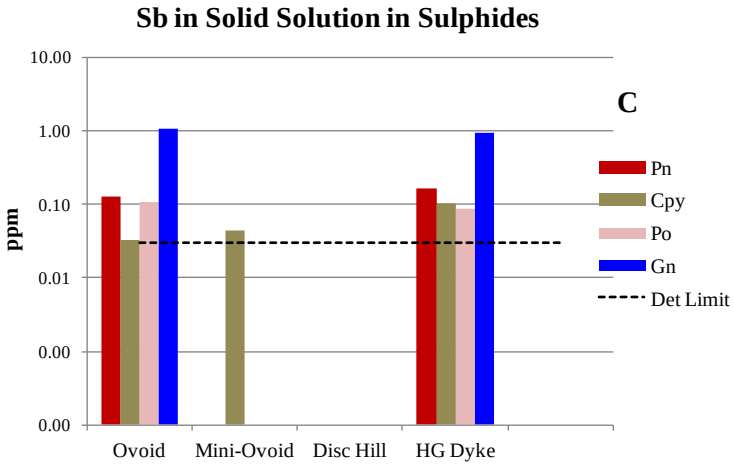


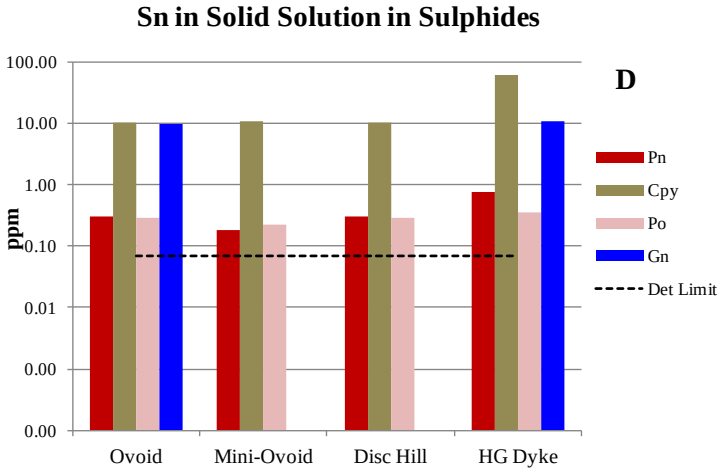


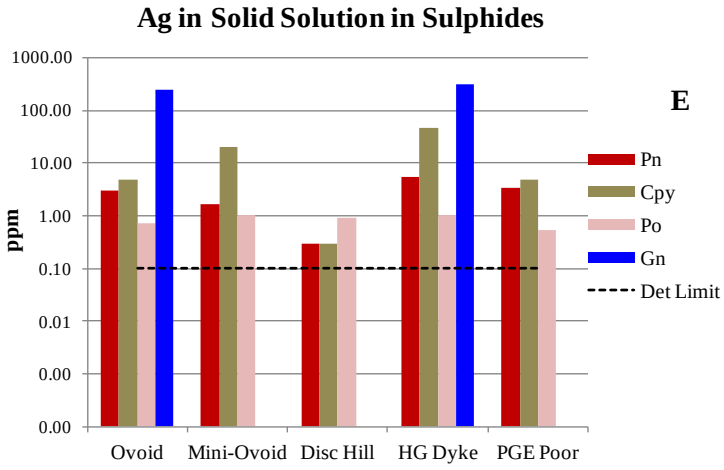


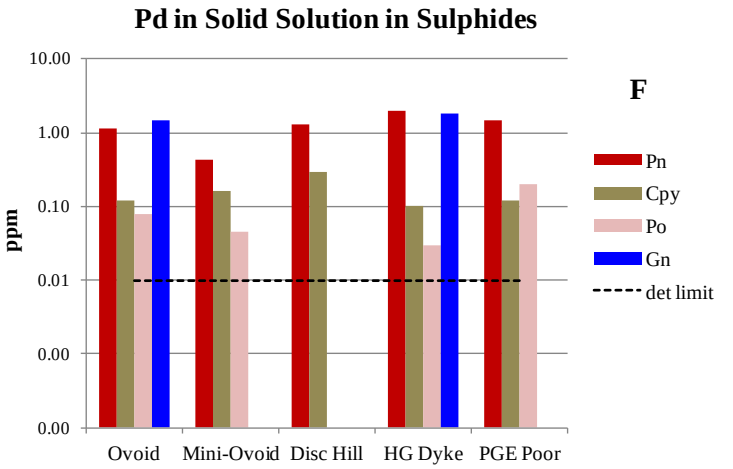


**Figures 3-12 A - F: Average Concentration (ppm) of As, Te, Sb, Sn, Ag and Pd in solid solution** in pentlandite (Pn), chalcopyrite (Cpy), pyrrhotite (Po) and galena (Gn) determined by LA-ICPMS. Y-axis is in log-scale. Error bars on Pd in pentlandite are provided to show the consistency throughout the deposit.

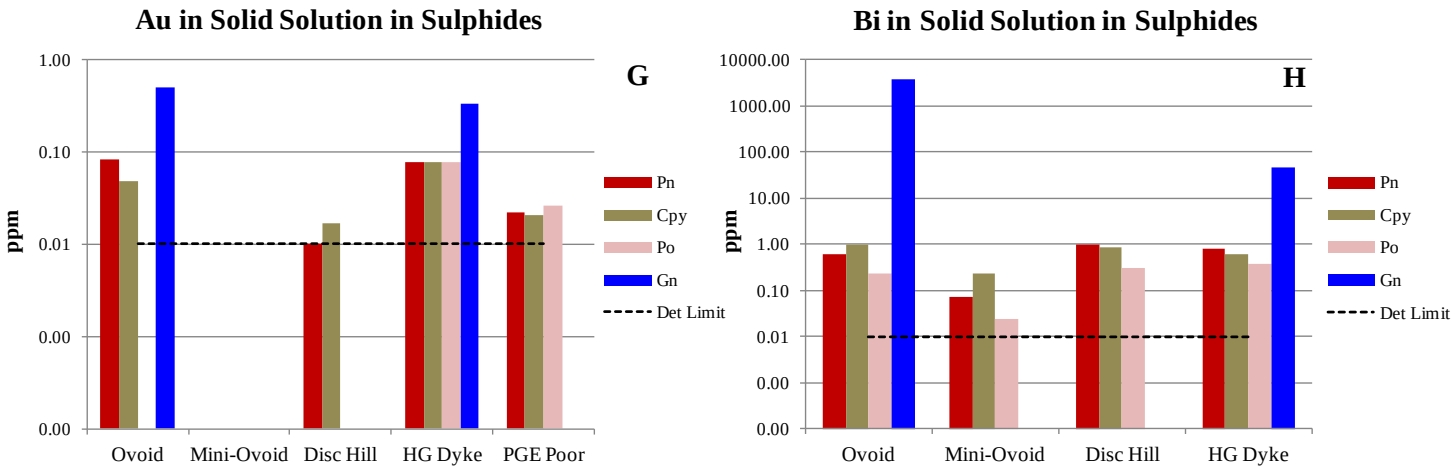


**Figures 3-11 G, H: Concentration (ppb) of Bi and Au solid solution** in pentlandite (Pn), chalcopyrite (Cpy), pyrrhotite (Po) and galena (Gn) determined by LA-ICPMS. Y-axis is in log-scale.

**A.** Trace Elements in Pn from the Ovoid

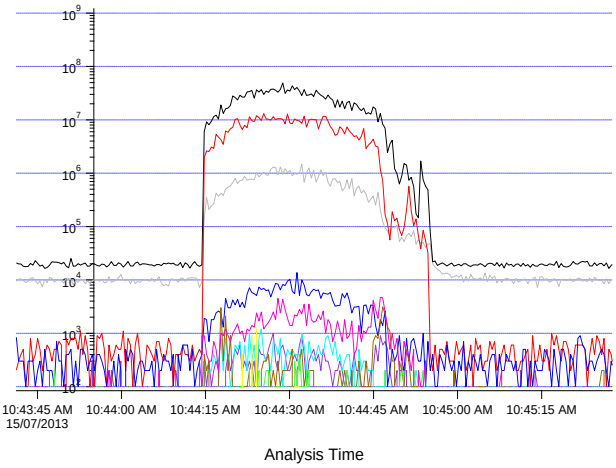


**B.** Trace Elements in Cpy from the Ovoid

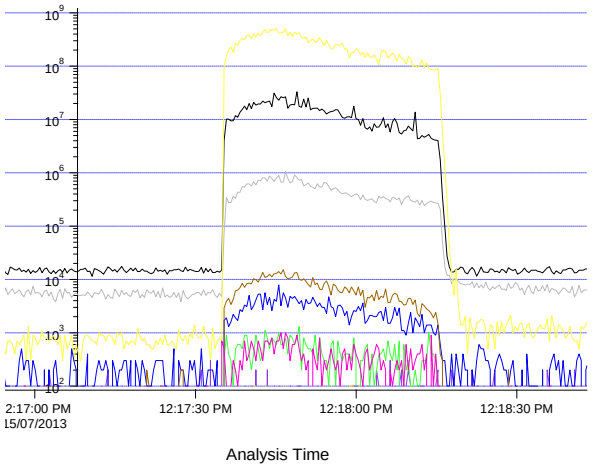


**C.** Trace Elements in Po from the Ovoid

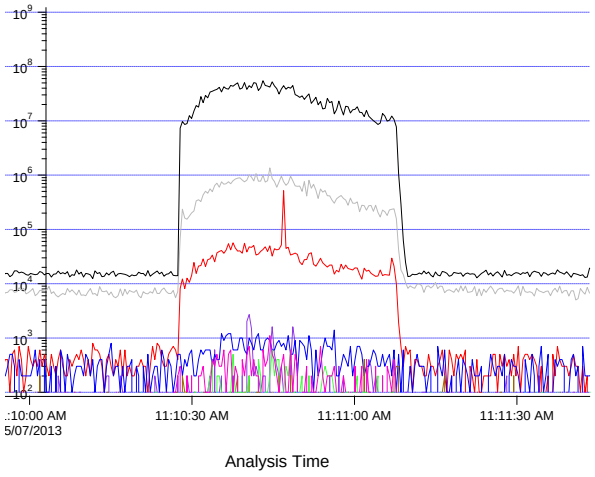


**D.** Trace Elements in Cpy from the Mini-Ovoid

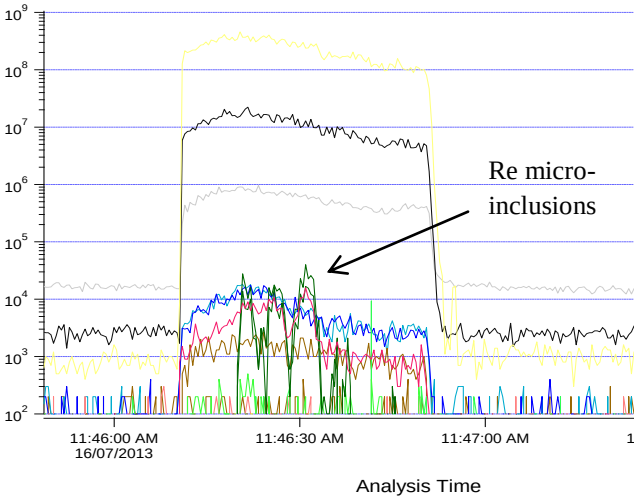


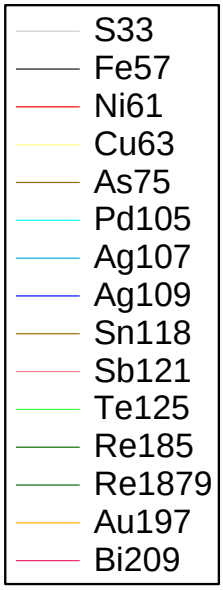


**Figures 3-12 A-D: Sample LA-ICPMS Time Resolved Spectra** in pentlandite (A), Chalcpyrite (B), Pyrrhotite (C) from the Ovoid and Chalcopyrite (D) from the Mini-Ovoid. Figure D shows Re micro-inclusions in chalcopyrite from the Mini-Ovoid

Palladium is the only PGE that is present in amounts that are significant compared to its average detection limit. It has consistently elevated concentrations in pentlandite (1–2 ppm) in all areas except for the Mini-Ovoid where the average concentration drops to 43 ppm. The abundances of Pd are similar in each zone and is the lowest in chalcopyrite and in pyrrhotite (<0.1ppm). Palladium also occurs at elevated concentrations in galena from the Ovoid (1.4 ppm) (Kelvin et al., 2011) and Southeast Extension zone (1.8 ppm) (Huminicki et al., 2008). The Pd in solid solution in pentlandite from the PGE poor DISS Ovoid (1.5ppm) sample is similar to the Pd in pentlandite in the PGE rich samples.

Where galena is present, it contains the greatest amount of Te, Sb, Ag, Bi and Au in solid solution compared to the other sulfide minerals.

Silver is present in solid solution in nearly all phases. Chalcopyrite carries the most abundant amount of Ag out of all major sulfide phases (between 4.2 and 47 ppm) except at Discovery Hill where it contains the least amount of Ag (0.3 ppm). Where galena is present (Ovoid and SE extension), it contains significantly higher amounts of Ag than the major sulfides (310 ppm in SE extension zone and 250 ppm in the Ovoid).

Gold is present in very low abundances (just above detection) within the major sulfide minerals in all areas except for the mini-Ovoid where it is present below the detection limit. The galena from the Southeast Extension Zone (0.3 ppm) and the Ovoid (0.5 ppm) contained the most abundant amount of Au out of all the sulfide minerals.

Tin is consistently very enriched in chalcopyrite compared to pentlandite and pyrrhotite, and to a lesser extent, galena. It is the most enriched in the Southeast Extension zone where the Sn assays are also the highest (63.2 ppb in chalcopyrite and 11.0 in galena).

Arsenic has the most variation in distribution within the sulfide minerals amongst each zone. In the Ovoid, As is the most abundant in pentlandite (1.14 ppm), and has the lowest abundance in chalcopyrite

(0.26 ppm). Arsenic is detected in low abundances in pentlandite and pyrrhotite (<0.2 ppm) in the Discovery Hill zone. It is present in the lowest concentration in the Mini-Ovoid.

Antimony was detected in very low amounts or was below detection limits in the major sulfide minerals. Discovery Hill and the Mini-Ovoid contain the lowest concentrations of Sb in solid solution (near or below detection limits), and the Ovoid and Southeast Extension Zone contain concentrations of Sb in solid solution just above the detection limits. In galena, Sb was present at slightly elevated levels (>0.96 ppm).

Although Re was not above detection limit in any sulfide, rare micro-inclusions are apparent in chalcopyrite analyzed from the Mini-Ovoid. An example of the Re mico-inclusions is shown in Figure 3-12D. This is consistent with the MLA data reported for the Mini-Ovoid.

*Assays*

The Fe, Cu Ni, S, PGE and semi-metal assay results are presented in Table 5. Variations in the concentrations of trace semi-metals (Bi, Sb, Te, As and Sn) are apparent between the samples selected from the different ore zones. The hornblende-gabbro dyke samples contain a much greater enrichment of Sn, As, and Pb than the samples from the Ovoid and Discovery Hill. In the Ovoid, Mini-Ovoid and Discovery Hill, As is below detection limit.

The semi-metal to PGE ratio is also provided in the table. The Ovoid has the lowest (average) PGE to semi ratio of 74, and the Mini-Ovoid has the highest at 210. The PGE to semi-metal ratio of the hornblende-gabbro dyke is 111.

Even though the semi-metal concentrations are low in the unmineralized rock units, their occurrence may be significant and an attempt was made to define a relationship between the country rocks and the unmineralized gabbros and troctolites. In order to illustrate the semi-metal content in the country rocks relative to the unmineralized troctolite and gabbro, the average concentrations of semi-metals in the

country rock units were normalized to the average concentrations of semi-metals in the unmineralized troctolites and gabbros. Figures 3-13 and 3-14 plot this relationship. Values that are above one are enriched compared to the troctolite or gabbro.

According to these plots, Tasiuyak gneisses, Enderbitic gneisses, and granite are enriched in Se, Sn and Sb compared to the unmineralized troctolite units. Tellurium and Bi are more enriched the unmineralized troctolite compared to the country rocks. Arsenic is only enriched in diorite and tonalite relative to the troctolite.

The unmineralized gabbros appear to be close to or slightly more enriched in Sn, Sb, Te and Bi than most country rocks. Arsenic is more enriched in diorite, tonalite and granite than the unmineralized gabbro. The gabbro is more enriched in As than Tasiuyak and Enderbitic gneisses.

Rhenium is enriched in Tasiuyak and Enderbite gneisses and in the Voisey's Bay granites relative to both unmineralized troctolite and unmineralized gabbro.

**Table 3-5: Assays Results of Country Rock, Voisey's Bay unmineralized rocks and mineralized samples.**

| Element | | Ir | Ru | Rh | Pt | Pd | Au | Re | Fe | Ni | Cu | S | Pb | Zn | Ag | Co | Bi | Se | As | Sn | Sb | Te | Semi-metal/PGE ratio |
|---|---|---|---|---|---|---|---|---|---|---|---|---|---|---|---|---|---|---|---|---|---|---|---|
| Unit | | ppb | ppb | ppb | ppb | ppb | ppb | ppb or ppm | % | % or ppm | % or ppm | % | ppm | ppm | ppm | ppm | ppm | ppm | ppm | ppm | ppm | ppm | |
| L.O.D. | | 1 | 1 | 1 | 1 | 1 | 1 | 1 | 0.01 | | | | 0.5 | 0.2 | 0.05 | 0.1 | 0.02 | 0.1 | 0.1 | 1 | 0.1 | 0.1 | |
| Method | | NF | NF | NF | NF | NF | NF | NF | TD-MS | ICPMS | ICPMS | ICPMS | TD-MS | TD-MS | TD-MS | TD-MS | TD-MS | TD-MS | TD-MS | TD-MS | TD-MS | TD-MS | |
| **Rock Type** | **Location** | | | | | | | | | | | | | | | | | | | | | | |
| **Country Rock** | | | | | | | | | | | | | | | | | | | | | | | |
| PTG | Dico Hill | | | | | | | 0.0005 | 3.97 | 55.9 | 21.2 | | 27.4 | 88.7 | 0.025 | 342 | 0.04 | 0.05 | 0.05 | 0.5 | 0.2 | 0.2 | |
| PTG | cheeks | | | | | | | 0.0005 | 12.4 | 252 | 27.8 | | 2.5 | 159 | 0.025 | 135 | 0.02 | 0.4 | 0.05 | 2 | 0.1 | 0.05 | |
| PTG | cheeks | | | | | | | 0.007 | 0.94 | 7.5 | 11.7 | | 25.4 | 23.7 | 0.025 | 400 | 0.05 | 0.05 | 0.05 | 0.5 | 0.2 | 0.2 | |
| PTG | cheeks | | | | | | | 0.018 | 5.81 | 17 | 3.6 | | 1.6 | 25.5 | 0.025 | 500 | 0.03 | 0.05 | 0.05 | 3 | 0.4 | 0.2 | |
| PTG | N of Mushuau | | | | | | | 0.0005 | 4.57 | 22.3 | 4.7 | | 2 | 61.7 | 0.025 | 58.4 | 0.07 | 0.05 | 0.05 | 1 | 0.1 | 0.1 | |
| PTG | Old Joe | | | | | | | 0.002 | 8.03 | 76 | 5.9 | | 7.4 | 74.3 | 0.025 | 305 | 0.01 | 0.05 | 0.05 | 0.5 | 0.05 | 0.05 | |
| PTG | Dico Hill | | | | | | | 0.001 | 5.21 | 11.6 | 11.7 | | 12.6 | 83 | 0.025 | 63.3 | 0.01 | 0.2 | 0.05 | 0.5 | 0.05 | 0.05 | |
| Tonalite (EO) | Dico Hill | | | | | | | 0.0005 | 3.86 | 26.5 | 2.1 | | 10.4 | 83.2 | 0.025 | 87.9 | 0.01 | 0.05 | 0.5 | 0.5 | 0.05 | 0.05 | |
| Qtz Diorite (EO) | Dico Hill | | | | | | | 0.0005 | 3.34 | 19.3 | 30.3 | | 11.3 | 80.7 | 0.13 | 106 | 0.03 | 0.05 | 1.2 | 0.5 | 0.05 | 0.2 | |
| EO | Mushuau | | | | | | | 0.0005 | 2.24 | 18.7 | 20.2 | | 9.3 | 55.4 | 0.025 | 173 | 0.01 | 0.05 | 0.05 | 0.5 | 0.05 | 0.2 | |
| EO | Mushuau | | | | | | | 0.002 | 1.37 | 13.6 | 36.8 | | 8 | 35.3 | 0.06 | 305 | 0.02 | 0.05 | 0.05 | 0.5 | 0.2 | 0.05 | |
| EO | N. of East Deeps | | | | | | | 0.003 | 3.36 | 32.9 | 26.9 | | 13.2 | 64.6 | 0.025 | 74.5 | 0.02 | 0.05 | 0.05 | 0.5 | 0.05 | 0.05 | |
| **Voisey's Bay Intrusive Rocks** | | | | | | | | | | | | | | | | | | | | | | | |
| **Unmineralized** | | | | | | | | | | | | | | | | | | | | | | | |
| Granite | E. of East Deeps | | | | | | | 0.0005 | 2.06 | 4.2 | 4.3 | | 16.1 | 52.9 | 0.05 | 299 | 0.01 | 0.05 | 0.05 | 0.5 | 0.05 | 0.05 | |
| Granite | Dico Hill | | | | | | | 0.0005 | 2.01 | 7.7 | 9 | | 16.7 | 38.9 | 0.025 | 306 | 0.04 | 0.05 | 0.05 | 1 | 0.5 | 0.1 | |
| Granite-Syenite | E. of East Deeps | | | | | | | 0.002 | 2.53 | 104 | 81.9 | | 27.4 | 36.1 | 0.025 | 69.3 | 0.01 | 0.3 | 0.4 | 2 | 0.05 | 0.05 | |
| Gabbro | Dico Hill | | | | | | | 0.0005 | 4.07 | 30.5 | 36.2 | | 15.9 | 89.4 | 0.025 | 110 | 0.04 | 0.05 | 0.2 | 1 | 0.05 | 0.1 | |
| Gabbro | Dico Hill | | | | | | | 0.0005 | 5.89 | 38 | 83.2 | | 8.8 | 104 | 0.025 | 96.5 | 0.03 | 0.05 | 0.05 | 3 | 0.4 | 0.2 | |
| Gabbro | Dico Hill | | | | | | | 0.0005 | 7.28 | 36.2 | 7 | | 3.8 | 107 | 0.025 | 84.3 | 0.04 | 0.05 | 0.05 | 2 | 0.4 | 0.05 | |
| Troctolite | VB Troctolite | | | | | | | 0.0005 | 6.06 | 397 | 306 | | 3.6 | 93.4 | 0.24 | 102 | 0.03 | 0.05 | 0.05 | 0.5 | 0.05 | 0.2 | |
| **Low min.** | | | | | | | | | | | | | | | | | | | | | | | |
| Gabbro | SE Extension | | | | | | | 0.004 | 8.51 | 2950 | 898 | | 12.5 | 74.2 | 0.33 | 189 | 0.16 | 1.2 | 0.05 | 2 | 0.05 | 0.05 | |
| Gabbro | Dico Hill | | | | | | | 0.0005 | 8.57 | 1110 | 834 | | 4.2 | 73.7 | 0.32 | 137 | 0.09 | 0.7 | 0.05 | 0.5 | 0.1 | 0.2 | |
| Troctolite | VB Troctolite | | | | | | | 0.017 | 12.8 | 1610 | 1270 | | 7.2 | 184 | 0.74 | 212 | 0.19 | 1 | 0.05 | 2 | 0.05 | 0.05 | |
| Troctolite | VB Troctolite | | | | | | | 0.007 | 10.8 | 2910 | 1420 | | 44.5 | 103 | 0.5 | 217 | 0.13 | 2.9 | 0.05 | 2 | 0.05 | 0.2 | |
| **Mineralized** | | | | | | | | | | | | | | | | | | | | | | | |
| BS0218 | Troc. Feed (Ov) | < 1 | 1 | 2 | 33 | 85 | 19 | 16 | 23.6 | 1.51 | | | 53.7 | 300 | 2.06 | 500 | 0.44 | 9.2 | 0.05 | 1 | 0.05 | 1.2 | 22.64 |
| BS0265 | Mini-Ovoid | 3 | 3 | 8 | < 1 | 93 | < 1 | 52 | 35.2 | 2.60 | 5.5 | 15 | 8 | 401 | 22.7 | 500 | 0.79 | 14.2 | 0.05 | 7 | 0.05 | 0.4 | 77.48 |
| BS0241 | Inner Ovoid | 1 | < 1 | 5 | 158 | 463 | 84 | 32 | 46.7 | 3.20 | 2.4 | 26 | 1686 | 179 | 15 | 500 | 7.39 | 47.3 | 0.05 | 3 | 0.05 | 5.9 | 26.14 |
| BS0207 | Inner Ovoid | < 1 | < 1 | 3 | 614 | 503 | 297 | 18 | 49 | 4.50 | 2.5 | 27 | 1201 | 187 | 26 | 500 | 6.91 | 63 | 0.05 | 5 | 0.1 | 11.6 | 21.13 |
| DF6063 | Inner Ovoid | < 1 | < 1 | 4 | 325 | 412 | 51 | 22 | 49 | 4.30 | 1.1 | 30 | 819 | 629 | 30.5 | 500 | 1.59 | 53.4 | 0.05 | 6 | 0.05 | 8.7 | 22.12 |
| DF6055 | Inner Ovoid | 1 | < 1 | 4 | 2180 | 2490 | 209 | 25 | 52.6 | 5.10 | 4.2 | 29 | 712 | 609 | 28 | 500 | 13.8 | 60 | 0.05 | 7 | 1.1 | 25.7 | 10.19 |
| VX49277 | Disco Hill | < 1 | 11 | 5 | 338 | 324 | 488 | 30 | 27.7 | 2.59 | 1.12 | 15.7 | 67.2 | 101 | 6.7 | 500 | 1.54 | 50.5 | 0.05 | 6 | 0.05 | 4.8 | 18.35 |
| VX49289 | Disco Hill | < 1 | 12 | 6 | 80 | 288 | 454 | 25 | 28.1 | 1.42 | 7.32 | 11 | 30.1 | 348 | 83.5 | 500 | 1.36 | 50.3 | 0.05 | 11 | 0.05 | 9.1 | 55.85 |
| MH-028A[1] | H.G. Dyke, SEE | <det | <det | 0.62 | 3430 | 2150 | 12900 | | 6.7 | | | | 5000 | 88.3 | 100 | 120 | 173 | 19.7 | 37 | 200 | 0.9 | 31.8 | 79.33 |
| MH-028B[1] | H.G. Dyke, SEE | <det | <det | <det | 272 | 231 | 281 | | 10.9 | | | | 1330 | 132 | 29.5 | 163 | 15.5 | 2.4 | 32.8 | 17 | 0.05 | 2.3 | 134.49 |
| MH-035 | H.G. Dyke, SEE | | | | | | | | 8.03 | | | | 5000 | 145 | 100 | 153 | 77.2 | 14.4 | 42.8 | 133 | 0.3 | 11.6 | |
| MH-036 | H.G. Dyke, SEE | | | | | | | | 6.89 | | | | 3890 | 132 | 91.1 | 106 | 65.3 | 7.9 | 51 | 83 | 0.2 | 3.3 | |

1. PGE values from Huminicki (2008); PTG = Proterozoic Tasiuyak Gneiss, EO= Enderbitic Orthogneiss NF = PGE analysis by Ni Fire Assay; TD-MS = Trace element analysis by Total Digestion ICPMS; SEE = Southeast Extension; Values with "<" are below lower detection limit; Values with ">" are above upper detection limit; Values highlighted in grey are below detection limit, but were estimated to be half of the detection limit for the purpose of calculating the average concentrations; blank spaces indicate that no analysis was completed

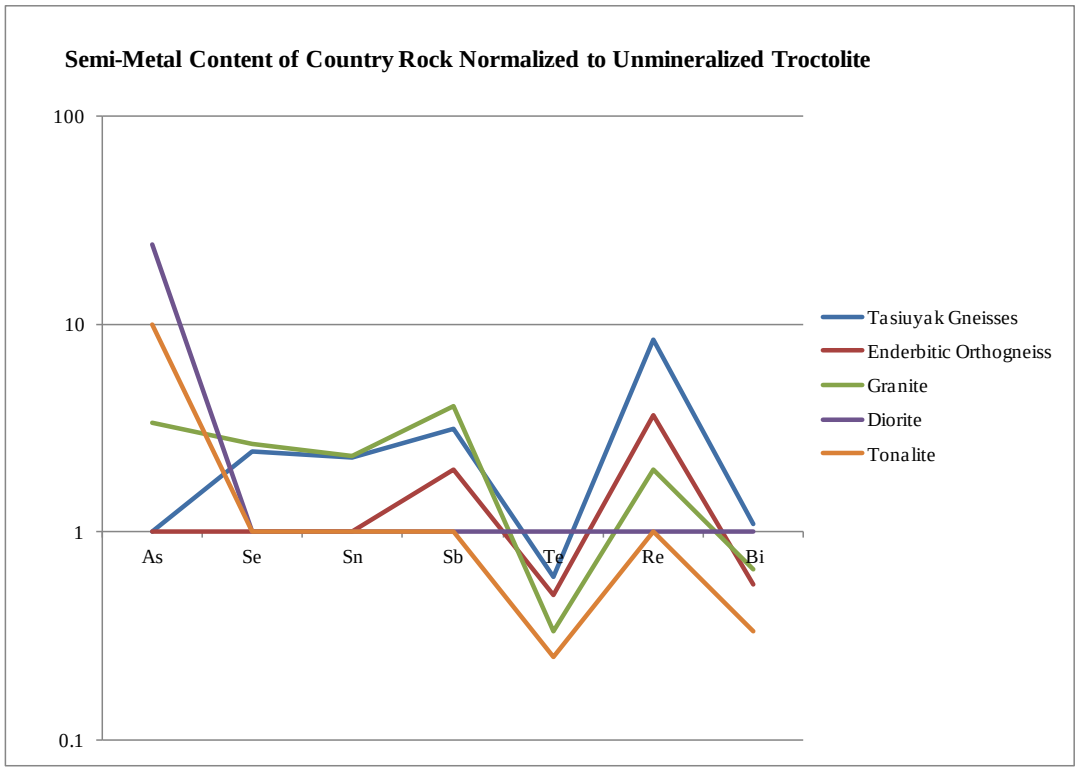


**Figure 3-13: Average concentration of semi-metals (As, Se, Sn, Sb, Te and Bi) in country rock (Tasiuyak and enderbitic gneisses) normalized to the average concentrations of semi-metals in unmineralized troctolite**.

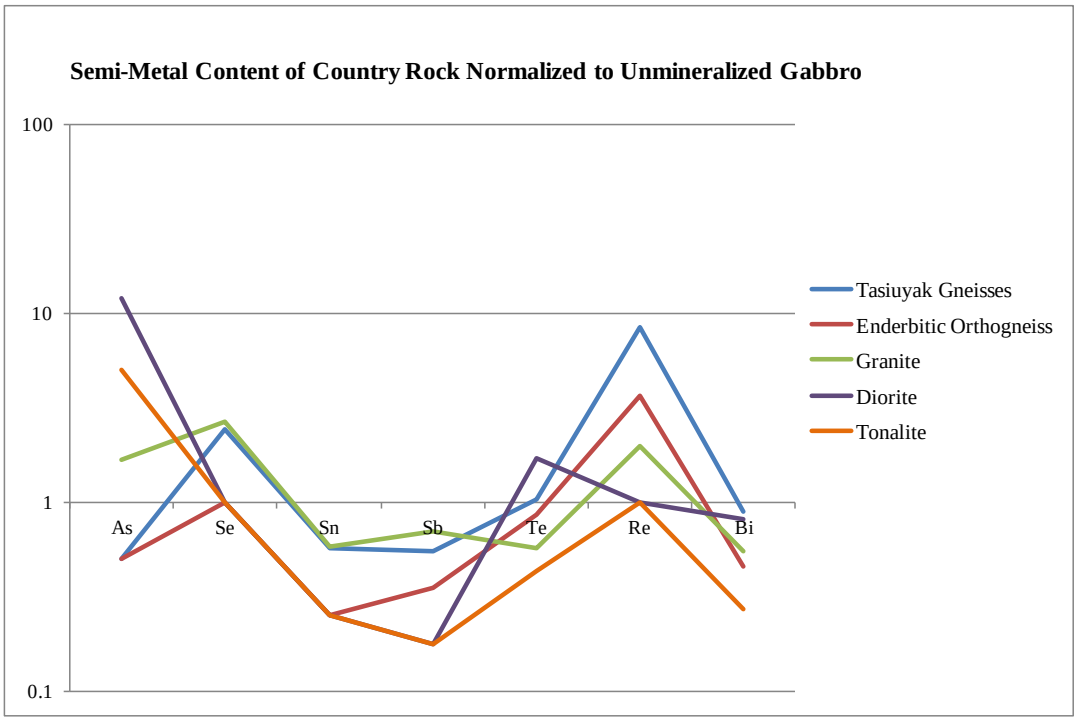


**Figure 3-14: Average concentration of semi-metals (As, Se, Sn, Sb, Te and Bi) in country rock (Tasiuyak and enderbitic gneisses) normalized to the average concentrations of semi-metals in unmineralized gabbro.**

*Mineral Deportment of Semi-Metals*

A mass distribution (deportment) of Pd, As, Sn, Sb, Te, Bi, Pd and Au has been calculated based on the combined geochemical and mineralogical results. In some cases, a distribution could not be calculated due to undetectable or very low assay levels of some metals, or undertermined amounts of metals in solid solution in some phases. The results of the deportment calculations are presented in Figures 3-15A through 3-15E.

With the exception of Bi in the Ovoid, all semi-metals were strongly distributed to discrete minerals phases (>70% element mass). Only 5.2% of the Bi in the Ovoid is distributed to discrete PMM. This is due to the high amount of Bi (~3000ppm average) in galena. Galena from the hornblende-gabbro dyke only carries <1% of the total bismuth in solid solution likely due to the higher PGE content available to complex with Bi. Where galena is present, it carries large proportions of dissolved Te (5.9-23.0%) and Bi (3.4-9.8%) in solid solution compared to the other sulfide phases even though galena is only present in trace amounts.

In all areas analyzed, the majority of Pd (78% in the Ovoid to 96% in the hornblende-gabbro dyke) is carried by discrete minerals phases containing Bi, Sn or Te. The greatest distribution of Pd in pentlandite occurs in the Ovoid (14%) where the semi-metal/PGE ratio (74.0) is the lowest.

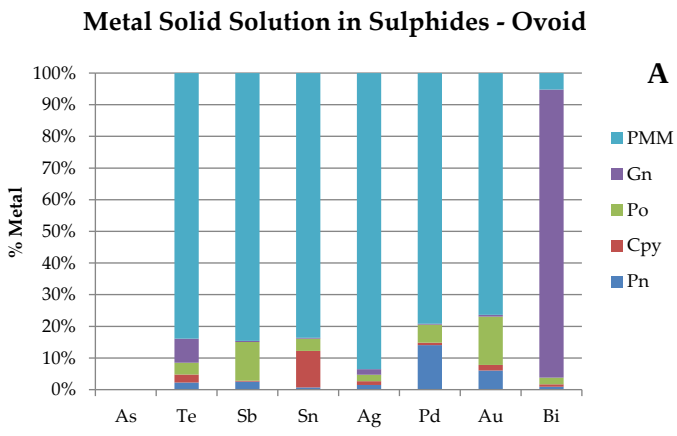


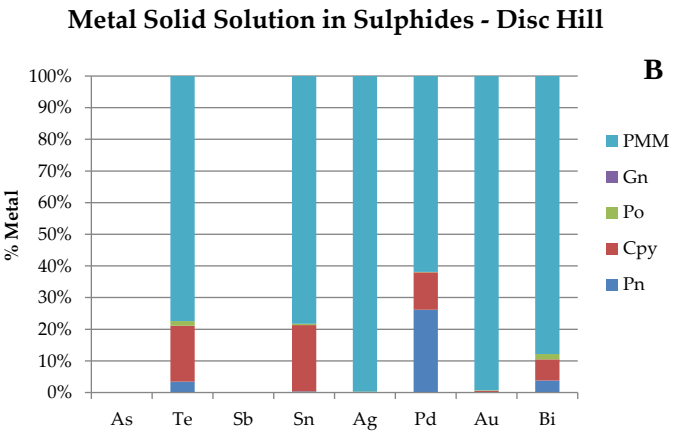


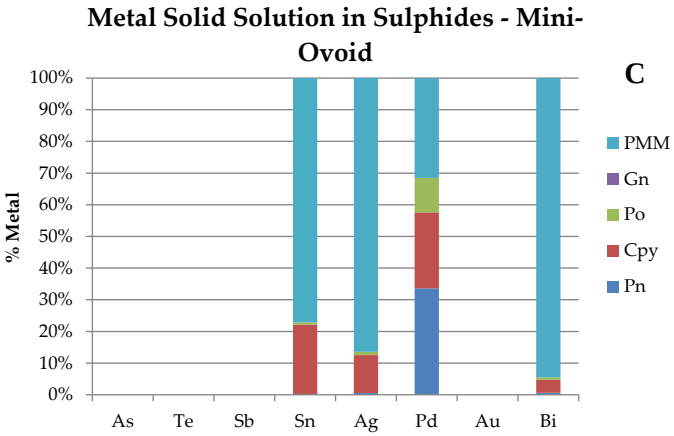


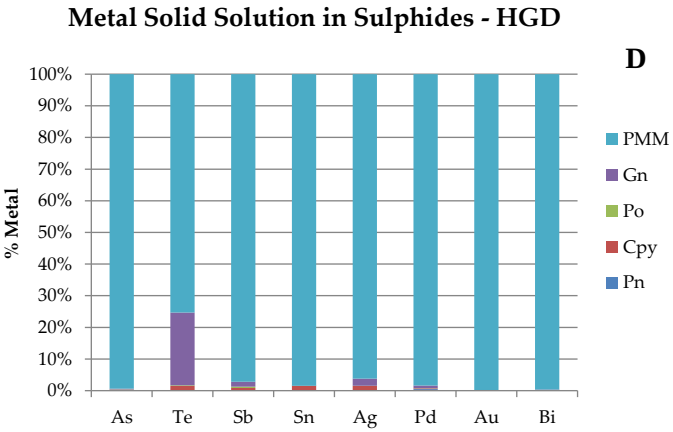


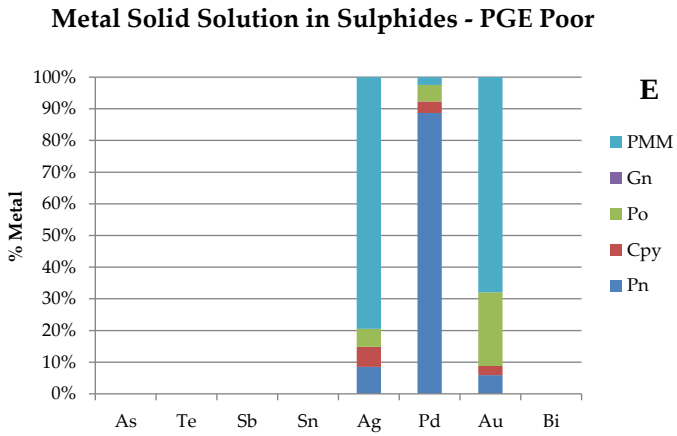


**Figures 3-15 A – F. Arsenic, Sb, Sn, Te, Bi, Pd distributions amongst sulfides and PMM phases**. Pn=pentlandite, Cpy=chalcopyrite, Po=pyrrhotite, Gn=galena. For the Mini-Ovoid sample, the amount of Te in solid solution calculated from the modal abundances of the sulfides and the LA-ICPMS results marginally exceeded the total Te concentration in the sample and could not be calculated; although volynskite and stutzite were detected in the mini-Ovoid, the amount of Te deported to discrete PMM is negligible compared to the amount of Te dissolved in solid solution in sulfides.

## Discussion

*Role of Semi-Metals in PMM Crystallization at Voisey's Bay*

Based on the large number of grain boundary associations of PMM with galena and pentlandite, and the fact that Pd, Au and Ag occur mostly as mineral phases containing Bi, Te, As, Sn and Sb, it is likely that most of the PMM at Voisey's Bay crystallized from a Pd, Au, Ag semi-metal melt, derived from Cu-, ISS-rich sulfide melt, either through extreme differentiation or immiscibility.

Cabri and Laflamme (1976) and Helmy et al. (2007), (2008) and (2013a,b) demonstrated the strong control of semi-metals on PGE crystallization. In magmas that are enriched in semi-metals such as As, Te, Sb, and Bi, the metals complex with PGE at super solidus temperatures, perhaps to form nano-sized clusters that will nucleate to form early crystallizing phases, or late-stage immiscible melts (Helmy et al., 2013a,b). After forming semi-metal complexes, the surface properties of the clusters, rather than sulfide mineral-melt partition coefficients, dominantly control how the PGE are concentrated within in the sulfide system (Helmy et al., 2013a).

Pt-arsenide complexes may have formed at high temperatures. Sperrylite is always found in our samples as large, easily liberated, euhedral grains, suggesting that they crystallized early in the crystallization history of the sulfide magma, allowing them to grow unconstrained by adjacent minerals. Helmy et al. (2013b) found that in the Pt-arsenide system, sperrylite is a liquidus phase below 1230 °C. In the Ovoid samples, sperrylite hosts inclusions of froodite and galena. This association is consistent with the results reported by Helmy et al. (2103a), who proposed that PGE-semi-metals complexes may nucleate at high temperatures and continue to crystallize at lower temperatures.

If semi-metals are not enriched in the initial melt, or if the semi-metal/PGE ratio is low, sulfide mineral-melt partition coefficients become the most effective control of PGE distribution, allowing PGE to be dissolved into solid solution in the sulfide phases. This is reflected in the deportment of Pd in our

Voisey's Bay samples. Out of all the samples with elevated PGE concentrations, the Ovoid samples contain the lowest distribution of Pd into PMM and, coincidentally, also have the lowest average semi-metal/PGE ratio.

Little to no Pd is found in solid solution in chalcopyrite in any of the samples, which suggests that Pd is incompatible in Cu-rich ISS in the presence of semi-metal complexes. Peredoegova (1998) proposed that Pd is incorporated into pentlandite during recrystallization of the ISS. Naldrett (2000) attributed the large grained pentlandite present in the Ovoid samples to exsolution of pentlandite from the MSS at higher temperatures (500 °C) due to the higher metal to sulphur ratio. Palladium is present in significant amounts in pentlandite at Voisey's Bay, as documented in Chapter 2 and shown in Fig. 13-5 of this Chapter. Lightfoot et al. (2011) suggested that Pd was incorporated into the pentlandite during subsolidus exsolution from MSS. Thus, Pd may not be in the chalcopyrite because it is more strongly partitioned to the Bi-Te complexes or into the exsolved pentlandite rather than the Cu rich melt.

Research on the partitioning of Pb and Sn during a fractionation of an Fe-Ni-Cu sulfide magma is limited. Galena has not been considered in experimental studies on the partitioning behaviour of PGE in sulfide minerals. This may be due to the fact that galena is normally present in only minor to trace amounts, or as accessory minerals in Fe-Ni-Cu magmatic sulfide deposits, or because PGE associations with galena are not found at other deposits. However, since Pb and Sn are strongly associated with semi-metals, Pt and Pd in the Voisey's Bay samples, these elements are probably related to the semi-metal melt and may influence the crystallization sequence of the PGM at this deposit. Thus, the partitioning of Pb and Sn in the fractionating sulfide magma is important for interpreting a genetic model for the crystallization of PGE.

Based on our results, we can make some inferences regarding partitioning of Pb and Sn. Our results of Sn in solid solution in the sulfide phases show that Sn is partitioned into chalcopyrite in preference to galena,

pentlandite and pyrrhotite. This suggests that Sn is partitioned into the Cu-rich ISS. It has been proposed for other PGE bearing deposits that the PGM exsolved from the ISS sulfide phases at subsolidus temperatures (e.g. Dare, et al., 2011). The fact that Sn is more strongly partitioned into the ISS in Voisey's Bay samples may imply the possibility that Sn bearing PMM (mainly paolovite, $Pd_2Sn$ from the hornblende-gabbro dyke) could exsolve from the ISS; however, no Pd was found in significant proportions in solid solution in chalcopyrite in any deposits studied at Voisey's Bay. A model incorporating exsolution of Sn PGM from the Cu ISS would require further explanation to address the lack of PGE in chalcopyrite. Dare et al. (2011) suggested that the Pd is diffused from the ISS during low temperature recrystallization. A second explanation is that the Sn PGM do not exsolve from the ISS but, instead, begin to accumulate as nanoclusters at high temperatures as proposed by Helmy et al. (2013b) and evolve to form as constituents of the semi-metal PGE melt. Remaining Sn that is not associated with Pd (or other PGE) may then be partitioned into the ISS at the appropriate temperature.

The relationship of galena to magnetite implies that galena is present in the most fractionated regions of the Ovoid. Huminicki (2007) and Huminicki et al. (2012) reported a magnetite-rich zone at the inner region of the Ovoid, and at the boundary of this zone, the PGE and Pb concentrations are elevated. Naldrett et al. (2000b) and Naldrett (2011) proposed that $O_2$ was fractionated into the center of the Ovoid because the ore body crystallized as a closed system. By extension, the strong association of PGM and semi-metal phases, particularly froodite and other Bi and Te phases, with galena suggests that the semi-metal melt coexisted with galena or a Pb-S melt in the most fractionated regions.

Where galena is occurs, it contains the majority of Bi and Te present in solid solution. Galena also hosts PMM inclusions and attachments more commonly than any other sulfide mineral. In the case of the Ovoid, the association of galena to magnetite in the fractionated regions provides stronger evidence for galena crystallization from a Pb and semi-metal rich melt rather than crystallization of galena from exsolution from ISS crystals. The EPMA results showed that sperrylite contains minor amounts of Pb

(0.25%), which indicates that Pb was also present during high temperature nucleation of the PGE semi-metal complexes.

*Hydrothermal Remobilization*

The PGE mineralogy at Voisey's Bay does not appear to have been upgraded by hydrothermal activity. Even in areas where the sulfide mineralization is disseminated amongst silicate, most PMM are associated with sulfide phases. In particular, in Discovery Hill and in the Mini-Ovoid, the PMM are fine inclusions in the sulfide phases, indicating that crystallization of the PMM is associated with the sulfide liquid. The sulfide mineralogy that hosts the inclusions appears to be strictly magmatic and do not contain lower temperature sulfides such as pyrite (Naldrett et al., 2000a). Only minor amounts of hydrous silicate minerals (biotite and amphibole) were identified in the disseminated sulfide samples. The PMM in the Ovoid samples are also primarily magmatic in origin because they show similar associations to the sulfides and no association to any silicate minerals.

Huminicki et al. (2008) showed that hydrothermal fluids did not affect PGE mineralization or transport and introduce new PGE and semi-metals into the sulfide system. The hornblende-gabbro dyke hydrous phases contained low Cl contents and did not show any evidence of Cl complexing to PGE because there was no correlation between Cl and PGE. Microprobe and LA-ICPMS of that area also revealed that Sn and Pb were transported from the sulfides into amphibole rather than hydrous phases transporting these elements to the system. This may indicate that the hydrothermal fluids are not the cause of crystallization of the different PGM assemblages (e.g., paolovite) in the hornblende-gabbro dyke compared to other ore zones.

*Origin of Semi-Metals*

A notable difference observed between the PMM across the Voisey's Bay deposit is the types of semi-metals that complex to PGE, and the concentrations of PGE, Ag and Au. Tin PGM occur in the Southeast Extension zone and not in the other studied parts of the deposit. Native-Ag also contributes to 24% of the PMM mass in the Southeast Extension zone, whereas no native-Ag and lower abundances of Ag minerals were detected in the Ovoid, Mini-Ovoid and Discovery Hill. Furthermore, the Ovoid and Discovery Hill samples are much less enriched in Pd, Pt, Ag and Au than in the Southeast Extension zone dyke.

A probable explanation for the variability of semi-metals between the Ovoid regions, Discovery Hill and the hornblende gabbro dyke is that the semi-metals are contributed to the system through crustal contamination in a heterogeneous fashion. If the contaminants were localized, they may have delivered different semi-metals to different parts of the sulfide body. Secondly, the Southeast Extension zone sample was specifically taken from an area where sulfide mineralization is hosted by a hornblende-gabbro dyke, whereas the other samples in this study are from areas where the sulfide mineralization is hosted by troctolite or olivine-gabbro. The magmas of the hornblende-gabbro, olivine-gabbro and troctolite may have traversed different crustal rocks prior to final emplacement, and scavenged different semi-metals from them.

The semi-metal assay results of the local country rocks normalized to unmineralized troctolite and gabbro indicate that, in troctolite-hosted mineralization (Ovoid regions and Discovery Hill), contamination from country rocks is possible for Se, Sn and Sb from either Voisey's Bay granites or Tasiuyak gneisses. Because the Voisey's Bay granites were emplaced after the troctolite, and hydrothermal upgrading of metals has been ruled out, the most significant source of Se, Sn and Sb contamination is the Tasiuyak gneisses. This is consistent with the presence of variably digested and reacted inclusions of Tasiuyak paragneiss in conduit breccia rocks of the deposit (Li and Naldrett, 2000). Bismuth is only slightly enriched in the Tasiuyak gneisses compared to the troctolite. Arsenic is enriched in the Enderbitic diorite

and tonalite, but they are not known to be abundant in mineralized samples that are hosted by troctolite. The source of contamination of Bi and As in the troctolite thus may have been localized enrichments within the Tasiuyak and/or Enderbite units.

For the unmineralized gabbro, Se could have been added to the magma through country rock contamination from Tasiuyak gneisses, and As and Te through contamination from Enderbitic diorite. Both Sn and As are enriched in the mineralized samples of the Southeast Extension zone compared to the mineralized samples from the Ovoid regions and Discovery Hill. The variation in As (observed in both assays and PGM) between the troctolite hosted mineralization and the gabbro hosted mineralization could be the result of localized contamination of As from Enderbitic tonalitic-dioritic rock suites to the gabbros in the Southeast Extension zone.

Although the average concentration of Sn in Tasiuyak gneisses is lower than the average concentration of Sn in the gabbro, some of the Tasiuyak gneisses samples do contain elevated Sn (up to 3 ppm). Because the Tasiuyak gneisses do not have a homogenous mixture of minerals and could have variable compositions depending on location, it is possible that the Tasiuyak that were assimilated by the gabbros contained higher amounts of Sn than the Tasiuyak gneisses that are with the troctolite. This is demonstrated in the wider range of Sn concentrations in the Tasiuyak gneiss than in the other rock units analyzed (Tasiuyak ranges from below detection limit to 3ppm, whereas analysed samples of Enderbitic gneiss are all below detection limit). In some cases, the Tasiuyak gneisses contain sulfides that may be enriched heterogeneously in semi metals and may be the source of the semi-metals.

The notion that semi-metals are inherited from crustal sources by localized contamination has been suggested for the Sudbury deposits (Cabri and Laflamme, 1976; Dare et al., 2011) and for Platreef, Bushveld deposit (Hutchison and MacDonald, 2008). Furthermore, crustal contamination by country rock gneisses is widely recognized as the trigger for sulfur saturation in the parent gabbro-troctolite magmas at Voisey's Bay (Li and Naldrett, 2000; Ripley et al., 200; Lambert et al., 2000; Lightfoot et al., 2011). It

appears that crustal contamination not only led to the formation of sulfide magmas at Voisey's Bay, but also the crystallization of precious metal minerals through the introduction of semi-metal contaminants to the magmas. The Voisey's Bay results indicate that, even where PGE concentrations are very low in parent silicate magmas, PGMs may crystallize, provided that there are sufficient quantities of semi-metal ligands present to nucleate PGE-complexes.

*Evolution and Distribution of PGM in Sulfide Metals*

In the PGE poor DISS Ovoid sample (from drill hole BS0218), which represents a less fractionated area of the Ovoid (or MSS cumulates), the Pd concentration in pentlandite is similar to that in the inner Ovoid samples (~1.4ppm in the pentlandite), and the semi-metal to PGE ratio is similar in both sample types (20 in the PGE enriched samples in the Ovoid and 22 in the PGE poor sample); however, the Pd distribution in the PGE poor sample reveals that nearly all of the total Pd is in solid solution in pentlandite rather than deported to PGM, whereas only 22% of the Pd in the inner Ovoid samples occurs in solid solution in pentlandite. This result is not entirely consistent with the predictions presented in Helmy et al. (2007 and 2010). Based on their prediction, the Pd deportment should be similar in both the PGE poor sample and those in PGE rich samples (Ovoid centre) since their semi-metal to PGE ratios are similar. As an explanation, we suggest that in areas where semi-metals and PGE concentrations are sufficient to produce complexes, the proportion of PGE that is carried by discrete phases is also dependent on the degree of fractionation that has taken place within a sulfide melt. Sulfide that represents MSS cumulates would have captured less of the differentiated melt, contain lower absolute concentrations of semi-metals, and thus would accommodate a higher proportion of the total PGE (Pd) in solid solution in sulfides.

In summary, the amount of PGE in solid solution in sulfide phases is dependent on a combination of three factors: 1) incompatibility of the PGE into the early crystallizing MSS; 2) the presence of semi-metals in

the parent magma and the amount of assimilation that has occurred to incorporate external sources of semi-metals; and, 3) the degree of fractionation that has occurred within a sulfide melt.

The gabbro magmas contained more significant proportions of semi-metals than the troctolite magmas, and, consequently, the semi-metal to PGE ratio is higher in the hornblende-gabbro dyke mineralization than in the PGE rich Ovoid samples. The Sn and As bearing PGE in the hornblende-gabbro dyke would have formed PGE semi-metal complexes early in the crystallization history of the parent magmas, preventing significant amounts of Pt and Pd to enter solid solution in sulfide phases. This process may have delivered the PGM to a localized domain (the inner dyke) by entrainment in fractionating liquids. Thus, the concentration of significant (and perhaps economic) quantities of PGE (and Au or Ag) into localized domains may be strongly dependent on the semi-metal concentration of the parental magma.

Semi-metal control over PGE distribution is also apparent in the Ovoid samples. The semi-metal to PGE ratio in the Ovoid is lower than in the hornblende-gabbro dyke (due to lack of Sn and As), and because of this, less PGE semi-metal melt was able to accumulate at high temperatures and more Pd was able to dissolve in pentlandite and galena, diluting the overall Pd grade of the Ovoid compared to the hornblende-gabbro dyke (larger amounts of pentlandite to accept Pd). Evidence for this is seen in the Pd deportments that have a lower proportion of the Pd distributed to PGM relative to the hornblende-gabbro dyke samples (78% in the Ovoid compared to 97% in the hornblende-gabbro dyke). The semi-metal (As, Bi, Te and Pb) complexes could have carried Pt and Pd to the centre of the Ovoid in fractionated melts during cooling, depleting the outer Ovoid in PGE (represented by the PGE poor DISS Ovoid sample). If the troctolite that hosts the Ovoid mineralization would have acquired more semi-metals, perhaps a domain richer in PGM could have developed in the Ovoid. The fact that semi-metals are present in variable proportions in various parts of the ore system raises the possibility that undiscovered domains rich in PGE are present in less explored areas of the Voisey's Bay deposits.

Although there was semi-metal control on PGM distribution at Voisey's Bay, insufficient amounts of PGE were available to accumulate high-grade PGM occurrences in studied parts of the deposit. For example, in the Mini-Ovoid and Discovery Hill, the Pd concentrations are the lowest resulting in much higher semi-metal to PGE ratios; however the Pd concentrations are too low to accumulate Pd rich domains. Excess semi-metals (such as the Te and Bi) are dissolved into the sulfide phases, which is evident in the semi-metal deportment (Figure 12).

PMM occurrences in the Mini-Ovoid are the most different from the the other areas of Voisey's Bay deposit. No galena or sperrylite, and a much lower abundance of Pd-PGM were detected in the Mini-Ovoid. Conversely, this sample contains several grains of Ir-As and Re-Cu phases, which are associated with pentlandite, pyrrhotite and chalcopyrite. Rhenium could have been inherited from Tasiuyak gneisses because Tasiuyak gneisses are enriched in Re compared to the unmineralized gabbros and troctolites (Lambert et al., 2001).

The low abundances of Pt and Pd in the Mini-Ovoid sample and the presence of Ir and Re phases would imply exsolution of the Re and Ir phases from MSS crystals since it has been suggested that Re and Ir partition into the MSS (Fleet et al., 1993; Barnes et al., 1997). The high proportion of Pd in solid solution in pentlandite (68.5%) and the high semi-metal to PGE ratio (78) is further indication that the Mini-Ovoid sample is representative of a poorly differentiated melt that crystallized at high temperatures. High temperature crystallization of pentlandite in the Mini-Ovoid sample is consistent with its high Ni contents (EPMA, Table 4) compared to in the main Ovoid samples analyzed in this study (Naldrett et al., 1999).

*Sequence of PMM Crystallization at Voisey's Bay*

Considering the results and discussion above, a model for the crystallization of PGE, Au and Ag minerals at Voisey's Bay may be formulated: it is summarized in Figure 13A through 13E with the main points as follows:

1) As external sulfur was added to the Voisey's Bay Intrusion from the Tasiuyak paragneiss (e.g. Li and Naldrett, 2000) crustal contamination also added external Se, Sb, Sn, Te, Pb and Bi from local Tasiuyak gneisses, and As from tonalitic-dioritic Enderbite gneisses. The semi-metal contamination was most likely localized along the conduit feeder system of the Voisey's Bay parent silicate magma. Depending on the location, each part of the conduit system, different semi-metals were concentrated into different areas of the magma body (Figure 13A).
2) Once sulfur saturation occurred and temperatures cooled to *ca.* 1200 °C, an Fe-Cu-Ni rich sulfide melt segregated from the silica magma. At these high temperatures, As formed complexes with Pt and early sperrylite crystallization began. Over time sperrylite grew into large euhedral crystals; Bi, Te, Sn (in SE-Extension zone) and Sb (if present) complex with Pd to form nano-size clusters. The nano-clusters nucleated and led to the accumulation of a semi-metal rich melt (Figure 13B).
3) At 900ºC, ISS segregated from MSS. The semi-metal-PGE clusters became entrained in the ISS where they began to accumulate larger pools of semi-metal-rich melt that later precipitated PGM. The semi-metal melt also scavenged Au and Ag locally (Figure 13C and D).
4) At temperatures of 500-800 ºC, Pd, Pt, Au and Ag rich domains began to develop. Pentlandite exsolved from pyrrhotite (Naldrett et al., 2000) and incorporated "uncomplexed" Pd. Volynksite and stutzite crystallized followed by galena and chalcopyrite, froodite, michenerite, stutzite, electrum, Bi-Te, Ag-Bi-Te and Bi. (Quantitative compositions of volynskite and Bi-Te phase would be needed in order to estimate crystallization temperatures; Babanly et al., 2005.) Tiny

nano-clusters of PGE and bimutho-tellurides complexes that were not entrained into the semi-metal melt crystallized as very fine to sub-micron inclusions in sulfides (Figure 13E).

5) Altaite exsolved from galena (in Ovoid, based on mass ratio of PbTe/Te in galena of 0.02), and Ni-As (in Discovery Hill) exsolved from pentlandite. The Ir-As-S(?) phase and the Re-Cu-S(?) phase exsolved from MSS cumulates (in Mini-Ovoid, similar to sulpharsenides in Dare et al., 2010).

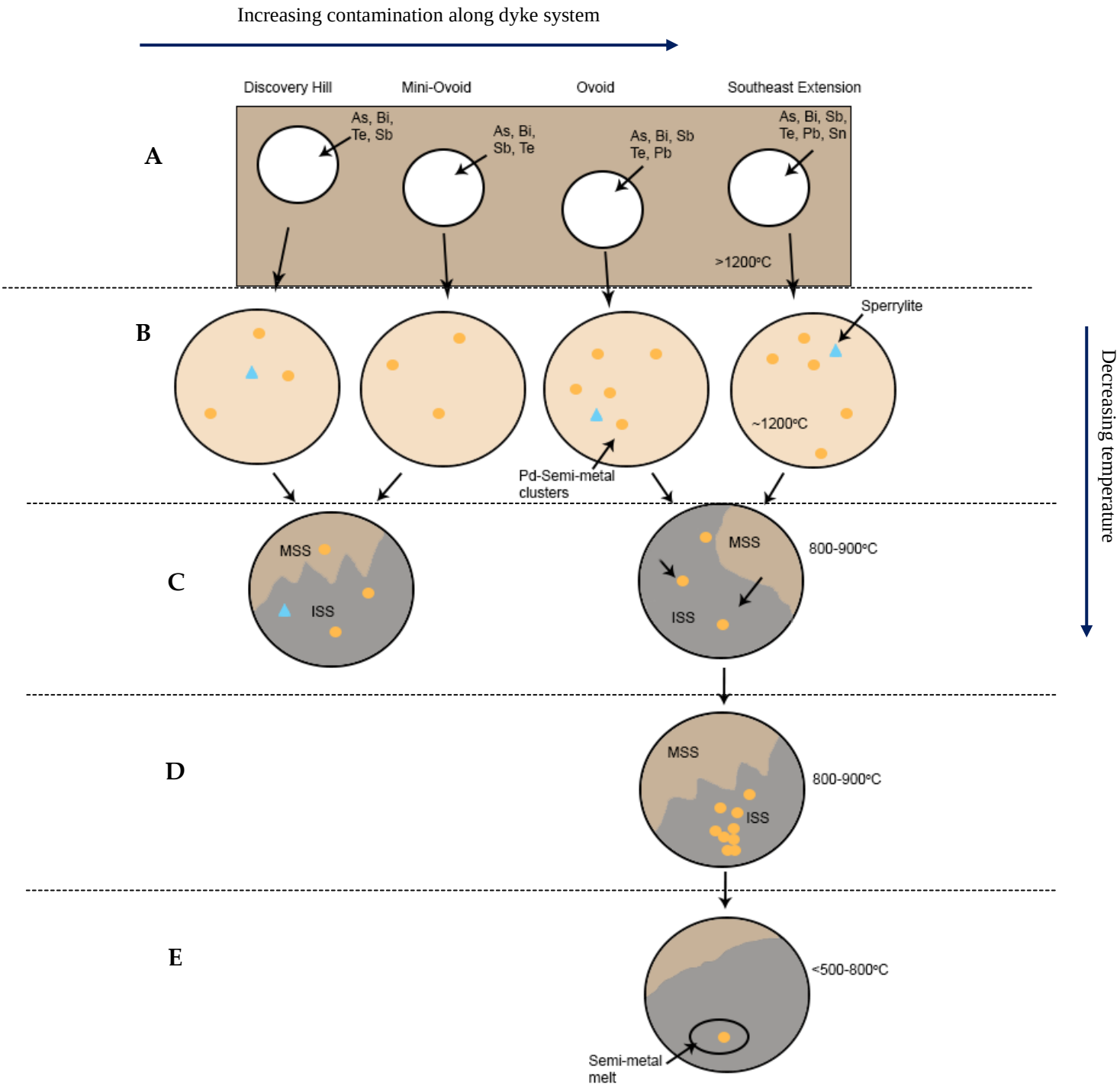


**Figure 3-16, A-E: Model for Crystallization of PGM and PMM**; **A.** Contamination of As, Bi, Te, Sn, Sb (and Se) from Tasiuyak Paragneiss & Enderbite Orthogneiss to silicate parental melts; **B.** Early complexing of semi-metals and PGE (Pd and Pt); **C.** Continuous growth of PGE semi-metal clusters; **D.** Accumulation of semi-metal PGE clusters by entrainment in fractionated liquids and by attraction of surface properties; **E.** Development of PGE enriched domains in fractionated regions; crystallization of PGM continues after this stage; Pd enters pentlandite and galena.

This model can be applied to the samples from each area of Voisey's Bay presented in this study. In the samples where the semi-metal and Pd concentrations were low, any Pd PGM and PMM were normally found as very fine inclusions in pentlandite and sometimes pyrrhotite. The idea that semi-metals and PGE begin to complex early at high temperatures would explain the very fine grain sizes observed in the Mini-Ovoid and Discovery Hill samples, and possibly any sub-micron particles documented from other deposits (summarized in Howell and MacDonald, 2010). Because the mass distribution of Te and Bi showed little deportment to pentlandite and pyrrhotite, it is less likely that any bismuthotelluride phases exsolved at low temperatures where these phases occur as fine textures in pyrrhotite and pentlandite. When the concentration of Pd and semi-metals are lower, the nano-clusters cannot as easily accumulate during fractionation. Where the concentrations are higher, such as in the Ovoid and Southeast Extension zone, the nano-clusters become entrained in the fractionating ISS and are able to accumulate at a higher rate to form the semi-melt.

Although it is not completely understood how galena is related to the semi-metal rich melt, we recognize that it is an important carrier of most semi-metals, Pd, Au and PMM grains at Voisey's Bay. Galena is also present where Ag and Pd contents are the highest. Galena may be a component of the ISS, which easily incorporated remaining semi-metals and Pd into solid solution, and formed textures with minerals derived from the co-existing semi-metal rich melt. Another possibility is that Pb was also enriched in the semi-metal melt, and exsolved some of the semi-melt minerals, such as Bi-Te and altaite, at low temperatures. To improve understanding of the role of Pb during PGE mineralization, investigations of occurrences of galena at other PGE bearing deposits are suggested given that galena seems to be a dominant host for many Pd and semi-metal occurrences.

**Conclusion**

The precious-metal (including PGE) geochemistry and mineralogy the Mini-Ovoid and Discovery Hill zones of the Voisey's Bay deposit were evaluated and compared to previously documented occurrences

from the Ovoid and Southeast Extension zone. Major differences observed between PMM assemblages across the deposit are due to localized contamination that has added different semi-metals into the silicate-sulfide liquid at each zone (in particular, Sn in the Southeast Extension zone). Evidence for this can be observed in the enrichment patterns of As, Se, Sb, Sn, Te and Bi in Tasiuyak and Enderbitic country rock relative to unmineralized troctolites and gabbros.

In the Mini-Ovoid sample, no galena or sperrylite was detected. Extremely fine grains of Ir-As-S(?) and Re-Cu-S(?) phases were identified in pentlandite, pyrrhotite and chalcopyrite and may indicate that the Mini-Ovoid sample crystallized under higher temperature conditions than the other deposits.

A plausible model for the formation and mineralization of precious metals at Voisey's Bay involves: incorporation of semi-metals during crustal contamination, and early complexing of semi-metals and PGE at high temperature, which leads to early sperrylite crystallization and formation of a differentiated semi-metal-Pd melt. The predicted model is based on the following observations:

- Large, euhedral, easily liberated sperrylite occurrences are occasionally associated with other PMM and galena;
- Deportment of much of the Pd and semi-metals at Voisey's Bay to discrete precious metal mineral phases;
- Sporadic, fine-grained inclusions of Ag, Pd and Pb rich minerals in pentlandite and sometimes pyrrhotite.
- Associations of Pd-PGM and other PMM with galena and other ISS phases.

The results presented in this paper indicate that PGM are able to crystallize at low-grade deposits if semi-metals are present in large enough quantities. The semi-metals (As, Te, Sn and Bi) are shown to have a critical influence over the distribution of Pd and Pt at the Voisey's Bay deposits. The higher semi-metal to PGE ratio in the hornblende-gabbro dyke mineralization was sufficient to accumulate high grade precious-metal domains. The Ovoid region may also contain domains of high grade Pd in the most

fractionated regions, but the Pd concentrations are less significant than the domains in the hornblende-gabbro dyke due to a lower semi-metal to PGE ratio. The localized semi-metal variation throughout Voisey's Bay deposits introduces the possibility that small-scale domains containing enrichments of Pt, Pd, Au and Ag may exist at undeveloped areas of Voisey's Bay.

## References


Amelin, Y., Li, C., Naldrett, A.J. (1999) Geochronology of the Voisey's Bay intrusion, Labrador, Canada by precise U-Pb dating of coexisting baddeleyite, zircon and apatite. Lithos v 47, p 33-51

Amelin, Y., Li, C., Valeyev, O., Naldrett, A.J. (2000) Nd-Pb-Sr isotope systematics of crustal assimilation in the Voisey's Bay and Mushuau intrusions, Labrador, Canada. Economic Geology, v. 95, p. 815–830.

Barnes, S-J., Naldrett, A.J., Gorton, M.P. (1985) The origin of platinum-group elements in terrestrial magmas. Chemical Geology v 53, p 303-323

Babanly, M.B., Shykhyev, Y.M., Babanly, N.B., Yusibov, Y.A. (2005) Phase equilibria in the Ag-Bi-Te system. Physiochemical Analysis of Inorganic Systems v 52, p 487-493

Cabri, L.J., Laflamme, J.H.G. (1976) The mineralogy of the platinum-group elements from some copper-nickel deposits of the Sudbury area, Ontario. Economic Geology v 71, p 1159-1195

Cabri, L.J., Rudashevsky, N.S., Rudashevsky, V.N. & Oberthür, T. (2008): Electric-Pulse Disaggregation (EPD), Hydroseparation (HS) and their use in combination for mineral processing and advanced characterization of ores. Can. Mineral Processors, 40th Annual Meeting, Proc., Pap. 14, p. 211-235.

Dare, A.S., Barnes, S-J., Prichard, H.M., Fisher, P.C. (2010) The timing and formation of platinum-group minerals from the Creighton Ni-Cu-Platinum-group element sulfide deposit, Sudbury, Canada: early crystallization of PGE-rich sulfarsenides. Economic Geology v 105, p 1071-1096

Dare, A.S., Barnes, S-J., Prichard, H.M., Fisher, P.C. (2014) Mineralogy and geochemistry of Cu-rich ores from the McCreedy East Ni-Cu-PGE deposit (Sudbury, Canada); implications for the behavior of platinum group and chalcophile elements at the end of crystallization of a sulfide liquid. Economic Geology v 109, p 343-366

Evans-Lamswood, D.M., Butt, D.P., Jackson, R.S., Lee, D.V., Muggridge, M.,G., Wheeler, R.I. and Wilton, D.H.C. (2000) Physical controls associated with the distribution of sulfides in the Voisey's Bay Ni-Cu-Co deposit, Labrador. Economic Geology v 95, p. 749-769

Fandrich, R., Gu, Y., Burrows, D., and Moeller, K. (2007). Modern SEM-based mineral liberation analysis: International Journal of Mineral Processing, v. 84, p. 310–320.

Farrow, C.E.G., Watkinson, D.H. (1999), An evaluation of the role of fluids in Ni-Cu-PGE-bearing, mafic ultramafic systems: Geological Association of Canada Short Course, v 13, p 31-98

Fleet, M.E., Stone, W.E. (1991) Partitioning of platinum-group elements in the Fe-Ni-S system and their fractionation in nature. Geochimica and Cosmochimica v 55, p 245-253

Hanley, J. (2005), The aqueous geochemistry of the platinum-group elements (PGE) in surficial, low T hydrothermal and high-T magmatic hydrothermal environments: Mineralogical Association of Canada Short Course v 35, p 35-56

Helmy, H.M., Baullhaus, C., Fronseca, R.O.C., Wirth, R., Nagel, T., Tredoux, M. (2013a) Noble metal and nanoclusters and nanoparticles precede mineral formation in magmatic sulfidesulfide melts. Nature Communications 4, Article 2405

Helmy, H.M., Ballhaus, C., Fronseca, R.O.C. (2013b) Fractionation of platinum, palladium, nickel, and copper in sulfide-arsenide systems at magmatic temperature. Contib Mineral Petrol v 166, p 1725-1737

Helmy, H.M., Ballhaus, C., Wohlgemuth-Ueberwasser, C., Fonseca, R.O.C., Laurenz, V. (2010) Partitioning of Se, As, Sb, Te and Bi between monosulfide solid solution and sulfide metl - application to magmatic sulfide deposits. Geochimica and Cosmochimica v 74, p 6174-6179

Helmy, H.M., Ballhaus, C., Berndt, J., Bockrath, C., Wohlgemuth-Ueberwasser, C. (2007) Formation of Pt, Pd and Ni tellurides: experiments in sulfide-telluride systems. Contributions to Mineralogy and Petrology v 153, p 577-591

Hill, R.E.T. (1984) Experimental study of phase relations at 600ºC in a portion of the Ni-Fe-Cu-S system and its applications to natural sulfide assemblages, in Buchanan, D.L., and Jones, M.J., eds., Sulfide deposits in mafic and ultramafic rocks: Institute of Mining and Metallurgy Special Publication, p 14-21

Holwell, D.A., McDonald, I. (2010) A review of the behavior of platinum-group elements within natural magmatic sulfide ore systems. Platinum Metals Rev v 54, p 26-36

Huminicki, M.A.E., Sylvester, P.J., Lastra, R., Cabri, L.J., Evans-Lamswood, D., Wilton, D.H.C. (2008) First report of platinum-group minerals from a hornblende-gabbro dyke in the vicinity of the Southeast Extension Zone of the Voisey's Bay Ni-Cu-Co deposit, Labrador. Mineralogy and Petrology v 92, p 129-164

Huminicki, M.A.E., Sylvester P J, Shaffer M, Wilton D H C, Evans-Lamswood D, Wheeler R I (2012) Systematic and Integrative Ore Characterization of Massive Sulfide Deposits: An Example from Voisey's Bay Ni-Cu-Co Ovoid Orebody. Exploration and Mining Geology v 20, p 53-86

Huminicki, M.A.E., Sylvester, P.J., Cabri, L.J., Lesher, C.M., and Tubrett, M. (2005) Quantitative mass balance of platinum-group elements in the Kelly Lake Ni-Cu-PGE deposit, Copper Cliff offset, Sudbury. Economic Geology, v. 100, p. 1631–1646.

Huminicki, M.A.E (2007) A comprehensive geological, petrological, and geochemical evaluation of the Voisey's Bay Ni-Cu-Co sulfide deposit: an integration of empirical data and process mechanics, PhD Thesis, Memorial University of Newfoundland

Hutchinson, D., McDonald, I. (2008) Laser ablation ICP-MS study of platinum-group elements in sulfides from the Platreef at Turfspruit, northern limb of the Bushveld Complex, South Africa: Mineralium Deposita v 43, p. 695–711.

Kelvin, M.A., Sylvester, P.J., Cabri, L.J. (2011) Mineralogy of rare occurrences of precious-metal-enriched massive sufide in the Voisey's Bay Ni–Cu–Co Ovoid deposit, Labrador, Canada. Canadian Mineralogist v 49, p 1505-1522.

Lambert, D.D., Frick, L.R., Foster, J.G., Li, C., Naldrett, A.J. (2000) Re-Os isotope systematics of the Voisey's Bay Ni-Cu-Co magmatic sulfide system, Labrador, Canada: II. Implications for parental magma chemistry, ore genesis, and metal redistribution. Economic Geology v 95, p 867-888

Lambert, D.D., Foster, J.G., Frick, L.R., Li, C., Naldrett, A.J. (1999) Re-Os isotopic systematics of the Voisey'sBay Ni-Cu-Co magmatic ore system, Labrador, Canada. Lithos v 47, p 69-88

Li, C., Naldrett, A. J. (2000) Melting Reactions of Gneissic Inclusions with Enclosing Magma at Voisey's Bay, Labrador, Canada: Implications with Respect to Ore Genesis. Economic Geology v 95, p. 801-814

Li, C., Lightfoot, P.C., Amelin, Y., Naldrett, A.J. (2000) Contrasting petrological and geochemical relationships in the Voisey's Bay and Maushuau Intrusions, Labrador, Canada: Implications for ore genesis. Economic Geology v 95, p 771-799

Lightfoot, P.C., Keays, R.R., Evans-Lamswood, D., Wheeler, R. (2011) S Saturation History or Nain Plutonic Suite mafic intrustions: origin of the Voisey's Bay Ni-Cu-Co sulfide deposit, Labrador, Canada. Miner Deposita v 47 p 25-50

Mulligan, R., Jambor, J.L. (1968) Tin-bearing silicates from skarn in the Cassiar District, northern British Columbia, Canadian Mineralogist, v 9, p 358-370

Mulholland, I.R. Malayaite and tine-bearing garnet from a skarn at Gumble, NSW, Australia, Mineralogical Magazine v 48, p 27-30

Naldrett, A.J. (2010) From the mantle to the bank: the life of a Ni-Cu-(PGE) sulfide deposit. South African Journal of Geology v 113, p 1-32

Naldrett, A.J., Singh, J., Kristic, S., Li, C. (2000a) The mineralogy of the Voisey's Bay Ni-Cu-Co deposit, Northern Labrador, Canada: Influence of oxidation state on textures and mineral compositions. Economic Geology v 95, p 889-900

Naldrett, A.J., Asif, M., Krstic, S., Li, C. (2000b) The composition of mineralzation at the Voisey's Bay Ni-Cu sulfide deposit, with special reference to platinum-group elements: Economic Geology v 95, p 845-865

Peregoedova, A.V. (1998) The experimental study of Pt-Pd-partitioning between monosulfide solid solution and Cu-Ni sulfide melt at 900-840ºC. In 8th International Platinum Symposium abstracts. Geol Soc South Africa and South African Inst Min Metall, Symposium Series, S18, p 325-373

Pina, R., Gervilla, F., Barnes, S-J., Ortega, L., Lunar, R. (2012) Distribution of platinum-group and chalcophile elements in the Aguablanca Ni-Cu sulfide deposit (SW Spain): Evidence from a LA-ICP-MS study. Chemical Geology v 302-303, p 61-75

Rawlings-Hinchey, A.M., Sylvester, P.J., Myers, J.S., Dunning, G.R. and Kosler, J. (2003). Paleoproterozoic crustal genesis: calc-alkaline magmatism of the Torngat orogen, Voisey's Bay area, Labrador. Precambrian Research v 125, p 55-85.

Ripley, E.M., Park, Y-R. (2000) Oxygen isotope studies of the Voisey's Bay Ni-Cu-Co deposit, Labrador, Canada. Economic Geology. v 95 p 831-844

Ripley, E.M., Park, Y-R., Li, C., Naldrett, A.J. (1999) Sulfur and oxygen isotopic evidence of country rock contamination in the Voisey's Bay Ni-Cu-Co deposit, Labrador, Canada. Lithos v 47, p 53-68

Ryan, B. (2000) The Nain-Churchill boundary and the Nain Plutonic Suite: A regional perspective on the geological setting of the Voisey's Bay Ni-Cu-Co deposit. Economic Geology v 95, p 703-724

Sylvestster, P.J. (2001) A practical guide to the platinum-group element analysis of sulfides by laser-ablation ICPMS. In Laser-Ablation ICPMS in the Earth Sciences. Principles and Applications (P. Sylvester, ed.). Mineral. Assoc. Can., Short Course 29, p. 203-211.

Sylvester, P.J., Cabr i, L.J., Tubrett , M.N., Peregoedovava, A., McMahon, G., Laflamme, J.H.G. (2005) Synthesis and evaluation of a fused pyrrhotite standard reference material for platinum group element and gold analysis by laser ablation – ICPMS. Proc. 10th Int. Platinum Symp. (Oulu), Extended Abstr. Vol., p 16-20.

# CHAPTER 4: CONCLUSION AND RECOMMENDATIONS

This thesis has provided a clearer understanding of the PGE occurrences and their potential for recovery within the Ovoid deposit and regions of the Discovery Hill and Mini-Ovoid deposit. The samples that were chosen for this study represent areas of Voisey's Bay deposit that contain elevated levels of Pt+Pd, and Au or Ag. Samples containing elevated concentrations of Pd and Pt from the Ovoid were the main focus of this study, but occurrences from areas of Discovery Hill and the Mini-Ovoid were also analyzed for comparison. The results were compared to previously documented occurrences from a hornblende-gabbro dyke in the Southeast Extension zone.

The primary objectives of this thesis were: 1) to identify the potential for recovering PGE from Voisey's Bay deposit if future exploration reveals domains of economically significant concentrations of PGE; and, 2) to define a model for the genesis of the PGE at Voisey's Bay which could have useful references to the evolution of Voisey's Bay and other deposits with similar mineralization styles. These objectives were most effectively addressed through preparation of a mass-balance and a quantitative distribution of Pt, Pd, Au and Ag occurrences at Voisey's Bay. A rigorous characterization of PGM and PMM acquired by MLA was performed. Characteristics such as grain size and association were documented for each PGM and PMM detected. The MLA results were combined with the concentrations of Pd, Pt and other semi-metals in solid solution in sulfide phases determined by LA-ICPMS to produce a distribution of Pd, Pt, Ag and Au, and semi-metals (As, Sn, Te and Bi).

The following points summarize the significant results of the mass-balance calculations and the main conclusions specific to ore processing of Pt, Pd, Au and Ag at Voisey's Bay:

- In the Ovoid samples, the dominant PGMs that were detected include froodite and sperrylite. Rare grains of michenerite were also detected; the PMM detected include stutzite, volynskite and electrum.

- Sperrylite contributes to the majority of total PGM+PMM weight% (90%) due to its large grain size (>80μm) and may be easily liberated during routine grinding in the milling circuit.
- The majority of froodite grains occur as fine inclusions (<10μm) in pentlandite or galena, but several larger grains (>30μm) distribute the mass of froodite to 30-50μm. The fine froodite inclusions would be difficult to liberate during routine grinding and could be recovered to the Ni or Cu concentrates; the larger grains, which make up the majority of the mass of Pd, would be easier to liberate and could potentially be recovered during flotation or gravity concentration methods.
- Only Pd and Ag were found in significant concentrations in solid solution in pentlandite and galena, ranging from 1.2 to 199 ppm. The mass balance estimates that the majority of Pt, Pd, Au and Ag occur as discrete mineral phases rather than in solid solution (77.3-99.0%). Approximately 23% of the Pd was distributed to either galena or pentlandite in solid solution.
- Considering the results of the mass balance, it was estimated that a large portion of Pd could be recovered to the Ni concentrate, and ~33% of the total Pd is associated with galena as inclusions or in solid solution. Recovery of that 33% is dependent on recovery of galena.
- The most significant conclusion is that recovery of a large proportions of the Pt, Pd and Ag is possible because most of the PGE and PMM mass are either associated with recoverable sulfides (galena, pentlandite and chalcopyrite), or large enough to be concentrated alone. Very little mass is associated with pyrrhotite that would be rejected to the tailings in order to reduce $SO_2$ emissions during smelting of pyrrhotite.

Not only has this quantitative distribution of PGE and PM provided useful applications to ore processing, it has also improved our understanding of their occurrences in relation to the genetic history of Voisey's Bay deposit. Quantifying the occurrences of Pd, Pt, Ag, Au and other semi-metals offers more meaningful insight into the crystallization history of the PGM at Voisey's Bay than interpretation based only on speculation of average concentrations of PGE in solid solution and the

types of PGE and PM mineral phases present. The quantitative distribution of the PGE occurrences has allowed us to directly compare the proportions of PGE dissolved in solid solution in the Ovoid, Mini-Ovoid, Discovery Hill and the Southeast Extension zone. The results indicate that the distribution and type of Pd, Pt, Au and Ag occurrences that will crystallize is dependent on semi-metal content (in this case As, Bi, Sn and Te) of the parental sulfide melt, incompatibility of the precious metals within early crystallizing MSS, and the degree of fractionation of the of the magma.

The majority of the conclusions related to crystallization history were drawn from comparisons of the selected samples. Our comparisons also involved assay analysis of country rock that is local to Voisey's Bay intrusion that aided in the interpretation of semi-metal origins. It was shown that the PGM and PMM phases in the centre of the Ovoid differ from those within the inner hornblende-gabbro dyke in the Southeast Extension zone and to occurrences the Mini-Ovoid.

Our model proposes that interaction of Voisey's Bay magma with crustal Tasiuyak paragneisses has contaminated the system with As, Bi, Sn and Te. The contamination is localized and delivers a heterogenous combination of the semi-metals to the magmas that now occupy separate regions of the deposit. The semi-metals are a key component for the onset of Pt, Pd and Ag mineralization. Early on in the magma development, As, Bi, Sn and Te may complex to Pt, Pd or Ag at high temperatures and form the basis of differtentiated melt rich in precious metals. This melt may co-exist with the Cu-rich ISS although they are potentially immiscible. The PGE mineralizations in the inner Ovoid and the hornblende-gabbro dyke represent crystallization of the differentiated melt that is enriched in variable proportions of As, Te, Bi, Sn, Pb and Sb. The samples from the Mini-Ovoid and the outer region of the Ovoid, represent MSS cumulates or magmas that crystallized at higher temperatures. The proposed model is based on a number of observations which are listed below:

- 77% of the mass of Pd, Pt, Ag and Au are present as mineral phases complexed to Bi, As, Te and Sb in the Ovoid and 98% of the mass in the hornblende-dyke occur as discrete mineral phases containing Sn, Bi, As, Te and Sb.
- A PGE poor disseminated sample from the outer region of the Ovoid contains >85% of Pd in solid solution in pentlandite.
- In Discovery Hill, the dominant PGM is sperrylite, and only rare michenerite was detected. Stutzite, volynskite and electrum are present.
- The Mini-Ovoid sample contained only a few PGM grains which included froodite and rare grains of an Ir-As phase. Rare Re-Cu-S was also detected. The majority of the Pd in the Mini-Ovoid is present in solid solution in pentlandite.

The results presented in this study suggest that PGM (and PMM) are able to crystallize at low-grade deposits if sufficient concentrations of semi-metals are available in the parent magma to complex to PGE, Au and Ag. Complexing of semi-metals to PGE at high temperatures may increase the potential to precipitate domains rich in PGE, which may be the case for the inner Ovoid and the inner region of the hornblende-gabbro dyke in the Southeast extension zone at Voisey's Bay. Recovery of Pd, Pt, Au and Ag from these areas is possible since majority of mass could be recovered to the Ni or Cu concentrate or is present as grains large enough to be recovered alone.

The following recommendations are suggested for furture analysis to further improve the understanding of PGM occurrences at the Voisey's Bay deposit:

- A more robust data-set of massive sulfide samples from the mid Ovoid region which integrates chemical assay with mineralogical data may reveal if a distinct precious-metal enriched zone is present in the Ovoid deposit, or any other areas of Voisey's Bay deposit.

- Analysis of Pd and Pt rich samples from other areas of Voisey's Bay deposit such as Reid Brook, Eastern Deeps and the centre regions of the Mini-Ovoid identify whether any precious-metals in these areas are associated with bismuth-tellurides.

# APPENDIX 1: ASSAY DATA (ICP-MS AND NI FIRE ASSAY)

Analysis for Fe, S, Co, Ni and Cu by solution ICP-MS analysis was carried out at Memorial University. The remaining elements were analyzed by total acid digestion followed by ICP-MS and were performed at Actlabs Ltd in Ancaster, Ontario.

| | | Element | Ir | Ru | Rh | Pt | Pd | Au | Re | Fe | Ni | Cu | S | Pb | Li | Na | Mg | Al | K | Ca | Cd | V | Cr |
|---|---|---|---|---|---|---|---|---|---|---|---|---|---|---|---|---|---|---|---|---|---|---|---|
| | | Unit | ppb | ppb | ppb | ppb | ppb | ppb | ppb or ppm | % | % or ppm | % or ppm | % | ppm | ppm | % | % | % | % | % | ppm | ppm | ppm |
| | | L.O.D. | 1 | 1 | 1 | 1 | 1 | 1 | 1 | 0.01 | | | | 0.5 | 0.5 | 0.01 | 0.01 | 0.01 | 0.01 | 0.01 | 0.1 | 1 | 0.5 |
| | | Method | NI-FAMS | NI-FAMS | NI-FAMS | NI-FAMS | NI-FAMS | NI-FAMS | NI-FAMS | TD-MS | ICPMS | ICPMS | ICPMS | TD-MS | TD-MS | TD-MS | TD-MS | TD-MS | TD-MS | TD-MS | TD-MS | TD-MS | TD-MS |
| **Rock Type** | **Description** | **Location** | | | | | | | | | | | | | | | | | | | | | |
| **Country Rock** | | | | | | | | | | | | | | | | | | | | | | | |
| Proterozoic Tasiuyak Paragnei | Meta-Quartz Diorite | Dico Hill | | | | | | | < 0.001 | 3.97 | 55.9 | 21.2 | | 27.4 | 14.3 | 1.99 | 1.49 | 8.18 | 1.52 | 1.13 | 0.2 | 90 | 57.5 |
| Proterozoic Tasiuyak Paragnei | Garnet Amphibolite | cheeks | | | | | | | < 0.001 | 12.4 | 252 | 27.8 | | 2.5 | 7.8 | 2.15 | 5.32 | 6.83 | 0.22 | 5.37 | 0.2 | 191 | 40.8 |
| Proterozoic Tasiuyak Paragnei | Quartzite | cheeks | | | | | | | 0.007 | 0.94 | 7.5 | 11.7 | | 25.4 | 11.2 | > 3.00 | 0.24 | 7.61 | 1.65 | 1.11 | < 0.1 | 13 | 3.7 |
| Proterozoic Tasiuyak Paragnei | Quartzite | cheeks | | | | | | | 0.018 | 5.81 | 17 | 3.6 | | 1.6 | 4.8 | 0.19 | 0.07 | 0.44 | 0.11 | 0.17 | 0.1 | 146 | 117 |
| Proterozoic Tasiuyak Paragnei | Meta-Sediment | N of Mushuau | | | | | | | < 0.001 | 4.57 | 22.3 | 4.7 | | 2 | 5.8 | 0.08 | 8.1 | 2.42 | 0.19 | 13.7 | 0.2 | 55 | 12.8 |
| Proterozoic Tasiuyak Paragnei | Meta-Pelite | Old Joe | | | | | | | 0.002 | 8.03 | 76 | 5.9 | | 7.4 | 19.7 | 0.88 | 1.76 | 7.75 | 1.51 | 1.22 | 0.1 | 75 | 135 |
| Proterozoic Tasiuyak Paragnei | Garnet Tasiuyak Gneis | Dico Hill | | | | | | | 0.001 | 5.21 | 11.6 | 11.7 | | 12.6 | 9.6 | 1.7 | 0.52 | 6.82 | 2.37 | 1.9 | 0.2 | 22 | 19.8 |
| Enderbitic Orthogneiss | Enderbitic/Orthogneiss | Mushuau | | | | | | | < 0.001 | 2.24 | 18.7 | 20.2 | | 9.3 | 11.3 | > 3.00 | 0.78 | 8.73 | 0.39 | 2.84 | < 0.1 | 43 | 10.7 |
| Enderbitic Orthogneiss | Enderbitic/Orthogneiss | Mushuau | | | | | | | 0.002 | 1.37 | 13.6 | 36.8 | | 8 | 10.6 | > 3.00 | 0.47 | 8.54 | 0.37 | 2.64 | < 0.1 | 24 | 4.6 |
| Enderbitic Orthogneiss | Enderbitic Gneiss | North of Eastern Deeps | | | | | | | 0.003 | 3.36 | 32.9 | 26.9 | | 13.2 | 12.1 | 0.93 | 0.96 | 5.08 | 1.29 | 0.55 | 0.1 | 57 | 47.2 |
| **Voisey's Bay Intrusive Rocks** | | | | | | | | | | | | | | | | | | | | | | | |
| **Unmineralized** | | | | | | | | | | | | | | | | | | | | | | | |
| Tonalite | Tonalite | Dico Hill | | | | | | | < 0.001 | 3.86 | 26.5 | 2.1 | | 10.4 | 13.7 | > 3.00 | 1.63 | 9.94 | 0.56 | 4.88 | < 0.1 | 85 | 16.7 |
| Quartz Diorite | Qtz Diorite | Dico Hill | | | | | | | < 0.001 | 3.34 | 19.3 | 30.3 | | 11.3 | 13.8 | > 3.00 | 1.39 | 8.85 | 0.8 | 4.07 | < 0.1 | 45 | 11.5 |
| Gabbro | Meta-Gabbro | Dico Hill | | | | | | | < 0.001 | 4.07 | 30.5 | 36.2 | | 15.9 | 17 | > 3.00 | 1.71 | 8.93 | 1.9 | 4.26 | 0.1 | 90 | 24.3 |
| Gabbro | Meta-Gabbro | Dico Hill | | | | | | | < 0.001 | 5.89 | 38 | 83.2 | | 8.8 | 11.4 | > 3.00 | 2.2 | 9.19 | 0.54 | 5.47 | 0.2 | 149 | 36.9 |
| Gabbro | Gabbro | Dico Hill | | | | | | | < 0.001 | 8.57 | 1110 | 834 | | 4.2 | 10.3 | 2.14 | 5.44 | 8.48 | 0.21 | 5.08 | 0.3 | 36 | 39.2 |
| Gabbro | Gabbro | Dico Hill | | | | | | | < 0.001 | 7.28 | 36.2 | 7 | | 3.8 | 17.8 | > 3.00 | 2.95 | 8.91 | 0.39 | 6.17 | 0.2 | 214 | 64.4 |
| Gabbro | Gabbro | Southeast Extension | | | | | | | 0.004 | 8.51 | 2950 | 898 | | 12.5 | 7.7 | > 3.00 | 2.4 | 7.27 | 0.48 | 5.11 | 0.5 | 50 | 40.7 |
| Granite | VB Granite | Dico Hill | | | | | | | < 0.001 | 2.01 | 7.7 | 9 | | 16.7 | 8.5 | 2 | 0.18 | 6.18 | 0.77 | 0.98 | < 0.1 | 29 | 4 |
| Granite-Syenite | VB Granite-Syenite | East of Eastern Deeps | | | | | | | 0.002 | 2.53 | 104 | 81.9 | | 27.4 | 13 | 2.09 | 0.11 | 5.78 | 3.15 | 0.57 | 0.1 | 1 | 4.8 |
| Granite | Granite | East of Eastern Deeps | | | | | | | < 0.001 | 2.06 | 4.2 | 4.3 | | 16.1 | 7.6 | 2.12 | 0.12 | 5.57 | 1.34 | 0.83 | < 0.1 | 5 | 3.6 |
| Troctolite | Troctolite | VB Troctolite | | | | | | | 0.017 | 12.8 | 1610 | 1270 | | 7.2 | 8.2 | 0.59 | > 10.0 | 1.99 | 0.22 | 2.82 | 1 | 55 | 2270 |
| Troctolite | Troctolite | VB Troctolite | | | | | | | 0.007 | 10.8 | 2910 | 1420 | | 44.5 | 5.1 | 2.53 | 2.78 | 8.27 | 0.46 | 4.64 | 0.6 | 35 | 58.8 |
| Troctolite | Troctolite | VB Troctolite | | | | | | | < 0.001 | 6.06 | 397 | 306 | | 3.6 | 11.5 | 2.67 | 3.38 | > 10.0 | 0.68 | 5.35 | 0.2 | 35 | 96.8 |
| **Mineralized** | | | | | | | | | | | | | | | | | | | | | | | |
| BS0218 | Disseminated Sulphide | Troctolite Feeder (Ovo | < 1 | 1 | 2 | 33 | 85 | 19 | 16 | 23.6 | | | | 53.7 | 3.9 | 1.66 | 2.99 | 5.82 | 0.27 | 3.85 | 1.5 | 46 | 84.9 |
| BS0265 | Semi-Massive Sulphide | Mini-Ovoid | 3 | 3 | 8 | < 1 | 93 | < 1 | 52 | 35.2 | 2.6 | 5.5 | 15 | 8 | 4.9 | 0.531 | 1.23 | 3.32 | 0.86 | 2.34 | 8.2 | 81 | 202 |
| BS0241 | Massive Sulphide | Inner Ovoid | 1 | < 1 | 5 | 158 | 463 | 84 | 32 | 46.7 | 3.2 | 2.4 | 26 | 1686 | < 0.5 | 0.034 | < 0.01 | 0.02 | < 0.01 | < 0.01 | 5.5 | 60 | < 0.5 |
| BS0207 | Massive Sulphide | Inner Ovoid | < 1 | < 1 | 3 | 614 | 503 | 297 | 18 | 49 | 4.5 | 2.5 | 27 | 1201 | < 0.5 | 0.07 | < 0.01 | 0.04 | 0.01 | < 0.01 | 6.8 | 13 | 2.7 |
| DF6063 | Massive Sulphide | Inner Ovoid | < 1 | < 1 | 4 | 325 | 412 | 51 | 22 | 49 | 4.3 | 1.1 | 30 | 819 | < 0.5 | 0.041 | 0.04 | 0.06 | 0.01 | 0.12 | 18.2 | 13 | 1.9 |
| DF6055 | Massive Sulphide | Inner Ovoid | 1 | < 1 | 4 | 2180 | 2490 | 209 | 25 | 52.6 | 5.1 | 4.2 | 29 | 712 | < 0.5 | 0.034 | 0.01 | 0.02 | < 0.01 | < 0.01 | 27.3 | 8 | < 0.5 |
| VX49277 | Disseminated Sulphide | Disco Hill | < 1 | 11 | 5 | 338 | 324 | 488 | 30 | 27.7 | 2.59 | 1.12 | 15.7 | 67.2 | 2.5 | 0.47 | 1 | 1.8 | 0.1 | 1.38 | 6 | 13 | 20.1 |
| VX49289 | Semi-Massive Sulphide | Disco Hill | < 1 | 12 | 6 | 80 | 288 | 454 | 25 | 28.1 | 1.42 | 7.32 | 11 | 30.1 | 1.5 | 0.02 | 0.7 | 0.31 | < 0.01 | 1.48 | 28.1 | 12 | < 0.5 |
| MH-028A | Semi-Massive Sulphide | H.G. Dyke, SEE | | | | | | | | 6.7 | | | | > 5000 | 13.5 | 2.7 | 4.8 | > 10.0 | 0.6 | 7.14 | 74.3 | 21 | 44.9 |
| MH-028B | Semi-Massive Sulphide | H.G. Dyke, SEE | | | | | | | | 10.9 | | | | 1330 | 10.7 | > 3.00 | 3.9 | 9.55 | 0.9 | 7.3 | 17.4 | 38 | 37.6 |
| MH-035 | Semi-Massive Sulphide | H.G. Dyke, SEE | | | | | | | | 8.03 | | | | > 5000 | 12.8 | 2.86 | 4.7 | > 10.0 | 0.6 | 6.77 | 45.3 | 28 | 90.8 |
| MH-036 | Semi-Massive Sulphide | H.G. Dyke, SEE | | | | | | | | 6.89 | | | | 3890 | 78.1 | 2.87 | 4.2 | > 10.0 | 0.6 | 6.9 | 25.3 | < 1 | 82.2 |

| Mn | Hf | Er | Be | Ho | Ag | Cs | Co | Eu | Bi | Se | Zn | Ga | As | Rb | Y | Sr | Zr | Nb | Mo | In | Sn | Sb | Te | Ba | La | Ce | Pr | Nd | Sm | Gd | Tb | Dy | Ge | Tm | Yb | Lu | Ta | W | Tl | Th | U |
|---|---|---|---|---|---|---|---|---|---|---|---|---|---|---|---|---|---|---|---|---|---|---|---|---|---|---|---|---|---|---|---|---|---|---|---|---|---|---|---|---|
| ppm | ppm | ppm | ppm | ppm | ppm | ppm | ppm | ppm | ppm | ppm | ppm | ppm | ppm | ppm | ppm | ppm | ppm | ppm | ppm | ppm | ppm | ppm | ppm | ppm | ppm | ppm | ppm | ppm | ppm | ppm | ppm | ppm | ppm | ppm | ppm | ppm | ppm | ppm | ppm | ppm |
| 1 | 0.1 | 0.1 | 0.1 | 0.1 | 0.05 | 0.05 | 0.1 | 0.05 | 0.02 | 0.1 | 0.2 | 0.1 | 0.1 | 0.2 | 0.1 | 0.2 | 1 | 0.1 | 0.1 | 0.1 | 1 | 0.1 | 0.1 | 1 | 0.1 | 0.1 | 0.1 | 0.1 | 0.1 | 0.1 | 0.1 | 0.1 | 0.1 | 0.1 | 0.1 | 0.1 | 0.1 | 0.05 | 0.1 | 0.1 |
| TD-MS | TD-MS | TD-MS | TD-MS | TD-MS | TD-MS | TD-MS | TD-MS | TD-MS | TD-MS | TD-MS | TD-MS | TD-MS | TD-MS | TD-MS | TD-MS | TD-MS | TD-MS | TD-MS | TD-MS | TD-MS | TD-MS | TD-MS | TD-MS | TD-MS | TD-MS | TD-MS | TD-MS | TD-MS | TD-MS | TD-MS | TD-MS | TD-MS | TD-MS | TD-MS | TD-MS | TD-MS | TD-MS | TD-MS | TD-MS | TD-MS |
| 362 | 3.7 | 2.3 | 0.7 | 0.8 | < 0.05 | 0.54 | 342 | 1.86 | 0.04 | < 0.1 | 88.7 | 18.2 | < 0.1 | 84.9 | 21.1 | 352 | 149 | 5.4 | 0.4 | < 0.1 | < 1 | 0.2 | 0.2 | 1410 | 107 | 213 | 23 | 78.1 | 10.4 | 6 | 0.7 | 3.7 | 0.7 | 0.4 | 2.3 | 0.3 | 0.3 | > 200 | 0.74 | 38.9 | 1.5 |
| 1570 | 1.7 | 3.8 | 1.6 | 1.3 | < 0.05 | 0.07 | 135 | 2.14 | 0.02 | 0.4 | 159 | 20.1 | < 0.1 | 2.7 | 35.1 | 264 | 36 | 12.4 | 0.3 | < 0.1 | 2 | 0.1 | < 0.1 | 68 | 26 | 58 | 8 | 32.1 | 6.7 | 6.3 | 1.1 | 6.6 | 0.4 | 0.6 | 3.4 | 0.5 | 0.7 | > 200 | < 0.05 | 1.5 | 0.1 |
| 170 | 1.5 | 0.4 | 1.2 | 0.1 | < 0.05 | 0.14 | 400 | 0.62 | 0.05 | < 0.1 | 23.7 | 16.7 | < 0.1 | 41.8 | 4 | 332 | 66 | 2.5 | 0.2 | < 0.1 | < 1 | 0.2 | 0.2 | 1350 | 40.1 | 74.1 | 7.1 | 21.8 | 2.5 | 1.6 | 0.2 | 0.8 | 0.2 | < 0.1 | 0.4 | < 0.1 | 0.3 | > 200 | 0.33 | 9 | 0.4 |
| 233 | 8.5 | 0.2 | 0.5 | < 0.1 | < 0.05 | < 0.05 | > 500 | 0.08 | 0.03 | < 0.1 | 25.5 | 6.8 | < 0.1 | 5.2 | 1 | 15 | 315 | 8.6 | 1 | < 0.1 | 3 | 0.4 | 0.2 | 62 | 5.8 | 9.7 | 0.9 | 2.9 | 0.3 | 0.2 | < 0.1 | 0.1 | 0.1 | < 0.1 | 0.3 | < 0.1 | 0.6 | > 200 | < 0.05 | 2.8 | 0.4 |
| 1640 | 0.6 | 0.6 | 1.7 | 0.2 | < 0.05 | 0.1 | 58.4 | 0.4 | 0.07 | < 0.1 | 61.7 | 9.6 | < 0.1 | 8.7 | 8.2 | 101 | 21 | 3.4 | 0.3 | < 0.1 | 1 | 0.1 | 0.1 | 47 | 6.6 | 12.8 | 1.6 | 5.9 | 1.2 | 1.1 | 0.2 | 1.1 | 0.1 | < 0.1 | 0.6 | < 0.1 | 0.2 | 198 | < 0.05 | 1.2 | 0.6 |
| 570 | 4.7 | 2.9 | 1.4 | 1.1 | < 0.05 | 0.41 | 305 | 1.27 | < 0.02 | < 0.1 | 74.3 | 20.9 | < 0.1 | 75.3 | 28.2 | 111 | 185 | 8.5 | < 0.1 | < 0.1 | < 1 | < 0.1 | < 0.1 | 556 | 51.6 | 106 | 11.6 | 40.7 | 6.3 | 5.4 | 0.9 | 5.5 | 0.7 | 0.4 | 2.4 | 0.3 | 0.3 | > 200 | 0.38 | 10.6 | 0.6 |
| 724 | 2.8 | 6.7 | 1.1 | 2.1 | < 0.05 | 0.55 | 63.3 | 2.39 | < 0.02 | 0.2 | 83 | 11.5 | < 0.1 | 62.1 | 51.2 | 280 | 128 | 3.5 | < 0.1 | < 0.1 | < 1 | < 0.1 | < 0.1 | 2050 | 24.6 | 48.1 | 5.7 | 22.7 | 4.5 | 5.7 | 1.1 | 8.4 | 0.3 | 1 | 6.8 | 1.1 | 0.1 | 25.9 | 0.3 | 2.9 | 0.4 |
| 210 | 0.9 | 0.3 | 1.3 | 0.1 | < 0.05 | 0.06 | 173 | 1.02 | < 0.02 | < 0.1 | 55.4 | 18.6 | < 0.1 | 14.7 | 2.8 | 608 | 39 | 2 | < 0.1 | < 0.1 | < 1 | < 0.1 | 0.2 | 945 | 28.7 | 46.7 | 4.6 | 14.9 | 1.9 | 1.3 | 0.1 | 0.6 | 0.2 | < 0.1 | 0.2 | < 0.1 | 0.1 | > 200 | 0.11 | 0.4 | < 0.1 |
| 159 | 1.3 | < 0.1 | 1.1 | < 0.1 | 0.06 | < 0.05 | 305 | 0.88 | 0.02 | < 0.1 | 35.3 | 21.1 | < 0.1 | 1.5 | 0.6 | 638 | 59 | 1.1 | 0.3 | < 0.1 | < 1 | 0.2 | < 0.1 | 551 | 23.4 | 32.9 | 2.8 | 8.5 | 0.8 | 0.5 | < 0.1 | 0.1 | 0.1 | < 0.1 | < 0.1 | < 0.1 | 0.2 | > 200 | < 0.05 | 0.2 | < 0.1 |
| 332 | 3 | 1.7 | 1.4 | 0.6 | < 0.05 | 0.67 | 74.5 | 0.88 | 0.02 | < 0.1 | 64.6 | 10.4 | < 0.1 | 51.2 | 16.8 | 122 | 117 | 5.1 | < 0.1 | < 0.1 | < 1 | < 0.1 | < 0.1 | 490 | 30.7 | 60.3 | 7.1 | 25.1 | 4.6 | 4.2 | 0.6 | 3.4 | 0.6 | 0.3 | 1.6 | 0.2 | 0.6 | 167 | 0.24 | 8.8 | 1.2 |
| 595 | < 0.1 | 0.8 | 1.6 | 0.3 | < 0.05 | < 0.05 | 87.9 | 1.7 | < 0.02 | < 0.1 | 83.2 | 24.7 | 0.5 | 4.9 | 8.3 | > 1000 | 5 | 2.8 | < 0.1 | < 0.1 | < 1 | < 0.1 | < 0.1 | 883 | 35.2 | 67.7 | 8.2 | 31.7 | 5.1 | 3.3 | 0.4 | 1.8 | 0.4 | < 0.1 | 0.6 | < 0.1 | < 0.1 | 158 | < 0.05 | 0.2 | < 0.1 |
| 511 | < 0.1 | 0.7 | 1.4 | 0.3 | 0.13 | < 0.05 | 106 | 1.45 | 0.03 | < 0.1 | 80.7 | 22 | 1.2 | 6.7 | 7.9 | > 1000 | 5 | 1.2 | 0.7 | < 0.1 | < 1 | < 0.1 | 0.2 | 1240 | 33.4 | 64.1 | 7.9 | 31.2 | 5 | 3.3 | 0.4 | 1.8 | 0.4 | < 0.1 | 0.5 | < 0.1 | < 0.1 | 105 | 0.07 | 0.1 | < 0.1 |
| 644 | 1.2 | 1.2 | 2.6 | 0.5 | < 0.05 | 0.29 | 110 | 1.8 | 0.04 | < 0.1 | 89.4 | 21.7 | 0.2 | 53.6 | 12.4 | > 1000 | 54 | 6.9 | 0.4 | < 0.1 | 1 | < 0.1 | 0.1 | 1410 | 43.7 | 88 | 10.8 | 40.5 | 6.4 | 4.3 | 0.5 | 2.6 | 0.4 | 0.2 | 0.9 | 0.1 | 0.1 | > 200 | 0.39 | 0.9 | 0.2 |
| 894 | 1.9 | 3.3 | 2 | 1.2 | < 0.05 | 0.15 | 96.5 | 1.8 | 0.03 | < 0.1 | 104 | 24.8 | < 0.1 | 13.3 | 30.9 | 685 | 72 | 11.4 | 0.6 | < 0.1 | 3 | 0.4 | 0.2 | 451 | 48.1 | 97.8 | 12.4 | 47.6 | 8.9 | 7.1 | 1.1 | 6.2 | 0.3 | 0.5 | 2.8 | 0.4 | 0.5 | > 200 | 0.09 | 2.1 | 0.4 |
| 808 | 0.2 | 0.4 | 0.3 | 0.1 | 0.32 | < 0.05 | 137 | 0.74 | 0.09 | 0.7 | 73.7 | 12.5 | < 0.1 | 1.8 | 3.7 | 423 | 9 | 1.4 | 0.3 | < 0.1 | < 1 | 0.1 | 0.2 | 146 | 3.7 | 8.1 | 1.1 | 4.7 | 0.9 | 0.9 | 0.1 | 0.8 | 0.4 | < 0.1 | 0.3 | < 0.1 | 0.1 | 170 | < 0.05 | 0.3 | < 0.1 |
| 1220 | 0.7 | 1.9 | 1.2 | 0.7 | < 0.05 | 0.06 | 84.3 | 1.2 | 0.04 | < 0.1 | 107 | 20.9 | < 0.1 | 8.3 | 18.7 | 534 | 20 | 6 | 0.4 | < 0.1 | 2 | 0.4 | < 0.1 | 224 | 14.7 | 30.7 | 3.9 | 16.9 | 3.7 | 3.6 | 0.5 | 3.5 | 0.2 | 0.3 | 1.6 | 0.2 | 0.3 | 195 | 0.07 | 0.5 | 0.2 |
| 764 | 0.5 | 1.5 | 1 | 0.6 | 0.33 | 0.09 | 189 | 1.5 | 0.16 | 1.2 | 74.2 | 19.8 | < 0.1 | 7.7 | 14.9 | > 1000 | 16 | 1 | 0.1 | < 0.1 | 2 | < 0.1 | < 0.1 | 135 | 18.4 | 41 | 5.5 | 24.3 | 4.8 | 4.1 | 0.6 | 3.2 | 0.4 | 0.2 | 1.2 | 0.2 | < 0.1 | 53.9 | 0.05 | 0.5 | 0.1 |
| 149 | 3.3 | 0.8 | 1.2 | 0.3 | < 0.05 | 0.08 | 306 | 1.27 | 0.04 | < 0.1 | 38.9 | 17.2 | < 0.1 | 21.3 | 7.3 | 272 | 140 | 5.1 | 0.5 | < 0.1 | 1 | 0.5 | 0.1 | 1600 | 27.9 | 54.4 | 5.7 | 20.6 | 2.9 | 2.1 | 0.2 | 1.4 | 0.2 | 0.1 | 0.7 | 0.1 | 0.3 | > 200 | 0.31 | 2 | 0.3 |
| 242 | 2.9 | 3.4 | 2.7 | 1.4 | < 0.05 | 0.94 | 69.3 | 0.26 | < 0.02 | 0.3 | 36.1 | 20.3 | 0.4 | 136 | 33.6 | 21.8 | 63 | 29.2 | 1.3 | < 0.1 | 2 | < 0.1 | < 0.1 | 59 | 139 | 314 | 38.7 | 138 | 24.6 | 15.3 | 1.7 | 8.4 | 0.3 | 0.4 | 2.4 | 0.4 | 0.9 | 169 | 0.76 | 25.9 | 1 |
| 204 | 1.6 | 1.2 | 1 | 0.4 | 0.05 | 0.09 | 299 | 1.8 | < 0.02 | < 0.1 | 52.9 | 18.9 | < 0.1 | 24.9 | 11.5 | 185 | 83 | 1.3 | 0.8 | < 0.1 | < 1 | < 0.1 | < 0.1 | 1760 | 25.5 | 49.5 | 5.3 | 19.6 | 3.4 | 2.9 | 0.4 | 2.2 | 0.4 | 0.2 | 1 | 0.1 | < 0.1 | > 200 | 0.26 | 1.3 | 0.3 |
| 1340 | 0.4 | 0.8 | 0.5 | 0.3 | 0.74 | 0.16 | 212 | 0.64 | 0.19 | 1 | 184 | 5.7 | < 0.1 | 6 | 8.1 | 86.3 | 17 | 0.4 | 0.5 | 0.1 | 2 | < 0.1 | < 0.1 | 114 | 6.3 | 15.7 | 2.2 | 9.7 | 2.1 | 2 | 0.3 | 1.6 | 0.3 | 0.1 | 0.6 | < 0.1 | < 0.1 | > 200 | 0.11 | 0.3 | < 0.1 |
| 768 | 0.2 | 1.5 | 0.9 | 0.6 | 0.5 | 0.22 | 217 | 1.55 | 0.13 | 2.9 | 103 | 16.7 | < 0.1 | 9.6 | 15.1 | 475 | 9 | 0.9 | < 0.1 | 0.2 | 2 | < 0.1 | 0.2 | 293 | 14.5 | 34.6 | 4.8 | 20.7 | 4.2 | 3.8 | 0.6 | 3.1 | 0.4 | 0.2 | 1.2 | 0.2 | < 0.1 | > 200 | 0.22 | 0.6 | 0.4 |
| 695 | 0.9 | 1.6 | 1.3 | 0.6 | 0.24 | 0.3 | 102 | 1.64 | 0.03 | < 0.1 | 93.4 | 25.1 | < 0.1 | 20 | 15.9 | 486 | 33 | 0.8 | < 0.1 | < 0.1 | < 1 | < 0.1 | 0.2 | 379 | 21.1 | 47.3 | 6.2 | 26.3 | 5.1 | 4.2 | 0.6 | 3.3 | 0.3 | 0.2 | 1.2 | 0.2 | < 0.1 | 29 | 0.07 | 2.5 | 0.3 |
| 1360 | 0.7 | 0.6 | < 0.1 | 0.2 | 2.06 | 0.09 | > 500 | 0.85 | 0.44 | 9.2 | 300 | 12.2 | < 0.1 | 1.9 | 6.1 | 413 | 43 | 1 | < 0.1 | 0.3 | 1 | < 0.1 | 1.2 | 193 | 6.1 | 14.9 | 2.2 | 8.6 | 1.8 | 1.5 | 0.2 | 1.2 | 1.2 | < 0.1 | 0.5 | < 0.1 | < 0.1 | 2.5 | 0.18 | 0.8 | < 0.1 |
| 547 | 0.9 | 0.6 | 0.2 | 0.2 | 22.7 | 0.18 | > 500 | 0.71 | 0.79 | 14.2 | 401 | 10.7 | < 0.1 | 25 | 5.1 | 184 | 47 | 1.8 | 1.6 | 0.4 | 7 | < 0.1 | 0.4 | 42 | 8.1 | 21 | 2.9 | 10.7 | 1.9 | 1.6 | 0.2 | 1.2 | 1.5 | < 0.1 | 0.5 | < 0.1 | < 0.1 | 4.7 | 0.43 | 0.6 | 0.1 |
| 487 | 0.2 | < 0.1 | < 0.1 | < 0.1 | 15 | 0.08 | > 500 | < 0.05 | 7.39 | 47.3 | 179 | 1 | < 0.1 | < 0.2 | 0.2 | 0.6 | 25 | 2.1 | 2.6 | 0.5 | 3 | < 0.1 | 5.9 | < 1 | 0.2 | 0.4 | < 0.1 | 0.3 | < 0.1 | < 0.1 | < 0.1 | < 0.1 | 2.3 | < 0.1 | < 0.1 | < 0.1 | < 0.1 | 5.4 | 0.31 | 0.9 | < 0.1 |
| 591 | 0.3 | < 0.1 | < 0.1 | < 0.1 | 26 | 0.09 | > 500 | < 0.05 | 6.91 | 63 | 187 | 1 | < 0.1 | < 0.2 | 0.2 | 0.6 | 34 | 2.3 | 3.3 | 0.6 | 5 | 0.1 | 11.6 | 2 | < 0.1 | 0.2 | < 0.1 | < 0.1 | < 0.1 | < 0.1 | < 0.1 | < 0.1 | 2.9 | < 0.1 | < 0.1 | < 0.1 | < 0.1 | 16.3 | 0.28 | 0.6 | < 0.1 |
| 418 | 0.4 | 0.2 | < 0.1 | < 0.1 | 30.5 | 0.09 | > 500 | 0.21 | 1.59 | 53.4 | 629 | 0.7 | < 0.1 | 0.3 | 1.7 | 51.2 | 30 | 8.4 | 3 | 2.1 | 6 | < 0.1 | 8.7 | 9 | 8.2 | 16.7 | 1.9 | 5.5 | 0.8 | 0.6 | < 0.1 | 0.4 | 3.1 | < 0.1 | 0.2 | < 0.1 | < 0.1 | 0.1 | 0.56 | 5.7 | < 0.1 |
| 366 | 0.2 | < 0.1 | < 0.1 | < 0.1 | 28 | 0.08 | > 500 | < 0.05 | 13.8 | 60 | 609 | 0.6 | < 0.1 | < 0.2 | 0.1 | 0.5 | 18 | 1.7 | 5.9 | 2.5 | 7 | 1.1 | 25.7 | 1 | 0.1 | 0.2 | < 0.1 | < 0.1 | < 0.1 | < 0.1 | < 0.1 | < 0.1 | 7.5 | < 0.1 | < 0.1 | < 0.1 | < 0.1 | 0.3 | 4.45 | 0.6 | < 0.1 |
| 396 | 0.3 | 0.3 | < 0.1 | 0.1 | 6.7 | < 0.05 | > 500 | 0.41 | 1.54 | 50.5 | 101 | 4.1 | < 0.1 | 1.7 | 3.9 | 131 | 27 | 2.6 | 1.7 | 0.4 | 6 | < 0.1 | 4.8 | 77 | 3.6 | 8.8 | 1.2 | 5.1 | 1 | 1 | 0.1 | 0.7 | 1.6 | < 0.1 | 0.3 | < 0.1 | 0.2 | 33.7 | 0.29 | 0.3 | < 0.1 |
| 373 | 0.1 | < 0.1 | < 0.1 | < 0.1 | 83.5 | < 0.05 | > 500 | 0.08 | 1.36 | 50.3 | 348 | 1.2 | < 0.1 | 0.7 | 0.8 | 9.4 | 16 | 1.1 | 2.5 | 1.9 | 11 | < 0.1 | 9.1 | 17 | 1.5 | 3.1 | 0.3 | 1.2 | 0.2 | 0.2 | < 0.1 | 0.2 | 1.2 | < 0.1 | < 0.1 | < 0.1 | 0.1 | 54.9 | 0.12 | 0.3 | 0.2 |
| 678 | 1 | 0.9 | 0.4 | 0.3 | > 100 | < 0.05 | 120 | 1.19 | 173 | 19.7 | 88.3 | 15.9 | 37 | 8 | 10.2 | 642 | 53 | 3.7 | 0.3 | 2.2 | > 200 | 0.9 | 31.8 | 258 | 8.5 | 20 | 2.7 | 11.7 | 2.4 | 2.3 | 0.3 | 1.7 | 0.9 | 0.1 | 0.7 | < 0.1 | 0.2 | 109 | 16.7 | 0.8 | < 0.1 |
| 1490 | 0.7 | 3.5 | 1.5 | 1.3 | 29.5 | 0.07 | 163 | 3.04 | 15.5 | 2.4 | 132 | 26.5 | 32.8 | 14.4 | 43.2 | 534 | 40 | 2.4 | 0.5 | 0.9 | 17 | < 0.1 | 2.3 | 559 | 31 | 73.8 | 10.5 | 45.8 | 9.4 | 9.5 | 1.2 | 7 | 0.7 | 0.5 | 2.7 | 0.4 | < 0.1 | 14.1 | 8.48 | 1.1 | 0.2 |
| 859 | 1.2 | 1.3 | 0.5 | 0.5 | > 100 | < 0.05 | 153 | 1.47 | 77.2 | 14.4 | 145 | 17 | 42.8 | 13.3 | 15.3 | 617 | 57 | 5.4 | 0.4 | 1.6 | 133 | 0.3 | 11.6 | 253 | 13 | 30 | 4.1 | 17.7 | 3.6 | 3.6 | 0.5 | 2.6 | 1 | 0.2 | 1 | 0.1 | 0.3 | 127 | 3.2 | 0.6 | < 0.1 |
| 777 | 0.7 | 1.1 | 0.8 | 0.4 | 91.1 | 0.09 | 106 | 1.44 | 65.3 | 7.9 | 132 | 18.1 | 51 | 14.6 | 13.5 | 606 | 33 | 3.5 | 0.2 | 0.9 | 83 | 0.2 | 3.3 | 320 | 15.1 | 32.7 | 4.3 | 17.2 | 3.3 | 3.2 | 0.4 | 2.3 | 0.8 | 0.2 | 0.9 | 0.1 | < 0.1 | 38.8 | 4.11 | 0.8 | 0.1 |

# APPENDIX 2: NOTES ON MINERAL LIBERATION ANALYSIS

| | |
|---|---|
| Instrument | FEI Quanta 400 or FEI 650FEG |
| Voltage | 25 kV |
| Beam Current | 10 nA |
| Working Distance | 12.0 mm |
| MLA Scan | GXMAP, XBSE and SPS |

**Notes**: The following points list information regarding instrument set-up, MLA data processing and limitions of the measurements.

- Each identified PGM was checked by driving back to its respective location in the polished section with the SEM to ensure that the grains detected were not artifacts produced by X-ray overlap near grain boundaries at small grain-sizes.
- Over 100,000 particles were scanned over multiple MLA measurements and only ~200-300 precious-metal minerals were identified due to the overall low PGE grade in the sample. Although efforts were made to maximize the number of particles detected by measuring replicate polished sections, the low grade of PGE and low number of grains detected reduces the consistency of the the particle statistics. It should be noted that PGM grains with large grain sizes such as sperrylite may have a significant influence over the mass distribution of the PGM phases.
- Instrument magnification set-up produced a 1 pixel = 0.98 by 0.98 µm spacing. Grains that are <1-2µm may not be detected.
- The volume of a particle is calculated based on an equivalent circle diameter determined by the total measured pixel area.
- The mass is calculated from the the volume, nominal density of the mineral phase and the EPMA elemental percents; Liberation is based on estimated area of the mineral of interest that is exposed (>90% free of attachments/inclusions is liberated, <90% is attached and completely enclosed is an inclusion); The grain size, association and liberation of each idenfified PGM was documented.

# APPENDIX 3: ELECTRON PROBE MICROANALYSIS

| | | Cu | Ni | Fe | S | Co | Se | Pb | Bi | Ag | Sb | Pd | As | Elemental Totals |
|---|---|---|---|---|---|---|---|---|---|---|---|---|---|---|
| Units | | Wt% | Wt% | Wt% | Wt% | Wt% | Wt% | Wt% | Wt% | Wt% | Wt% | Wt% | Wt% | |
| | | | | | | | **Ovoid** | | | | | | | |
| Galena | | | | | | | | | | | | | | |
| *Avemge LOD* | | *0.02* | | | *0.04* | | | *0.12* | *0.19* | *0.06* | *0.05* | *0.13* | *0.02* | |
| | 34 | 0.00 | | | 13.36 | | | 86.96 | 0.00 | 0.00 | 0.00 | 0.00 | 0.00 | 100.33 |
| | 35 | 0.00 | | | 13.49 | | | 86.49 | 0.14 | 0.02 | 0.00 | 0.00 | 0.00 | 100.13 |
| | 36 | 0.00 | | | 13.45 | | | 87.43 | 0.11 | 0.00 | 0.03 | 0.00 | 0.00 | 101.02 |
| | 37 | 0.02 | | | 13.36 | | | 86.68 | 0.26 | 0.02 | 0.00 | 0.00 | 0.00 | 100.33 |
| | 38 | 0.00 | | | 13.49 | | | 86.99 | 0.01 | 0.00 | 0.00 | 0.00 | 0.00 | 100.49 |
| | 39 | 0.00 | | | 13.47 | | | 85.89 | 0.13 | 0.01 | 0.00 | 0.00 | 0.00 | 99.49 |
| | 40 | 0.02 | | | 13.36 | | | 87.21 | 0.16 | 0.00 | 0.00 | 0.00 | 0.00 | 100.76 |
| | 41 | 0.01 | | | 13.56 | | | 87.44 | 0.00 | 0.00 | 0.00 | 0.00 | 0.00 | 101.01 |
| | 42 | 0.04 | | | 13.30 | | | 87.51 | 0.06 | 0.07 | 0.00 | 0.00 | 0.00 | 100.99 |
| | 43 | 0.00 | | | 13.47 | | | 86.80 | 0.17 | 0.00 | 0.00 | 0.00 | 0.00 | 100.43 |
| | 44 | 0.02 | | | 13.27 | | | 86.66 | 0.22 | 0.00 | 0.00 | 0.00 | 0.00 | 100.16 |
| | 45 | 0.00 | | | 13.43 | | | 86.70 | 0.21 | 0.00 | 0.00 | 0.04 | 0.00 | 100.38 |
| | 46 | 0.04 | | | 13.53 | | | 87.11 | 0.17 | 0.06 | 0.00 | 0.00 | 0.00 | 100.91 |
| | 47 | 0.00 | | | 13.56 | | | 86.87 | 0.24 | 0.04 | 0.00 | 0.00 | 0.00 | 100.71 |
| | 48 | 0.00 | | | 13.27 | | | 86.43 | 0.25 | 0.02 | 0.00 | 0.00 | 0.00 | 99.97 |
| | 49 | 0.00 | | | 13.27 | | | 85.99 | 0.12 | 0.05 | 0.00 | 0.00 | 0.00 | 99.43 |
| | 50 | 0.03 | | | 13.56 | | | 88.17 | 0.31 | 0.05 | 0.00 | 0.02 | 0.00 | 102.15 |
| | 51 | 0.06 | | | 29.30 | | | 0.00 | 0.05 | 0.02 | 0.00 | 0.00 | 0.04 | 29.46 |
| | 52 | 0.03 | | | 13.33 | | | 86.29 | 0.25 | 0.00 | 0.00 | 0.00 | 0.00 | 99.90 |
| | 53 | 0.03 | | | 13.36 | | | 86.73 | 0.03 | 0.00 | 0.00 | 0.00 | 0.00 | 100.16 |
| | 54 | 0.00 | | | 9.09 | | | 0.00 | 57.10 | 0.00 | 0.13 | 0.01 | 0.01 | 66.33 |
| | 55 | 0.00 | | | 8.95 | | | 0.00 | 57.14 | 0.00 | 0.09 | 0.00 | 0.00 | 66.18 |
| | 56 | 0.27 | | | 13.49 | | | 87.16 | 0.00 | 0.00 | 0.00 | 0.00 | 0.00 | 100.92 |
| | 57 | 0.00 | | | 13.63 | | | 87.10 | 0.12 | 0.00 | 0.00 | 0.02 | 0.00 | 100.88 |
| | 58 | 0.01 | | | 13.27 | | | 85.41 | 0.24 | 0.00 | 0.00 | 0.00 | 0.00 | 98.92 |
| Pentlandite | | | | | | | | | | | | | | |
| Average LOD | | *0.03* | *0.02* | *0.01* | *0.03* | *0.01* | *0.00* | | | | | | | |
| 241 | Pn1 | 0.00 | 31.46 | 34.47 | 33.05 | 1.10 | 0.00 | NA | NA | NA | NA | NA | NA | 100.08 |
| | Pn2 | 0.00 | 31.31 | 34.54 | 32.90 | 1.11 | 0.00 | NA | NA | NA | NA | NA | NA | 99.86 |
| | Pn3 | 0.00 | 31.31 | 34.38 | 33.05 | 1.14 | 0.00 | NA | NA | NA | NA | NA | NA | 99.88 |
| | Pn4 | 0.00 | 31.42 | 34.04 | 33.03 | 1.13 | 0.00 | NA | NA | NA | NA | NA | NA | 99.61 |
| | Pn5 | 0.00 | 31.12 | 34.92 | 33.00 | 1.00 | 0.00 | NA | NA | NA | NA | NA | NA | 100.04 |
| | Pn6 | 0.00 | 31.09 | 34.67 | 32.91 | 0.93 | 0.00 | NA | NA | NA | NA | NA | NA | 99.60 |
| | Pn7 | 0.00 | 31.23 | 34.49 | 32.88 | 0.98 | 0.00 | NA | NA | NA | NA | NA | NA | 99.57 |
| | Pn8 | 0.02 | 31.25 | 34.53 | 32.86 | 1.00 | 0.00 | NA | NA | NA | NA | NA | NA | 99.67 |
| | Pn9 | 0.00 | 31.24 | 34.48 | 32.96 | 1.07 | 0.00 | NA | NA | NA | NA | NA | NA | 99.74 |
| | Pn10 | 0.00 | 32.28 | 33.38 | 32.87 | 1.12 | 0.00 | NA | NA | NA | NA | NA | NA | 99.66 |
| 207 | Pn1 | 0.00 | 30.93 | 34.63 | 32.84 | 1.08 | 0.00 | NA | NA | NA | NA | NA | NA | 99.48 |
| | Pn2 | 0.00 | 31.24 | 34.40 | 32.85 | 1.14 | 0.00 | NA | NA | NA | NA | NA | NA | 99.63 |
| | Pn3 | 0.52 | 29.02 | 32.47 | 31.68 | 0.92 | 0.00 | NA | NA | NA | NA | NA | NA | 94.60 |
| | Pn4 | 0.00 | 30.96 | 33.98 | 33.23 | 1.04 | 0.00 | NA | NA | NA | NA | NA | NA | 99.22 |
| | Pn5 | 0.00 | 31.32 | 34.38 | 32.88 | 1.01 | 0.00 | NA | NA | NA | NA | NA | NA | 99.60 |
| | Pn6 | 0.00 | 31.21 | 34.60 | 33.02 | 1.07 | 0.00 | NA | NA | NA | NA | NA | NA | 99.90 |
| | Pn7 | 0.00 | 31.20 | 34.41 | 32.74 | 1.04 | 0.00 | NA | NA | NA | NA | NA | NA | 99.39 |
| | Pn9 | 0.00 | 31.37 | 34.68 | 32.96 | 0.99 | 0.00 | NA | NA | NA | NA | NA | NA | 100.00 |
| | Pn10 | 0.01 | 31.26 | 34.60 | 33.05 | 1.01 | 0.00 | NA | NA | NA | NA | NA | NA | 99.93 |
| 6055 | Pn1 | 0.00 | 31.51 | 33.98 | 33.10 | 1.29 | 0.00 | NA | NA | NA | NA | NA | NA | 99.89 |
| | Pn2 | 0.00 | 31.11 | 34.55 | 33.23 | 1.10 | 0.00 | NA | NA | NA | NA | NA | NA | 99.99 |
| | Pn3 | 0.00 | 31.56 | 34.13 | 33.16 | 1.02 | 0.00 | NA | NA | NA | NA | NA | NA | 99.87 |
| | Pn4 | 0.00 | 31.53 | 33.96 | 33.09 | 1.18 | 0.00 | NA | NA | NA | NA | NA | NA | 99.77 |
| 6063 | Pn1 | 0.00 | 31.00 | 34.47 | 33.09 | 1.01 | 0.00 | NA | NA | NA | NA | NA | NA | 99.57 |
| | Pn2 | 0.00 | 30.98 | 34.61 | 33.27 | 1.02 | 0.00 | NA | NA | NA | NA | NA | NA | 99.87 |
| | Pn3 | 0.00 | 31.16 | 34.39 | 33.20 | 1.07 | 0.00 | NA | NA | NA | NA | NA | NA | 99.82 |
| | Pn4 | 0.00 | 30.99 | 34.59 | 33.18 | 1.01 | 0.00 | NA | NA | NA | NA | NA | NA | 99.77 |
| | Pn5 | 0.00 | 30.79 | 33.43 | 33.11 | 0.96 | 0.00 | NA | NA | NA | NA | NA | NA | 98.28 |

| | | | | | | | | | | | | | | |
|---|---|---|---|---|---|---|---|---|---|---|---|---|---|---|
| Chalcopyrite | | | | | | 1.05 | | | | | | | | |
| *Average LOD* | | *0.03* | *0.02* | *0.01* | *0.03* | *0.01* | *0.00* | | | | | | | |
| | Cpy | 20.42 | 11.78 | 32.27 | 33.97 | 0.31 | 0.00 | NA | NA | NA | NA | NA | NA | 98.76 |
| | Cpy1 | 34.14 | 0.02 | 31.07 | 34.84 | 0.00 | 0.00 | NA | NA | NA | NA | NA | NA | 100.07 |
| | Cpy2 | 34.45 | 0.09 | 31.04 | 34.42 | 0.00 | 0.00 | NA | NA | NA | NA | NA | NA | 100.00 |
| | Cpy3 | 34.10 | 0.00 | 31.04 | 34.81 | 0.00 | 0.00 | NA | NA | NA | NA | NA | NA | 99.95 |
| | Cpy4 | 29.67 | 3.97 | 31.46 | 34.41 | 0.10 | 0.00 | NA | NA | NA | NA | NA | NA | 99.61 |
| | Cpy5 | 31.59 | 2.63 | 30.95 | 34.25 | 0.03 | 0.00 | NA | NA | NA | NA | NA | NA | 99.44 |
| | Cpy6 | 33.93 | 0.01 | 31.17 | 34.58 | 0.00 | 0.00 | NA | NA | NA | NA | NA | NA | 99.69 |
| | Cpy7 | 33.81 | 0.04 | 30.93 | 34.24 | 0.00 | 0.00 | NA | NA | NA | NA | NA | NA | 99.01 |
| | Cpy8 | 33.81 | 0.03 | 30.89 | 34.69 | 0.00 | 0.00 | NA | NA | NA | NA | NA | NA | 99.41 |
| | Cpy9 | 33.78 | 0.04 | 31.06 | 34.65 | 0.00 | 0.00 | NA | NA | NA | NA | NA | NA | 99.53 |
| | Cpy10 | 33.59 | 0.08 | 30.73 | 34.26 | 0.00 | 0.00 | NA | NA | NA | NA | NA | NA | 98.65 |
| | Cpy11 | 33.83 | 0.01 | 30.85 | 34.61 | 0.00 | 0.00 | NA | NA | NA | NA | NA | NA | 99.31 |
| | Cpy12 | 33.78 | 0.01 | 31.17 | 34.56 | 0.00 | 0.00 | NA | NA | NA | NA | NA | NA | 99.53 |
| | Cpy13 | 33.51 | 0.36 | 30.97 | 34.48 | 0.00 | 0.00 | NA | NA | NA | NA | NA | NA | 99.32 |
| | Cpy14 | 33.38 | 0.56 | 31.02 | 34.52 | 0.01 | 0.00 | NA | NA | NA | NA | NA | NA | 99.50 |
| Pyrrhotite | | | | | | | | | | | | | | |
| *Average LOD* | | *0.03* | *0.02* | *0.02* | *0.03* | *0.01* | *0.00* | | | | | | | |
| | Po1 | 0.06 | 0.09 | 64.15 | 35.68 | 0.00 | 0.00 | NA | NA | NA | NA | NA | NA | 99.98 |
| | Po2 | 0.00 | 0.28 | 62.40 | 37.06 | 0.00 | 0.00 | NA | NA | NA | NA | NA | NA | 99.75 |
| | Po3 | 0.00 | 0.31 | 62.61 | 36.79 | 0.00 | 0.00 | NA | NA | NA | NA | NA | NA | 99.70 |
| | Po4 | 0.00 | 0.13 | 64.11 | 35.68 | 0.00 | 0.00 | NA | NA | NA | NA | NA | NA | 99.91 |
| | Po5 | 0.01 | 0.17 | 62.58 | 37.05 | 0.00 | 0.00 | NA | NA | NA | NA | NA | NA | 99.82 |
| | Po1 | 0.03 | 0.23 | 62.74 | 37.15 | 0.00 | 0.00 | NA | NA | NA | NA | NA | NA | 100.15 |
| | Po2 | 0.03 | 0.06 | 64.66 | 35.58 | 0.00 | 0.00 | NA | NA | NA | NA | NA | NA | 100.33 |
| | Po3 | 0.02 | 0.06 | 64.51 | 35.14 | 0.00 | 0.00 | NA | NA | NA | NA | NA | NA | 99.73 |
| | Po4 | 0.06 | 0.29 | 62.42 | 37.01 | 0.00 | 0.00 | NA | NA | NA | NA | NA | NA | 99.78 |
| | Po5 | 0.01 | 0.20 | 63.72 | 36.09 | 0.00 | 0.00 | NA | NA | NA | NA | NA | NA | 100.03 |
| | Po6 | 0.03 | 0.24 | 62.67 | 37.17 | 0.00 | 0.00 | NA | NA | NA | NA | NA | NA | 100.11 |
| | Po1 | 0.03 | 0.10 | 62.43 | 36.82 | 0.00 | 0.00 | NA | NA | NA | NA | NA | NA | 99.38 |
| | Po2 | 0.01 | 0.13 | 64.14 | 35.77 | 0.00 | 0.00 | NA | NA | NA | NA | NA | NA | 100.05 |
| | Po3 | 0.02 | 0.30 | 62.26 | 36.80 | 0.00 | 0.00 | NA | NA | NA | NA | NA | NA | 99.37 |
| | Po4 | 0.00 | 0.25 | 62.47 | 36.95 | 0.00 | 0.00 | NA | NA | NA | NA | NA | NA | 99.67 |
| | Po5 | 0.01 | 0.08 | 64.29 | 35.44 | 0.00 | 0.00 | NA | NA | NA | NA | NA | NA | 99.81 |
| | Po1 | 0.01 | 0.30 | 62.50 | 36.85 | 0.00 | 0.00 | NA | NA | NA | NA | NA | NA | 99.66 |
| | Po2 | 0.00 | 0.28 | 62.73 | 37.04 | 0.00 | 0.00 | NA | NA | NA | NA | NA | NA | 100.04 |
| | Po3 | 0.00 | 0.29 | 62.42 | 36.94 | 0.00 | 0.00 | NA | NA | NA | NA | NA | NA | 99.64 |
| | Po4 | 0.02 | 0.37 | 62.41 | 36.86 | 0.00 | 0.00 | NA | NA | NA | NA | NA | NA | 99.66 |
| | Po5 | 0.00 | 0.32 | 62.29 | 36.81 | 0.00 | 0.00 | NA | NA | NA | NA | NA | NA | 99.42 |

**Mini Ovoid**

| | | | | | | | | | | | | | | |
|---|---|---|---|---|---|---|---|---|---|---|---|---|---|---|
| Pentlandite | | | | | | | | | | | | | | |
| Average LOD | | *0.03* | *0.02* | *0.01* | *0.03* | *0.01* | *0.00* | | | | | | | |
| | | 0.00 | 33.95 | 31.10 | 32.98 | 1.24 | 0.00 | NA | NA | NA | NA | NA | NA | 99.27 |
| | | 0.00 | 34.28 | 30.99 | 33.06 | 1.32 | 0.00 | NA | NA | NA | NA | NA | NA | 99.64 |
| | | 0.00 | 34.28 | 31.07 | 33.15 | 1.03 | 0.00 | NA | NA | NA | NA | NA | NA | 99.52 |
| | | 0.00 | 34.14 | 30.59 | 33.16 | 1.24 | 0.00 | NA | NA | NA | NA | NA | NA | 99.13 |
| | | 0.03 | 34.32 | 30.88 | 32.94 | 1.11 | 0.00 | NA | NA | NA | NA | NA | NA | 99.27 |
| | | 0.10 | 33.96 | 30.59 | 32.99 | 1.24 | 0.00 | NA | NA | NA | NA | NA | NA | 98.89 |
| | | 0.00 | 34.10 | 30.92 | 32.96 | 1.18 | 0.00 | NA | NA | NA | NA | NA | NA | 99.16 |
| Chalcopyrite | | | | | | 1.19 | | | | | | | | |
| *Average LOD* | | *0.03* | *0.02* | *0.02* | *0.03* | *0.01* | *0.00* | | | | | | | |
| | | 31.59 | 2.63 | 30.95 | 34.25 | 0.03 | 0.00 | | | | | | | 99.44 |
| | | 34.10 | 0.00 | 31.04 | 34.81 | 0.00 | 0.00 | | | | | | | 99.95 |
| | | 33.93 | 0.01 | 31.17 | 34.58 | 0.00 | 0.00 | | | | | | | 99.69 |
| | | 33.81 | 0.04 | 30.93 | 34.24 | 0.00 | 0.00 | | | | | | | 99.01 |
| | | 33.81 | 0.03 | 30.89 | 34.69 | 0.00 | 0.00 | | | | | | | 99.41 |
| | | 33.78 | 0.04 | 31.06 | 34.65 | 0.00 | 0.00 | | | | | | | 99.53 |
| | | 33.59 | 0.08 | 30.73 | 34.26 | 0.00 | 0.00 | | | | | | | 98.65 |
| | | 33.83 | 0.01 | 30.85 | 34.61 | 0.00 | 0.00 | | | | | | | 99.31 |
| | | 33.78 | 0.01 | 31.17 | 34.56 | 0.00 | 0.00 | | | | | | | 99.53 |
| Pyrrhotite | | | | | | | | | | | | | | |
| *Average LOD* | | *0.03* | *0.02* | *0.02* | *0.03* | *0.01* | *0.00* | | | | | | | |
| | | 0.00 | 0.58 | 61.78 | 37.14 | 0.00 | 0.00 | | | | | | | 99.50 |
| | | 0.01 | 0.53 | 61.79 | 37.03 | 0.00 | 0.00 | | | | | | | 99.36 |
| | | 0.01 | 0.49 | 62.06 | 37.12 | 0.00 | 0.00 | | | | | | | 99.68 |
| | | 0.03 | 0.25 | 61.39 | 37.79 | 0.00 | 0.00 | | | | | | | 99.46 |
| | | 0.00 | 0.59 | 61.79 | 37.07 | 0.00 | 0.00 | | | | | | | 99.45 |
| | | 0.03 | 0.22 | 61.08 | 37.69 | 0.00 | 0.00 | | | | | | | 99.02 |
| | | 0.00 | 0.55 | 61.76 | 37.24 | 0.00 | 0.00 | | | | | | | 99.55 |
| | | | 0.46 | | | | | | | | | | | |

| Discovery Hill | | | | | | | | | | | | | | |
|---|---|---|---|---|---|---|---|---|---|---|---|---|---|---|
| Pentlandite | | | | | | | | | | | | | | |
| Average LOD | | *0.03* | *0.02* | *0.02* | *0.03* | *0.01* | *0.00* | | | | | | | |
| | | 0.00 | 32.04 | 32.75 | 33.04 | 1.46 | 0.00 | NA | NA | NA | NA | NA | NA | 99.29 |
| | | 0.01 | 32.77 | 32.36 | 33.10 | 1.27 | 0.00 | NA | NA | NA | NA | NA | NA | 99.51 |
| | | 0.00 | 32.31 | 32.36 | 32.93 | 1.41 | 0.00 | NA | NA | NA | NA | NA | NA | 99.00 |
| | | 0.00 | 32.30 | 32.41 | 33.14 | 1.40 | 0.00 | NA | NA | NA | NA | NA | NA | 99.24 |
| | | 0.01 | 32.88 | 32.17 | 33.17 | 1.24 | 0.00 | NA | NA | NA | NA | NA | NA | 99.48 |
| | | | | | | 1.36 | | NA | NA | NA | NA | NA | NA | 1.36 |
| | | | | | | | | NA | NA | NA | NA | NA | NA | 0.00 |
| Chalcopyrite | | | | | | | | | | | | | | |
| *Average LOD* | | *0.03* | *0.02* | *0.02* | *0.03* | *0.01* | *0.00* | | | | | | | |
| | | | | | | | | | | | | | | 0.00 |
| | | | | | | | | | | | | | | 0.00 |
| | | | | | | | | | | | | | | 0.00 |
| | | | | | | | | | | | | | | 0.00 |
| | | | | | | | | | | | | | | 0.00 |
| | | | | | | | | | | | | | | 0.00 |
| | | | | | | | | | | | | | | 0.00 |
| | | | | | | | | | | | | | | 0.00 |
| Pyrrhotite | | | | | | | | | | | | | | |
| *Average LOD* | | *0.03* | *0.02* | *0.02* | *0.03* | *0.01* | *0.00* | | | | | | | |
| | | 0.00 | 0.44 | 61.77 | 36.90 | 0.00 | 0.00 | | | | | | | 99.12 |
| | | 0.00 | 0.38 | 61.90 | 37.04 | 0.00 | 0.00 | | | | | | | 99.32 |
| | | 0.00 | 0.47 | 61.95 | 36.81 | 0.00 | 0.00 | | | | | | | 99.22 |
| | | 0.02 | 0.35 | 62.06 | 36.95 | 0.00 | 0.00 | | | | | | | 99.37 |
| | | 0.01 | 0.38 | 62.19 | 36.97 | 0.00 | 0.00 | | | | | | | 99.56 |
| | | | | | | | | | | | | | | 0.00 |
| | | | | | | | | | | | | | | 0.00 |

Vaules highlighted in grey are below detection limit. Values highlighted in brown had low element totals.

**PGM, PMM and other Trace Minerals**

| Element | | Fe | Ni | Pt | S | Pd | Te | Pb | Sb | Ag | Bi | As | Au | Se | Ir | Cu | Re | Cd | Zn | Element Totals |
|---|---|---|---|---|---|---|---|---|---|---|---|---|---|---|---|---|---|---|---|---|
| *Avenge LOD* | | *0.02* | *0.02* | *0.14* | *0.04* | *0.05* | *0.09* | *0.10* | *0.05* | *0.08* | *0.15* | *0.10* | *0.12* | *0.19* | *0.14* | *0.00* | | | | |
| Sperrylite | Ovoid | 0.13 | 0.02 | 57.62 | 0.00 | 0.00 | 0.00 | 0.27 | 3.23 | 0.00 | 0.05 | 38.57 | 0.00 | 0.00 | 0.00 | 0.00 | | | | 99.88 |
| Sperrylite | Disc. Hill | 0.00 | 0.01 | 57.01 | 0.00 | 0.03 | 0.00 | 0.18 | 0.06 | 0.00 | 0.00 | 43.28 | 0.00 | 0.41 | NA | | | | | 100.99 |
| Sperrylite | Disc. Hill | 0.25 | 0.06 | 56.80 | 0.00 | 0.07 | 0.00 | 0.19 | 0.05 | 0.01 | 0.00 | 42.73 | 0.00 | 0.00 | NA | | | | | 100.17 |
| Sperrylite | Disc. Hill | 0.03 | 0.03 | 57.07 | 0.00 | 0.00 | 0.02 | 0.28 | 0.08 | 0.01 | 0.00 | 42.38 | 0.00 | 1.00 | NA | 0.00 | | | | 100.90 |
| | | | | | | | | | | | | | | | | | | | | |
| *Avenge LOD* | | *0.02* | *0.02* | *0.07* | *0.02* | *0.06* | *0.10* | *0.07* | *0.05* | *0.10* | *0.19* | *0.11* | *0.08* | *0.19* | *0.08* | *0.00* | | | | |
| Froodite | Ovoid | 0.70 | 0.02 | 0.00 | 0.05 | 22.61 | 0.07 | 0.00 | 0.00 | 0.10 | 78.00 | 0.06 | 0.49 | 0.00 | 0.00 | 0.00 | | | | 102.10 |
| Froodite | Ovoid | 0.06 | 0.02 | 0.00 | 0.02 | 22.60 | 0.08 | 0.00 | 0.00 | 0.11 | 77.16 | 0.33 | 0.70 | 0.00 | 0.00 | 0.00 | | | | 101.08 |
| Froodite | Ovoid | 2.05 | 1.33 | 0.04 | 0.21 | 21.23 | 0.00 | 0.00 | 0.00 | 0.00 | 74.77 | 0.07 | 0.59 | 0.00 | 0.00 | 0.00 | | | | 100.29 |
| Bismuth | Ovoid | 0.07 | 0.04 | 0.01 | 13.46 | 0.00 | 0.01 | 83.93 | 0.00 | 0.04 | 0.00 | 0.93 | 0.01 | 0.31 | 0.04 | 0.00 | | | | 98.85 |
| | | | | | | | | | | | | | | | | | | | | |
| *Avenge LOD* | | *0.02* | *0.02* | *0.08* | *0.03* | *0.05* | *0.12* | *0.10* | *0.05* | *0.08* | *0.50* | *0.13* | *0.08* | *0.18* | *0.08* | *0.02* | | | | |
| PbTe | Ovoid | 0.01 | 0.01 | 0.00 | 0.78 | 0.01 | 35.41 | 55.62 | 0.21 | 0.00 | 7.87 | 0.59 | 0.00 | 0.11 | 0.01 | 0.00 | | | | 100.63 |
| PbTe | Ovoid | 0.31 | 0.00 | 0.00 | 0.89 | 0.00 | 35.40 | 63.69 | 0.21 | 0.00 | 0.00 | 0.30 | 0.06 | 0.08 | 0.00 | 0.00 | | | | 100.93 |
| | | | | | | | | | | | | | | | | | | | | |
| Average LOD | | *0.02* | *0.02* | *0.07* | *0.02* | *0.03* | *0.15* | *0.07* | *0.04* | *0.06* | *0.11* | *0.10* | *0.08* | *0.17* | *0.07* | *0.08* | | | | |
| NiSb | Ovoi | 3.93 | 30.68 | 1.25 | 2.85 | 2.35 | 0.00 | 0.00 | 60.20 | 0.07 | 0.09 | 0.23 | 0.00 | 0.00 | 0.03 | 0.00 | | | | 101.68 |
| | | | | | | | | | | | | | | | | | | | | |
| Average LOD | | 0.04 | 0.03 | 0.11 | 0.03 | 0.10 | 0.25 | 0.13 | 0.09 | 0.19 | 0.30 | 0.18 | 0.15 | 0.37 | 0.13 | 0.06 | 0.14 | 0.00 | 0.00 | |
| AuAg2 | Ovoid | 0.22 | 0.26 | 0.06 | 0.07 | 0.00 | 0.00 | 0.00 | 0.00 | 42.17 | 0.54 | 0.01 | 57.14 | 0.00 | 0.03 | 0.00 | 0.01 | 0.00 | 0.00 | 100.51 |
| Bismuth | Ovoid | 0.33 | 0.32 | 0.00 | 0.00 | 0.73 | 0.04 | 0.00 | 0.01 | 0.00 | 100.19 | 0.26 | 0.15 | 0.07 | 0.00 | 0.00 | 0.00 | 0.00 | 0.00 | 102.11 |
| | | | | | | | | | | | | | | | | | | | | |
| Average LOD | | *0.03* | *0.03* | *0.10* | *0.04* | *0.05* | *0.14* | *0.09* | *0.06* | *0.10* | *0.20* | *0.15* | *0.12* | *0.26* | *0.11* | *0.14* | *0.12* | *0.00* | *0.00* | |
| PdSbTe1 | Ovoid | 28.24 | 27.92 | 1.01 | 28.80 | 1.31 | 2.83 | 0.00 | 2.84 | 0.00 | 1.47 | 0.11 | 0.02 | 0.00 | 0.00 | 0.00 | 0.05 | 0.00 | 0.00 | 94.59 |
| | | | | | | | | | | | | | | | | | | | | |
| Average LOD | | 0.03 | 0.03 | 0.10 | 0.03 | 0.06 | 0.17 | 0.09 | 0.17 | 0.11 | 0.19 | 0.16 | 0.12 | 0.25 | 0.11 | 0.05 | 0.00 | 0.10 | 0.06 | |
| CdS1 (Southeast Extension 2 | | 5.43 | 0.02 | 0.00 | 28.10 | 0.00 | 0.00 | 0.01 | 0.00 | 0.00 | 0.00 | 0.00 | 0.00 | 0.12 | 0.00 | 0.72 | 0.00 | 37.44 | 29.55 | 101.38 |

# APPENDIX 4: LA-ICPMS of Elements of Interest

Instrument Parameters

| | |
|---|---|
| Instrument: | Element-XR HR-ICPMS (Geolas 193 nm excimer laser) or Quadrupole ICP-MS Electron X Series II (ArF Resonetic Resolution M-50 193nm excimer laser system) |
| Fluence: | 5.0-6.0 J/cm$^2$ |
| Spot Size: | 30-40 µm |
| Repitition Rate: | 10 Hz |
| Calibration Standards: | Po 41, Po 698, Po 727, MASS1, Nist 610 |

**Notes**:

The LA-ICP-MS systems were equipped with a light microscope to enable viewing of the sample surface through a computer monitor. The mineral grains that were chosen for anlaysis were based on previous SEM-MLA results, or were chosen by inspection under the light microscope.

Where possible, the full suite of elements were analyzed or monitored per individual grain. These elements include $S^{33}$, $S^{34}$, $Ti^{47}$, $Ti^{49}$, $Fe^{57}$, $Ni^{61}$, $Cu^{63}$, $Zn^{66}$, $As^{75}$, $Ru^{99}$, $Ru^{101}$, $Ru^{102}$, $Rh^{103}$, $Pd^{105}$, $Pd^{106}$, $Pd^{108}$, $Ag^{107}$, $Ag^{109}$, $Cd^{111}$, $Sb^{121}$, $Sb^{123}$, $Te^{125}$, $Hf^{177}$, $Hf^{178}$ $Ta^{181}$, $Re^{187}$ $Os^{189,}$ $Ir^{191}$, Ir 193, $Pt^{194}$, $Pt^{195}$, $Au^{197}$, $Bi^{209}$; Selected elements were quantified using a combination of the above listed synthetic calibration standards. Each standard was ablated between sets of 6 to 8 spot analyses in order to correct for drift and perform elemental quantifications and calibrations. Fe or S that was determined by EPMA in the mineral phases were used for internal calibrations. The ablation time consisted of approximately 60-90s per grain, and approximately 20-30s of background was collected before and after ablation.

Off-line data reduction calculations, including background subtraction, were made using Iolite software package (supported by Igor Pro 6) or LAMTRACE software package (an application of Lotus 1,2,3) specifically designed for processing raw data generated by LA-ICPMS. Corrections to the light element PGE interferences were made using the methods described in Sylvester (2001). The possible isotopic interferences that were corrected for in these samples include $^{40}Ar^{65}Cu$ on $^{105}Pd$, $^{40}Ar^{66}Zn$ on $^{106}Pd$ and $^{40}Ar^{68}Zn$ on $^{108}Pd$; $^{40}ArNi^{61}$ on $^{101}Ru$, and $^{40}Ar^{62}Ni$ on $^{102}Ru$ and $^{102}Pd$. Measurements requiring corrections greater than 50% were not included in the data-set. The concentrations of Rh in galena and chalcopyrite could not be determined because of the large interferences (>95%) of $^{206}Pb^{2+}$ and $^{40}Ar^{63}Cu$, respectively, on $^{103}Rh$ (100% isotopic abundance).

Occasionally, subsurface micro-inclusions that contained elements of interest were present in some mineral grains that were analyzed. In these cases, count intervals used for the data reduction were selected as appropriately as possible based on inspection of the time resolved spectra.

Analyses highlighted in grey are below detection limit. Values highlighted in green were too close to detection limit, or required too many corrections due to interferences or inclusions to be confidently used for interpretation. Elements that are listed as analyzed that are not provided in the tables below did not contain any analyses that were above detection limit or were not statistically significant.

# Trace-Elements in Solid Sution in Sulphides (ppm)

**Trace Elements and PGE in Sulphide Minerals Analyzed by LAICPMS**

| Sample | Analysis# | Mineral | Ru | Rh | Pd | Os | Ir | Pt | Au | Ag | As | Sb | Te | Bi | Sn |
|---|---|---|---|---|---|---|---|---|---|---|---|---|---|---|---|
| Units | | | ppm | ppm | ppm | ppm | ppm | ppm | ppm | ppm | ppm | ppm | ppm | ppm | ppm |
| *Average L.O.D.* | | | | | *0.01* | *0.01* | *0.01* | *0.01* | *0.01* | *0.1* | *0.07* | *0.03* | *0.2* | *0.01* | *0.07* |
| **Ovoid** | | | | | | | | | | | | | | | |
| BS0218 | jl13B05 | Cpy | | | 0.03 | 0.02 | 0.01 | <0.00508 | 0.02 | 1.25 | 0.07 | <0.029 | | | |
| | jl13B06 | Cpy | | | 0.10 | 0.00 | 0.01 | 0.02 | <0.0129 | 2.18 | 0.08 | <0.033 | | | |
| | jl13B07 | Cpy | | | 0.07 | <0.00474 | <0.00712 | <0.00951 | 0.01 | 2.21 | <0.050 | <0.033 | | | |
| | jl13B08 | Cpy | | | 0.37 | <0.0284 | 0.00 | <0.0118 | 0.03 | 16.96 | 0.18 | <0.035 | | | |
| | jl13B09 | Cpy | | | 0.05 | 0.00 | <0.00266 | <0.00825 | <0.0109 | 4.84 | <0.066 | <0.042 | | | |
| | jl13B10 | Cpy | | | 0.08 | <0.00584 | 0.05 | 0.01 | <0.0103 | 2.32 | <0.055 | <0.032 | | | |
| | | | | | 0.12 | 0.01 | 0.02 | 0.01 | 0.02 | 4.96 | 0.11 | #DIV/0! | | | |
| | my25D05 | Pn | | | 1.77 | <0.0272 | 0.02 | 0.02 | <0.0301 | 0.88 | 0.20 | <0.0815 | | | |
| | my25D06 | Pn | | | 0.94 | <0.0293 | 0.01 | 0.02 | 0.01 | 0.34 | 0.23 | <0.0342 | | | |
| | my25D07 | Pn | | | 1.95 | 0.02 | <0.0144 | 0.02 | 0.02 | 10.90 | 0.21 | <0.0331 | | | |
| | my25D08 | Pn | | | 1.25 | <0.0212 | 0.02 | 0.01 | <0.00970 | 1.34 | 0.38 | <0.0365 | | | |
| | my25D09 | Pn | | | 2.21 | 0.03 | <0.00623 | 0.01 | <0.0138 | 5.24 | 0.84 | <0.0435 | | | |
| | my25D10 | Pn | | | 0.72 | <0.0397 | <0.0187 | 0.01 | 0.03 | 1.76 | 0.07 | <0.0358 | | | |
| | | | | | 1.47 | 0.02 | 0.02 | 0.01 | 0.02 | 3.41 | 0.32 | #DIV/0! | | | |
| | my25C05 | Po | | | 0.41 | 0.04 | 0.01 | 0.02 | 0.01 | 0.40 | 0.15 | 0.25 | | | |
| | my25C08 | Po | | | 0.14 | 0.01 | <0.00682 | 0.03 | 0.06 | 0.32 | 0.30 | <0.0241 | | | |
| | my25C09 | Po | | | 0.07 | 0.01 | 0.01 | 0.02 | 0.02 | 0.41 | 0.18 | 0.12 | | | |
| | my25C11 | Po | | | 0.22 | 0.01 | <0.00851 | 0.01 | <0.109 | 1.36 | 0.19 | <0.0344 | | | |
| | my25C12 | Po | | | 0.17 | 0.02 | 0.01 | 0.01 | 0.02 | 0.40 | 0.87 | 0.06 | | | |
| | my25C13 | Po | | | 0.20 | <0.0127 | 0.01 | <0.00863 | 0.01 | 0.27 | 0.47 | <0.0334 | | | |
| | | | | | 0.20 | 0.02 | 0.01 | 0.02 | 0.03 | 0.53 | 0.36 | 0.14 | | | |
| | | | | | | | | | | | | | | | |
| DF6055 | jl13C05 | Cpy | | | 0.11 | <0.00161 | <0.00317 | 0.01 | 0.03 | 1.68 | <0.018 | <0.011 | | | |
| | jl13C06 | Cpy | | | 0.02 | 0.00 | <0.00076 | 0.00 | 0.02 | 0.99 | 0.05 | 0.01 | | | |
| | jl13C07 | Cpy | | | 0.08 | 0.00 | <0.00394 | <0.00267 | 0.09 | 4.75 | 0.07 | <0.020 | | | |
| | jl13C08 | Cpy | | | 0.02 | <0.00785 | 0.00 | <0.00402 | <0.00760 | 4.57 | 0.05 | <0.022 | | | |
| | | | | | | | | | | | | | | | |
| | my25E05 | Pn | | | 0.12 | 0.04 | 0.02 | <0.0168 | <0.0122 | 1.65 | <2.44 | <0.0490 | | | |
| | my25E06 | Pn | | | 1.72 | 0.02 | <0.0215 | 0.01 | <0.0131 | 0.29 | 0.05 | 0.04 | | | |
| | my25E07 | Pn | | | 3.76 | <0.0450 | <0.0147 | 0.04 | 0.04 | 0.93 | 0.27 | 0.03 | | | |
| | my25E08 | Pn | | | 1.07 | 0.04 | 0.03 | <0.0192 | 0.02 | 0.90 | 0.59 | 0.04 | | | |
| | my25E09 | Pn | | | 2.39 | <0.0186 | <0.00900 | 0.02 | 0.10 | 0.77 | 0.62 | 0.04 | | | |
| | my25E10 | Pn | | | 0.46 | <0.0333 | 0.02 | 0.04 | <0.0130 | 0.28 | 0.76 | 0.03 | | | |
| | | | | | | | | | | | | | | | |
| | my25A05 | Po | | | 0.77 | 0.01 | <0.0125 | 0.20 | 0.14 | 3.33 | 0.25 | <0.0367 | | | |
| | my25A07 | Po | | | 0.13 | 0.01 | 0.01 | 0.01 | 0.10 | 2.07 | 0.29 | 0.07 | | | |
| | my25A09 | Po | | | 0.22 | 0.01 | <0.00608 | 0.01 | 0.00 | 1.68 | 0.60 | 0.05 | | | |
| | my25A10 | Po | | | 0.39 | 0.03 | 0.01 | 0.01 | 0.02 | 0.68 | 0.23 | 0.05 | | | |
| | my25A11 | Po | | | 0.31 | 0.01 | 0.01 | 0.01 | 0.01 | 1.85 | 0.19 | <0.0530 | | | |
| | my25A12 | Po | | | 0.04 | 0.01 | 0.04 | <0.00634 | 0.06 | 0.72 | <0.123 | 0.19 | | | |
| | | | | | | | | | | | | | | | |
| | jl22A05 | Gn | | | 0.88 | <0.194 | <0.0843 | <0.149 | 0.42 | 50.46 | <1.134 | 0.19 | | | |
| | jl22A06 | Gn | | | 0.48 | <0.208 | <0.165 | <0.166 | 0.14 | 453.54 | <1.830 | 2.54 | | | |
| | jl22A07 | Gn | | | 0.42 | <0.291 | <0.128 | <0.170 | 0.24 | 280.96 | <1.404 | <0.255 | | | |
| | jl22A08 | Gn | | | 0.79 | <0.316 | <0.186 | <0.203 | 0.49 | 120.30 | <1.534 | 0.43 | | | |
| | jl22A09 | Gn | | | | <0.186 | <0.121 | <0.185 | 0.25 | 73.73 | <1.570 | 0.65 | | | |
| | | | | | | | | | | | | | | | |
| | fe18A07 | Gn2 | | | 2.18 | <0.521 | <0.351 | <0.571 | 1.69 | 70.20 | <3.35 | 0.89 | 14900.00 | 3710.00 | |
| | fe18A09 | Gn3 | | | <1.67 | <0.884 | <0.462 | <0.774 | <0.407 | 108.00 | <4.57 | <1.05 | 3470.00 | 4630.00 | |
| | fe18A11 | Gn4 | | | 1.27 | <0.572 | <0.453 | <0.662 | 0.37 | 36.30 | <4.42 | <0.735 | 770.00 | 1810.00 | |
| | fe18A13 | Gn5 | | | 2.11 | <0.536 | <0.427 | <0.574 | 0.50 | 128.00 | <3.95 | 0.78 | 3550.00 | 5340.00 | |
| | | | | | | | | | | | | | | | |
| | | | | | | | | | | | | | | | |
| | fe1808 | PbTe | | | 0.67 | <0.224 | <0.151 | <0.189 | <0.121 | 233.00 | <1.48 | 1.05 | 3170.00 | 5530.00 | |
| | fe1810 | PbTe | | | 2.10 | <0.615 | <0.385 | <0.549 | <0.338 | 158.00 | <3.40 | <0.685 | 3000.00 | 4410.00 | |
| | fe1812 | PbTe | | | 3.26 | <1.00 | <0.458 | <0.670 | 0.58 | 49.50 | <4.55 | <0.885 | 3210.00 | 3170.00 | |
| | fe1814 | PbTe | | | 2.36 | <0.851 | <0.397 | <0.450 | <0.322 | 108.00 | <4.25 | 1.02 | 3120.00 | 4680.00 | |
| | | | | | | | | | | | | | | | |
| | | | | | | | | | | | | | | | |

| | | | | | | | | | | | | | | | |
|---|---|---|---|---|---|---|---|---|---|---|---|---|---|---|---|
| BS0241 | jl13D05 | Cpy | 0.03 | | 0.01 | 0.02 | 0.02 | 0.01 | 0.03 | 1.16 | <1.801 | <0.016 | | | |
| | jl13D06 | Cpy | 0.02 | | 0.22 | <0.00411 | 0.00 | 0.01 | 0.09 | 1.49 | 0.09 | 0.02 | | | |
| | jl13D07 | Cpy | <0.0174 | | 0.11 | 0.01 | <0.00347 | 0.01 | 0.03 | 0.87 | 0.13 | 0.02 | | | |
| | jl13D08 | Cpy | <0.0150 | | 0.08 | <0.00274 | 0.01 | 0.02 | 0.07 | 2.42 | 0.08 | 0.02 | | | |
| | | | | | | | | | | | | | | | |
| | se04B05 | Pn | | | 1.10 | 0.02 | 0.02 | <0.0340 | <0.0667 | 1.46 | <2.42 | 0.86 | | | |
| | se04B06 | Pn | | | 0.23 | <0.0253 | 0.00 | <0.0334 | <0.0484 | 1.53 | <0.206 | <0.102 | | | |
| | se04B07 | Pn | | | 0.93 | 0.03 | 0.01 | <0.0172 | <0.0420 | 13.93 | <2.19 | 1.58 | | | |
| | se04B08 | Pn | | | 0.89 | <0.0215 | 0.04 | <0.0261 | <0.0462 | 0.46 | <0.203 | <0.088 | | | |
| | se04B09 | Pn | | | 0.87 | 0.02 | <0.0140 | 0.01 | <0.0403 | 2.03 | <1.625 | 0.09 | | | |
| | se04B10 | Pn | | | 0.98 | <0.0215 | 0.01 | 0.02 | <0.0362 | 1.20 | <0.187 | <0.072 | | | |
| | | | | | | | | | | | | | | | |
| | my21A10 | Po | | | 0.21 | <0.0119 | 0.01 | 0.01 | 0.01 | 0.42 | 0.80 | 0.05 | | | |
| | my21A11 | Po | | | 0.23 | 0.02 | 0.02 | <0.0257 | 0.01 | 0.33 | 0.32 | <0.037 | | | |
| | my21A12 | Po | | | 0.15 | 0.02 | 0.01 | <0.00709 | 0.03 | 0.24 | 0.22 | <0.028 | | | |
| | my21A13 | Po | | | 0.35 | 0.04 | 0.01 | <0.0185 | 0.02 | 0.22 | 0.40 | <0.029 | | | |
| | my21A14 | Po | | | 0.21 | 0.01 | 0.02 | 0.02 | <0.00957 | 0.49 | 0.18 | <0.029 | | | |
| | my21A15 | Po | | | 0.19 | 0.01 | 0.02 | 0.01 | 0.02 | 0.57 | 0.52 | 0.10 | | | |
| | | | | | | | | | | | | | | | |
| | jl22B05 | Gn | | | 1.34 | <0.372 | <0.165 | <0.157 | 0.18 | 101.81 | <2.829 | <0.347 | | | |
| | jl22B06 | Gn | | | 0.83 | <0.343 | <0.146 | <0.284 | <0.139 | 556.42 | <3.536 | 0.41 | | | |
| | jl22B07 | Gn | | | 1.09 | <0.158 | <0.109 | <0.158 | <0.0980 | 116.94 | <1.937 | <0.209 | | | |
| | jl22B08 | Gn | | | 2.69 | <0.754 | <0.485 | <0.560 | <0.242 | 177.72 | <8.036 | <0.830 | | | |
| | jl22B09 | Gn | | | 0.86 | <0.271 | <0.118 | <0.184 | <0.150 | 147.17 | <3.090 | 0.34 | | | |
| | jl22B10 | Gn | | | 2.69 | <0.181 | <0.0903 | <0.157 | 0.33 | 108.18 | <2.349 | <0.283 | | | |
| | | | | | | | | | | | | | | | |
| | | | | | | | | | | | | | | | |
| BS0207 LU | | Cpy | | | 0.07 | NA | NA | 0.00 | 0.03 | 3.91 | 1.09 | 0.02 | 0.81 | 0.59 | 12.09 |
| BS0207 LU | | Cpy | | | 0.06 | NA | NA | 0.00 | 0.05 | 3.64 | 0.41 | 0.20 | 8.10 | 0.28 | 17.70 |
| BS0207 LU | | Cpy | | | 0.05 | NA | NA | 0.00 | 0.02 | 4.94 | 0.03 | 0.02 | 3.36 | 2.60 | 7.25 |
| BS0207 LU | | Cpy | | | 0.08 | NA | NA | 0.00 | 0.01 | 2.72 | 0.03 | 0.00 | 7.22 | 0.17 | 9.72 |
| BS0207 LU | | Cpy | | | 0.58 | NA | NA | 0.00 | 0.03 | 2.89 | 0.05 | 0.01 | 8.55 | 1.14 | 4.81 |
| BS0207 MUN | jl13E05 | Cpy | <0.0156 | | 0.07 | <0.00312 | <0.00206 | 0.02 | 0.02 | 1.70 | 0.27 | 0.02 | NA | NA | NA |
| BS0207 MUN | jl13E06 | Cpy | 0.01 | | 0.09 | 0.00 | 0.00 | 0.01 | 0.09 | 2.27 | 0.05 | 0.02 | NA | NA | NA |
| BS0207 MUN | jl13E07 | Cpy | 0.02 | | 0.03 | 0.00 | 0.00 | <0.00220 | 0.05 | 2.10 | 0.04 | <0.011 | NA | NA | NA |
| BS0207 MUN | jl13E08 | Cpy | 0.08 | | 1.11 | 0.01 | 0.01 | 0.01 | 0.01 | 5.67 | 0.24 | <0.018 | NA | NA | NA |
| | | | | | | | | | | | | | | | |
| BS0207 LU | | Pn | | | 1.36 | | | | | 4.05 | 1.02 | 0.03 | 0.77 | 0.23 | 0.05 |
| BS0207 LU | | Pn | | | 0.79 | | | | | 3.17 | 0.22 | 0.00 | 0.86 | 0.50 | 0.43 |
| BS0207 LU | | Pn | | | 2.19 | | | | | 1.99 | 0.23 | 0.14 | 7.67 | 0.29 | 0.05 |
| BS0207 LU | | Pn | | | 1.87 | | | | | 2.80 | 0.35 | 0.01 | 1.31 | 0.20 | 0.39 |
| BS0207 LU | | Pn | | | 0.47 | | | | | 2.68 | 0.42 | 0.01 | 0.54 | 0.41 | 0.11 |
| BS0207 LU | | Pn | | | 0.97 | | | | | 2.18 | 0.33 | 0.06 | 3.09 | 2.17 | 0.62 |
| BS0207 LU | | Pn | | | 0.58 | | | | | 4.13 | 0.64 | 0.26 | 12.30 | 2.11 | 0.29 |
| BS0207 LU | | Pn | | | 1.07 | | | | | 2.34 | 0.26 | 0.21 | 1.77 | 0.57 | 0.07 |
| BS0207 LU | | Pn | | | 0.57 | | | | | 3.46 | 0.14 | 0.03 | 0.16 | 0.11 | 0.04 |
| BS0207 LU | | Pn | | | 1.80 | | | | | 1.26 | 0.38 | 0.01 | 0.42 | 0.75 | 0.29 |
| BS0207 LU | | Pn | | | 0.49 | | | | | 3.89 | 0.10 | 0.03 | 0.54 | 0.37 | 0.06 |
| BS0207 LU | | Pn | | | 0.00 | | | | | 2.88 | 0.34 | 0.01 | 0.85 | 0.14 | 0.04 |
| BS0207 LU | | Pn | | | 1.13 | | | | | 2.16 | 0.13 | 0.15 | 6.20 | 0.19 | 0.02 |
| BS0207 LU | | Pn | | | 1.43 | | | | | 4.29 | 0.33 | 0.01 | 0.55 | 0.30 | 0.07 |
| BS0207 LU | | Pn | | | 0.37 | | | | | 5.71 | 0.61 | 0.06 | 3.36 | 0.55 | 0.29 |
| BS0207 LU | | Pn | | | 1.08 | | | | | 1.75 | 0.18 | 0.14 | 9.80 | 0.27 | 0.16 |
| BS0207 LU | | Pn | | | 0.47 | | | | | 4.57 | 0.46 | 0.02 | 0.29 | 2.09 | 0.25 |
| BS0207 LU | | Pn | | | 0.47 | | | | | 11.92 | 0.56 | 0.13 | 1.47 | 0.89 | 0.16 |
| BS0207 LU | | Pn | | | 2.07 | | | | | 1.99 | 0.76 | 0.02 | 1.65 | 0.34 | 3.80 |
| BS0207 LU | | Pn | | | 1.25 | | | | | 3.86 | 0.52 | 0.03 | 0.18 | 0.45 | 0.04 |
| BS0207 LU | | Pn | | | 0.68 | | | | | 1.98 | <6.5 | 0.03 | 0.28 | 0.62 | 0.59 |
| BS0207 LU | | Pn | | | 0.32 | | | | | 8.11 | 0.61 | 0.17 | 7.63 | 0.33 | 0.05 |
| BS0207 LU | | Pn | | | 0.96 | | | | | 4.28 | 0.35 | 0.02 | 0.49 | 0.78 | 0.10 |
| BS0207 LU | | Pn | | | 1.43 | | | | | 2.12 | 0.71 | 0.01 | 1.28 | 0.24 | 0.03 |
| BS0207 LU | | Pn | | | 1.54 | | | | | 3.54 | <1.7 | 0.02 | 0.57 | 0.14 | 0.03 |
| BS0207 LU | | Pn | | | 2.18 | | | | | 1.76 | 0.51 | 0.01 | 0.63 | 0.23 | 0.08 |

| | | | | | | | | | | | | | | | |
|---|---|---|---|---|---|---|---|---|---|---|---|---|---|---|---|
| BS0207 MUN | se04C05 | Pn | | | 1.06 | <0.0460 | <0.0302 | <0.0364 | <0.0558 | 0.80 | <0.290 | <0.117 | | | |
| BS0207 MUN | se04C06 | Pn | | | 1.06 | 0.01 | 0.00 | 0.06 | <0.0587 | 1.31 | <0.331 | <0.122 | | | |
| BS0207 MUN | se04C07 | Pn | | | 1.78 | 0.02 | 0.03 | <0.0342 | <0.0653 | 0.89 | <0.304 | <0.136 | | | |
| BS0207 MUN | se04C08 | Pn | | | 1.54 | <0.0335 | 0.07 | <0.0185 | 0.08 | 1.56 | <0.296 | <0.131 | | | |
| BS0207 MUN | se04C09 | Pn | | | 1.56 | <0.0442 | 0.03 | 0.03 | <0.0447 | 13.70 | 14.30 | 0.16 | | | |
| BS0207 MUN | se04C10 | Pn | | | <0.148 | <0.0553 | 0.01 | <0.0178 | <0.0459 | 5.99 | <0.247 | <0.124 | | | |
| BS0207 LU | | | | | | | | | | | | | | | |
| BS0207 LU | | Po | | | 0.02 | | | | | 0.73 | 0.51 | 0.01 | 2.59 | 0.59 | 1.70 |
| BS0207 LU | | Po | | | 0.01 | | | | | 0.54 | 0.61 | 0.03 | 1.08 | 0.20 | 0.05 |
| BS0207 LU | | Po | | | 0.00 | | | | | 0.48 | 0.65 | 0.04 | 0.44 | 0.30 | 0.14 |
| BS0207 LU | | Po | | | 0.02 | | | | | 0.35 | 0.31 | 0.01 | 0.36 | 0.10 | 0.04 |
| BS0207 LU | | Po | | | 0.00 | | | | | 0.34 | 0.14 | 0.00 | 0.26 | 0.11 | 0.11 |
| BS0207 LU | | Po | | | 0.01 | | | | | 1.44 | 0.25 | 0.02 | 0.26 | 0.25 | 0.14 |
| BS0207 LU | | Po | | | 0.00 | | | | | 0.54 | 0.22 | 0.01 | 0.22 | 0.17 | 0.05 |
| BS0207 LU | | Po | | | 0.02 | | | | | 0.39 | 0.18 | 0.02 | 0.32 | 0.10 | 0.10 |
| BS0207 MUN | my21A05 | Po | | | 0.08 | 0.02 | 0.02 | <0.0169 | <0.00626 | 0.28 | 0.08 | 0.04 | | | |
| BS0207 MUN | my21A06 | Po | | | 0.16 | 0.02 | 0.01 | 0.01 | 0.01 | 0.88 | 1.57 | <0.036 | | | |
| BS0207 MUN | my21A07 | Po | | | <0.0235 | 0.04 | 0.02 | <0.0162 | <0.00671 | 0.68 | 0.33 | <0.041 | | | |
| BS0207 MUN | my21A08 | Po | | | 0.43 | <0.0156 | 0.02 | 0.01 | <0.00870 | 0.26 | 0.61 | 0.05 | | | |
| BS0207 MUN | my21A09 | Po | | | 0.04 | 0.01 | 0.02 | 0.03 | <0.00668 | 0.81 | <0.062 | <0.036 | | | |
| BS0207 MUN | my21A10 | Po | | | 0.04 | 0.00 | <0.0276 | <0.0177 | 0.01 | 0.27 | 0.09 | <0.032 | | | |
| | | | | | | | | | | | | | | | |
| | jl22C05 | Gn | | | 3.46 | <0.615 | <0.243 | <0.380 | 0.44 | 89.10 | <5.92 | <0.419 | | | |
| | jl22C06 | Gn | | | 1.48 | <0.201 | <0.0963 | <0.196 | 0.15 | 347.00 | <1.51 | 0.60 | | | |
| | jl22C07 | Gn | | | 3.49 | <0.370 | <0.235 | <0.264 | 0.13 | 344.00 | <2.36 | <0.444 | | | |
| | jl22C08 | Gn | | | 1.23 | <0.298 | <0.228 | <0.167 | <0.141 | 56.70 | <2.12 | <0.432 | | | |
| | jl22C09 | Gn | | | 0.42 | <0.290 | <0.166 | <0.167 | <0.0941 | 745.00 | <2.02 | 0.74 | | | |
| | jl22C10 | Gn | | | 0.80 | <0.347 | <0.186 | <0.180 | <0.166 | 222.00 | <2.55 | <0.330 | | | |
| | | | | | | | | | | | | | | | |
| | | | | | | | | | | | | | | | |
| DF6063 | jl13F05 | Cpy | <0.0412 | | 0.15 | <0.00468 | <0.00438 | 0.01 | 0.02 | 7.40 | 0.07 | <0.039 | | | |
| | jl13F06 | Cpy | 0.22 | | 0.35 | <0.0133 | <0.0147 | <0.0157 | 0.17 | 39.66 | 0.20 | <0.071 | | | |
| | jl13F07 | Cpy | <0.0155 | | <0.00767 | <0.00191 | 0.00 | <0.00256 | 0.03 | 5.16 | 0.20 | 0.02 | | | |
| | jl13F08 | Cpy | | | | | | | | | | | | | |
| | | | | | | | | | | | | | | | |
| | se04D05 | Pn | | | 0.11 | 0.00 | 0.00 | <0.0255 | <0.0334 | 2.88 | <0.144 | <0.077 | | | |
| | se04D06 | Pn | | | 2.18 | <0.0224 | <0.0118 | <0.0480 | 0.21 | 0.88 | <0.212 | <0.105 | | | |
| | se04D07 | Pn | | | 1.50 | 0.01 | <0.0148 | 0.01 | <0.0366 | 1.08 | 0.34 | <0.129 | | | |
| | se04D08 | Pn | | | 1.07 | 0.02 | <0.0144 | <0.0234 | <0.0426 | 0.85 | 0.26 | <0.121 | | | |
| | se04D09 | Pn | | | <0.0795 | <0.0247 | 0.00 | <0.0182 | 0.05 | 5.23 | <0.122 | <0.061 | | | |
| | se04D10 | Pn | | | 1.65 | 0.02 | 0.01 | <0.0424 | <0.0333 | 1.07 | 0.36 | <0.153 | | | |
| | | | | | | | | | | | | | | | |
| | my25B05 | Po | | | <0.0798 | <0.0580 | <0.0137 | <0.0267 | 0.08 | 0.74 | <0.296 | <0.211 | | | |
| | my25B06 | Po | | | 0.22 | 0.02 | 0.02 | <0.0245 | <0.0167 | 0.25 | 0.29 | <0.0746 | | | |
| | my25B08 | Po | | | 0.18 | <0.0128 | 0.02 | 0.01 | <0.0149 | 1.39 | 0.60 | <0.0695 | | | |
| | my25B09 | Po | | | <0.0438 | <0.0397 | 0.02 | <0.0296 | 0.05 | 0.31 | 0.38 | <0.102 | | | |
| | my25B10 | Po | | | 0.15 | <0.0332 | <0.0158 | <0.00602 | 0.02 | 0.30 | <3.26 | <0.0751 | | | |
| | my25B11 | Po | | | <0.0397 | <0.0422 | <0.0162 | <0.00660 | 0.01 | 0.15 | <0.149 | 1.08 | | | |
| | | | | | | | | | | | | | | | |
| | jl22D05 | Gn | | | <1.80 | <1.14 | <1.08 | <1.07 | <0.568 | 244.00 | <7.00 | <1.53 | | | |
| | jl22D06 | Gn | | | <0.706 | <0.363 | <0.288 | <0.297 | 1.10 | 400.00 | <2.64 | 2.30 | | | |
| | jl22D07 | Gn | | | 1.69 | <0.364 | <0.176 | <0.226 | <0.135 | 335.00 | <2.00 | 0.98 | | | |
| | jl22D08 | Gn | | | 1.09 | <0.614 | <0.184 | <0.283 | 1.05 | 621.00 | <2.98 | 2.59 | | | |
| | jl22D09 | Gn | | | <0.512 | <0.288 | <0.253 | <0.186 | <0.105 | 569.00 | <2.28 | 1.34 | | | |
| | | | | | | | | | | | | | | | |

| Mini-Ovoid | | | | | | | | | | | | | | | |
|---|---|---|---|---|---|---|---|---|---|---|---|---|---|---|---|
| | | Cpy | | | 0.10 | | | | | 9.61 | 0.18 | 0.05 | 5.70 | 0.27 | 5.28 |
| | | Cpy | | | 0.09 | | | | | 5.97 | 0.24 | 0.03 | 3.60 | 0.11 | 15.45 |
| | | Cpy | | | 0.09 | | | | | 23.50 | 0.52 | 0.07 | 3.00 | 0.46 | 2.99 |
| | | Cpy | | | 0.12 | | | | | 24.30 | 0.19 | 0.03 | 8.70 | 0.09 | 12.87 |
| | | Cpy | | | 0.15 | | | | | 40.50 | 0.33 | 0.09 | 7.80 | 0.26 | 11.60 |
| | | Cpy | | | 0.13 | | | | | 17.20 | 0.09 | 0.03 | 9.90 | 0.22 | 18.60 |
| BS0265 | j113a07 | Cpy | <detection | not determ | 0.65 | | | <0.00280 | 0.01 | 3.58 | 0.03 | 0.03 | | | |
| | j113a08 | Cpy | <detection | not determ | 0.10 | | | 0.01 | 0.01 | 13.53 | 0.09 | 0.01 | | | |
| | j113a09 | Cpy | <detection | not determ | 0.10 | | | <0.00410 | <0.00784 | 4.03 | 0.03 | <0.021 | | | |
| | j113a10 | Cpy | <detection | not determ | 0.09 | | | <0.00365 | 0.01 | 130.16 | 0.03 | <0.013 | | | |
| | j113a11 | Cpy | <detection | not determ | 0.06 | | | 0.01 | <0.0114 | 9.14 | <0.047 | <0.037 | | | |
| | j113a12 | Cpy | <detection | not determ | 0.12 | | | <0.0118 | 0.01 | 13.27 | <0.041 | <0.035 | | | |
| | j113a13 | Cpy | <detection | not determ | 0.17 | | | 0.00 | 0.01 | 7.06 | 0.03 | <0.021 | | | |
| | j113a14 | Cpy | <detection | not determ | 0.03 | | | <0.00633 | 0.01 | 4.96 | <0.036 | <0.026 | | | |
| | j113a15 | Cpy | <detection | not determ | 0.06 | | | <0.00501 | <0.00786 | 5.53 | <0.039 | <0.022 | | | |
| | j113a16 | Cpy | <detection | not determ | 0.54 | | | <0.00561 | <0.00655 | 3.95 | 0.07 | <0.024 | | | |
| | | | | | | | | | | | | | | | |
| | | | | | 0.48 | | | | | | 0.36 | 0.04 | 1.93 | 0.08 | 0.06 |
| | | | | | 0.12 | | | | | | 0.75 | 0.04 | 10.40 | 0.01 | 0.03 |
| | | | | | 0.49 | | | | | | 0.24 | 0.01 | 0.30 | 0.01 | 0.06 |
| | | | | | 0.21 | | | | | | 0.58 | 0.06 | 7.10 | 0.12 | 0.05 |
| | | | | | 0.23 | | | | | | 0.40 | 0.01 | 1.28 | 0.17 | 0.04 |
| | | | | | 0.38 | | | | | | 0.57 | 0.00 | 16.30 | 0.11 | 0.19 |
| | | | | | 0.41 | | | | | | 0.22 | 0.01 | 0.70 | 0.01 | 0.05 |
| | | | | | 0.28 | | | | | | 0.28 | 0.00 | 2.15 | 0.04 | 0.04 |
| | | | | | 0.37 | | | | | | 0.05 | -0.05 | 2.01 | 0.01 | 0.51 |
| | | | | | 0.88 | | | | | | 0.54 | 0.02 | 5.60 | 0.17 | 0.81 |
| | se04A05 | Pn | | | <0.0643 | <0.0279 | <0.00931 | <0.0170 | <0.128 | 4.21 | 0.34 | <0.0575 | | | |
| | se04A06 | Pn | | | 0.12 | 0.04 | 0.05 | 0.01 | <0.0428 | 0.76 | 0.15 | <0.0518 | | | |
| | se04A07 | Pn | | | 0.80 | <0.0198 | 0.02 | <0.0152 | <0.0414 | 0.57 | <0.165 | 0.08 | | | |
| | se04A08 | Pn | | | 1.01 | <0.0129 | 0.02 | <0.0121 | <0.0417 | 0.41 | 0.31 | <0.0529 | | | |
| | se04A09 | Pn | | | 0.27 | 0.04 | 0.02 | <0.00685 | <0.0349 | 1.04 | <0.143 | <0.0475 | | | |
| | se04A10 | Pn | | | <0.0672 | <0.0132 | 0.00 | 0.02 | <0.0400 | 2.94 | 0.17 | <0.0547 | | | |
| | | | | | **0.43** | | | | | | | | | | |
| | | | | | 0.04 | | | | | 1.05 | | | 6.90 | 0.04 | 1.10 |
| | | | | | 0.03 | | | | | 0.64 | | | 7.40 | 0.02 | 0.04 |
| | | | | | 0.02 | | | | | 0.68 | | | 8.80 | 0.04 | 0.12 |
| | | | | | 0.07 | | | | | 0.48 | | | 8.10 | 0.01 | 0.04 |
| | | | | | 0.04 | | | | | 0.45 | | | 5.10 | 0.01 | 0.13 |
| | | | | | 0.01 | | | | | 2.23 | | | 3.20 | 0.04 | 0.22 |
| | | | | | 0.01 | | | | | 0.62 | | | 6.90 | 0.02 | 0.06 |
| | | | | | 0.03 | | | | | 0.54 | | | 10.80 | 0.01 | 0.14 |
| | my21B04 | Po | | | 0.10 | 0.07 | 0.02 | <0.00689 | <0.00780 | 0.46 | 0.54 | <0.050 | | | |
| | my21B05 | Po | | | 0.10 | 0.07 | 0.02 | <0.0136 | <0.0103 | 3.34 | 0.15 | <0.046 | | | |
| | my21B06 | Po | | | 0.05 | 0.06 | <0.0184 | 0.02 | <0.00575 | 0.67 | <0.060 | <0.045 | | | |
| | my21B08 | Po | | | 0.48 | 0.06 | 0.01 | <0.00990 | <0.0109 | 0.68 | 0.55 | <0.052 | | | |
| | my21B09 | Po | | | <0.0189 | <0.00867 | <0.00835 | 0.03 | 0.09 | 10.15 | 0.32 | <0.041 | | | |

| Disovery Hill | | | | | | | | | | | | | | | |
|---|---|---|---|---|---|---|---|---|---|---|---|---|---|---|---|
| VX49289 | mr29B05 | Po | | | <0.412 | 0.02 | 0.00 | 0.00 | <0.0474 | 0.32 | 0.00 | <0.131 | | | |
| | mr29B06 | Po | | | <0.432 | 0.00 | 0.00 | 0.00 | <0.0404 | 0.34 | 0.16 | <0.112 | | | |
| | mr29B07 | Po | | | <0.434 | 0.00 | 0.00 | 0.00 | <0.0461 | 3.26 | 0.00 | <0.114 | | | |
| | mr29B08 | Po | | | <0.457 | 0.00 | 0.01 | 0.00 | <0.0370 | 0.35 | 0.00 | <0.149 | | | |
| | mr29B09 | Po | | | <0.552 | 0.00 | 0.01 | 0.00 | <0.0433 | 0.41 | 0.00 | <0.0975 | | | |
| | mr29B10 | Po | | | <0.572 | 0.00 | 0.00 | 0.00 | <0.0532 | 0.26 | 0.00 | <0.131 | | | |
| | | | | | | | | | | | | | | | |
| | mrB2911 | Pn | | | 1.83 | <0.0262 | <0.0117 | <0.0205 | 0.05 | 0.44 | 0.00 | <0.123 | | | |
| | mrB2912 | Pn | | | 0.76 | <0.0634 | <0.0128 | <0.0223 | 0.00 | 0.44 | 0.00 | <0.176 | | | |
| | mrB2913 | Pn | | | 1.61 | <0.0594 | <0.0167 | <0.0386 | 0.00 | 0.14 | 0.21 | <0.135 | | | |
| | mrC2905 | Pn | | | 1.47 | <0.0289 | <0.0129 | <0.0334 | 0.00 | 0.00 | 0.00 | <0.212 | | | |
| | mrC2906 | Pn | | | 1.54 | <0.0785 | <0.0125 | <0.0322 | 0.00 | 0.00 | 0.32 | <0.170 | | | |
| | mrC2907 | Pn | | | 0.00 | <0.0296 | <0.0185 | <0.0379 | 0.04 | 0.21 | 0.00 | <0.161 | | | |
| | | | | | | | | | | | | | | | |
| | mr29C08 | Cpy | | | <0.430 | 0.00 | 0.00 | 0.00 | 0.00 | 8.76 | 0.00 | <0.112 | | | |
| | mr29C09 | Cpy | | | <0.352 | 0.02 | 0.00 | 0.00 | 0.02 | 0.65 | 0.00 | <0.104 | | | |
| | mr29C10 | Cpy | | | <0.407 | 0.00 | 0.00 | 0.00 | 0.04 | 0.69 | 0.29 | <0.101 | | | |
| | mr29C11 | Cpy | | | <0.371 | 0.00 | 0.00 | 0.00 | 0.00 | 6.36 | 0.00 | <0.0793 | | | |
| | mr29C12 | Cpy | | | <0.446 | 0.00 | 0.00 | 0.02 | 0.03 | 8.81 | 0.00 | <0.0884 | | | |
| | mr29C13 | Cpy | | | <0.423 | 0.01 | 0.02 | 0.00 | 0.00 | 0.43 | 0.00 | <0.117 | | | |
| | | | | | | | | | | | | | | | |
| VX49277 | mr29D05 | Po | | | <0.544 | 0.02 | 0.00 | <0.0285 | 0.00 | 0.39 | 0.21 | <0.123 | | | |
| | mr29D06 | Po | | | <0.557 | 0.00 | 0.01 | <0.0317 | 0.00 | 1.02 | 0.19 | <0.145 | | | |
| | mr29D07 | Po | | | <0.530 | 0.00 | 0.00 | <0.0129 | 0.00 | 1.41 | 0.00 | <0.156 | | | |
| | mr29D08 | Po | | | <0.689 | 0.00 | 0.00 | <0.0193 | 0.04 | 0.59 | 0.00 | <0.153 | | | |
| | mr29D09 | Po | | | <0.576 | 0.00 | 0.00 | <0.0197 | 0.00 | 2.17 | 0.45 | <0.173 | | | |
| | mr29D10 | Po | | | <0.675 | 0.00 | 0.00 | <0.0291 | 0.00 | 0.20 | 0.70 | <0.182 | | | |
| | | | | | | | | | | | | | | | |
| | mr29D08 | Pn | | | 0.00 | 0.00 | <0.0328 | 0.00 | 0.00 | 0.55 | 0.00 | <0.222 | | | |
| | mr29D09 | Pn | | | 0.97 | 0.00 | <0.0241 | 0.00 | 0.00 | 1.16 | 0.72 | <0.185 | | | |
| | mr29D10 | Pn | | | 0.00 | 0.00 | <0.0126 | 0.00 | 0.00 | 0.23 | 0.00 | <0.181 | | | |
| | mr29E05 | Pn | | | 0.98 | 0.02 | <0.0155 | 0.00 | 0.05 | 0.00 | 0.25 | <0.224 | | | |
| | mr29E06 | Pn | | | 2.16 | 0.00 | <0.0136 | 0.01 | 0.00 | 0.24 | 0.36 | <0.165 | | | |
| | mr29E07 | Pn | | | 1.84 | 0.00 | <0.0190 | 0.00 | 0.00 | 0.29 | 0.28 | <0.163 | | | |
| | | | | | | | | | | | | | | | |
| | mr29E08 | Cpy | | | 37.40 | 0.01 | 0.00 | <0.0201 | 0.04 | 0.15 | 2.44 | <0.122 | | | |
| | mr29E09 | Cpy | | | 1.60 | 0.00 | 0.00 | <0.0291 | 0.07 | 0.37 | 1.94 | <0.143 | | | |
| | mr29E10 | Cpy | | | 0.85 | 0.00 | 0.00 | <0.0499 | 0.00 | 0.00 | 1.57 | <0.102 | | | |
| | mr29E11 | Cpy | | | 0.00 | 0.00 | 0.01 | <0.0233 | 0.00 | 0.23 | 1.56 | <0.110 | | | |
| | m | Cpy | | | 0.00 | 0.00 | 0.00 | <0.0270 | 0.06 | 1.15 | <51.8 | <0.125 | | | |
| | mr29E13 | Cpy | | | 0.00 | 0.00 | 0.00 | <0.0193 | 0.02 | 0.12 | 1.20 | <0.120 | | | |
| | mr29E14 | Cpy | | | 0.63 | 0.04 | 0.00 | <0.0229 | 0.00 | 0.00 | 1.83 | <0.143 | | | |

# APPENDIX 5: CALCULATIONS

**Calculations used for modal mineral abundances based on assays (chapter 3)**

% Chalcopyrite = Cu assay/(%Cu EPMA/100)

% Penlandite = Ni assay/(%Ni EPMA/100)

% Pyrrhotite = (S assay - ((%Cpy*S EPMA in Cpy)+(%Pn*S EPMA in Pn)))/(S EPMA Po)

Other (mostly Mt in massive sulfide samples) = 100 - (%Cpy + %Pn +%Po)

**Calculated Mineralogy (wt%)**

| | Pn | Cpy | Po | Gn | Other |
|---|---|---|---|---|---|
| Ovoid | 11.76 | 5.88 | 69.11 | 0.17 | 13.06 |
| MO | 7.26 | 13.79 | 22.37 | 0.00 | 56.57 |
| DISS O | 5.12 | 2.65 | 22.13 | 0.01 | 70.10 |
| DH SM | 7.85 | 3.29 | 11.96 | 0.01 | 27.18 |
| DH DISS | 4.30 | 21.13 | 5.84 | 0.00 | 23.61 |
| SE | 0.29 | 2.50 | 1.83 | 0.58 | 94.80 |

Ovoid is based on assay data for the average of the 4 massive sulfide samples.
Other category is mostly magnetite in the massive sulfide samples (Ovoid) and silicates in the disseminated sampels.

Pn=pentlandite; Cpy=chalcpyrite; Po=pyrrhotite; Gn=galena.

**Deportment Calculations:**

Element in Solid Solution =(Element in Pn)*Modal Pn + (Element in Cpy)*Modal Cpy + (Element in Po)*Modal Po + (Element in Gn)*Modal Gn)

Element deported to PGM or PMM = Element Assay - Element in Solid Solution

Calculated Mass Distributions (mass% of Metal in sample)

| | | As | Te | Sb | Sn | Ag | Pd | Au | Bi |
|---|---|---|---|---|---|---|---|---|---|
| Ovoid | Pn | ND | 2.26 | 2.51 | 0.70 | 1.46 | 14.09 | 6.02 | 0.93 |
| | Cpy | ND | 2.54 | 0.32 | 11.56 | 1.17 | 0.73 | 1.80 | 0.76 |
| | Po | ND | 3.68 | 12.24 | 3.82 | 2.06 | 5.72 | 15.25 | 2.11 |
| | Gn | ND | 7.62 | 0.31 | 0.33 | 1.75 | 0.27 | 0.54 | 91.00 |
| | PMM | ND | 83.90 | 84.62 | 83.59 | 93.55 | 79.19 | 76.38 | 5.20 |
| Mini-Ovoid | Pn | ND | ND | ND | 0.19 | 0.53 | 33.62 | ND | 0.66 |
| | Cpy | ND | ND | ND | 21.94 | 12.01 | 23.99 | ND | 4.12 |
| | Po | ND | ND | ND | 0.74 | 1.00 | 10.89 | ND | 0.70 |
| | Gn | ND | ND | ND | 0.00 | 0.00 | 0.00 | ND | 0.00 |
| | PMM | ND | ND | ND | 77.14 | 86.46 | 31.50 | ND | 94.53 |
| Disc Hill | Pn | ND | 3.44 | ND | 0.32 | 0.04 | 26.14 | 0.13 | 3.79 |
| | Cpy | ND | 17.66 | ND | 20.99 | 0.08 | 11.85 | 0.44 | 6.66 |
| | Po | ND | 1.46 | ND | 0.43 | 0.18 | 0.15 | 0.12 | 1.73 |
| | Gn | ND | 0.00 | ND | 0.00 | 0.00 | 0.00 | 0.00 | 0.00 |
| | PMM | ND | 77.43 | ND | 78.26 | 99.70 | 61.87 | 99.31 | 87.82 |
| HG Dyke | Pn | 0.30 | 0.10 | 0.13 | 0.00 | 0.02 | 0.49 | 0.00 | 0.00 |
| | Cpy | 0.06 | 1.36 | 0.72 | 1.46 | 1.47 | 0.21 | 0.03 | 0.02 |
| | Po | 0.05 | 0.20 | 0.43 | 0.01 | 0.02 | 0.05 | 0.02 | 0.01 |
| | Gn | 0.25 | 23.00 | 1.53 | 0.06 | 2.26 | 0.88 | 0.03 | 0.34 |
| | PMM | 99.35 | 75.34 | 97.18 | 98.47 | 96.24 | 98.37 | 99.92 | 99.63 |
| PGE poor | Pn | ND | ND | ND | ND | 8.47 | 88.66 | 5.87 | ND |
| | Cpy | ND | ND | ND | ND | 6.37 | 3.68 | 2.89 | ND |
| | Po | ND | ND | ND | ND | 5.66 | 5.21 | 23.29 | ND |
| | Gn | ND | ND | ND | ND | 0.00 | 0.00 | 0.00 | ND |
| | PMM | ND | ND | ND | ND | 79.49 | 2.46 | 67.95 | ND |